



HAL
open science

Novel insights into the role of fetal hemoglobin in spleen function, red cell survival and ineffective erythropoiesis in sickle cell disease

Sara El Hoss

► **To cite this version:**

Sara El Hoss. Novel insights into the role of fetal hemoglobin in spleen function, red cell survival and ineffective erythropoiesis in sickle cell disease. *Tissues and Organs* [q-bio.TO]. Université Paris Cité, 2019. English. NNT : 2019UNIP7140 . tel-03127209

HAL Id: tel-03127209

<https://theses.hal.science/tel-03127209>

Submitted on 1 Feb 2021

HAL is a multi-disciplinary open access archive for the deposit and dissemination of scientific research documents, whether they are published or not. The documents may come from teaching and research institutions in France or abroad, or from public or private research centers.

L'archive ouverte pluridisciplinaire **HAL**, est destinée au dépôt et à la diffusion de documents scientifiques de niveau recherche, publiés ou non, émanant des établissements d'enseignement et de recherche français ou étrangers, des laboratoires publics ou privés.

Université de Paris

École Doctorale Bio Sorbonne Paris Cité–ED 562

UMR_S 1134 Biologie Intégrée du Globule Rouge

Novel Insights into the Role of Fetal Hemoglobin in Spleen Function, Red Cell Survival and Ineffective Erythropoiesis in Sickle Cell Disease

Sara El Hoss

Thèse de doctorat : Physiologie et Pathophysiologie

Dirigée par Dr. Wassim El Nemer

Présentée et soutenue publiquement à Paris le 24 Septembre 2019

Devant le jury composé de

Pr. Olivier Hermine	Université de Paris	Président
Pr. Corinne Pondarré	Université Paris XII	Rapportrice
Pr. Ashley M. Toye	University of Bristol	Rapporteur
Dr. Narla Mohandas	New York Blood Center	Examineur
Dr. Sandrina Kinet	Université de Montpellier	Examinatrice
Dr. Valentine Brousse	Université de Paris	Examinatrice
Dr. Wassim El Nemer	Université de Paris	Directeur de thèse



Dedication:

This work is dedicated to a whole nation and not to a person

To my childhood in Nigeria, to Africa, to where the heart will always be ...

Acknowledgment

I actually prefer to write a chapter 4 to avoid this roller coaster of emotions I will have ahead. I did not know this will be the hardest part of writing a thesis till I decided to sit and write it and ended up staring at my screen for an hour... My PhD was the best experience I ever had, I loved every part of it the scary, the stressing, the overworking, the funny, the happy and the exciting parts, I loved living them all and all of this won't have been possible or will not be the same without all the people I will list below.

I would like to start by thanking my PhD director (and my favorite person) Dr. Wassim El Nemer. Wassim, I really don't think words will do justice to how grateful and thankful I am to you. Thank you for believing in me, for listening to me, for endlessly teaching me, for giving me all the opportunities I needed to grow and shape myself into becoming a researcher. Thank you for your cheerleading sessions before every talk, thank you for your forever positive attitude that made everything easier, thank you for teaching me that after every "down" we will witness an "up"! You are truly one of kind! (*Blue team* all the way!)

This journey will not have been the same without the amazing Dr. Brousse! Valentine first of all thank you for always challenging me and pushing me to become better, please don't stop doing that! Thank you for showing me that patients' matter and that it is never just a blood tube. Thank you for sharing with me your love for the spleen, I ended up loving this mysterious organ too! (and I will always come over for food ;))

Dr. Yves Colin, the BBB (Best Big Boss), thank you for having me in your research unit. Thank you for your continuous support during my PhD, and for your availability when needed! (P.S Can I still use your cave after I finish?)

Dr. Caroline Le Van Kim, thank you for having me in the team and for your support during my PhD. Many thanks Caroline for advising me to be part of the representatives for the doctorate school, it was such an amazing experience that I really enjoyed!!

I would like to thank Pr. Olivier Hermine, Pr. Corinne Pondarré, Pr. Ashley Toyé, and Dr. Sandrina Kinet, members of my thesis jury, for the time they dedicated to evaluate this work.

Dr. Narla Mohandas, thank you for being part of my thesis jury and for a very nice collaboration. Working with you was an honor. Thank you for having me in your lab during my PhD and for all the fruitful scientific discussions. Thank you for introducing me to Hongxia

with whom I share the love of research. This collaboration was very rich for me and for that I will always be intensively grateful!

Michael Dussiot, « the AMNIS expert », thank you for making me discover the wonders of the AMNIS! And now I just can't live without it ;) Thanks for all the scientific discussions, working with you is a pleasure!

During my PhD I had the chance to share my office with the lovely Dr. Claudine Lapoumèroulie. Claudine mille merci d'être un soutien constant, je suis vraiment chanceuse de t'avoir dans ma vie. Merci de m'avoir enseigné la culture cellulaire, la langue française, l'histoire de France, de m'avoir emmenée à l'opéra, m'avoir nourrie de foie gras et de fromage, m'avoir fait aimer *longchamps*, Paris et aimer devenir Parisienne !

Pr. Jacques Elion thank you for all your support, for the rich scientific discussions, for helping me connect with an international scientific network and for the cheese and wine discussions too. I hope to always have the opportunity to learn from you!

My PhD experience will not have been the same without the sweetest Sylvie Cochet. Merci Sylvie d'être la reine de la biochimie et de m'avoir appris à faire un Western Blot qui fonctionne ! Merci de partager ta paillasse avec moi, d'avoir toujours une solution pour tout ! Merci de m'apprendre des proverbes français et l'histoire de France et me nourrir de bonbons du nord et pour ton soutien sans fin ! Tu es incroyable !!

This PhD will have not been possible without the support, love and care provided by my amazing friends (my 7bbs!!!):

- Maria (my Miga) sharing a project with you was extremely fun! Thank you for listening to me when I needed you, I can't thank you enough for always being here for me through thick and thin! You are truly a remarkable person and I will miss you bigtime!!
- Ralf, Papito, thank you for adding the fun and chill aspect to the blue team, I am grateful for having you always around, sorry for all the complains and thank you for all the listening!
- Martina! My favorite Italian! I can't imagine these four years without your happy energy all around! Thanks for sharing the episodes of "weekends in the lab" with me! Thanks for introducing me to Giulia and so thanks for all the pasta ;)
- Mahmoud thanks for supporting my endless jokes, may your future be germ free ;)

Jean-Philippe Semblat, my office neighbor, I can't thank you enough for supporting me as an office neighbor, I'm sure it was a lot of work! Thank you for sponsoring this PhD with endless cookies supply and motivational pitch talks! Thank you for all the discussions we have!

Sandrine L., my erythropoiesis partner in crime! Thank you for sharing L2 moments with me! It was stressful and you made it fun! To many more years of teasing Claudine together!

Karim, thank you for sharing with me the "let us save Africa" passion! Hopefully to future collaborations together!

Marc (a.k.a Marco des Isles) thank you for your support and suggestions to our projects! Discussing with you was always a pleasure! Hopefully I will end up visiting the Guadeloupe.

Aurélie, Camille, Benoît H., Alioune, Charlotte and Mallorie you guys are awesome in every way!! I am grateful that I had the chance to get to know you.

Arnaud, thanks for all the advice discussions and support!

Yann, even with the 8,802 km between Paris and Brazil, I can't count the number of times you repeated the phrase "you can do it" since I met you! Merci!

Auria sharing the last step of my journey with you was a great experience! I wish you only success for your future.

Patricia, Mariano, Marie-Catherine, Mickaël, Claude L., Claude H., Olivier, Sandrine G., Pascal, Dominique, Abdallah, Lucie, Emmanuelle, Hugo, Manon, Sophie, Sarah, Mélanie, Anna, Irene, Nelly, Marilou, Zaineb, Sébastien, Célia, Benoît G., Romain, Slim, Alexandra, Leonardo, Asma and the rest of the INSERM unit 1134 (and the Guadeloupe team) with whom I shared lunch, coffee and lab meetings thank you for being part of this journey!

A special thanks go to the chefs of the canteen at INTS for feeding us every day! Because life is oriented around the lunch break!

Dr. Walid Moubayed, the real inspiration behind the phrase that anything is possible!! Thank you for believing in my dreams.

My family, Dad Mom Mehio Yara Stephanie and Hasan I love you all!!! Your support for every step I take is what keeps me going forward. Dad, this 200 pages of science is for you!

Bénédictte, Jules and Agathe thank you for cheering me up when it was hard and thank you for simply existing in my life.

Shaza, Hala, Sherine, Takla, Tania, Reina, Mira, and Abdallah twice a year is not enough! Thank you for the welcome back/goodbye gatherings, thank you for the supportive phone calls and texts and I'm sorry for my minimal availability I was trying to make this thesis happen...

This work will not have happened without the nurses of Necker Hospital (Hôpital de Jour), this amazing group of people made everything easier! Dr. Valentine Brousse and Dr. Bénédicte Boutonnat – Faucher thank you for taking care of all the patients.

To all the patients and their parents, I hope this work will help change something or will be a step toward a change. I cannot be more grateful for your support and belief in this work. I promise to continue working...

Finally, to France thank you for the opportunities, the challenges, the teaching and the memories. Thank you for making me feel at home ❤️

Table of Content

ABSTRACT	1
RÉSUMÉ.....	3
ABBREVIATIONS.....	5
INTRODUCTION.....	9
1. Sickle cell disease.....	10
1.1 Epidemiology	10
1.2 Pathophysiology	12
1.2.1 HbS polymerization	14
1.2.2 Disease onset and hemoglobin switching	14
1.2.3 Main dysfunctions in the red blood cell.....	17
1.2.4 Main clinical features.....	18
1.3 Environmental and genetic modifiers of disease severity	22
1.3.1 Fetal Hemoglobin.....	23
1.3.2 α -thalassemia	24
1.4 Treatments	24
1.4.1 Hydroxycarbamide	25
1.4.2 Blood Transfusion	26
1.4.3 Hematopoietic stem cell transplantation.....	27
1.4.4 Gene therapy	27
2 The human spleen.....	29
2.1 Structure and function of the spleen.....	29
2.1.1 The red pulp.....	29
2.1.2 The white pulp	31
2.1.3 The perifollicular zone	32
2.2 Measurements of spleen function.....	32
3 The spleen in sickle cell disease.....	33
3.1 Early and progressive loss of spleen function	33
3.1.1 Pathophysiology of SCD splenic damage.....	34
3.2 Consequences of loss of spleen function.....	35
3.3 Clinical manifestation of the spleen	36
3.3.1 Acute splenic sequestration	36
3.3.2 Splenomegaly.....	37
3.3.3 Hypersplenism	38

4	Erythropoiesis.....	38
4.1	Developmental waves of erythropoiesis.....	38
4.2	Human erythropoiesis at steady state	39
4.3	The erythroblastic island	41
4.4	Regulation of erythropoiesis.....	43
4.5	Ex vivo culture systems of erythropoiesis.....	45
4.6	Monitoring of erythropoiesis	47
4.7	Ineffective erythropoiesis in erythroid disorders.....	48
4.7.1	<i>Ineffective erythropoiesis in hemoglobinopathies</i>	48
	OBJECTIVES	51
	<i>CHAPTER I: Novel Insights into Spleen Function and Determinants of Spleen Injury in SCA</i>	
	<i>Children: A Longitudinal Study</i>	53
	RESULTS.....	54
	A novel non-invasive method to measure the splenic filtration function in humans	55
	<i>Novel template to quantify HJB-RBCs using imaging flow cytometry (IFC)</i>	55
	<i>Validation of the IFC-based technique</i>	58
	<i>Measuring %HJB-RBCs with conventional flow cytometry</i>	60
	Insights into determinants of spleen injury in sickle cell anemia.....	62
	<i>Description of the cohort</i>	62
	<i>Evidence of very early loss of spleen function</i>	63
	<i>Impaired deformability of RBCs increases with time and impacts spleen function</i>	66
	<i>Adhesion properties of red cells</i>	67
	<i>Adhesion properties and spleen function</i>	70
	Decreased red cell deformability plays a role in ASS occurrence.....	71
	DISCUSSION	73
	PATIENTS & METHODS.....	79
	Patients and blood samples.....	80
	HJB-RBCs quantification.....	81
	<i>Sample preparation</i>	81
	<i>Imaging Flow Cytometry assay</i>	81
	<i>Flow Cytometry assay</i>	82
	<i>Blood smears and May-Grünwald-Giemsa staining</i>	82
	Spleen scintigraphy	83
	Quantification of Irreversibly Sickled Cells (ISCs)	84
	Flow cytometry analysis.....	84
	Flow adhesion assays	85

<i>Culture of TrHBMECs in Vena8 Endothelial+ biochips</i>	85
<i>Coating of channels with laminin</i>	86
<i>Preparation of blood samples</i>	86
<i>Adhesion assays under flow conditions</i>	86
Immunoprecipitation and Western blot analyses.....	86
Statistics	87
CHAPTER II: New Insights into the Expression and Cellular Distribution of HbF, and the Effect of Hydroxycarbamide	88
RESULTS	89
Early survival advantage of F-cells during erythroid maturation.....	90
High, medium and low % of HbF within F-cells in non-treated patients.....	91
F-cells with low levels of HbF are lysed upon mechanical challenge.....	93
HbF expression and distribution in infancy.....	94
Impact of HC on HbF expression and cellular distribution.....	95
Effect of HC on RBC mechanical properties	97
Relationship between %HbF and %F-cells according to age or HC treatment.....	98
Effect of HC treatment on the distribution of High and Low F-cells.....	100
DISCUSSION	103
PATIENTS & METHODS	107
Patients	108
Flow Cytometry and Imaging Flow Cytometry	108
<i>HbF staining and analysis</i>	108
<i>Irreversibly Sickled Cells Quantification</i>	108
Hemolysis and HbF measurements	109
Statistics	110
CHAPTER III: Anti-apoptotic Role of Fetal Hemoglobin During Human Terminal Erythroid Differentiation Regulates Ineffective Erythropoiesis in Sickle Cell Disease	111
RESULTS	112
Cell death during the terminal stages of erythroid differentiation in bone marrow of SCD patients	113
Hypoxia-induced cell death during <i>in vitro</i> terminal erythroid differentiation	114
F-cells are enriched during SCD erythroid differentiation.....	118
HSP70 is sequestered in the cytoplasm of non-F-cells.....	120
Induction of HbF by pomalidomide protects against cell death.....	128
DISCUSSION	130
MATERIALS & METHODS	135
Biological samples	136

Antibodies and fluorescent dies	136
In vitro differentiation of human erythroid progenitors	137
Imaging Flow Cytometry analysis of human bone marrow samples	137
Flow cytometry.....	138
<i>Surface marker staining</i>	138
<i>Enucleation analysis</i>	138
<i>Apoptotic cells</i>	138
<i>HbF and HSP70 staining</i>	139
Cytospin	139
Cell fractionation and Western blot.....	139
Confocal Microscopy and Proximity Ligation Assay	140
Statistics	141
CONCLUSIONS & PERSPECTIVES	142
BIBLIOGRAPHY	145
APPENDIX	173
Article 1	174
Article 2.....	179
Article 3.....	189
Article 4.....	200
Review.....	210

ABSTRACT

Sickle cell disease (SCD) is caused by a single point mutation in the β -globin gene generating sickle hemoglobin (HbS). Hypoxia drives HbS polymerization that is responsible for red blood cell (RBC) sickling and reduced deformability. In SCD, splenic dysfunction results in life-threatening complications, particularly in early childhood. During the course of the disease, the spleen functionally declines and anatomically disappears, although with great individual variability depending on modulating genetic and environmental factors. The key modulator of disease severity is fetal hemoglobin (HbF), as the presence of HbF inhibits HbS polymerization, thus delaying and preventing severe complications, ameliorating patients' quality of life and increasing survival. There is a rather well characterized hetero cellular concentration of HbF and distribution in circulating RBCs but the role of HbF during erythropoiesis, is poorly documented.

With the aim of better understanding the role of HbF in spleen function, red cell survival and ineffective erythropoiesis we investigated 1) the natural history of spleen dysfunction in SCD children, 2) the cellular expression and distribution of HbF in SCD children, in untreated patients and patients treated with Hydroxycarbamide and 3) ineffective erythropoiesis and the role of HbF during terminal erythropoiesis.

We developed a flow cytometry high-throughput method to measure splenic filtration function and showed that splenic loss of function is present very early in life at 3-6 months in SCD children and further declines with age. We also highlighted that irreversibly sickled cells (ISCs) are a potential contributor to acute splenic sequestration (ASS) which in turn results in further loss of splenic function. In the second part of this work, we set up an original approach to determine HbF distribution per cell. Using a longitudinal cohort of patients treated with hydroxycarbamide (HC - an inducer of HbF), we showed that HC has a global positive impact on RBCs, by not only increasing HbF content but also by increasing the volume of all RBCs independent of HbF. We moreover showed that High F-cells are a more precise marker of HC efficacy. In the last part of the thesis, we showed for the first time clear evidence of ineffective erythropoiesis in SCD and revealed a new role of HbF during terminal erythropoiesis protecting erythroblasts from apoptosis.

In conclusion, this work shows that HbF has an additional beneficial effect in SCD by not only conferring a preferential survival of F-cells in the circulation but also by decreasing ineffective erythropoiesis. Importantly, it suggests that the delay in hemoglobin switch in SCD might be also due to an enrichment in F-erythroblasts during terminal erythroid differentiation occurring very early in infancy, shortly after birth.

Keywords: Sickle Cell Disease, Red Blood Cells, Fetal Hemoglobin, Irreversibly Sickled Cells, Spleen, Acute Splenic Sequestration, Hydroxycarbamide, Ineffective Erythropoiesis, Apoptosis

RÉSUMÉ

La drépanocytose est une maladie génétique héréditaire récessive causée par la substitution d'un acide aminé dans la chaîne β -globine aboutissant à la production d'hémoglobine anormale (HbS). Dans des conditions hypoxiques, l'HbS polymérise entraînant une falciformation et une perte de déformabilité des globules rouges (GR). Au cours de la drépanocytose, le dysfonctionnement splénique entraîne des complications potentiellement mortelles, en particulier chez les jeunes enfants. Généralement, une asplénie fonctionnelle précède la survenue d'une asplénie anatomique avec cependant une grande variabilité inter-individuelle du fait de facteurs modulateurs génétiques et environnementaux. L'hémoglobine fœtale (HbF) est le principal modulateur de la gravité de la maladie, car la présence d'HbF inhibe la polymérisation d'HbS, retardant et prévenant ainsi les complications graves, améliorant la qualité de vie des patients et augmentant leur survie. Il existe une hétérogénéité assez bien caractérisée de la concentration et de la distribution cellulaire d'HbF dans les GR circulants, mais le rôle de l'HbF au cours de l'érythropoïèse est mal documenté.

Dans le but de mieux comprendre le rôle de l'HbF dans la perte de fonctionnalité splénique, la survie des GR et l'érythropoïèse inefficace, nous avons étudié 1) l'histoire naturelle du dysfonctionnement splénique chez les enfants drépanocytaires, 2) l'expression cellulaire et la distribution de l'HbF comparativement chez les enfants, chez les patients naïfs et ceux traités par hydroxycarbamide (HC) et 3) le rôle de l'HbF au cours de l'érythropoïèse terminale.

Nous avons d'abord développé une méthode de cytométrie en flux à haut débit pour mesurer la fonction de filtration splénique et avons montré que la perte de fonction splénique est présente très tôt dans la vie, dès 3 à 6 mois chez les enfants drépanocytaires, puis diminue avec l'âge. Nous avons également mis en évidence que les cellules irréversiblement falciformées (ISC) jouaient un rôle dans la survenue de la séquestration splénique aiguë, laquelle entraîne à son tour une perte supplémentaire de fonction.

Dans la deuxième partie de ce travail, nous avons mis en place une approche originale pour déterminer la distribution d'HbF à l'échelle cellulaire. En utilisant une cohorte longitudinale de patients traités par HC (inducteur d'HbF), nous avons montré que celui-ci avait un impact positif global sur les GR, en augmentant non seulement le contenu en HbF, mais également le volume de tous les GR, indépendamment de leur contenu en HbF. Nous avons par ailleurs montré que les cellules riches en HbF (High-F) étaient un marqueur précis d'efficacité de l'HC.

Dans la dernière partie de la thèse, nous avons démontré pour la première fois une érythropoïèse inefficace chez les patients drépanocytaires et avons révélé un nouveau rôle de l'HbF au cours de l'érythropoïèse terminale, celui de protéger les érythroblastes de l'apoptose.

En conclusion, ce travail montre que l'HbF a un effet bénéfique supplémentaire sur la drépanocytose en conférant non seulement une survie préférentielle des cellules F dans la circulation, mais en diminuant également l'érythropoïèse inefficace. Ce résultat suggère que la persistance d'HbF dans la drépanocytose serait davantage la conséquence d'un enrichissement en F-érythroblastes au cours de la différenciation érythroïde terminale survenant peu après la naissance plutôt qu'un retard du switch des hémoglobines.

Mots-clés : Drépanocytose, Globules Rouges, Hémoglobine Fœtale, Cellules Irréversiblement Falciformées, Rate, Séquestration Splénique Aiguë, Hydroxycarbamide, Érythropoïèse Inefficace, Apoptose.

ABBREVIATIONS

7AAD: 7-Aminoactinomycin D
ACS: Acute Chest Syndrome
ASH: American Society of Hematology
ASS: Acute Splenic Sequestration
BFU-E: Burst-forming Unit-erythroid
CFU-E: Colony-forming Unit-erythroid
CMP: Common Myeloid Progenitors
CNRGS: Centre Nationale de Référence pour les Groupes Sanguins
DAPI: 4',6-diamidino-2-phenylindole
DNA: Deoxyribonucleic Acid
ECL: Enhanced Chemiluminescence
EDTA: Ethylenediaminetetraacetic acid
EFS: Etablissement Français du Sang
EMeA: European Medicines Agency
EMP: Erythro-myeloid Progenitors
EPO: Erythropoietin
EPOR: Erythropoietin Receptor
FACS: Fluorescence-activated Cell Sorting
FDA: Food and Drug Administration
FVS: Fixable Viability Stain
GPA: Glycophorin A
GC: Germinal Center
Hb: Hemoglobin
HbF: Fetal Hemoglobin
HbS: Sickled Hemoglobin
HC: Hydroxycarbamide
HIF: Hypoxia Inducible Factor
HJB: Howell-Jolly Bodies
HSCs: Hematopoietic Stem Cells
HSCT: Hematopoietic Stem Cell Transplantation

HSP70: Heat Shock Protein 70
HU: Hydroxyurea
HPFH: Hereditary Persistence of Fetal Hemoglobin
HPLC: High Performance Liquid Chromatography
IFC: Imaging Flow Cytometry
IL-3: Interleukin 3
IL-6: Interleukin 6
IRB: Institutional Review Board
ISCs: Irreversibly Sickled Cells
Lu/BCAM: Lutheran Basal Cell Adhesion Molecule
MCHC: Mean Cell Hemoglobin Concentration
MCV: Mean Corpuscular Volume
MEPs: Megakaryocytic-erythroid Progenitors
MGG: May-Grünwald-Giemsa
N/C: Nucleus/Cytoplasm
NFkB: Nuclear Factor kB
NO: Nitric Oxide
O₂⁻: Superoxide
OH: Hydroxyl
PAS: Protein A Sepharose
PI: Propidium Iodide
PLA: Proximity Ligation Assay
POM: Pomalidomide
PS: Phosphatidylserine
PSA: Projected Surface Area
RBC: Red Blood Cell
RNA: Ribonucleic Acid
SCA: Sickle Cell Anemia
SCD: Sickle Cell Disease
SS RBCs: Sickled Red Blood Cells

TBS: Tris Buffer Saline

TCD: Trans Cranial Doppler

TrHBMEC: Transformed Human Bone Marrow Endothelial Cells

TNF- α : Tumor Necrosis Factor - alpha

UN: United Nations

VOC: Vaso-occlusive Crisis

WBC: White Blood Cells

WHO : World Health Organization

INTRODUCTION

1. Sickle cell disease

1.1 Epidemiology

Sickle cell disease (SCD) is a genetic recessive inherited disease and one of the most common severe monogenic disorders worldwide (Weatherall, Hofman, Rodgers, Ruffin, & Hrynkow, 2005). Clinical expression occurs in childhood, few months after birth. The disease is due to a single mutation in the β -globin chain (β^S) resulting in hemoglobin (Hb) polymerization and red blood cell (RBC) sickling. The sickle shaped erythrocyte was first described by James Herrick in 1910, after the examination of a patients' blood sample and commented as follows: "The shape of the reds was very irregular, but what especially attracted attention was the large number of thin, elongated, sickle shaped and crescent-shaped forms" (Figure 1) (Herrick, 2001). Later on, in 1949 Linus Pauling and his group examined the physical and chemical properties of hemoglobin from SCD patients and compared it to hemoglobin in healthy individuals. They were able to discover that HbS had an abnormal electrophoretic mobility, thus they classified SCD as a "molecular disease" (Pauling & Itano, 1949).

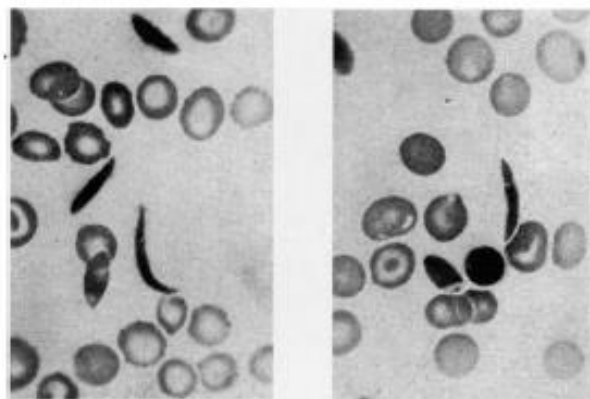


Figure 1: **Photomicrographs showing the elongated form of erythrocytes** (Herrick, 2001).

SCD has been recognized as a global public health problem by the World Health Organization (WHO) in 2006, the United Nations (UN) and the American Society of Hematology (ASH) in 2016. To date, around 300,000 newborns are affected yearly by the disease, and this number is expected to rise to 400,000 by 2050 (Piel, Hay, Gupta, Weatherall, & Williams, 2013). The vast

majority of affected births occur in African countries, with Nigeria, the Democratic Republic of Congo and India being the most impacted countries due to the selection for carriers through their survival advantage in malaria endemic regions (Piel, Steinberg, & Rees, 2017) (Figure 2A). Due to slave trading and voluntary migration, the distribution of SCD has spread far beyond its origins and is present worldwide, reaching in some countries, like the United States of America and Brazil, percentages as high as African areas of high prevalence (Figure 2A) (Piel, Rees, & Williams, 2014; Piel et al., 2017). An epidemiological study carried by Piel et al. estimate that the overall number of births affected by sickle cell anemia (SCA) between 2010 and 2050 to be 14,242,000, with approximately 88% in sub-Saharan Africa (Figure 2B) (Piel et al., 2013).

Due to lack of early diagnosis and effective treatment, it has been reported that 50-90% of the newborns die in the first few years of life (Grosse et al., 2011). However, in lower-income countries, life expectancy has improved significantly with increased number of affected babies and children surviving till adulthood, requiring diagnosis and treatment (Piel et al., 2017). Nevertheless, life expectancy for patients with SCD is reduced by about 30 years, even with the best medical care.

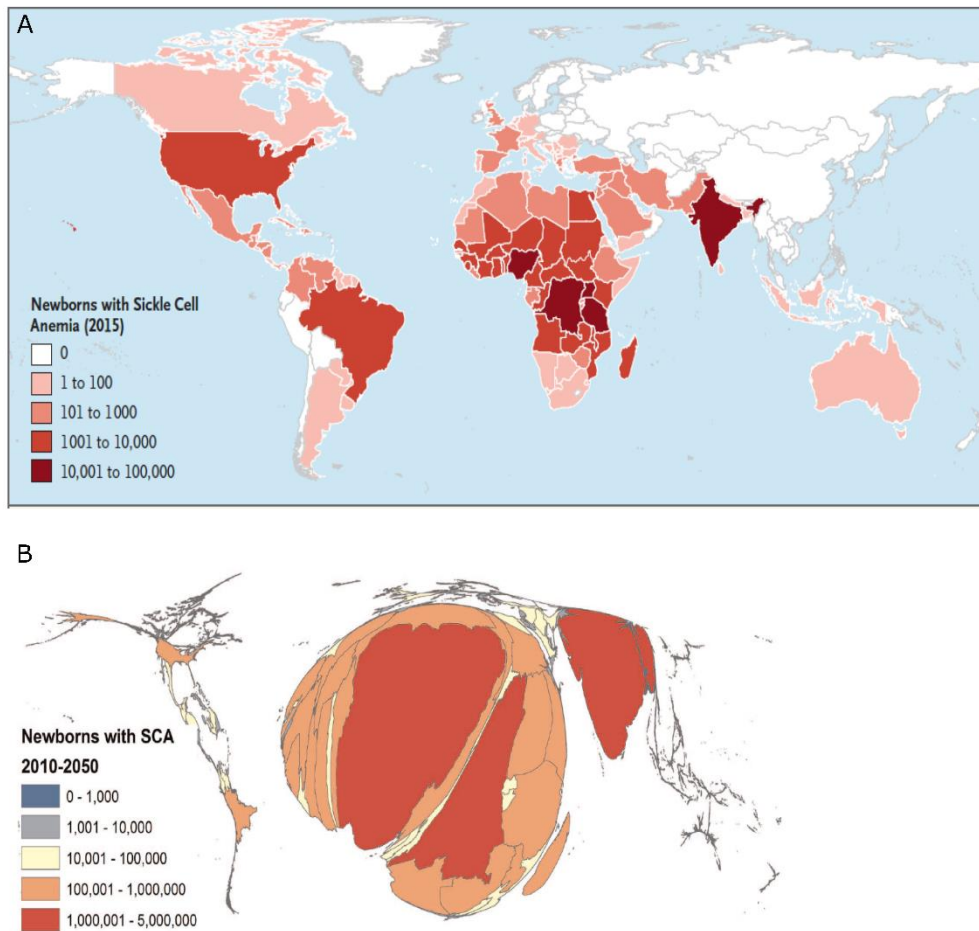


Figure 2: **Global burden of SCD.** (A) A map showing the number of newborns with SCD in 2015 (Piel et al., 2017). (B) Cartogram of the estimated number of newborns with SCD between the year 2010 and 2050 (Piel et al., 2013).

1.2 Pathophysiology

Adult functional hemoglobin is a tetramer formed of 2 α -globin and 2 β -globin polypeptide chains with an iron containing porphyrin ring known as heme, which is required for effective oxygen transport (Sankaran & Orkin, 2013). In SCD, the 17th nucleotide (thymine) is mutated to adenine (c.20A>T), resulting in a glutamic acid to valine substitution at the sixth amino acid of β globin (β^S) (Ingram, 1956). SCD is the consequence of this mutation on both alleles or the association of the β^S -mutation with another mutation of the β -globin gene, including β -thalassemia mutations that hinder the production of β -globin. The β^S -mutation produces a hydrophobic motif in the sickled hemoglobin (HbS) tetramer that results in binding between $\beta 1$

and $\beta 2$ chains of two deoxygenated hemoglobin molecules (see next paragraph). This crystallization produces a polymer nucleus that grows rapidly and forms long fibers in the erythrocyte, increasing cell rigidity, disrupting its architecture and elasticity, and increasing dehydration, ultimately leading to erythrocyte sickling (Brugnara, Bunn, & Tosteson, 1986; Rees, Williams, & Gladwin, 2010). These abnormalities impact the life span and rheological properties of RBCs resulting in hemolysis (and anemia) and a likelihood of small blood vessels occlusion (Figure 3) (Steinberg, 2008).

Other forms of SCD include coinheritance of β^S -mutation with other qualitative β -globin gene variants, including C (Glu6Lys, SCD-SC), D-Punjab (Glu121Gln), E (Glu26Lys) and O-Arab (Glu121Lys) or quantitative β -globin gene variants (S/β^0 -thalassemia and S/β^+ thalassemia). Sickle Cell Anemia (SCA) refers to the SS and S/β^0 -thalassemia genotypes, which are associated with the most severe phenotypes (Mburu & Odame, 2019).

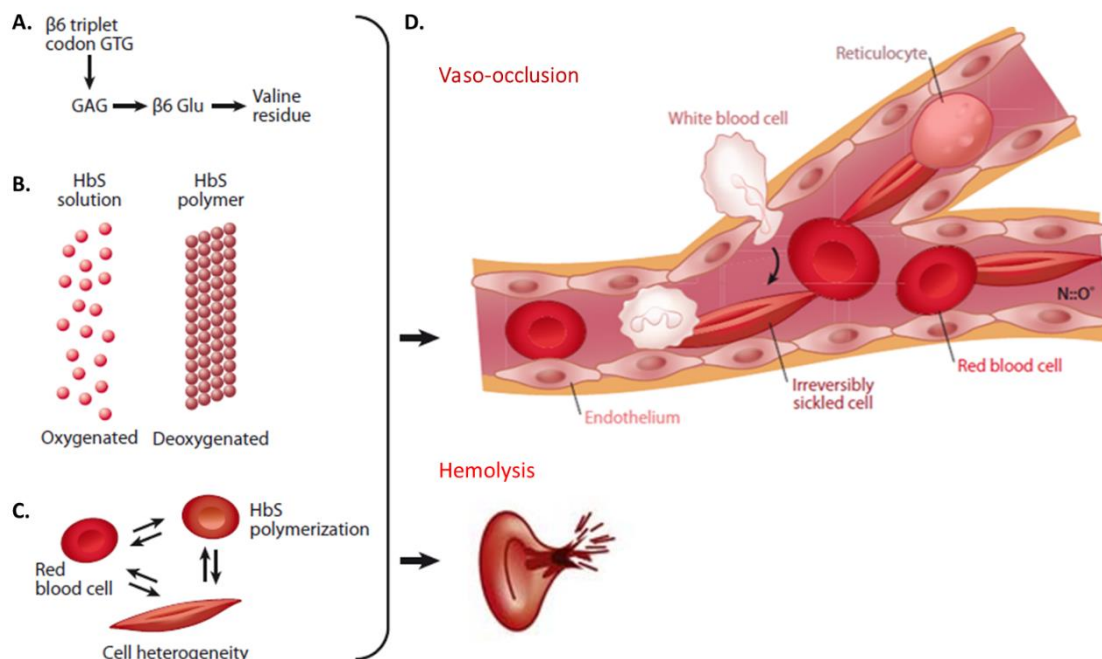


Figure 3: Pathophysiology of Sickle Cell Disease. (A) Point mutation in SCD. (B) Polymerization of hemoglobin S (HbS) under deoxygenation. (C) Red blood cell (RBC) change in response to HbS polymerization. (D) Cells in microvasculature: *Vaso-occlusion* initiated by a reticulocyte adhering to endothelium, trapping irreversibly sickled cells (ISCs) and forming aggregates with white blood cells; *Erythrocyte hemolysis* (Steinberg, 2008).

1.2.1 HbS polymerization

The rate and extent of HbS polymerization is dependent on the extent and duration of hemoglobin deoxygenation, the intracellular HbS concentration, and the presence of fetal hemoglobin (HbF) in the RBC, which can effectively reduce the concentration of HbS (Rees et al., 2010). During deoxygenation which follows the passage of the RBC in the microcirculation, the hemoglobin undergoes conformational changes. The sickled hemoglobin under deoxygenation (deoxyHbS) has a quaternary structure that differs from the oxygenated HbS (oxyHbS). The deoxyHbS molecules then collide, interact and nucleate rapidly forming the stiff polymer fiber (Figure 4). Cycles of polymerization and depolymerization cause irreversible damage to the sickle erythrocyte membrane cytoskeleton, accounting for the presence of irreversibly sickled cells (ISCs) in the peripheral blood of the patients (Lux, John, & Karnovsky, 1976; Odièvre, Verger, Silva-Pinto, & Elion, 2011; Steinberg, 2008).

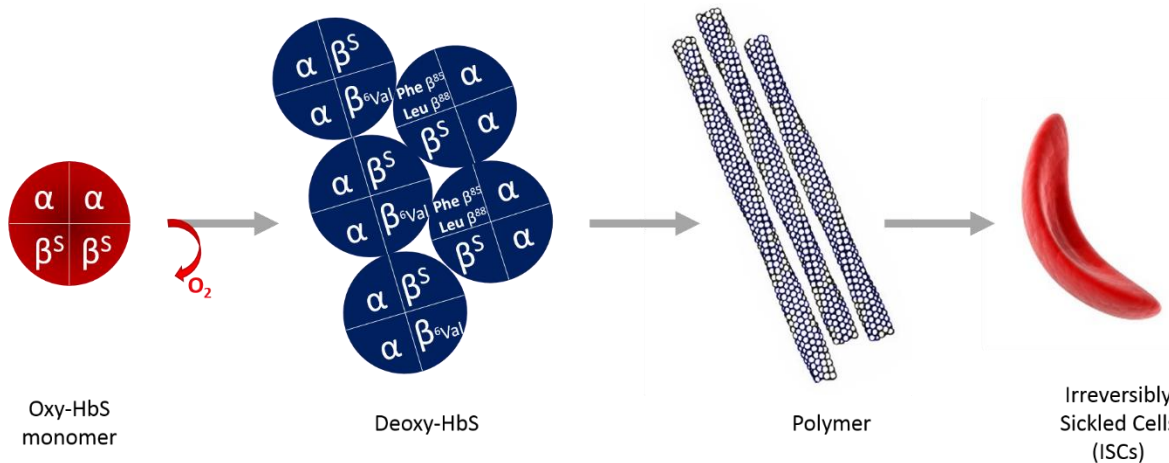


Figure 4: **Polymerization of deoxy-HbS.** At low oxygen pressure, deoxy-HbS polymerizes and forms stiff polymer fibers that deform the RBC, leading to irreversibly sickled cell (ISCs). Figure adapted from Odièvre et al. 2011.

1.2.2 Disease onset and hemoglobin switching

In SCD children, the first months of life are a time with a low incidence of complications, a state attributable to the sustained level of protective fetal hemoglobin (HbF). HbF has a pivotal

anti-polymerization effect on the mutant hemoglobin (HbS). As the physiological switch from HbF to HbS progresses, increased polymerization of HbS occurs resulting in multiple and inter-related downstream effects, mainly vaso-occlusion, hemolysis, inflammation, increased cell adhesion, endothelial dysfunction and decreased NO bioavailability (Couque et al., 2016).

The switching from embryonic, to fetal then to adult globin genes occurs during development through a series of two hemoglobin switches (Sankaran & Orkin, 2013). Humans have five functional β -like globin genes which are: embryonic (HBE1), fetal (HBG1, HBG2) and adult (HBD and HBB). There are three major functional α -like globin genes: embryonic (HBZ) and adult (HBA1 and HBA2). These genes allow the production of different hemoglobins during development: embryonic Hb ($\alpha 2\varepsilon 2$), fetal ($\alpha 2\gamma 2$), and adult ($\alpha 2\beta 2$). In SCD, the adult hemoglobin is formed of $\alpha 2\beta^S 2$ (Figure 5). In primitive erythroid cells we observe a switch from the embryonic to the fetal globins, the latter overlapping with the onset of definitive erythropoiesis (Nandakumar, Ulirsch, & Sankaran, 2016). After birth, fetal globin expression is gradually replaced by the adult globin expression (Figure 6).

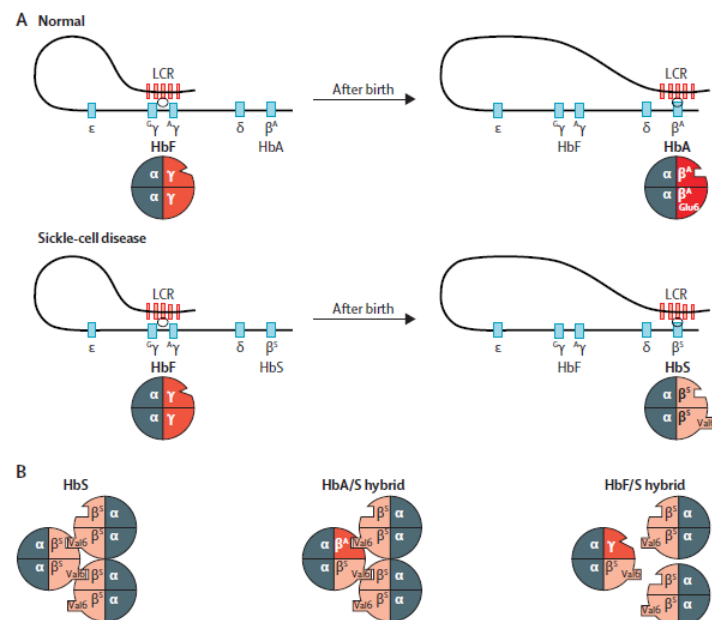


Figure 5: Fetal and sickled hemoglobin. The predominant hemoglobin before birth is fetal hemoglobin (HbF; $\alpha_2\gamma_2$). After birth, HbA gradually predominates. Sickle cell disease, due to its β^S mutation of β -globin, only manifests after birth. (B) Sickle hemoglobin (HbS) tetramers have a tendency to polymerize under deoxygenated conditions. The anti-sickling effect of HbF exceeds that of HbA (Lette & Bauer, 2016).

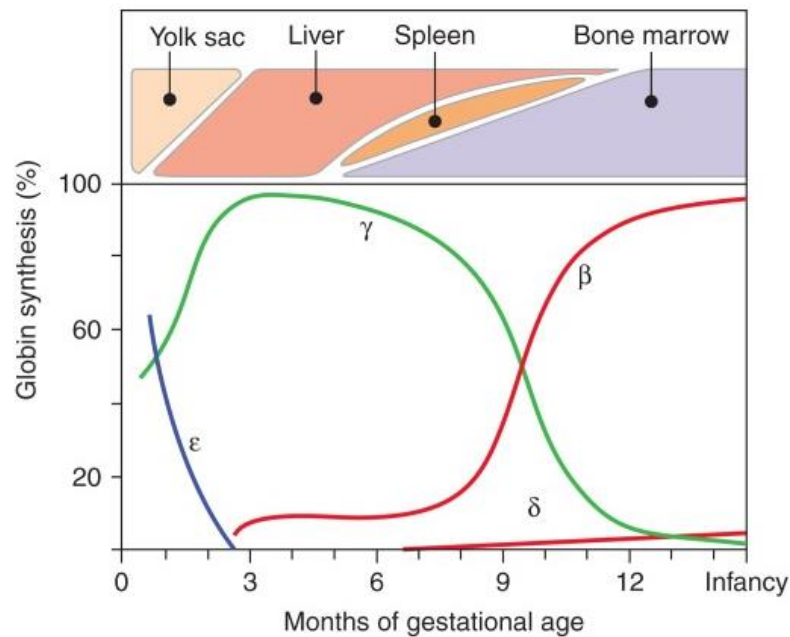


Figure 6: **The fetal-to-adult hemoglobin switch.** The switch as observed in healthy individuals, in the top panel the sites of production are shown. Lower panel: the levels of the various β -like globin molecules are shown (embryonic in blue, fetal in green and adult in red) (Sankaran & Orkin, 2013).

The understanding of the fetal to adult hemoglobin switching has been of great interest in sickle cell disease due to the therapeutic relevance of fetal hemoglobin in SCD. For instance, individuals with hereditary persistence of fetal hemoglobin (HPFH) have reduced disease severity when associated with SCD (Galanello et al., 2009).

At the molecular level, the multi-zinc finger containing transcriptional regulator, BCL11A, has been identified as the main regulator of the fetal to adult hemoglobin switch and HbF silencing (Sankaran et al., 2008). BCL11A is known to bind to the β -globin enhancer and to the intergenic region between the HBG1 and HBD gene, the latter being often deleted in HPFH individuals. Another important regulator of HbF is MYB, whose reduction was shown to induce HbF production although the mechanism behind this remains to be discovered (Sankaran & Nathan, 2010; Sankaran et al., 2013). Another important regulator of HbF is KLF1, whose mutation has been associated with increased HbF (Sankaran & Orkin, 2013) (Figure 7).

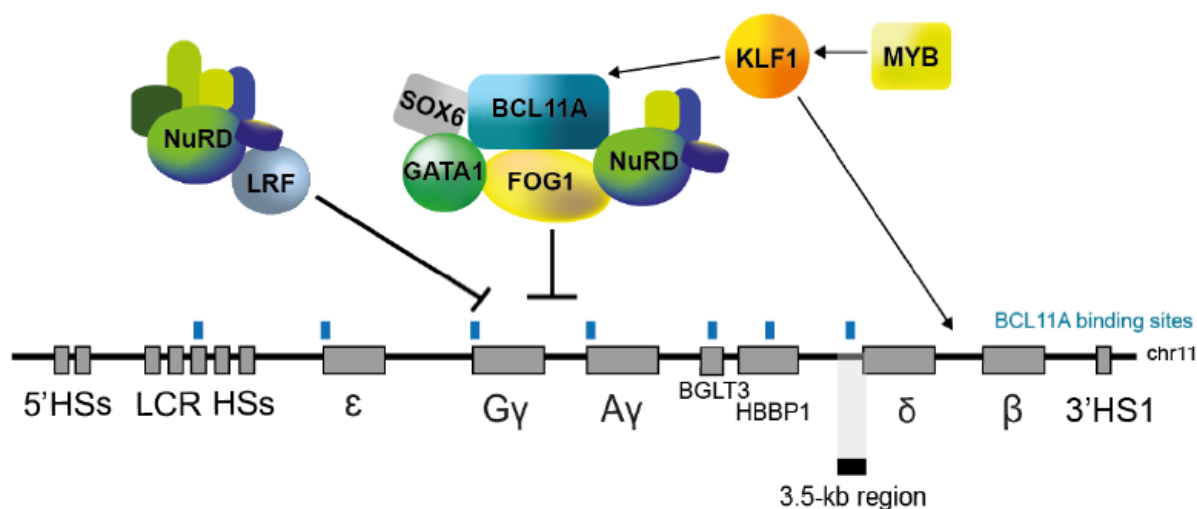


Figure 7: **Key regulators of fetal to adult globin switch.** The expression of BCL11A is positively regulated by KLF1, which in turn is upregulated by MYB. Additionally, KLF1 favors fetal-to-adult Hb switching by directly activating β -globin gene expression (Cavazzana, Antoniani, & Miccio, 2017).

Fetal hemoglobin expression varies between patients and more specifically it can vary at the erythrocyte level. The presence of HbF inhibits HbS polymerization and the concentration of HbF within each cell and the distribution among all cells influence the heterogeneity of erythrocytes in the circulation (Steinberg, 2008). Thus studying HbF cellular distribution is critical to the understanding of disease severity.

1.2.3 Main dysfunctions in the red blood cell

The HbS polymers, and even the high concentration of unpolymerized HbS damage the erythrocyte and its membrane (de Jong, Larkin, Styles, Bookchin, & Kuypers, 2001). The formation of these polymer fibers triggers a cascade of various abnormalities within the cell that participate to the overall pathophysiological mechanism. One important consequence is cellular dehydration due to the activation of ion channels, such as the KCl co-transport system and the Ca^{2+} -dependent K channel (Gardos channel) resulting in loss of potassium. Dehydration increases the intracellular Hb concentration which in turn favors HbS polymerization (Odievre et al., 2011; Steinberg, 2008; Stuart & Nagel, 2004). In addition, Hb hemichromes concentrates lead to the liberation of Fe^{3+} and the development of an oxidized environment in the cells.

Another consequence is the loss of the normal asymmetry of the phospholipid membrane and the exposure of the anionic phosphatidylserine (PS) on the cell surface (Stuart & Nagel, 2004). Lastly, these membrane changes lead to the production of microparticles in the circulation (Romana, Connes, & Key, 2018) (Figure 8).

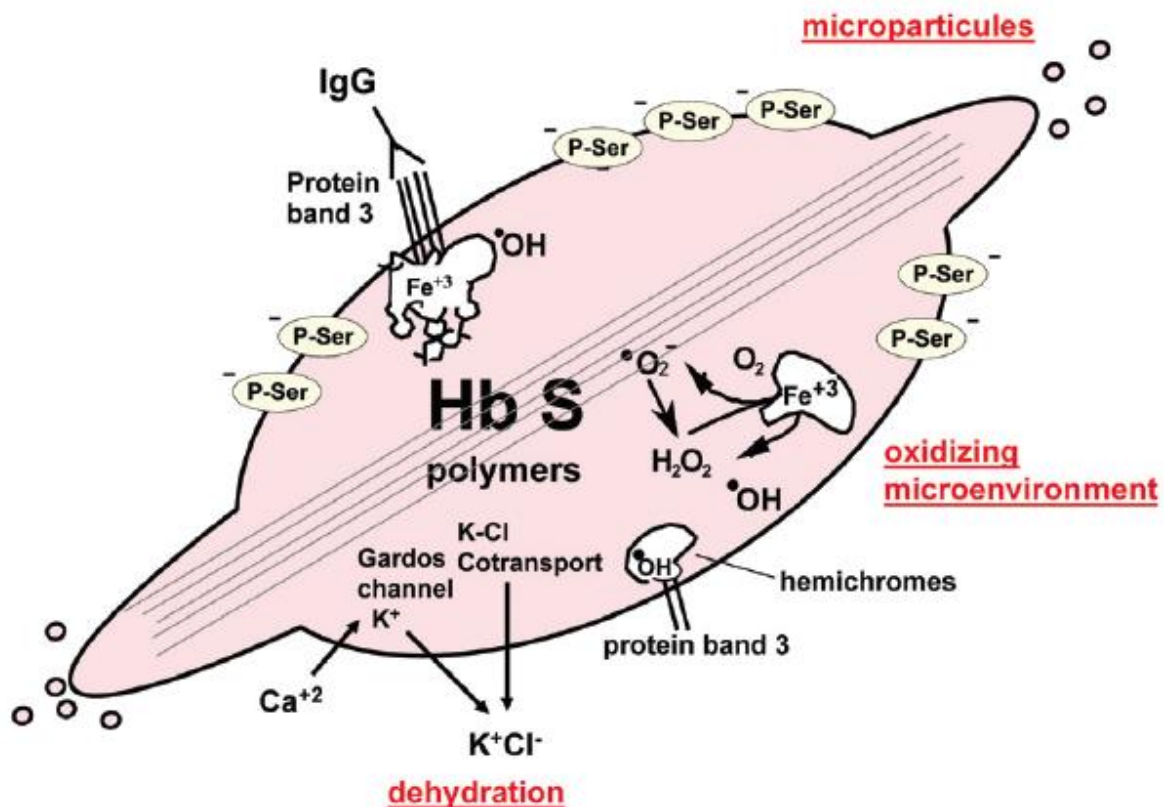


Figure 8: **Alterations in the sickle red blood cell.** Formation of the deoxy-HbS polymer fibers triggers a series of changes of the red blood cell membrane. Ion channels are affected and their dysfunction is responsible for a cellular dehydration which, in a vicious circle, favors deoxy-HbS polymerization. The liberation of heme and Fe^{3+} favors an oxidizing microenvironment. Exposure of anionic phosphatidylserines at the external side of the membrane creates a procoagulant surface. Finally, microparticles are released (Labie & Elion, 1999; Odievre et al., 2011).

1.2.4 Main clinical features

The primary trigger in SCD is HbS polymerization resulting in RBC sickling. The main clinical features of SCD are painful vaso-occlusive crisis and hemolytic anemia leading to multiple acute and chronic organ damage, with the spleen being the first organ to be affected (see section 3).

A. The vaso-occlusive crisis

Vaso-occlusive crisis (VOC) is one of the main acute complications of SCD. VOC is thought to be caused by the entrapment of erythrocytes and leukocytes in the microcirculation causing vascular obstruction and tissue ischemia. As a consequence, the patients experience episodes of pain, acute chest syndrome (ACS), osteonecrosis, organ injury, and early mortality (Manwani & Frenette, 2013).

Vaso-occlusive obstruction might first occur in small capillaries by the entrapment of sickled RBCs and their adhesion to the vascular endothelium, together with the adhesion of platelets and leukocytes (Figure 9) (Kaul, Fabry, & Nagel, 1996). Although VOC requires HbS polymerization and erythrocyte sickling, inflammation plays a crucial role. Studies on transgenic SCD mice showed that treatment of these mice with inflammatory drugs increases endothelial-leukocyte-erythrocyte cellular interactions resulting in microvascular occlusion and ischemia, which further promotes tissue injury mediated by reperfusion (Frenette, 2002; Turhan, Weiss, Mohandas, Coller, & Frenette, 2002). Both reperfusion and ischemia cause oxidant stress that in turn activates inflammatory pathways, increasing the expression of endothelial adhesive molecules which increases inflammatory cytokines and leukocytosis (Rees et al., 2010; Turhan et al., 2002).

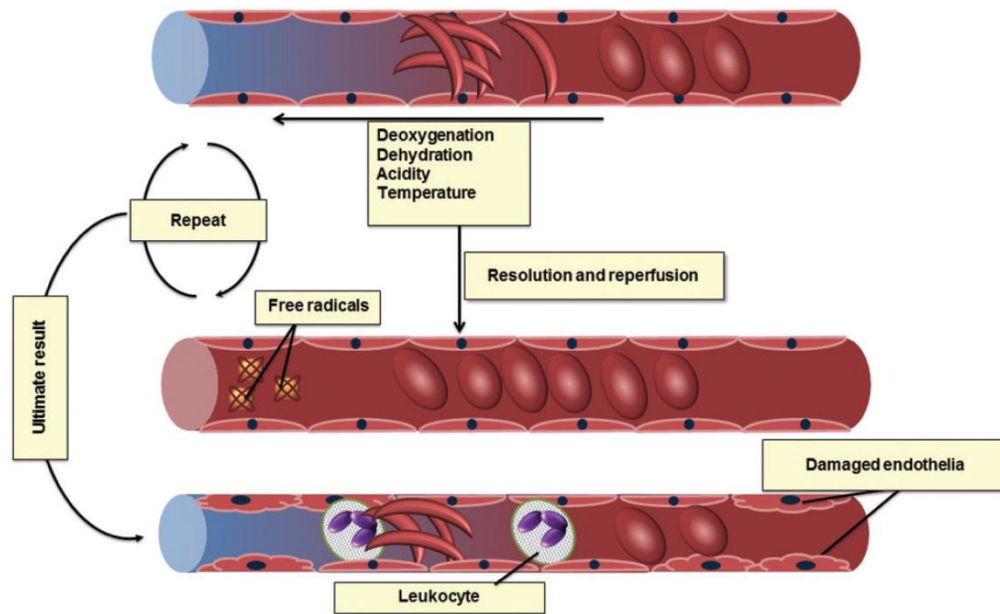


Figure 9: **Mechanism of sickle vaso-occlusion.** RBC damage and sickling occur as a result of polymerization of deoxy-HbS and also high concentrations of unpolymerized HbS, modulated by cellular contents of HbF, RBC cation and water content, pH, temperature, and mechanical stresses that result in membrane damage. Hemolytic anemia and vaso-occlusion cause tissue hypoxia; when this occlusion is resolved and perfusion is reestablished in the hypoxic tissue free radicals are produced. These free radicals damage the endothelial cells making them pro-adhesive for RBCs and leukocytes. The vascular wall ultimately becomes more vulnerable to occlusion (Habara & Steinberg, 2016).

Recent studies showed the critical role of neutrophil adhesion in vaso-occlusion, particularly in the first step. After this initial adhesion, neutrophils interact with circulating sickle RBCs leading to transient or prolonged obstruction of venular blood flow (Figure 10). Delayed cellular passage favors polymerization, sickling, and vaso-occlusion during microvasculature transit. Additional circulating cells (platelets, and “stress” reticulocytes i.e immature erythrocytes that are found in individuals with hemolytic disease) display adhesive ligands that facilitate erythrocyte-endothelial interactions.

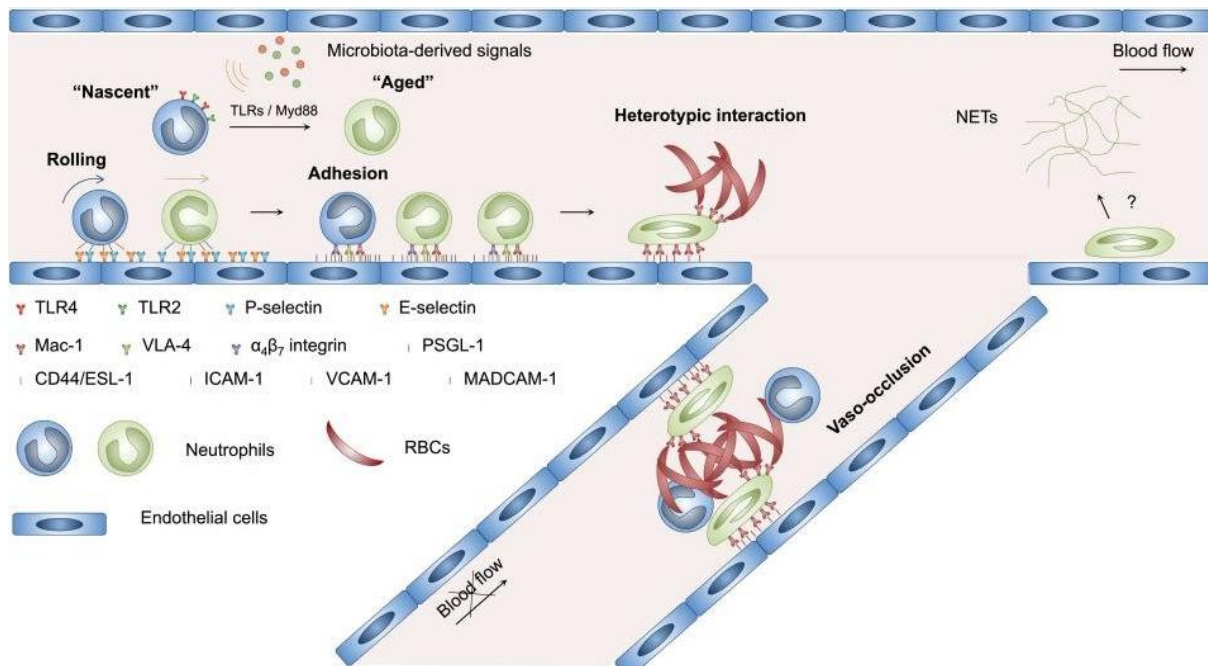


Figure 10: **Multicellular and multistep model of vaso-occlusion in SCD.** Sickle cell vaso-occlusion arises from a cascade of interactions among RBCs, neutrophils, and endothelial cells. Activation of endothelial cells, white blood cell (WBC) adhesion to the endothelium, SS RBC interaction with adhering WBCs, and progressive blockade (Zhang, Xu, Manwani, & Frenette, 2016).

B. Hemolytic anemia

Hemolysis leads to the release of hemoglobin into the circulation during intravascular hemolysis or within organs when it is extravascular. Hemolysis causes anemia in SCD patients together with other complications which include progressive vasculopathy, leg ulceration, priapism, stroke, glomerulopathy and pulmonary hypertension (Rees et al., 2010). It has been estimated that at steady state, hemolysis occurs mainly extravascularly (two-thirds) leading to erythrophagocytosis of dense, dehydrated and damaged SS RBCs by reticuloendothelial cells. However, red cell destruction can take place intravascularly (one-third), potentially releasing several grams of hemoglobin into the plasma daily, accounting for very little to up to 30% of total hemolysis (Steinberg, 2008; Wood, K. C., Hsu, & Gladwin, 2008).

Free plasma hemoglobin generates reactive oxygen species such as the hydroxyl ($\cdot\text{OH}$) and superoxide (O_2^-) radical and potent scavengers of nitric oxide (NO). NO is normally produced by the endothelium and regulates basal vasodilator tone, and inhibits platelet and hemostatic

activation and transcriptional expression of nuclear factor κ B (NF κ B)-dependent adhesion molecules. The release of hemoglobin into the plasma during hemolysis potently inhibits endothelial NO signaling, leading to endothelial cell dysfunction and NO resistance (Odievre et al., 2011).

Hemolysis also releases erythrocyte arginase-1 into plasma. Arginase metabolizes plasma arginine into ornithine, decreasing the substrate for NO synthesis and the bioavailability of NO. Thus the mechanism of NO depletion is double: destruction of NO by free Hb and reduced NO production by depletion of its precursor (Figure 11) (Odievre et al., 2011; Rees et al., 2010).

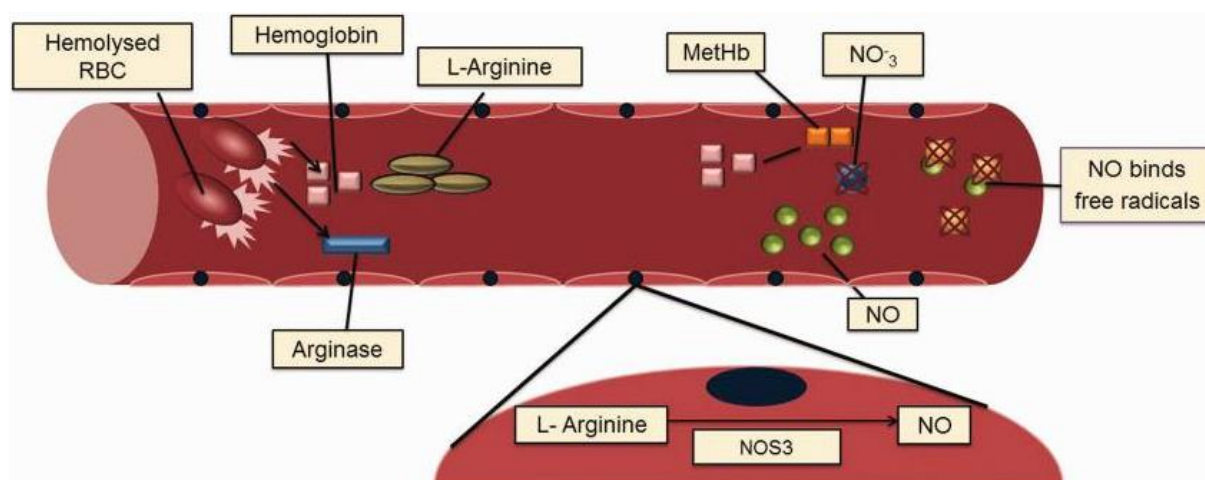


Figure 11: **Hemolysis-related endothelial dysfunctions.** With intravascular hemolysis, RBCs release hemoglobin and arginase. Arginine is the precursor for NO production by the endothelium via NOS3. Arginase degrades L-arginine, the NOS3 substrate, causing reduced NO production. Free plasma Hb interacts with NO producing methemoglobin and nitrate depleting NO. These mechanisms occur during steady state and the amount of intravascular hemolysis varies among patients (Habara & Steinberg, 2016).

1.3 Environmental and genetic modifiers of disease severity

The clinical expression of SCD is highly variable. Environmental factors can play a role in phenotypic variability of the disease. Previous studies have shown the effect of rainy season in tropical countries on episodes of acute pain and others have shown the effect of windy weather on increased occurrence of pain. However, more studies are required in this aspect (Jones et al., 2005; Redwood, Williams, Desal, & Serjeant, 1976; Rees et al., 2010). At the cellular level,

heterogeneity arises from differences in RBC intrinsic characteristics like heterocellular HbF distribution, HbS concentration (Serjeant, Serjeant, & Mason, 1977), hydration and density (Fabry et al., 1984; Noguchi, Torchia, & Schechter, 1983), and the cells environmental transitions from vessels to capillaries, laminar to turbulent flow, and normoxia to hypoxia (Kato, Gladwin, & Steinberg, 2007). Genetic modifiers play also a crucial role, the two best established genetic modifiers of SCD severity are fetal hemoglobin and α -thalassemia co-inheritance (Rees et al., 2010).

1.3.1 Fetal Hemoglobin

Fetal hemoglobin persistence in SCD patients has been very well established as a key point in amelioration of disease severity and prediction of increased life expectancy (John et al., 1984; Platt et al., 1994). HbF concentration in SCD patients can vary between 1% to 30% and it is inherited as a quantitative genetic trait. There are 3 major loci that have been identified that account for 50% variation in HbF expression; the Xmn1 polymorphism in the promoter gene of the G γ globin genes, the HMIP locus on chromosome 6q23.3 and BCL11A on chromosome 2 (Lettre et al., 2008; Menzel et al., 2007; Thein et al., 2007). Defining these loci has proven to be very important in gene therapy approaches for SCD patients.

In healthy adults, HbF accounts for less than 1% of total hemoglobin and is restricted to a small subset of RBCs (2%) called F-cells (Boyer, Belding, Margolet, & Noyes, 1975; Boyer et al., 1977; Wood, W. G., Stamatoyannopoulos, Lim, & Nute, 1975). In SCD the expression of HbF is higher than in healthy individuals and varies considerably among patients. Although the reasons of this increased expression are not completely elucidated, stress erythropoiesis and preferential survival of F-cells are known contributing factors (Stamatoyannopoulos, Veith, Galanello, & Papayannopoulou, 1985). As a matter of fact, it has been shown that F-cells survive longer in the circulation than non-F-cells (Dover, Boyer, Charache, & Heintzelman, 1978). This preferential survival of F-cells is also supported by studies showing that the

percentage of mature F-cells is higher than that of reticulocytes expressing HbF within the same SCD patient (Franco et al., 2006; Maier-Redelsperger, Elion, & Girot, 1998). But, HbF is unevenly distributed among F-cells and its cellular concentration needs to reach a minimal threshold to exert its protective polymer-inhibiting effect (Noguchi, Rodgers, Serjeant, & Schechter, 1988). The relationship between the expression level of HbF in F-cells and the impact on RBC morphology and survival is poorly understood.

1.3.2 *α-thalassemia*

The coinheritance of α -thalassemia with SCD improves hemoglobin levels, and results in a lower mean corpuscular volume (MCV), a lower mean cell hemoglobin concentration (MCHC), a reduction of the number of irreversibly sickled cells and a decrease in hemolysis (Piel et al., 2017). By decreasing the hemoglobin concentration in the red cells, α -thalassemia decreases the tendency of HbS polymerization and hence hemolysis rates. From a clinical perspective, α -thalassemia reduces the risk of stroke, pain frequency, leg ulcers, priapism and gall stones in SCD patients (Rees et al., 2010). α -thalassemia trait is present in up to 30% of SCD patients of African origin and more than 50% of patients from India and Saudi Arabia (Higgs et al., 1982; Kar et al., 1986; Padmos et al., 1991).

1.4 Treatments

Although SCD was discovered decades ago, treatments remain limited. Health and survival of children with SCD have improved considerably with the implementation of newborn screening, penicillin prophylaxis, pneumococcal immunization and education about disease complications. Erythrocyte transfusions, hydroxycarbamide treatment (also called hydroxyurea-HU) and hematopoietic stem-cell transplantation, and very recently gene therapy, are the options that can significantly improve survival and quality of life in SCD.

1.4.1 Hydroxycarbamide

Hydroxycarbamide (HC) is the first and major US Food and Drug Administration (FDA) approved drug for SCD patients, along with the more recent approval of L-Glutamine. In the European Union, HC was approved by the European Medicines Agency (EMA) to be given to both adults and children with SCD in 2007 (Ware & Aygun, 2009). HC is a ribonucleotide reductase inhibitor initially used as a myelosuppressive agent that provides therapeutic benefit in SCD patients through multiple mechanisms of action. HC principally increases HbF levels leading to a decrease in HbS intracellular concentration and inhibition of HbS polymerization (Chen, M. C. et al., 2015). The mechanism of action of HC for HbF induction remains however only partially understood. Hydroxycarbamide's primary effect by increasing HbF levels in treated patients is to decrease intracellular sickling, which in turn decreases vaso-occlusion and hemolysis (Ware & Aygun, 2009). Long term studies on HC have proven the benefit of HC on both children and adults by reducing both complications of the disease and mortality (Bakanay et al., 2005; Steinberg et al., 2003; Ware & Aygun, 2009). The use of HC began 25 years ago (Figure 12) and studies in children were initiated in the 1990s (Kinney et al., 1999; Wang et al., 2001).

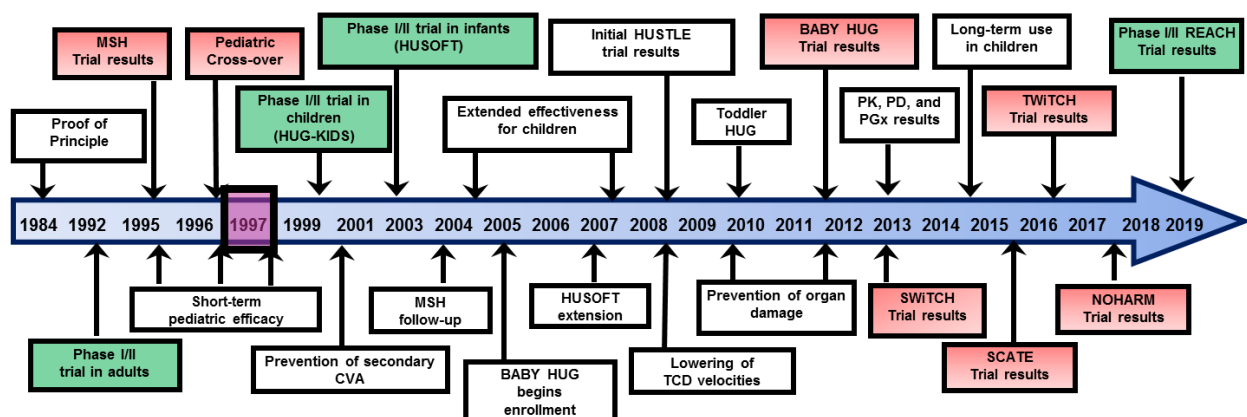


Figure 12: **Timeline of Hydroxycarbamide in clinical studies for the treatment of sickle cell disease** (courtesy of Dr. Russell Ware).

Growing evidence supports the fact that HC is a multi-target drug in SCD. Beyond HbF induction, the cytotoxic effects of HC also reduce the bone marrow production of neutrophils, reticulocytes, and platelets thus reducing important players of vaso-occlusion. At the cellular level, HC was shown to inhibit RBC adhesion to endothelial components by decreasing cAMP intracellular levels in RBCs (Bartolucci et al, Blood 2010) and endothelial cells (Chaar et al, J Biol Chem 2014) decreasing phosphorylation of adhesion molecules at the cell surface. In addition, the group of P. Frenette has shown that HC inhibits neutrophil adhesion to the vascular wall in a sickle mouse model of acute VOC by inhibiting their phosphodiesterase 9 (PDE9), increasing the levels of cGMP (Almeida et al., 2012). However, more studies are required to further explore the mechanisms of action of HC.

1.4.2 Blood Transfusion

Erythrocyte transfusion has a crucial role in the management of both acute and chronic complications of patients with SCD. Transfusion corrects anemia, decreases the relative percentage of sickle RBCs in the circulation and reduces hemolysis. All these effects are beneficial and have proven effective for the primary prevention of strokes and silent infarcts in children at risk. Erythrocytes can be given as a simple additive transfusion or by exchange. Exchange transfusion is more likely to be necessary if the initial Hb concentration is high, or if there is a need for a rapid decrease in HbS percentage without increasing the hematocrit and blood viscosity, typically in people with acute neurological symptoms. Chronic blood transfusion results however in iron overload, consequently iron chelation is mandatory in chronically transfused patients to avoid iron overload organ damage (Rees et al., 2010). Alloimmunization is another transfusion-related complication that occurs in 18 to 37% of transfused patients with SCD. The rate of sensitization decreases substantially when prophylactic antigen matching (PAM) is employed, even when patients are chronically transfused (Campbell-Lee et al., 2018; Rosse et al., 1990).

1.4.3 Hematopoietic stem cell transplantation

Hematopoietic stem cell transplantation (HSCT) was first used in SCD 25 years ago and is currently the only curative treatment for SCD. The goal is to successfully replace the host's bone marrow by a bone marrow from a healthy matched donor before development of organ dysfunction (Stuart & Nagel, 2004). However, its access is limited for several reasons, including donor availability and sociocultural and economic barriers, and it is only generally considered when serious complications have occurred, most often in children with cerebrovascular disease who are effectively dependent on transfusions. A recent study analyzed over 1000 HSCT performed with HLA matched related donors worldwide and demonstrated an overall survival of 92–94%, event-free survival of 82–86%, and a transplant related mortality of 7% (Gluckman et al., 2017).

The majority of HSCT has been performed in children from HLA-identical sibling donors resulting in high rates of survival (Khemani, Katoch, & Krishnamurti, 2019). Indeed, Gluckman et al. reported that the main predictors of event-free survival in HLA-identical HSCT were patients age and performance of HSCT after 2006 (Gluckman et al., 2017). The age of <15 years was reported as a significant determinant in the overall survival of patients (Bernaudin et al., 2007). An ongoing trial (NCT02766465, BMT CTN 1503), with estimated completion time in 2023, should provide results for the comparison of HSCT, Hydroxycarbamide and chronic blood transfusion in adolescents and young adults, thus giving a better perspective to the use of these different treatments (Khemani et al., 2019).

1.4.4 Gene therapy

Gene therapy has been considered a promising cure for SCD since the mid-1990s. Lentiviral vectors have been developed to insert γ -globin or modified β -globin genes engineered to reduce sickling into hematopoietic stem cells (Hoban, Orkin, & Bauer, 2016); these vectors are now in clinical trials and have yielded a promising initial result in 2017 in SCD. Ribeil and

collaborators published results of the first treated SCA patient, with lentiviral vector-mediated addition of an anti-sickling β -globin gene into autologous hematopoietic stem cells. Fifteen months after treatment, the level of therapeutic anti-sickling β -globin was high enough (approximately 50% of total β -like-globin chains) to correct the biologic hallmarks of the disease, with no recurrence of VOCs (Ribeil et al., 2017). Similar successful results with the same lentiviral vector have been reported recently in β -thalassemia (Thompson et al., 2018).

Newer gene editing approaches based on zinc-finger nucleases and transcription activator-like effector nucleases have been designed and tested for proof of principle in SCD. The development of CRISPR-Cas9 techniques, which enable the precise replacement of a specific region of DNA, is another promising gene therapy approach for SCD, currently tested only in mice and cultured human cells until the multiyear regulatory process is cleared for human trials (Kato et al., 2018).

For gene therapy or HSCT to be successful, an intact bone marrow and microenvironment in patients is required. However, the bone marrow content, precursor cells and the relationship with the stroma have very specific characteristics in patients with hemoglobinopathies, in particular in β -thalassemia. In β -thalassemia, anemia is both due to peripheral hemolysis and ineffective erythropoiesis which results in the bone marrow's impaired ability to produce terminally differentiated erythrocytes (Cavazzana, Ribeil, Lagresle-Peyrou, & Andre-Schmutz, 2017). Fewer studies have explored the bone marrow niche in SCD patients. Grasso et al. in 1975 performed an ultrastructural study of a bone marrow aspirate of an SCA patient which revealed the presence of hemoglobin S polymers in both reticulocytes and nucleated erythroblasts (Grasso, Sullivan, & Sullivan, 1975).

2 The human spleen

2.1 Structure and function of the spleen

The spleen is a combination of two main compartments, the red pulp and the white pulp, interconnected by the perifollicular zone that lies in between. These highly organized microanatomical structures serve the spleen's two main functions that are blood filtration and immune defense.

2.1.1 *The red pulp*

The red pulp represents the largest compartment of the spleen in humans (75%) and is mainly responsible for its filtering function. It is constituted of vascular structures, in particular specialized type of micro vessels called venous sinuses, in addition to classical capillaries, within a meshwork of cords. The cords are made of specialized fibroblasts and numerous macrophages lying upon a tridimensional network of reticular fibers, collagen type IV and laminin composing the extracellular matrix (Steiniger, B. S., 2015) (Figure 13).

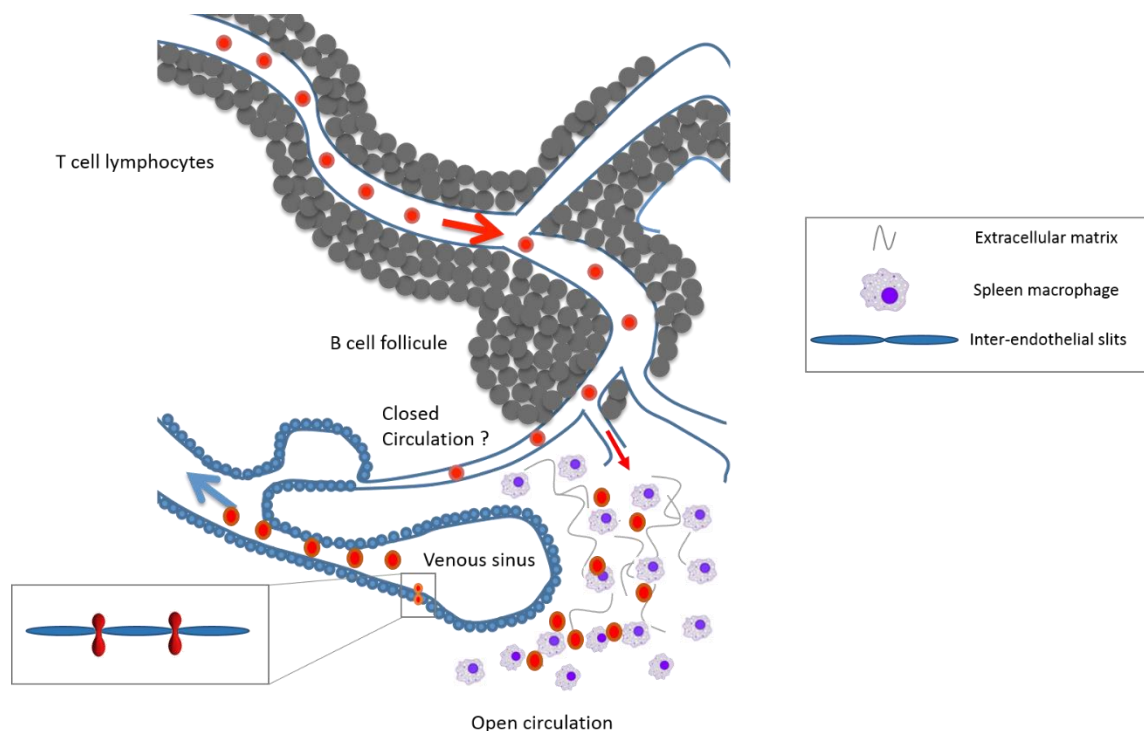


Figure 13: **Schematic diagram of the microcirculation in the human spleen.** A scheme showing the close cellular interaction in the filtering beds of the red pulp and the interendothelial slits that red blood cells need to squeeze through in order to join the venous circulation (El Hoss & Brousse, 2019).

The filtration in the red pulp is allowed by a unique microcirculation, which is termed open because when the arterial blood cells arrive into the cords of the red pulp, they exit their vascular endothelial-lined bed, thereafter flowing freely (Groom, Schmidt, & MacDonald, 1991; Steiniger, B., Bette, & Schwarzbach, 2011). Due to a high hematocrit (approximately 60%), blood cells not only percolate freely but also slowly, favoring a close and prolonged cell-cell contact (Figure 14). During these interactions, RBCs that are coated with antibodies or senescent or abnormally structured are cleared by the macrophages of the red pulp, thus giving the red pulp its erythrophagocytic characteristic (Mebius & Kraal, 2005). The collecting splenic sinuses, which will ultimately drain into portal veins, form a permeable vascular network with functional openings between the lining endothelial cells. These possibly dynamic slits, which are very narrow (1-3 μm wide), allow the passage of RBCs back to the venous circulation if they are deformable enough to squeeze through (Bowdler, 2002). During this vital checkpoint, an additional clearing process called pitting, allows the removal of unwanted material within

the RBCs (nuclear remnants or parasites for instance) while allowing the RBC to traverse. RBCs that are not deformable enough may be retained upstream of the sinus wall (Buffet et al., 2006; Safeukui et al., 2008) and thereafter phagocytized by specialized macrophages (Ganz, 2012). Consequently, if this checkpoint is altered, the removal of abnormal RBC, for example RBCs containing inclusion bodies, fails to happen and these are detected in the circulation. In splenectomized individuals or patients with a dysfunctional spleen like SCD patients, RBCs containing intracellular DNA remnants i.e. Howell-Jolly Bodies (HJB), are found in the peripheral blood (Sears & Udden, 2012).

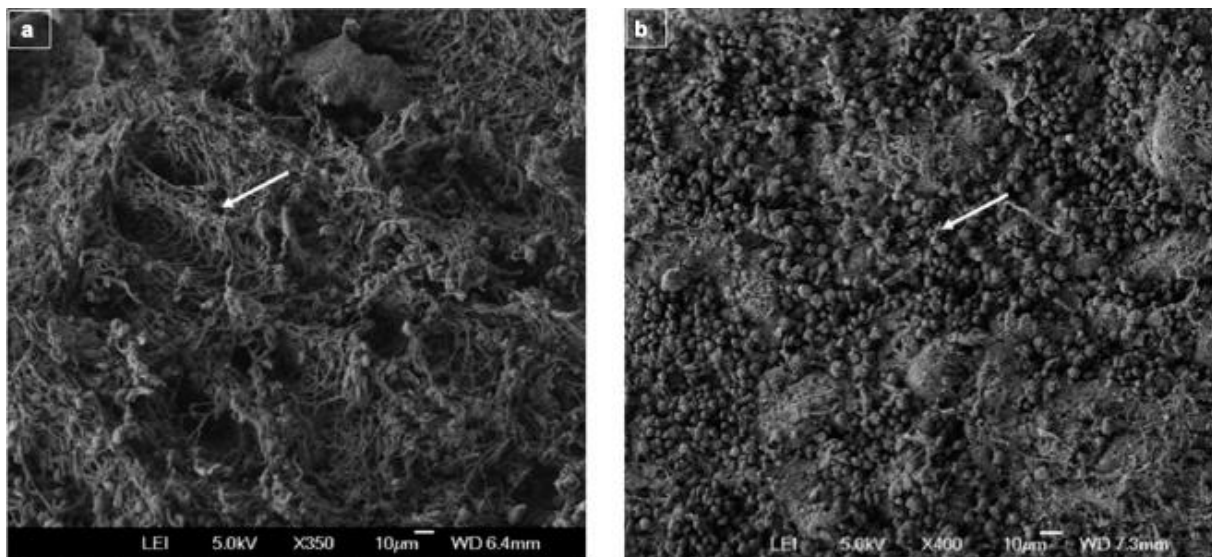


Figure 14: **Scanning electron microscopy micrograph of a spleen sample.** A scanning electron microscopy from a spleen of 5-year-old boy with sickle cell anemia showing the tridimensional reticular matrix of the red pulp (arrow). Bar = 10µm. B. Scanning electron microscopy micrograph of a spleen sample from a healthy adult showing red blood cells present in the filtering beds of the red pulp (arrow). Bar = 10µm (El Hoss & Brousse, 2019).

2.1.2 The white pulp

The white pulp of the human spleen consists of B lymphocytes found in the follicles and T lymphocytes mainly organized in sheaths surrounding arteries. B follicles are composed of a germinal center (GC) surrounded by a mantle zone. The GC consists of mainly B-cells and of T-cells in the periphery, very much like a lymph node structure (Steiniger, B. S., 2015). This compartment of the spleen is responsible for the recirculation and clearing of lymphocytes, and importantly, initiating an immune response for blood borne antigens. In particular, the follicular

B-cells initiate a T-cell dependent immune response, while IgM memory B-cells lining the mantle zone in the spleen initiate a T-cell independent response, critical for the phagocytosis of encapsulated bacteria, notably *Streptococcus pneumoniae*, *Neisseria meningitidis* and *Haemophilus influenza* (Booth, Inusa, & Obaro, 2010; Weller et al., 2004). Splenic dysfunction therefore leads to an increased susceptibility to encapsulated bacterial infections, notably pneumococcal infection. Indeed, T-independent clearance of polysaccharidic germs requires both an intact splenic filtration and an efficient opsonization by IgM antibodies.

2.1.3 The perifollicular zone

The perifollicular zone connects the white pulp and the red pulp. It is a zone of intense circulation and termination of many arterioles that open up in this area. Whether there exists within this zone an additional closed microcirculatory pathway that would allow pathogen or cellular escape from the filtering beds is still matter of debate (Steiniger, B. et al., 2011). Importantly, this zone is absent at birth in humans and becomes organized around 2 years of life, which explains the susceptibility to pneumococci in all very young children, let alone SCD (Steiniger, B., Barth, & Hellinger, 2001).

2.2 Measurements of spleen function

Assessment of spleen function has remained challenging up to date due to a relative lack of non-invasive, accurate and readily available tools to measure its specific filtering or immune function. Liver-spleen scintigraphic scanning has been and is possibly still the gold standard for assessing splenic function. This technique provides a qualitative and/or semi quantitative measurement of splenic function by evaluating the splenic uptake of either heat-denatured RBCs or nano colloids, labeled with technetium-99m (Ehrlich, Papanicolaou, Treves, Hurwitz, & Richards, 1982). While nanocolloids challenge the phagocytic ability of splenic macrophages, the heat-denatured RBCs challenge the mechanical filtration ability of the spleen (Adekile et al., 2002). Even though these techniques have proven reliable, they are time

consuming, invasive and not readily available. Counting of HJB-containing RBCs in circulation using May-Grunwald Giemsa staining on blood smears is one of the classical methods used to diagnose splenic dysfunction in clinical practice. This method is user-dependent and does not give exact percentages of HJB-containing RBCs because of the small number of counted cells (100-200 RBCs). Another similar commonly used method is to count “pitted” RBCs by interference contrast microscopy (Casper, Koethe, Rodey, & Thatcher, 1976). A flow cytometry-based method using propidium iodide (PI) was developed to count HJB-containing RBCs, a technique that requires cell fixation, RNA digestion steps and sample shipment to the laboratory (Harrod, Howard, Zimmerman, Dertinger, & Ware, 2007). Measuring spleen-related immune function is possible and relies on the peripheral blood analysis of splenic specific lymphocyte subsets, for instance IgM Memory B cells as a proportion of B cells. However, such analysis is time consuming, expensive and its clinical utility questionable as no discriminating threshold was associated with high sensitivity and specificity in a study that compared splenectomized patients with normal controls (Cameron et al., 2011).

3 The spleen in sickle cell disease

3.1 Early and progressive loss of spleen function

In sickling disorders, the spleen is an organ of early and major interaction. In SCA in particular, depending on the technique used, splenic loss of function is evidenced very early in infants. Pitted counts, for instance, were found in 23% of 130 homozygous infants at age 12 months, in 42% at age 24 months, and in 52% at age 36 months in a Jamaican cohort (Rogers, D. W., Serjeant, & Serjeant, 1982). Using a combination of HJB counts (quantified by flow cytometry), pitted cells and (99m) Tc sulfur-colloid liver-spleen scan in 193 infants 8 to 18 months of age, a more recent study demonstrated that loss of splenic function began before 12 months of age

in 86% of infants (Rogers, Z. R. et al., 2011). While this loss of function is a common feature in SCA, the age at which irreversible loss of the organ (autosplenectomy) occurs is variable, and reversal of splenic function with therapy has been described (see Appendix page 210). Without intervention, autosplenectomy, as evidenced by ultrasound scanning, was found in 35.7% of a cohort of 112 children with a means age of 12.3 years (range: 0 to 21) with SCD but in only 5% of children less than 5 years (Gale et al., 2016). In patients with other sickling genotypes (SC, S β +thalassemia for instance), spleen loss of function occurs later in life, and to a lesser extent than in patients with SCA (Lane et al., 1995).

3.1.1 Pathophysiology of SCD splenic damage

In patients with SCD, complications derive from both hemolysis and the entrapment of blood cells in small capillary networks causing vaso-occlusion and subsequent downstream ischemic damage. In the spleen however, the precise mechanism whereby damage occurs is not completely understood: in the splenic red pulp, RBCs are not contained in capillaries so that classical vaso-occlusion does not occur. The red pulp is instead congested by RBCs, implying an active flow rather than an upstream blockade (Figure 15). The term vaso-occlusion is therefore inappropriate when considering splenic damage. Congestion is most probably caused by sickle RBCs main characteristics, i.e. markedly reduced deformability and increased adhesion properties, favored by the splenic environment: slow transit time, high hematocrit, high concentration of specialized clearing macrophages. It is possible that an additional systemic signal (infectious for instance) may trigger further congestion. Consequences include hemorrhage followed by inflammation and fibrosis. Hypothetically hemodynamic diversion of RBCs towards other circulatory pathways shunting blood away from the filtration beds may occur. In addition, repeated acute or chronic hemolysis may result in low-grade iron deposit, inflammation and fibrosis. Up to date, however, there is no clear sequence of events or repeated pattern that may unequivocally explain the natural history of splenic pathological changes.

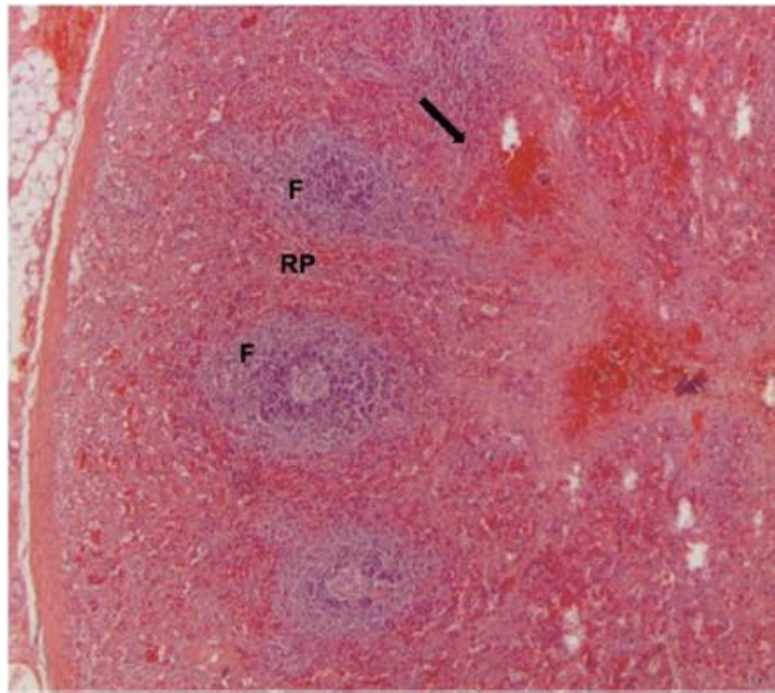


Figure 15: **Hematin eosin saffron-stained spleen sample of an SCD child.** Hematin eosin saffron-stained spleen following splenectomy for recurrent acute splenic sequestration in a 5-year-old girl with sickle cell anemia, showing intense red blood cell congestion or hemorrhage (black arrow). RP: Red pulp. F: Follicle. Original magnification x100 (El Hoss & Brousse, 2019).

3.2 Consequences of loss of spleen function

In SCD, splenic loss of function is the natural fate. Functional or anatomical asplenia is a common feature in sickling disorders although its onset may vary across genotypes and environments. Loss of spleen function results in an increased infectious susceptibility to encapsulated bacteria, first of all *Streptococcus pneumonia* (Booth et al., 2010). In high-income settings, the increased risk of invasive pneumococcal infection is well tackled by early diagnosis, penicillin prophylaxis, pneumococcal immunization and aggressive antibiotic treatment, so that infection-related mortality in childhood has drastically decreased (Gaston et al., 1986; Quinn, Rogers, McCavit, & Buchanan, 2010). By contrast, in sub Saharan Africa, where over 300,000 babies with sickling disorders are born annually, more than half of them will die by age 5 with infection and malaria being presumably the major contributors (Grosse et al., 2011; Ramakrishnan et al., 2010).

3.3 Clinical manifestation of the spleen

While splenic loss of function in SCD is in the majority of cases clinically silent, acute or chronic splenic complications may also occur which include acute splenic sequestration (ASS), splenomegaly and hypersplenism. These occur with a variable incidence, depending on age, genotype and various protective biological and genetic factors.

3.3.1 *Acute splenic sequestration*

Acute splenic sequestration (ASS) results from a brutal trapping of RBCs in the spleen. It is defined by the sudden enlargement of the spleen with an acute drop of Hb level $> 2\text{g/dL}$. The classic clinical signs are splenomegaly, abdominal pain and tenderness, pallor, and irritability or pain. ASS occurs in approximately 7 to 30% of infants with SCA (Brousse et al., 2012; Powell, Levine, Yang, & Mankad, 1992; Topley, Rogers, Stevens, & Serjeant, 1981). ASS is one of the earliest life-threatening complications seen in patients with SCD. Such a complication has been reported in a 5-week old and 4-month old (Airede, 1992; Walterspiel, Rutledge, & Bartlett, 1984). The median age range for this complication is between 6 months and 5 years, with a median age of 1.4 years in a French cohort study (Brousse et al., 2012). Predictive factors are still unknown.

Over 2/3 of infants (67%) experience more than one ASS episode, with a higher risk when ASS occurs before the age of 2. Precipitating factors are largely unknown although an infectious triggering event is often associated. Studies have reported an association between the occurrence of a parvovirus B19 infection and ASS and highlighted the need to monitor patients with an active parvovirus B19 infection for ASS episodes (Emond et al., 1985).

Despite the expected decline in spleen function with time, ASS, which presumably requires an active spleen to occur, has also been described in older patients, both in SCA and SC disease,

with a higher risk of a fatal outcome given the difficulty of recognition in adult patients (Naymagon, Pendurti, & Billett, 2015).

While there is a wide spectrum of severity, urgent treatment based on top-up transfusion or red blood cell exchange is mandatory as transfusion delay can lead to hypovolemic shock and death from acute anemia. ASS was considered as the second cause of death after infections in the first decade of life but ASS-related mortality has decreased in the last years in areas where neonatal screening is available and parental awareness allows prompt medical assistance in case of ASS (Emond et al., 1985; Powell et al., 1992; Telfer et al., 2007).

3.3.2 *Splenomegaly*

Splenomegaly is presumably the result of moderate trapping of rigid RBCs and translates into a limited enlargement of the spleen with no or very mild hematological consequences. Its prevalence is variable depending on genetic and environmental determinants. In a Jamaican setting, splenomegaly reached its highest incidence in the first year of life in patients with SCA, followed by progressive decrease (Rogers, D. W., Vaidya, & Serjeant, 1978). More recently, in the US, spleen volume assessed by ultrasonography in a large cohort of infants aged 7.5-18 months showed a mean volume significantly greater than normal age-matched controls (McCarville et al., 2011). Genetic modifiers of disease severity such as co inheritance of α -thalassemia or β -globin haplotypes associated with high HbF levels prolong spleen function and hence in certain cases splenomegaly to adulthood (Alsultan et al., 2014; Chopra, Al-Mulhim, & Al-Baharani, 2005; Embury, Clark, Monroy, & Mohandas, 1984).

Conflicting results about spleen size and function have been published. Increased pitted cells and HJB-containing RBCs together with decreased scintigraphic uptake have been reported in SCD patients suffering from an enlarged spleen, a finding that gave rise to the concept of functional asplenia i.e. a palpable spleen with decreased function (Pearson, Spencer, & Cornelius, 1969a). However, other studies show a significant inverted relationship between

pitted RBC count and spleen size (Adekile et al., 1993). It is now considered that there is no relationship between spleen size and function so that splenomegaly can result in either a normal or a decreased function (McCarville et al., 2011).

3.3.3 *Hypersplenism*

Hypersplenism is the consequence of chronic blood sequestration in the spleen with subsequent cytopenia. It occurs when the spleen is chronically enlarged and probably partly fibrotic, preventing it from shrinking back to a normal size, notably after transfusion. Hypersplenism has overlapping features with ASS or splenomegaly so that the diagnosis may sometimes be difficult and consequently the exact prevalence ill-defined. Like splenomegaly, hypersplenism has a higher frequency in patients with high HbF levels and co-inheritance of α -thalassemia (Singhal, Thomas, Kearney, Venugopal, & Serjeant, 1995).

4 Erythropoiesis

4.1 Developmental waves of erythropoiesis

During mammalian embryonic development, hematopoiesis occurs in three distinct waves. Most studies of this process have been done in mice by the groups of Palis and Yoder. In mice, the first wave of hematopoiesis, known as the primitive wave, is observed at embryonic day 7.5. During this stage primitive erythroblasts (nucleated megaloblastic erythroblasts) and platelet progenitor cells and macrophages are produced (Potts et al., 2014). During the second hematopoietic wave, erythro-myeloid progenitors (EMPs) develop at day 8.25 in the yolk sac. At this stage EMPs migrate from the yolk sac to the liver to produce erythroblasts (McGrath et al., 2011). At day 10.5, the third wave of hematopoiesis starts yielding hematopoietic stem cells (HSCs) which emerge from the hemogenic endothelium, known to be located in the umbilical, vitelline, cranial, yolk sac and placental region (Yoder, 2014). At this stage HSCs migrate to

the liver to undergo expansion before moving to the bone marrow where they are known to remain in an inactive state (Kiel et al., 2007). Of note, studies have shown that mutant mice unable to produce HSCs remain alive during embryonic stage via the EMPs (Figure 16) (Chen, M. J. et al., 2011).

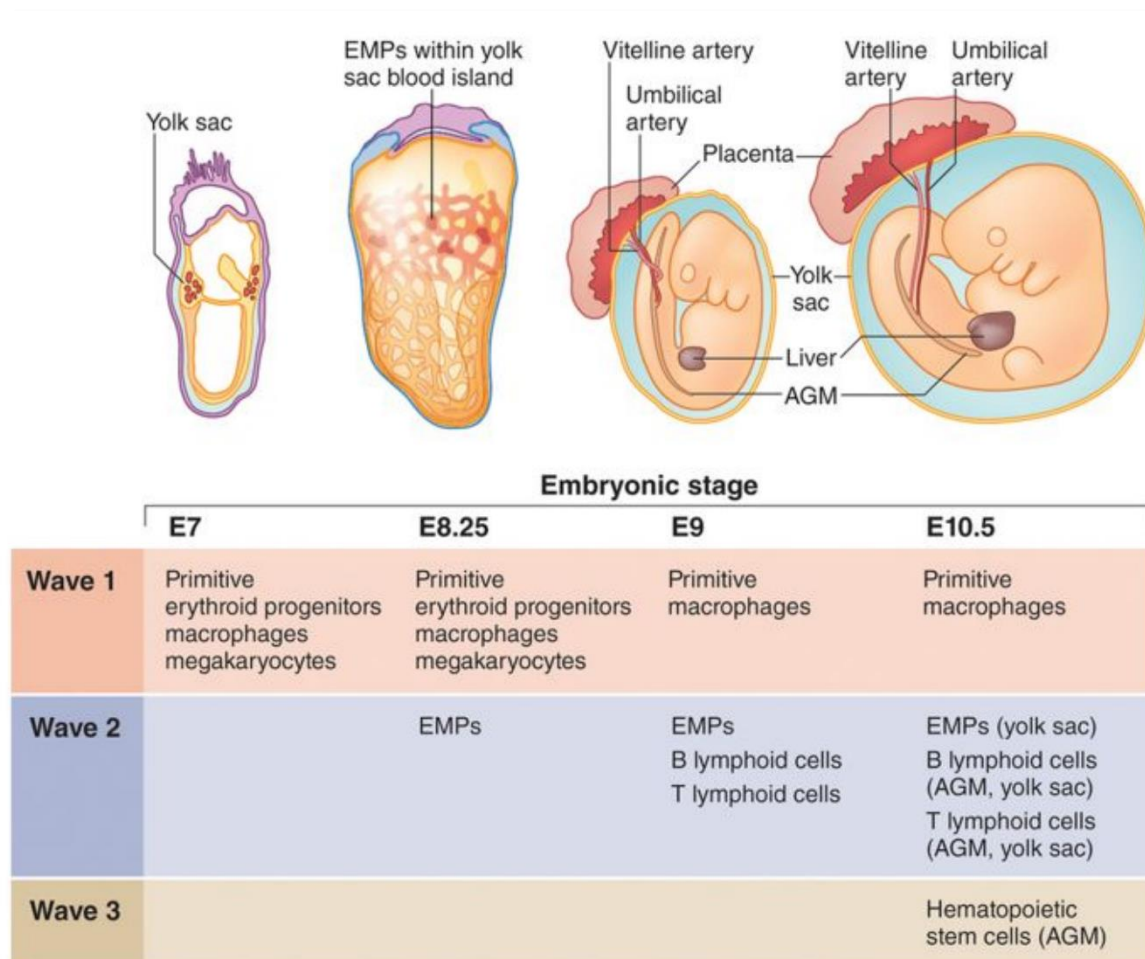


Figure 16: **The developmental waves of erythropoiesis** (Yoder, 2014).

4.2 Human erythropoiesis at steady state

Human erythropoiesis is a complex multi-step process that takes place in the bone marrow in adults, starting from a multipotent HSC and ending with an enucleated reticulocyte that exits the bone marrow and matures in the circulation to become an erythrocyte (Orkin, 2000). Erythropoiesis starts with an engagement phase, where HSCs give rise to the common myeloid

progenitors (CMPs) (Figure 17) (Orkin, 2000). The CMPs differentiate into the bipotent megakaryocytic-erythroid progenitors (MEPs) that have potential to form erythroid or megakaryocytic (Gregory & Eaves, 1977).

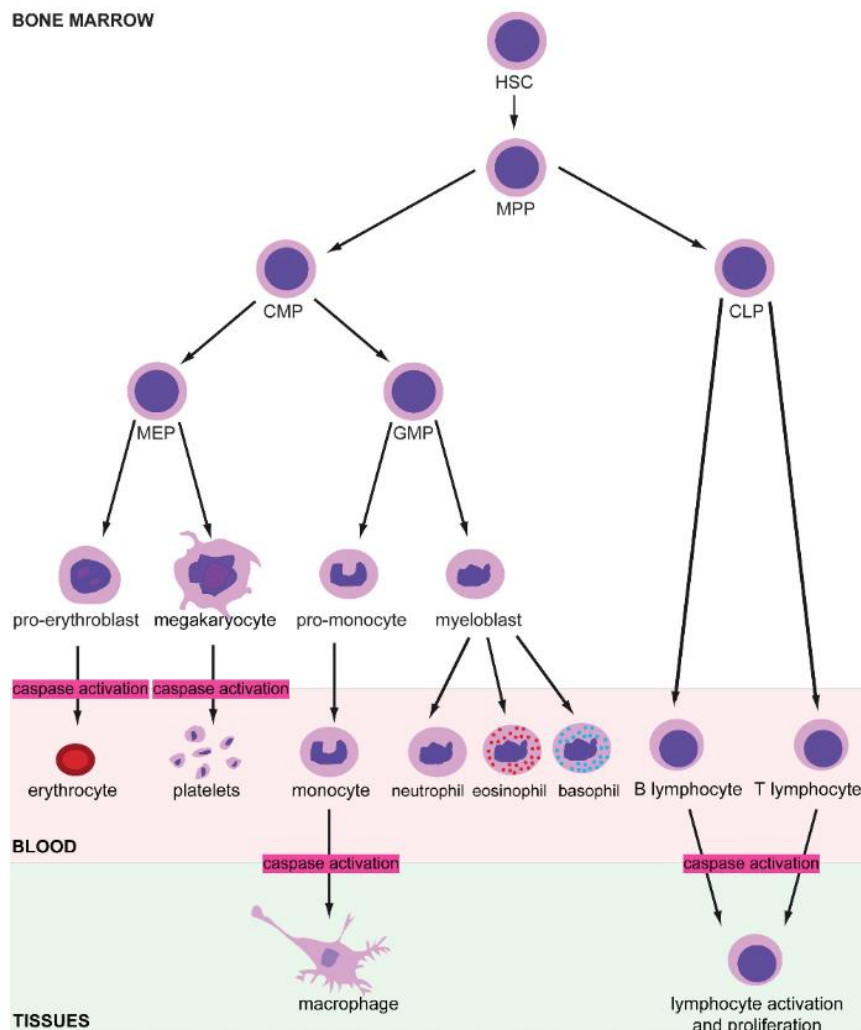


Figure 17: **Human hematopoiesis.** Hematopoietic stem cells can give rise to either common lymphoid or common myeloid progenitors. The myeloid progenitors are responsible for red cell formation (Solier, Fontenay, Vainchenker, Droin, & Solary, 2017).

Burst-forming unit-erythroid (BFU-E) are the first committed progenitors to the erythroid lineage downstream of the MEPs, that further differentiate into colony-forming unit-erythroid (CFU-E) (Gregory & Eaves, 1977). The CFU-E then enter the second phase of differentiation,

also called terminal differentiation, where the proerythroblast sequentially differentiates into basophilic, polychromatic and orthochromatic erythroblast. During the terminal phase hemoglobin is synthesized and nucleus condensation occurs, thus facilitating the enucleation process and giving rise to the reticulocyte, the immature erythrocyte (Granick & Levere, 1964). The reticulocyte exits the bone marrow and matures into the erythrocyte, the biconcave red blood cell. This mature red blood cell circulates in the bloodstream for a period of 120 days before being eliminated by the macrophages in the reticuloendothelial system (Figure 18) (Gifford, Derganc, Shevkoplyas, Yoshida, & Bitensky, 2006).

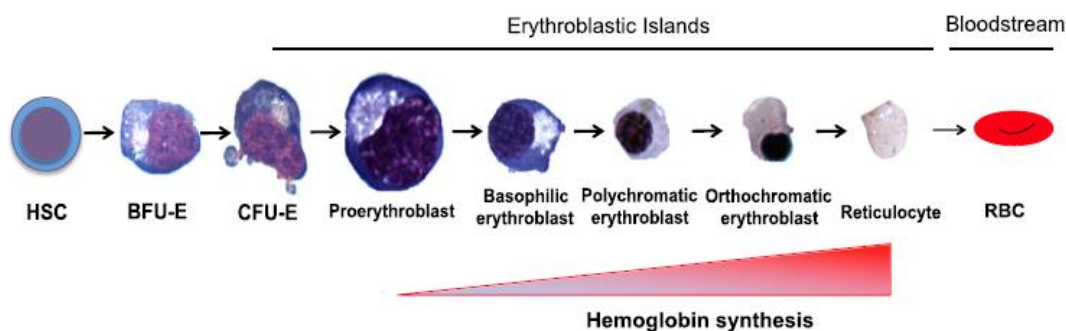


Figure 18: **Human erythropoiesis, for the hematopoietic stem cell to the mature red blood cell (RBC).** The differentiation from CFU-E to the reticulocyte takes place in the erythroblastic islands in the bone marrow niche (Zivot, Lipton, Narla, & Blanc, 2018).

4.3 The erythroblastic island

Mammalian erythroid differentiation occurs in specific niches in the bone marrow known as erythroblastic islands. These islands are constituted by one or two central macrophages surrounded by various erythroid cells at different stages of differentiation (Figure 19) (Lee et al., 1988). The central macrophage often does not have a round or oval shape but rather a star shape with very thin cytoplasmic extensions (Bessis & Breton-Gorius, 1962). The central macrophage plays a critical role in erythropoiesis, acting as an anchor to the erythroblasts providing cellular interactions required for differentiation and proliferation. Moreover, this macrophage is capable of phagocytosis of the extruded nuclei from terminally differentiated

erythroblasts (Seki & Shirasawa, 1965; Skutelsky & Danon, 1972). The central macrophage also plays a crucial role in heme synthesis as it directs the transfer of iron to the erythroid progenitors (Bessis & Breton-Gorius, 1962). Moreover, these erythroid niches are in a hypoxic microenvironments with an oxygen level between 1-7% (Mohyeldin, Garzon-Muvdi, & Quinones-Hinojosa, 2010; Yeo, Cosgriff, & Fraser, 2018).

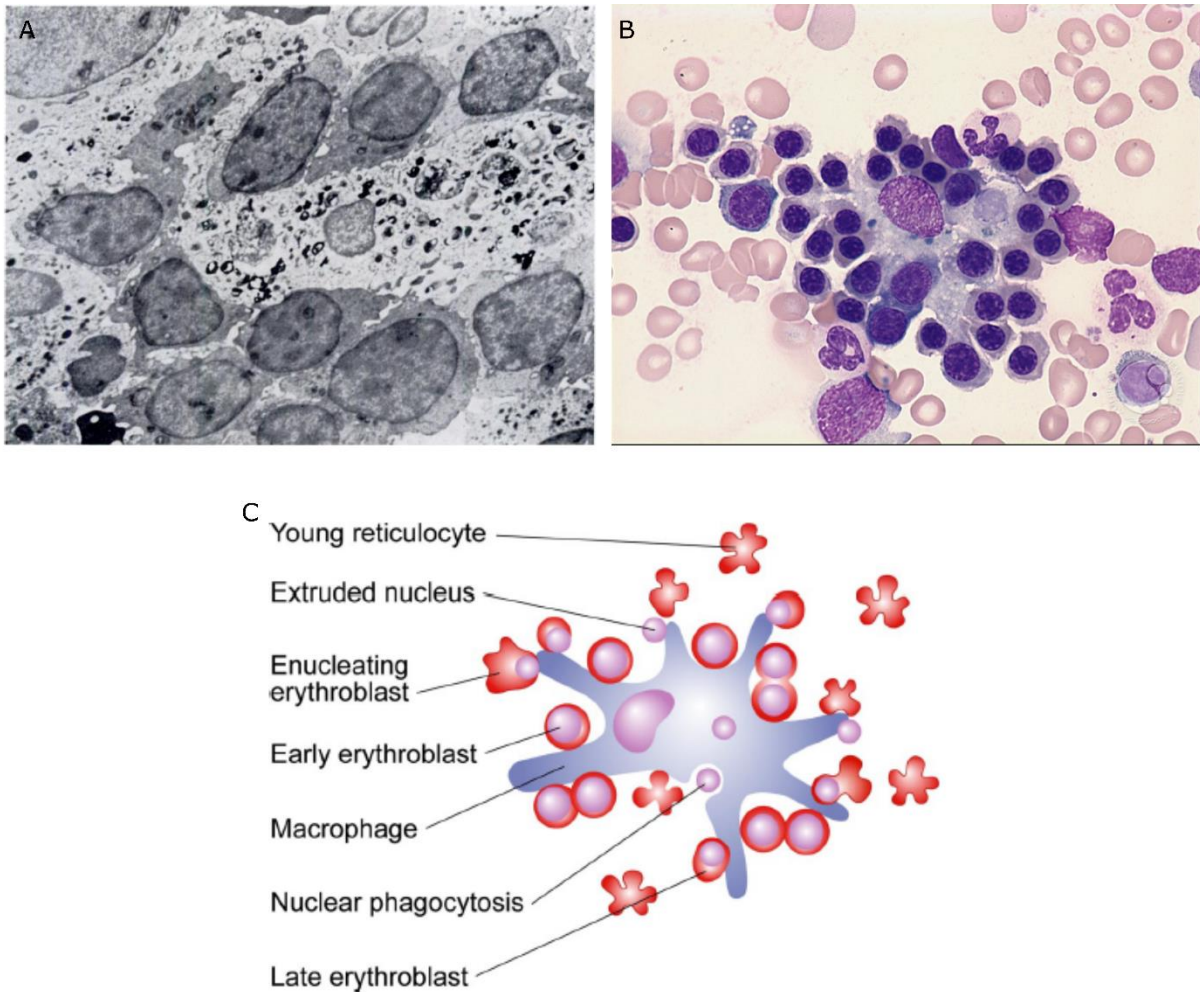


Figure 19: **The erythroblastic island.** (A) Electron microscopy image of erythroblasts surrounding the central macrophage which is seen to be containing some phagocytized inclusions (Bessis & Breton-Gorius, 1962). (B) May Grunwald Giemsa staining of an erythroblastic island (Author: Peter Maslak, Copyright © 2019 American Society of Hematology). (C) An illustration of the erythroblastic island with the star shaped central macrophage and early erythroblasts, late erythroblasts and enucleated reticulocytes (Chasis & Mohandas, 2008).

4.4 Regulation of erythropoiesis

The process of erythropoiesis is known to be mainly regulated by the humoral cytokine Erythropoietin (EPO). EPO is synthesized by the kidney and secreted in the blood stream where it targets erythroid progenitors in the bone marrow (Broxmeyer, 2013).

EPO is the primary mediator of hypoxic induction of erythropoiesis. During fetal development EPO is mainly produced by the liver while following birth the kidney accounts for 80% of EPO production. Hypoxia induces an increase in EPO production by the kidney, which in turn circulates in the plasma and binds to the EPO receptor which is abundantly expressed on erythroid progenitor cells, hence promoting viability, proliferation and terminal erythroid differentiation and ultimately increasing the red cell mass. The oxygen carrying capacity of the blood is therefore enhanced, increasing tissue oxygen tension and completing the feedback loop to suppress EPO production (Bunn, 2013) (Figure 20).

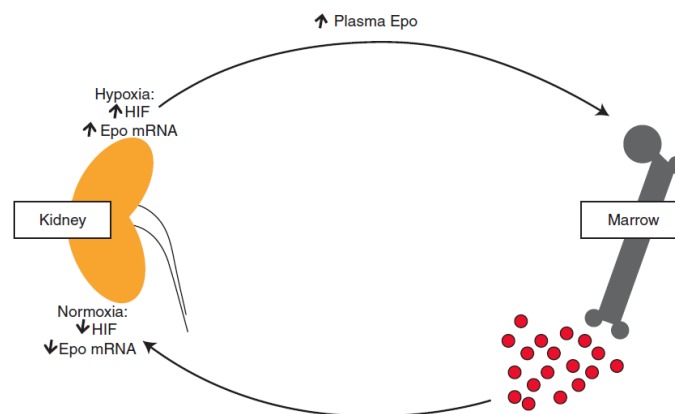


Figure 20: **Regulation of red cell production by EPO** (Bunn, 2013).

Both hypoxia inducible factor (HIF), which is regulated by hypoxia, and GATA binding proteins are involved in the process of EPO regulation. GATA-1, 2 and 3 have been shown to down-regulate EPO mRNA expression by binding to the EPO promoter region (Imagawa, Yamamoto, & Miura, 1997).

EPO-induced intracellular signaling during erythropoiesis is initiated by the binding of EPO to the Epo receptor (EPOR), a process that takes place from the CFU-E to the polychromatic stage (Wojchowski, Sathyanarayana, & Dev, 2010; Wu, H., Liu, Jaenisch, & Lodish, 1995). The binding of EPO to EPOR initiates the activation of the Janus kinase 2 (JAK2) and signal transducer and activator of transcription STAT5 pathway that plays a pivotal role in erythroid progenitor survival, proliferation and differentiation (Neubauer et al., 1998; Parganas et al., 1998). During erythroid differentiation, transcription factors GATA-1 and GATA-2 play an important role in the regulation of lineage-restricted gene expression. GATA-2 is required for the conservation and proliferation of hematopoietic stem and progenitor cells while GATA-1 is required for the terminal erythroid differentiation. Thus, a balance between GATA-1 and GATA-2 expression is critical throughout erythropoiesis to drive erythroid differentiation and the expression of the β -globin genes (Moriguchi & Yamamoto, 2014).

Caspase 3 is vital during erythroid differentiation, its signaling function begins at the late BFU-E stage, playing an important role in the expression of erythroid genes and of anti-apoptotic genes (Boehm et al., 2013; Krauss et al., 2005). Caspase-3 is thus transiently activated during erythroid differentiation and cleaves proteins that may prepare expel of mitochondria and enucleation by reticulocytes (Solier et al., 2017). Caspase 3 targets cells that strongly express the EPOR, and it is also known to play an important role in the GATA-1 signaling pathway (Boehm et al., 2013; Gregoli & Bondurant, 1999). Studies have shown that GATA-1 is protected from caspase-3 cleavage during terminal differentiation through its interaction with the chaperon Heat Shock Protein 70 (HSP70) (Ribeil et al., 2007). For this protection to occur, HSP70, which is expressed mainly in the cytoplasm, is translocated from the cytoplasm to the nucleus. This translocation takes place in the presence of EPO, with EPO depletion driving HSP70 nuclear export to the cytoplasm, GATA-1 cleavage and subsequent apoptosis (Figure 21).

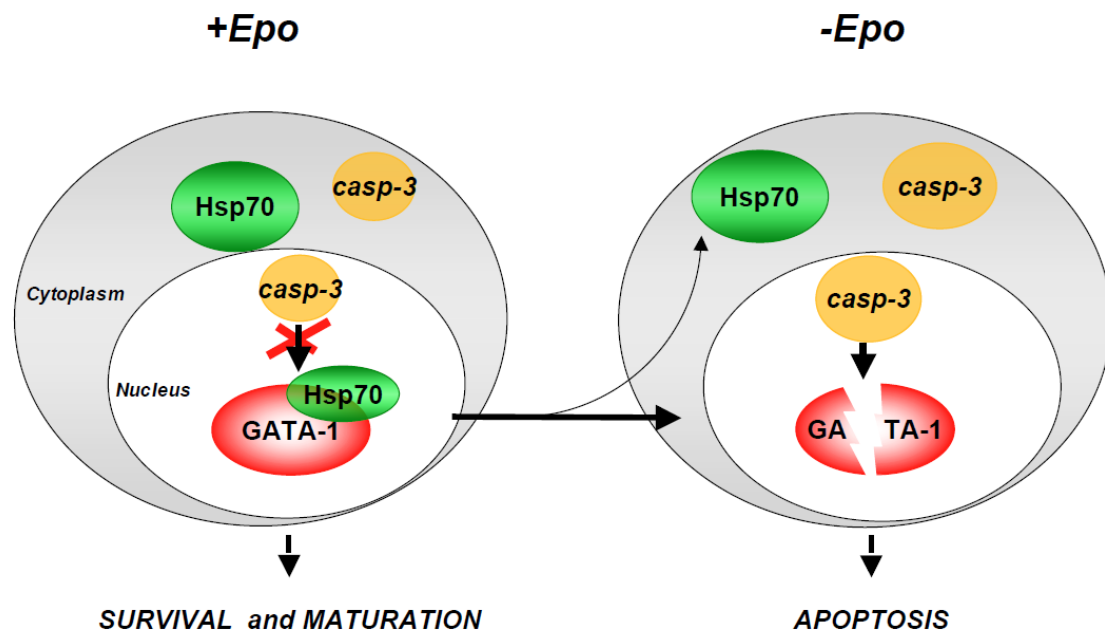


Figure 21: **GATA-1 protection by HSP70 during terminal erythroid differentiation** (Ribeil et al., 2007).

4.5 *Ex vivo* culture systems of erythropoiesis

For a better understanding of erythropoiesis and its pathologies, an *ex vivo* culture system is required. *Ex vivo* erythropoiesis can be established from different sources, such as hematopoietic progenitors isolated from peripheral blood or cord blood samples, human embryonic stem cells (ESCs) or induced pluripotent stem cells (iPSCs) (Giarratana et al., 2011; Palis, 2008; Tanavde et al., 2002).

The choice of an *ex vivo* culture system depends highly on the aim of the study. The focus of a study can be centered upon either a synchronous differentiation to specifically examine the different stages of erythropoiesis or a high final yield of reticulocytes, regardless of maintaining a synchronized system (Severn & Toyne, 2017). To achieve one of the above aims different *ex vivo* cultures containing different cytokine mix have been developed (Table 1).

Table 1: **The expansion rates and enucleation rates of different erythropoiesis protocols** (Severn & Toye, 2017)

Source and culture period	General protocol	Expansion	Enucleation rate	Key points	References
CB CD34 ⁺ 21 days	Three stage, serum free	2×10^5 fold	4%	Low enucleation rate	Neildez-Nguyen 2002
Peripheral blood MNC 13 days	HEMA culture	1×10^3 fold	–		Migliaccio <i>et al.</i>
Mobilized leukapheresis CD34 ⁺ 21 days	Three stage with co-culture	1.22×10^5 fold	98%	First co-culture with murine stromal cells	Giarratana <i>et al.</i> 2005
CB MNC, 60 days	Two stage, serum free	1×10^9	~100%	Prolonged expansion period	Leberbauer <i>et al.</i> 2005
CB CD34 ⁺ 20 days	Four stage	7×10^6 fold	77%		Miharada <i>et al.</i> 2006
CB MNC 21 days	Three stage, serum free with co-culture	8.2×10^3 fold	47%	Higher expansion rates when CB feeder cells used not BM feeder cells	Baek <i>et al.</i> 2008
Peripheral blood MNC	Three phase	3×10^8	80–90%	CD34 ⁺ population is important for expansion	van den Akker 2010
CB 33 days	Two stage	2.3×10^8	>90%	First demonstration of bioreactor use	Timmins <i>et al.</i> 2011
Peripheral blood MNC 14 days	HEMA culture	2.7×10^9	–	CFU and flow cytometry analysis	Tirelli <i>et al.</i> 2011
Peripheral blood CD34	Three stage	6.15×10^4 fold	68%	2.5 ml packed reticulocytes and transfusion of <i>in vitro</i> cultured reticulocytes	Giarratana <i>et al.</i> 2011
Peripheral blood CD34	Three stage	$>10^4$ fold	55–95%	5 ml packed reticulocytes	Griffiths <i>et al.</i> 2012
Peripheral blood CD34	Three stage	$>10^5$ fold	63%	10 ml packed reticulocytes under GMP conditions	Kupzig <i>et al.</i> 2017

Different laboratories have developed *ex vivo* culture protocols with various culture stages (Table 1). Principally a primary stage includes stem cell factor (SCF), interleukin-3 (IL-3) and erythropoietin (EPO), a secondary phase includes SCF, EPO and transferrin and the latter is followed by a terminal phase including EPO and holotransferrin (Severn & Toye, 2017). Alternatively, some laboratories include interleukin-6 (IL-6) in the first stage, to increase expansion prior to differentiation (Fibach, Manor, Oppenheim, & Rachmilewitz, 1989). The latter has proven useful in *ex vivo* culture of progenitors derived from patients with hematological pathologies, where isolation of progenitor cells is difficult (Reihani *et al.*, 2016).

4.6 Monitoring of erythropoiesis

To study erythropoiesis, it is important to be able to isolate erythroid progenitors and erythroblasts at different stages of development. To date, considerable progress has been made in the techniques focused on isolation and characterization of erythroid progenitors and erythroblasts using fluorescence-activated cell sorting (FACS)-based methods. The group of Mohandas Narla developed a FACS-based method using the expression of membrane proteins to distinguish between erythroblasts in the terminal erythroid differentiation. They identified that during erythroid differentiation the expression of the major red cell proteins increased while the expression of adhesion molecules decreased. More specifically they identified that the expression of both Glycophorin A (GPA) and Band 3 increased during erythroid differentiation, while the expression of $\alpha 4$ integrin decreased. Using these markers they developed a method to isolate highly purified populations of erythroblasts both *in vivo* and *in vitro* (Figure 22) (Hu et al., 2013).

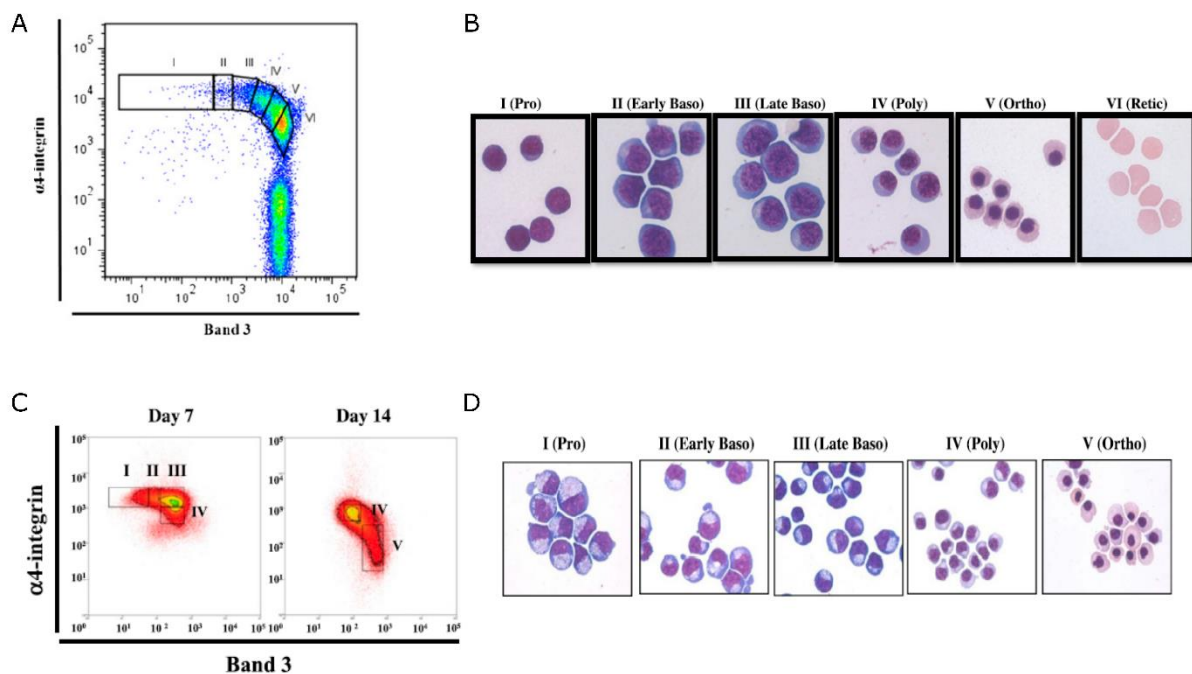


Figure 22: **Flow cytometry analysis for the isolation of human erythroblasts.** CD45- cells isolated from primary human bone marrow were stained for GPA, $\alpha 4$ integrin and band 3. (A) Plot of band 3 and $\alpha 4$ integrin of GPA positive cells. (B) Representative images of the sorted cells gated in A. (C) Invitro cultured erythroblasts stained with GPA, $\alpha 4$ integrin and band 3. (D) Representative images of erythroblasts morphology for the 6 distinct regions represented in C (Hu et al., 2013).

4.7 Ineffective erythropoiesis in erythroid disorders

Some erythroid disorders have known defects in erythroid differentiation, known as dyserythropoiesis defects, such as thalassemia syndromes, while others such as SCD have less characterized but the circulating red cells have defective function

4.7.1 *Ineffective erythropoiesis in hemoglobinopathies*

A. *α -thalassemia and β -thalassemia*

α -thalassemia is known to cause a reduction or absence in the α -globin chains leading to excess β -chains that form a precipitate within the developing red cell. These excess β -chains form tetramers in adults thus leading to hemolytic anemia and ineffective erythropoiesis. α -thalassemia patients have variable degree of anemia, the latter depending on the number of non-functional alpha globin genes (Kan & Nathan, 1968; Kan & Nathan, 1970).

β -thalassemia's are a group of recessive autosomal inherited disorders characterized by moderate to severe anemia because of altered or absent production of β -chain. In β -thalassemia, mutations in the β -gene create an imbalance between α and β -chains leading to the accumulation of α -tetramers in the cytoplasm. In β -thalassemia there are a multiplicity of different genetic mutations that give rise to a heterogeneous spectrum of clinical expression ranging from mild anemia to transfusion dependence. (Ribeil et al., 2013). Ineffective erythropoiesis is a characteristic of β -thalassemia, with high levels of apoptotic erythroblasts during the late stages of terminal differentiation, when there is marked increase in hemoglobin synthesis (Arlet et al., 2014; Arlet, Dussiot, Moura, Hermine, & Courtois, 2016; Rivella, 2009). Ineffective erythropoiesis is the major cause of anemia in β -thalassemia patients.

A recent study conducted in severe β -thalassemia patients (with no β -chain expression), demonstrated that HSP70 interacts directly with the free α -globin chains resulting in its

cytoplasmic sequestration (Arlet et al., 2014). As a consequence, GATA-1 is not protected from caspase-3 cleavage, which leads to end-stage maturation arrest and apoptosis in differentiating precursors, which causes anemia (Arlet et al., 2014). The resulting anemia induces a compensatory activation of erythropoiesis leading to increased proliferation of the erythroid progenitors in the bone marrow and resulting in medullary expansion (Figure23) (Arlet et al., 2016).

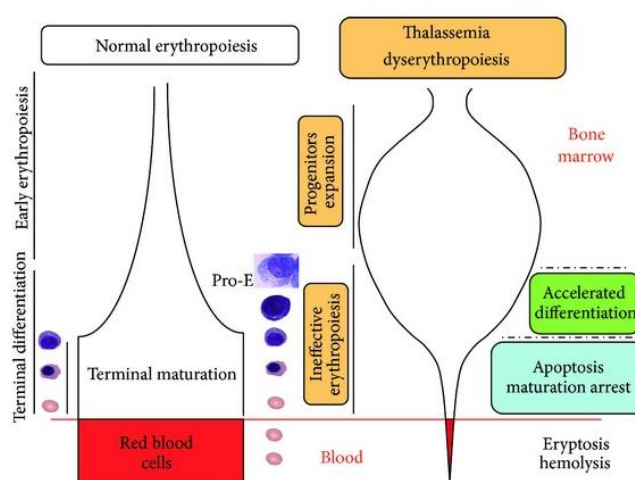


Figure 23: **Difference between normal and β -thalassemia ineffective erythropoiesis** (Ribeil et al., 2013).

B. *Sickle cell disease*

The marked decrease in life span of circulating red cells is the major determinant of chronic anemia in SCD and it is generally surmised that ineffective erythropoiesis contributes little to anemia. There is, however, a number of sporadic reports over the years suggestive of alterations during terminal erythroid differentiation in SCD. For example, erythroblasts differentiated *in vitro* or isolated from bone marrow of SCD patients were shown to sickle under hypoxic conditions (Hasegawa et al., 1998). Such sickling was also reported in the SAD mouse model, with altered morphology of late stage erythroid precursors within the bone marrow, with high levels of hemoglobin polymers and increased cell fragmentation occurring during medullary

endothelial migration of reticulocytes (Blouin, De Paepe, & Trudel, 1999). Finally, the study of Wu et. al. showed evidence of ineffective erythropoiesis occurring in the bone marrow of transplanted SCD patients with an imbalance favoring the survival of the donor erythroid progenitor cells (Wu, C. J. et al., 2005).

Despite these elements in the literature, there is no clear cellular and molecular demonstration of such ineffective erythropoiesis occurring in SCD patients. It is important to finely address this biological process in non-transplanted SCD patients, in the absence of conditioning and exogenous donor-related factors that can impact the hematopoietic niche and interfere with the survival of patient's erythroblasts.

OBJECTIVES

Fetal hemoglobin has proven to be a pivotal protective parameter in disease severity in SCD patients, preventing and delaying severe complications, and increasing survival (Platt et al., 1994). Several studies in the literature evaluated the beneficial role of HbF in SCD patients, however many questions remain to be addressed regarding cellular and molecular mechanisms by which this effect is exerted.

The aim of my thesis was to determine the role of fetal hemoglobin in spleen function, red cell survival and ineffective erythropoiesis in SCD patients. This was achieved by addressing the following points:

1. Evaluation of fetal hemoglobin in the natural history of spleen dysfunction in a longitudinal cohort of SCD children, and specifically in the occurrence of Acute Splenic Sequestration (ASS).
2. Study of the cellular expression and distribution of fetal hemoglobin in SCD children, in untreated patients and patients treated with Hydroxycarbamide.
3. Assessment of ineffective erythropoiesis in SCD patients and of the role of HbF as a protective factor against cell death during terminal erythroid differentiation

*CHAPTER I: Novel Insights into Spleen
Function and Determinants of Spleen
Injury in SCA Children: A Longitudinal
Study*

RESULTS

In sickle cell anemia the initiation of RBC abnormal properties takes place early in infancy during the hemoglobin switch from γ to β^S globin. HbS polymerization occurs and after several hypoxic cycles irreversibly sickled cells (ISCs), are formed. At this same period of time, in SCA infants, damage may occur in the spleen. Although splenic dysfunction is central to morbidity and mortality in children with SCA, the initiation and determinants of spleen injury, including acute splenic sequestration (ASS), are not fully established.

In this chapter, we set up and validated a high-throughput method to evaluate spleen function by measuring the percentage of circulating RBCs with Howell Jolly Bodies (%HJB-RBCs). Moreover, using our technique we investigated splenic loss of function in a longitudinal cohort of infants with SCA and explored the contribution of impaired RBC properties to splenic dysfunction (increased adhesion and decreased deformability).

[A novel non-invasive method to measure the splenic filtration function in humans](#)

The detection of red cells with Howell Jolly bodies and the liver-spleen scintigraphy scan are the currently used methods to assess splenic filtration function. The first is time consuming, and user-dependent. The second is quantitative but uses radioactive material in an invasive laborious manner. Here, we developed an automated, high throughput, non-invasive, and low-cost method to accurately measure splenic filtration function using flow cytometry. This part of the work was published in June 2018 in *Haematologica* as a Letter to the Editor (Appendix on page 174; DOI: 10.3324/haematol.2018.188920).

[Novel template to quantify HJB-RBCs using imaging flow cytometry \(IFC\)](#)

In this technique we used the Hoechst dye to stain the HJB, since Hoechst dye binds DNA and not RNA thus eliminating nonspecific labeling of reticulocytes. Using RBCs from non-SCA splenectomized patients we gated the Hoechst positive population. We observed high

percentages of Hoechst positive events (Table 1). We performed the staining in blood samples from control individuals, where little or no HJB-RBCs should be detected, and we did observe percentages higher than 1% (Table 1). The latter suggested the presence of false-positive events. To characterize these events, we used imaging flow cytometry (IFC), generated 50,000 pictures of RBCs and analyzed Hoechst positive events. We observed three categories of staining: Category 1 (RBC with HJB spots), Category 2 (RBC bound to Hoechst positive particles) and Category 3 (Hoechst positive particles) (Figure 1A and 1B). The Hoechst-positive particles were considered non-specific events, i.e. DNA released after lysis of neutrophils during the preparation steps. Thus, using specific features of staining localization in IFC analysis, we set up a template to quantify specifically the cells labeled in Category 1.

The Hoechst-positive population was gated with reference to a negative tube. To quantify the HJB-RBCs we developed a mask using the Modulation feature (a feature measuring the intensity range of an image normalized between 0 and 1) and the H Entropy feature (a texture feature used to determine if pixel values in an image follow a pattern or are randomly distributed). As shown in Figure 1C, using the H Entropy Mean_M07_Hoechst on the x-axis and the Modulation_Morphology (M07, Hoechst) on the y-axis, we set up the coordinates of the gate as: 3.356 – 5.9 on the x-axis and 0.38 – 0.456 on the Y-axis.

After applying our analysis template, we observed a decrease in the percentages of Hoechst positive events (Table 1). Moreover, all the pictures corresponding to Hoechst-positive events were HJB-RBCs, similar to those in Category 1.

Table 1: %Hoechst-positive events and %HJB-RBCs in splenectomized individuals (S), healthy donors (C) and SCA patients (P).

	Age (years)	%Hoechst-positive events	%HJB-RBCs
S1	66	13.00	9.80
S2	50	10.90	7.89
S3	34	10.90	9.43
S4	34	12.8	10.5
S5	8	12.9	10.4

S6	22	14.2	11.6
S7	11	7.8	6.2
S8	19	14.1	11.4
S9	9	12.8	10.2
S10	11	14.1	11.5
C1	45	1.30	0.30
C2	43	1.05	0.30
C3	38	1.20	0.60
C4	35	1.50	0.42
C5	31	1.10	0.30
C6	28	1.12	0.30
C7	27	1.30	0.00
P1	67	12.7	10.9
P2	61	13.4	10.59
P3	59	10.2	7.8
P4	59	18	15.8
P5	56	21.7	17.9
P6	53	9.3	7.85
P7	48	20.2	15.5
P8	40	21.6	17.5
P9	37	18.5	14.8
P10	36	14.1	11.5
P11	36	11.6	9.87
P12	1	3.2	2.24
P13	1	3.33	1.9
P14	1	0.51	0.32
P15	1	1.16	0.7
P16	1	0.29	0.06
P17	1	0.2	0.08
P18	1	0.09	0.07
P19	1	0.28	0.14
P20	1	0.08	0.02
P21	0.5	3.65	2.7
P22	0.5	1.3	0.6
P23	0.5	0.83	0.6
P24	0.5	0.82	0.61
P25	0.5	0.07	0.02
P26	0.5	0.09	0.02
P27	0.5	0.02	0.01
P28	0.5	0.2	0.03
P29	0.5	0.05	0.01
P30	0.5	3.14	2.3
P31	0.5	1.79	1.45
P32	0.5	0.33	0.23
P33	0.5	0.25	0.05
P34	0.5	1.23	0.71
P35	0.5	0.27	0.16
P36	0.5	0.2	0.11

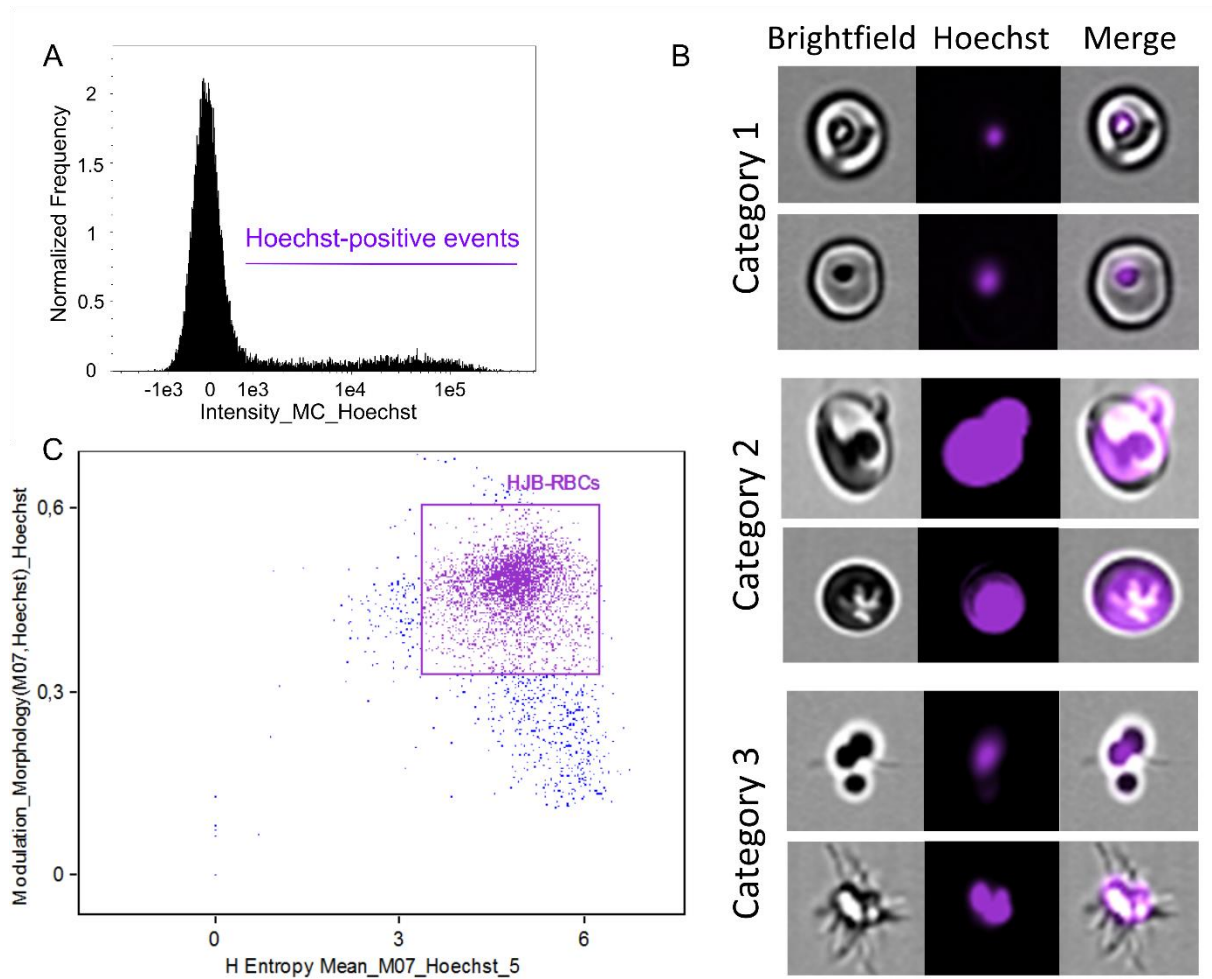


Figure 1: **Detecting Howell Jolly Bodies using Imaging Flow Cytometry.** (A) Histogram representing the intensity of Hoechst staining in a splenectomized individual. (B) Images from imaging flow cytometry (IFC) distinguishing 3 categories of cells: (1) RBCs with HJB-like spots, (2) RBCs bound to Hoechst-positive particles and (3) Hoechst-positive particles. (C) Dot plot representing the mask used to discriminate the HJB-RBCs from the non-specific staining using entropy mean feature on the x-axis and modulation morphology feature on the y-axis.

Validation of the IFC-based technique

To validate our method, we compared the percentage of HJB-RBCs obtained from the IFC-technique with those from the classical May-Grünwald-Giemsa (MGG) staining. HJB-RBCs were counted manually within a total of 3,000 RBCs (Figure 2A). The latter was performed on 10 splenectomized individuals (Figure 2B) and 11 SCA adults (P1 –P11 in Table 1) (Figure 2C). We observed no significant difference between both methods, thus confirming that our IFC-based method is robust.

We thereafter applied our IFC method to evaluate the %HJB-RBCs in 25 very young SCA children (P12-P36 in Table 1, age range: 6-12 months) who underwent technetium-99m RBC splenic scintigraphy. Patients were classified into 2 groups according to their splenic uptake percentage: [100%-50%] and [50%-0%]. The two groups displayed marked differences, with the [100%-50%] and [50%-0%] groups showing medians of 0.35% and 2.98% HJB-RBCs, respectively (Figure 2D).

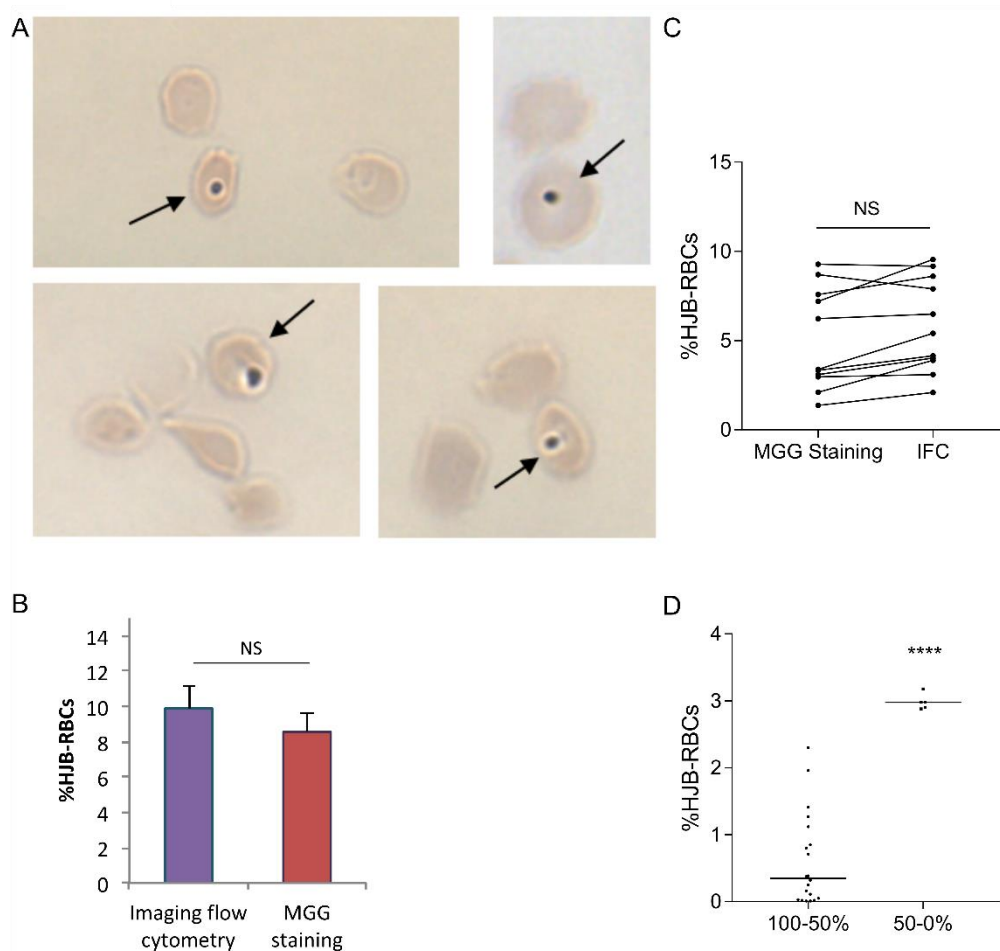


Figure 2: Validation of HJB-RBCs measurements performed by Imaging Flow Cytometry. (A) Images of HJB-RBCs colored by MGG staining taken from blood smears (magnification 20x). (B) 10 splenectomized individuals (Unpaired t test, $p = 0.07$) and (C) 11 SCA adult patients (Wilcoxon test, $p = 0.057$) (NS: non-significant). (D) Graphical representation of the percentage of HJB-RBCs by IFC in 20 SCA patients with a splenic uptake of 100-50% and 7 patients with a splenic uptake of 50-0% (Mann-Whitney test, **** $p < 0.0001$).

Measuring %HJB-RBCs with conventional flow cytometry

Imaging flow cytometry is a recent technology that is not present in all hospital and research centers. Therefore, to increase the possibility of the use of our method we aimed at refining the standard flow cytometry method in order to allow accurate evaluation of %HJB-RBCs using a classical flow cytometry.

We determined the %HJB-RBCs by flow cytometry in the group of 46 individuals with various splenic function (36 SCA patients, 10 splenectomized individuals and 7 non-splenectomized healthy donors). The percentage of total Hoechst-positive events, determined by standard flow cytometry, was plotted against the percentage of HJB-containing RBCs determined by IFC. We observed a robust linear regression between both parameters (Figure 3A), with the following equation: $y = 0.83x - 0.22$, where y is the %HJB-RBCs and x the % of Hoechst-positive events generated by flow cytometry. We further refined this equation by dividing the 53 samples into 3 groups and generated 3 equations based on 3 cut-offs of Hoechst-positive events: $< 0.5\%$, $0.5-3\%$ and $> 3\%$ (Figure 3B, C and D).

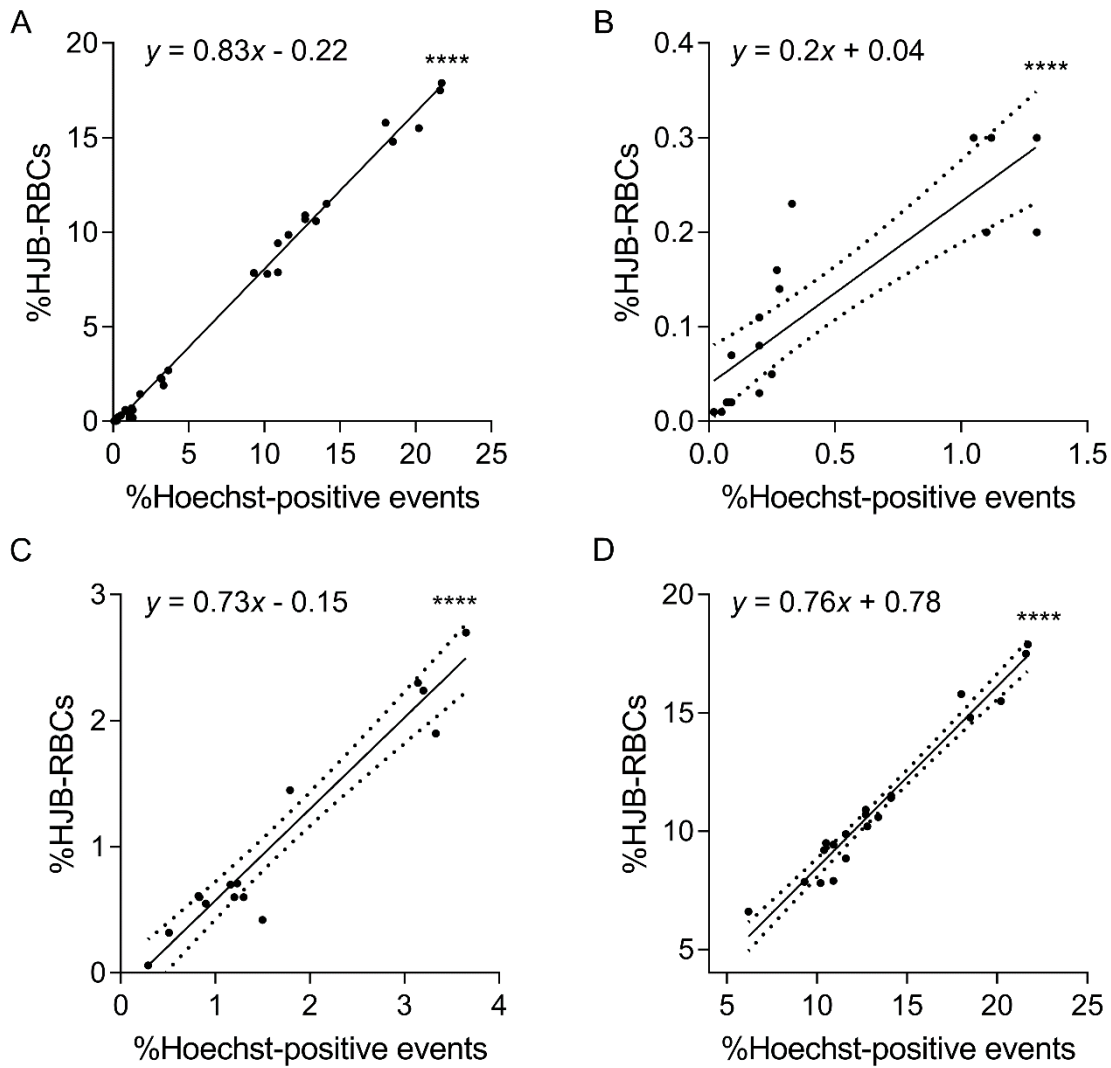


Figure 3: **Relationship between %Hoechst-positive events and %HJB-RBCs.** (A) Linear regression relationship between %Hoechst-positive events (x) and %HJB-RBCs (y) in 53 blood samples ($y=0.83x-0.22$). (B, C, D) Refinement of the linear regression according to 3 cut-offs of %Hoechst-positive events: (B) < 0.5% ($n=18$) ($y=0.2x + 0.04$), (C) 0.5-3.5% ($n=14$) ($y=0.73x-0.15$), and (D) > 3.5% ($n=21$) ($y=0.76x+0.78$). Correlation (Pearson's correlation coefficient) and Linear Regression, $p<0.0001$.

Insights into determinants of spleen injury in sickle cell anemia

In this part of the study, 57 SCA infants were included in a comprehensive longitudinal multi-center study for a total follow-up period of 24 months. The aim was to i) identify very early prognostic factors of clinical complications and ii) to evaluate spleen function at this very young age, knowing that spleen dysfunction is central to morbidity and mortality in young SCA children. This part of the project generated two publications. A paper in the American Journal of Hematology published in September 2018 (Appendix on page 179; DOI: 10.1002/ajh.25260), this first publication details the characteristics of the cohort and identifies early prognostic factors, that can predict severe outcomes in the first 2 years of life. A severe SCA-related event was defined as the occurrence of either an acute splenic sequestration (ASS), vaso-occlusive crisis (VOC) requiring hospitalization, acute chest syndrome, blood transfusion, conditional or abnormal trans cranial Doppler (TCD) or death. Multivariate analysis demonstrated that higher hemoglobin (Hb) concentration and fetal hemoglobin (HbF) level are the two independent protective factors [adjusted HRs (95% CI) 0.27 (0.11-0.73) and 0.16 (0.06-0.43) respectively]. These findings imply that early measurement of HbF and Hb levels can identify infants at high risk for severe complications who might maximally benefit from early disease modifying treatments. This part of the project will not be further developed in this result section. The second publication is published in Blood Advances Journal (Appendix page 200; DOI: 10.1182/bloodadvances.2019000106) and will be further developed.

Description of the cohort

A total of 57 infants (SS n=55; S β ^o n=2; 54.4% males) were included in this study and followed for a median of 19.4 months (range: 3.1-23.2). During the study period, 8 (17%) infants experienced at least one episode of acute splenic sequestration (ASS), at a median age of 13.4 months (range: 8.0-15.9), an incidence rate within an expected range (Brousse et al., 2012; Emond et al., 1985). Thirty-five (59%) remained asymptomatic during the follow up period and

14 (24%) experienced other SCD-related complications. Analysis was performed longitudinally in 47 patients of the cohort. Specific analysis was performed on 7 ASS patients compared to 22 asymptomatic non-transfused patients for whom samples were available for thorough analysis. This analysis was performed at two different time points of 3-6 months and 18 months. The mentioned time points represent the cohort before ASS (3-6 months) and after ASS (18 months). Note that during the study no infant was started on hydroxycarbamide, in line with European authorization licensing the drug in SCA for only children over 2 years. Moreover, patients transfused during the course of the study were excluded from the analysis.

Evidence of very early loss of spleen function

Spleen function was assessed using both a high throughput cytometry method for HJB-RBC counts and ^{99m}Tc heated RBC scintigraphy at two time points (3-6 and 18 months) in a cohort of 47 infants (2 patients were transfused during the study period and excluded from the analysis). Figure 4 explicits the exploration of splenic function performed on this cohort.

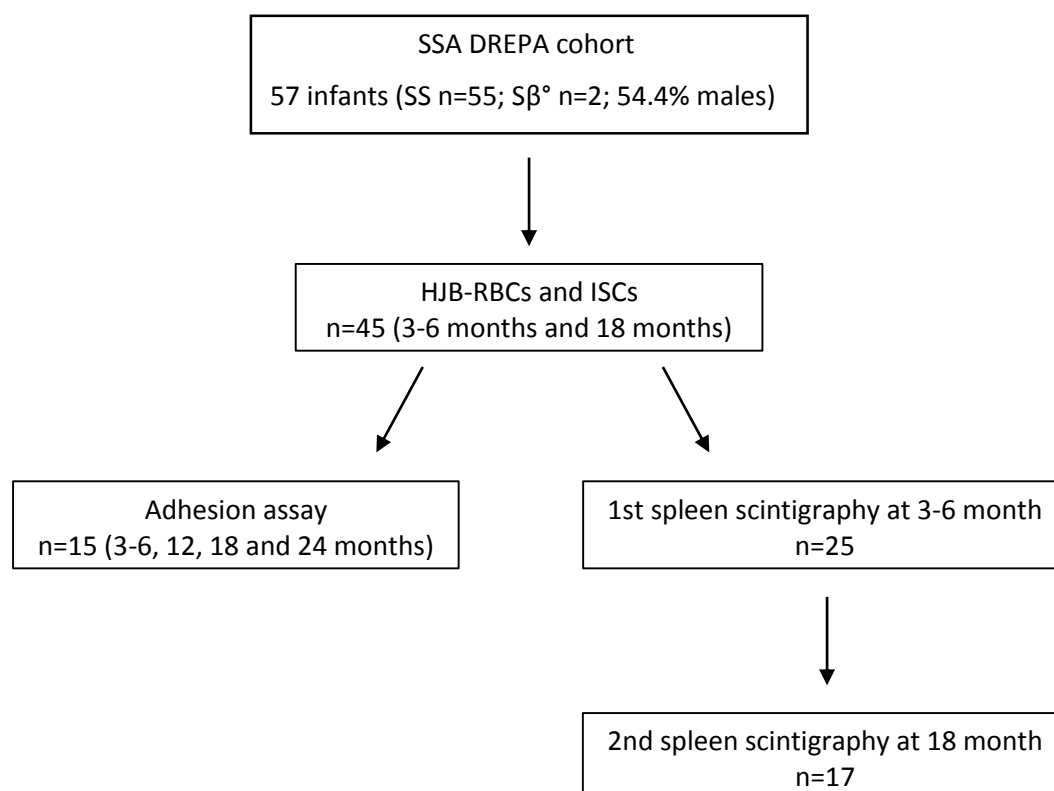


Figure 4: **Spleen exploration in the SSADREPA cohort.**

At enrollment, at a median age of 6 months (range: 2.75-8), the median %HJB-RBCs was low (0.3%, range: 0.01-2.9, n=45) and similar to an adult healthy control group, albeit with a different distribution range (0.3%, range: 0.01-0.6, n=7; $p=0.93$). Between enrollment and 18 months, the median %HJB-RBCs significantly increased, from 0.3% to 0.74% (range: 0.01-5.11%) (Figure 5A) (Table 2), illustrating the expected decline in spleen function. By contrast, HJB-RBCs counts on classical MGG blood smears were only slightly elevated in a very small proportion of patients and did not allow further interpretation by lack of sensitivity.

^{99m}Tc heated RBC splenic scintigraphy was performed in a subgroup of 25 patients (with comparable characteristics to the rest of the cohort) at a median age of 6.2 months (range: 4.9-8.0). There was a normal splenic uptake in 17 cases (68%) and a decreased uptake in 8 cases (32%) (Table 2). All scans were qualified as homogenous. Median splenic volume was 45 ml (range: 0-100), a volume increased compared to healthy age-matched controls (median 21 ml, range 14-42 ml) (Nemati et al., 2016). Only 28% of the patients had a spleen volume within the 5th and 95th percentile of age-matched healthy controls. There was no association between laboratory parameters including RBC indices (MCV, MCHC), hemolysis markers or %HbF measured at enrollment and the result of spleen scans at this age (Table 3). A second spleen scintigraphy, performed in 17 patients at a median age of 18.3 months (range: 16.6-19.5) showed a decreased splenic uptake in 7 (41.7%) and a stable scan in 9 (53%), further illustrating the decline of function with age except for 1 patient who had an unexpectedly increased splenic uptake (Table 2). At 18 months, a median splenic volume of 70 ml (range: 0-115) was measured, a volume increased compared to 31 ml (range: 10.59-65.4) in healthy controls. Only 16.7% of the patients had a spleen volume within the 5th and 95th percentile of age-matched healthy controls (Nemati et al., 2016). While 55.6% had an increased volume compared to normal, 27.8% of the patients had a decreased spleen volume. There was no correlation between splenic uptake and volume altogether or independently at each time point. Similarly, there was no

correlation between %HJB-RBCs and spleen volume demonstrating that spleen volume is not predictive of spleen function. At all time points, a significant correlation was found between %HJB-RBCs and splenic uptake (Figure 5B) ($R^2=0.69$, $p<0.0001$).

Table 2: Spleen function at 3-6 and 18 months of age in SCA children. Spleen function as measured by ^{99m}Tc heated RBC spleen scintigraphy (Splenic Uptake) and %HJB-RBCs. ND: not determined. *Only one blood sample was processed.

Age (months)	Splenic Uptake %	Patients N (%)	%HJB-RBCs Median (Range)
3-6	100-150	17 (68)	0.32 (0.01-1.27)
	75-100	3 (12)	0.16, 0.3 and 1.96
	50-75	1 (4)	ND
	25-50	2 (8)	0.05 and 3.18
	0-25	2 (8)	2.88 and 2.9
18	100-150	9 (50)	0.07 (0.01-1.3)
	75-100	2 (11.1)	0.8 and 1.41
	50-75	1 (5.6)	1.12
	25-50	2 (11.1)	2.98*
	0-25	4 (22.2)	4.77 (1.37-5.11)

Table 3: Comparison of routine laboratory parameters between patients with a normal spleen scan (100-150%) and abnormal spleen scan at inclusion (75-100%, 50-75%, 25-50% and 0-25%).

Variable	Median		p-value
	Normal	Abnormal	
Mean Corpuscular Volume	73.5 (67 - 77)	67.5 (63 - 71.8)	0.44
Mean Corpuscular Hemoglobin Concentration	25.3 (23.7 - 26.5)	23.2 (22.6 - 24.2)	0.14
Hemoglobin	9.2 (8.2 - 10)	8.8 (7.9 - 9.8)	0.76
Hematocrit	26 (24 - 28)	27 (23.5 - 28)	0.98
Reticulocytes	166 (129.5 - 200.5)	124.5 (104 - 155)	0.13
Fetal Hemoglobin	36 (26 - 42)	27.5 (21.5 - 42)	0.45

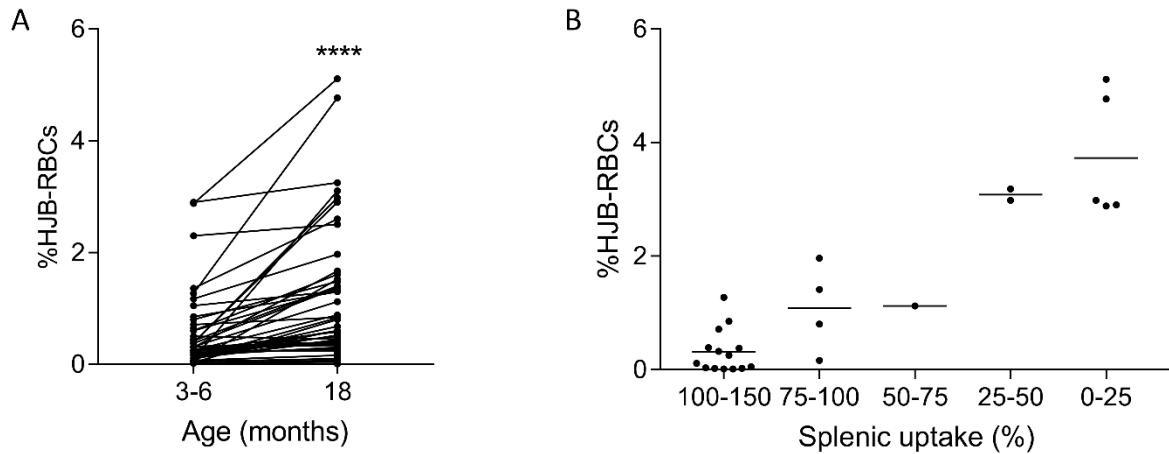


Figure 5: **HJB in SCA children.** (A) %HJB-RBCs determined by imaging flow cytometry (IFC) in 45 children at 3-6 months and 18 months. **** $p < 0.0001$, Wilcoxon paired test. (B) Distribution of %HJB-RBCs with respect to splenic uptake as measured by ^{99m}Tc heated RBCs spleen scintigraphy. Splenic uptake of 100-150% (n=15), 75-100% (n=4), 50-75% (n=1), 25-50% (n=2) and 0-25% (n=5).

Impaired deformability of RBCs increases with time and impacts spleen function

Irreversibly sickled cells (ISCs), a subpopulation of dense RBCs that are dehydrated and poorly deformable due to prolonged deoxygenation, were quantified as a surrogate of decreased RBC deformability thereby focusing on the subpopulation of dense cells with the most severe phenotype (Liu, Derick, & Palek, 1993). ISCs were measured using an IFC-based analysis developed in our laboratory and further detailed in the materials & methods section. ISCs were present at enrollment, with a median of 0.96% (range 0.08-2.9%) n=45. ISCs increased significantly at 18 months (1.71%, 0.47-6.21) (Figure 6A) (Table 2), similarly to %HJB-RBCs (Figure 5A). Pooling all time point measurements, there was significant positive correlation between %ISCs and %HJB-RBCs (Figure 6B), suggesting a relationship between altered RBC deformability and spleen loss of function. Expectedly, there was a positive correlation between %ISCs and splenic uptake by scintigraphy ($R^2=0.3$, *** $p=0.0005$) (Figure 6C). Since HbF modulates the polymerization of HbS and hence RBC deformability, we looked at the relationship between ISCs and HbF and found a significant correlation ($R^2=0.16$, *** $p < 0.0001$) (Figure 6D).

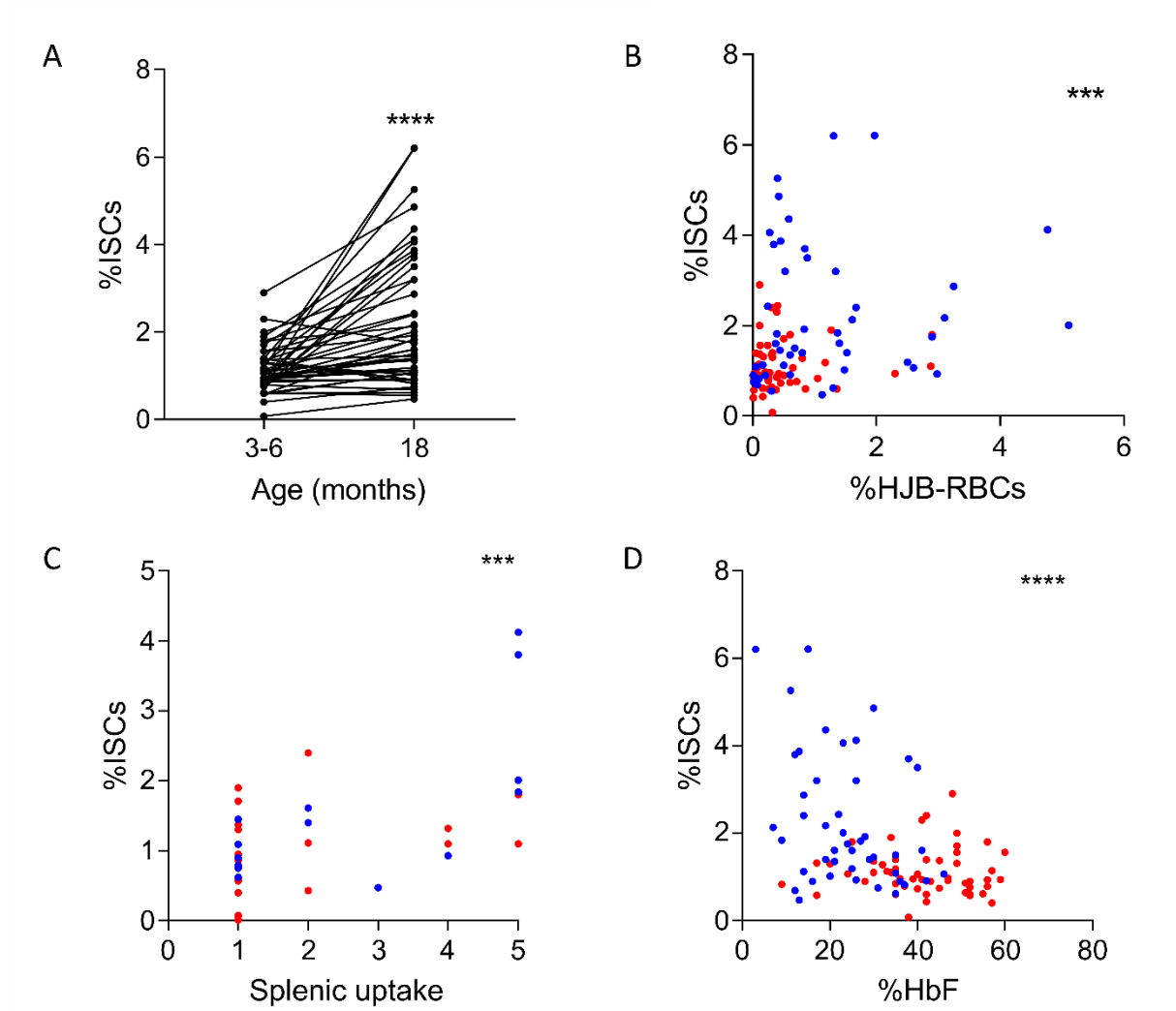


Figure 6: **HbF, ISCs and SCA children.** (A) %ISCs determined by IFC in 45 children at 3-6 and 18 months. **** $p < 0.0001$, Wilcoxon paired test (B) Spearman correlation between %ISCs and %HJB-RBCs at 3-6 (red dots) and 18 months (blue dots) (n=99). Spearman correlation between %ISCs and (A) splenic uptake [100-150%: (1), 75-100%: (2), 50-75%: (3), 25-50%: (4), 0-25%:(5)] (n=38) and (B) HbF (n=99) as measured by HPLC at 3-6 months (red dots) and 18 months (blue dots), *** $p < 0.0005$, **** $p < 0.0001$.

Adhesion properties of red cells

Increased RBC adhesion may contribute to the congestion of the red pulp of the spleen because of abnormal RBC interactions with cellular and matrix components (Brousse, Buffet, & Rees, 2014). We investigated RBC adhesion properties in a subgroup of 15 infants by first performing adhesion assays focusing on the receptor-ligand interaction between CD239/Lu/BCAM (Lutheran Basal Cell Adhesion Molecule) adhesion protein and laminin, known to drive

abnormal RBC adhesion in SCA (Bartolucci et al., 2010; El Nemer et al., 1998; Udani et al., 1998). Furthermore, Lu/BCAM has an increased expression on RBCs of SCA children (Brousse et al., 2014) and is known to adhere to laminin 521 (El Nemer et al., 1999) an important structural component of the spleen extracellular matrix. We also performed adhesion assays on TNF- α -activated endothelial cells, to have a more global and physiological approach including all adhesive interactions potentially involved in abnormal RBC adhesion to the endothelial wall.

Lu/BCAM-mediated adhesion to Laminin

RBC adhesion to immobilized laminin 521 was initiated as early as 3-6 months, with a significant progressive increase of the adhesion level at 12, 18 and 24 months (Figure 7A and 7B), indicating an early triggering of the RBC adhesive phenotype during the 2 first years of life. This increase was associated with increased Lu/BCAM expression per cell with age (Figure 7C). To test if the increase of RBC adhesion was secondary to the activation of Lu/BCAM, we determined the phosphorylation level of Lu/BCAM in the same blood samples at the 4 different time points. Lu phosphorylation began as early as 3-6 months, in accordance with the high adhesion levels observed at this stage. Lu phosphorylation rate did not differ significantly between 3-6 and 24 months, indicating that both Phospho-Lu and total Lu/BCAM were increasing at the same rate within this time frame (Figure 7D).

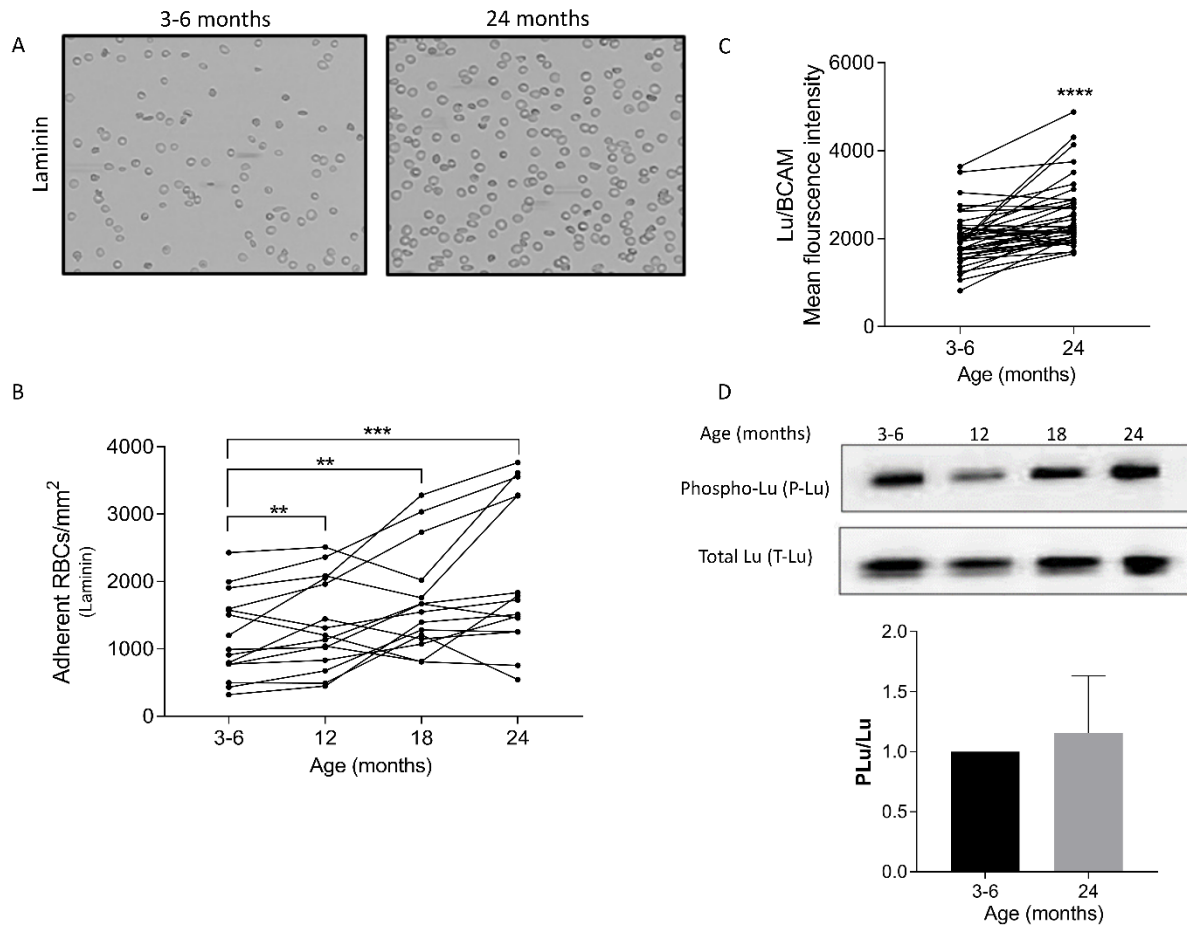


Figure 7: Lu/BCAM expression and mediated RBC adhesion. (A) Microscopy images of RBCs adhering to and laminin 521-coated microchannels at 3-6 months and 24 months. (B) The amount of adherent RBCs/mm² on laminin-coated channels (n=15) at 3-6, 9, 18 and 24 months; * $p < 0.05$, ** $p < 0.005$, *** $p < 0.001$, Wilcoxon test. (C) Mean fluorescence intensity of Lu/BCAM on mature RBCs; **** $p < 0.0001$, Wilcoxon test. (D) Phosphorylation of the long isoform Lu (upper panel) and total amount of protein (lower panel) as measured in one SCA infant at 3-6, 12, 18, and 24 months after precipitation using specific anti-Phospho Lu and anti-Lu antibodies respectively. Quantification of the ratio of Phospho-Lu/total Lu at 3-6 and 24 months in 15 SCA children.

RBC adhesion to endothelial cells

To assess sickle RBC adhesion properties under more physiological conditions, we performed adhesion assays using capillaries covered by endothelial cell monolayers. These assays were performed under inflammatory conditions because SCD patients exhibit an increase of circulating inflammatory cytokines believed to activate endothelial cells thus inducing their capacity to recruit circulating blood cells (Solovey et al., 1997). Due to the high rate of vaso-occlusive crises in the bone we chose to work with a cell line derived from the human bone marrow: transformed human bone marrow endothelial cells (TrHBMECs). Cell monolayers

were grown in 4 capillaries and were activated by TNF α to express inflammatory markers. Adhesion assays on TNF- α -activated endothelial cells showed that RBCs were adherent at 3-6 months, with a significant progressive increase of the adhesion level at 12, 18 and 24 months (Figure 8A and 8B), confirming very early onset of changes in RBC adhesive properties in SCA infants.

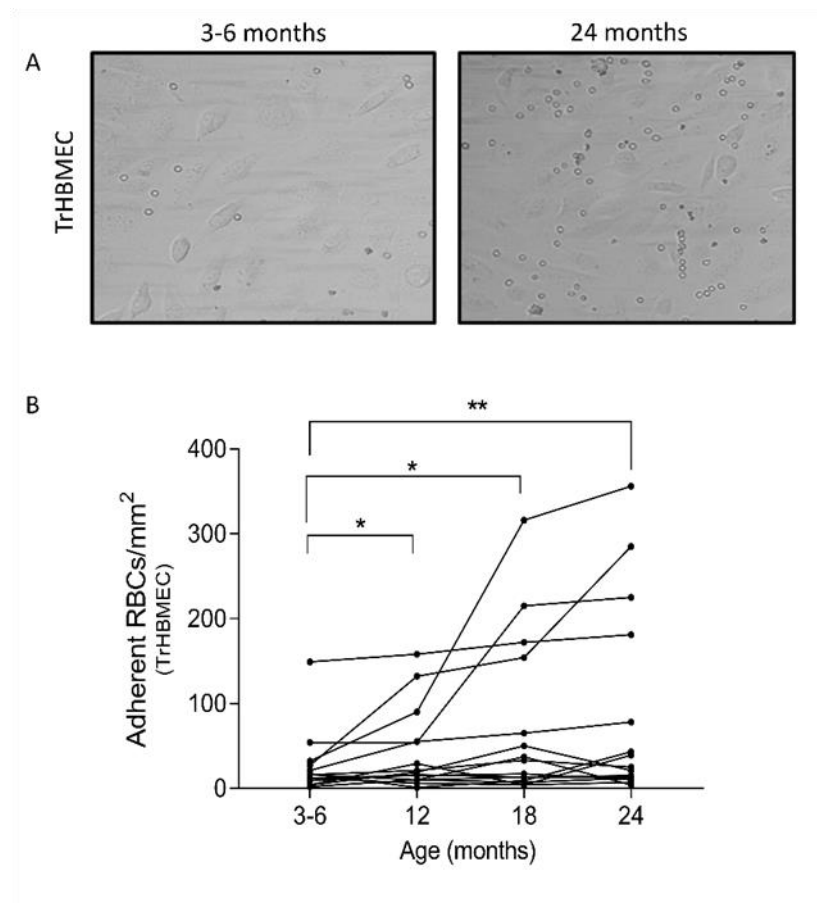


Figure 8: **RBC adhesion to endothelial cells.** (A) Microscopy images of RBCs adhering to TrHBMEC monolayers at 3-6 months and 24 months. (B) The amount of adherent RBCs/mm² on TrHBMEC-coated channels (n=15) at 3-6, 12, 18 and 24 months; * p <0.05, ** p <0.005, Wilcoxon test.

Adhesion properties and spleen function

We investigated if these changes in RBC adhesion properties affect spleen function by performing correlation analysis between the %HJB-RBCs and the amount of adherent cells on laminin and TrHBMECs, respectively. There was no correlation between the number of

adherent RBCs on laminin and the %HJB-RBCs ($p=0.39$) (Figure 9A), indicating that Lu/BCAM activation alone is not enough to induce spleen dysfunction. Interestingly, a positive correlation was found between the number of adherent cells on TrHBMECs and the %HJB-RBCs (Spearman's correlation $p<0.0001$ $R^2=0.42$) (Figure 9B) suggesting a relationship between abnormal RBC adhesion to endothelium, probably driven by several adhesion molecules, and spleen dysfunction.

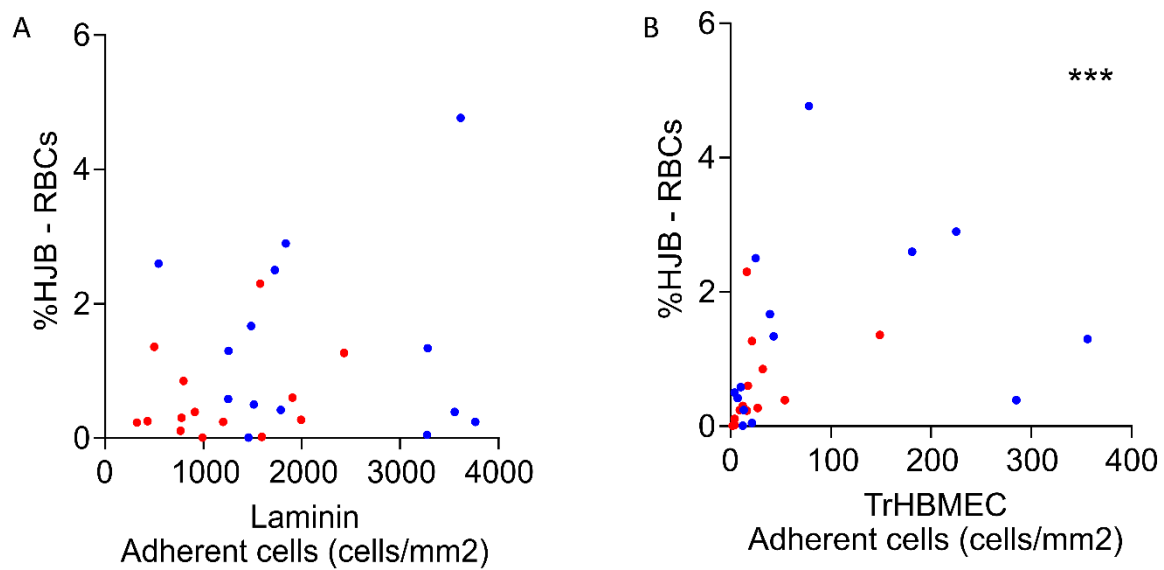


Figure 9: **Adhesion properties and spleen function.** Spearman correlation between %HJB-RBC and the amount of adherent RBCs/mm² on (A) Laminin ($p=0.39$ $R^2=0.027$) and (B) TrHBMEC ($p<0.0001$ $R^2=0.42$).

Decreased red cell deformability plays a role in ASS occurrence

During the study period, 8 (17%) infants experienced at least one episode of ASS, at a median age of 13.4 months (8.0-15.9), an incidence rate within an expected range (Brousse et al., 2012; Emond et al., 1985). Thirty-five remained asymptomatic during the follow up period and 14 experienced other SCD-related complications. Analysis was performed in 7 ASS patients compared to 22 asymptomatic non-transfused patients, for whom samples were available for thorough analysis.

At enrollment, comparison of %HJB-RBCs in infants who later experienced ASS with those who remained asymptomatic showed no significant difference, demonstrating similar spleen function in both groups at 3-6 months and excluding intrinsic abnormalities of the spleen filtration function in the ASS group at this stage. By contrast, at 18 months the %HJB-RBCs was significantly higher in the ASS group as compared to the asymptomatic group (Figure 10A), indicating altered spleen function after the occurrence of ASS.

Potential contributors to ASS such as Lu/BCAM-mediated increased adhesion and %ISCs were compared between both groups. No significant difference was noted between Lu/BCAM expression and Lu/BCAM mediated adhesion levels in these two groups at both time points (data not shown). While there was no difference at 18 months, patients from the ASS group had a significantly higher %ISCs at enrollment than those from the asymptomatic group (median: 1.61% versus 0.54%, $p = 0.0025$) (Figure 10B), suggesting that high levels of ISCs in the circulation might be a contributing factor to ASS.

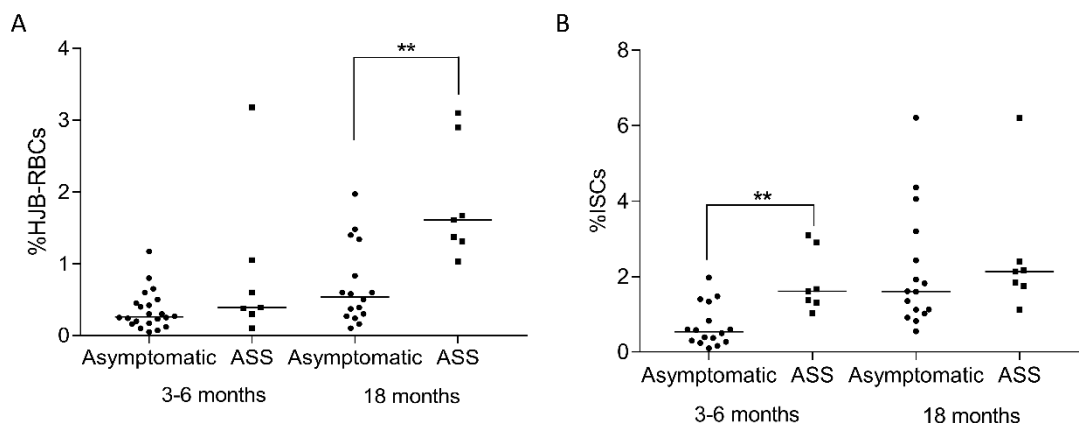


Figure 10: **HJB-RBCs and ISCs in asymptomatic and ASS infants.** Comparison of (A) %HJB-RBCs and (B) %ISCs at 3-6 months and 18 months in asymptomatic and ASS infants. Wilcoxon test. ** $p < 0.005$.

DISCUSSION

SCA is known to cause splenic dysfunction, with the spleen being the first organ to be severely injured resulting in substantial morbidity and mortality (Airede, 1992; Walterspiel et al., 1984). In clinical practice, exploration of splenic function is limited due to the lack of easy, high throughput, non-invasive tools. In addition, direct access to spleen histology is rare because autosplenectomy is the natural outcome in SCA. Monitoring spleen function has been neglected because the methods used are labor-intensive, such as counting HJB-RBCs, or invasive, such as the spleen-liver scintigraphy. The flow cytometry-based method that we set up is a robust non-invasive technique for the sensitive detection and evaluation of spleen filtration function. In contrast to previously published flow cytometry techniques, our method doesn't require cell fixation or RNA digestion steps (Harrod et al., 2007). Using our new technique and other known robust methods, the spleen scintigraphy, we were able to finely study spleen function in very young SCA patients.

Previous studies relying on pitted cells showed that spleen function was lost within the first 5 years of life in 90% of children with SCA (Brown et al., 1994). More recently, a study using liver spleen ^{99m}Tc colloid scan showed that in 12 infants with SCA less than 12 months, with the youngest aged 8 months, spleen function was impaired in 75 % of the cases (Rogers, Z. R. et al., 2011). Our study differs by exploring another aspect of splenic function (the filtration function) in a longitudinal manner and in a younger cohort. Splenic ^{99m}Tc heated RBC scintigraphy explores specifically the filtration function of the spleen as opposed to ^{99m}Tc colloid spleen scanning that measures the phagocytic uptake by splenic macrophages. Indeed, a previous study by Adekile (Adekile et al., 2002) using both methods, demonstrated a temporal loss of spleen function in a small series of patients with SCA, with an initial loss of the phagocytic function followed by the loss of the filtration function. Considering the very early alteration of the filtration function in our young infants (32% of patients had a decreased splenic uptake), our results suggest that onset of spleen phagocytic dysfunction may start earlier than 6

months. In fact, our highly sensitive method for measuring HJB indeed showed their presence in the circulation at this very young age. This data indicates that spleen dysfunction begins in the first semester of life in otherwise asymptomatic SCA infants with a sustained HbF level, reconciles our data with the results from the baseline splenic exploration of the BABYHUG trial mentioned above. Furthermore, because splenic function is immature in otherwise healthy infants below 2 years of age, our data support the additional infectious risk in infants with SCA. Although there may be a great variability between patients, these results argue for very early penicillin prophylaxis therapy in infants with SCA.

The longitudinal follow-up further allowed insights into the natural history of splenic decline of function and its relationship with spleen volume. Almost half of patients (42%) showed a decreased splenic function at 18 months i.e. within a year (increase of %HJB and decrease of splenic uptake). Furthermore, spleen volume measured by scintigraphy showed an increased volume in a majority of children and, importantly, did not correlate with function, a finding not only illustrating functional asplenia (Pearson, Spencer, & Cornelius, 1969b), but demonstrating that spleen volume is not predictive of spleen function. Importantly, the very significant correlation between %HJB-RBCs and results of splenic scintigraphy demonstrates that the measurement of %HJB-RBCs by flow cytometry may allow accurate evaluation of the spleen's filtration function in future studies. In clinical practice, this measurement could help monitor splenic function and guide the appropriate timing of splenectomy in very young children with recurrent ASS for instance, by demonstrating the absence of function and hence no additional infectious risk related to the surgical removal of the spleen. Beyond SCA, easily available measurement of HJB is a significant improvement given the growing suspected role of the spleen in the occurrence of severe complications such as auto-immune diseases, neoplasia, thrombo-embolic events and pulmonary hypertension in other hemolytic anemia patients and in healthy patients.

We chose to focus on sickle RBC adhesion and deformability properties as potential contributors to splenic injury because determinants of splenic injury in SCD are not known and because the splenic microcirculation specifically challenges these properties. Increased adhesion may play a role in spleen injury because increased adhesive properties of sickle RBCs prolong transit time in the red pulp, favor HbS polymerization and hence promote both sickling (and subsequent congestion) and increased cell-cell interactions (and subsequent phagocytosis) within the filtering beds. Here, we confirm the increase with time of the expression of Lu/BCAM on RBCs. We also show that Lu/BCAM is activated. We further show that this expression functionally translates into a significant increase in adhesion of RBCs on laminin-coated capillaries. Yet, no correlation (positive or negative) was observed between the percentage of adherent RBCs on laminin and the splenic function measured by %HJB-RBCs. This may perhaps pertain to the restricted interaction of Lu/BCAM with laminin 521, which may not be the major type of laminin present in the extracellular matrix of the spleen. Conversely, when adhesion assays were performed on endothelial cells (TrHBMECs), we not only observed a significant increase in the number of adherent RBCs with age, but we also observed a significant correlation with the %HJB-RBCs, implying a relation between spleen function and RBC adhesion. The activation of TrHBMECs leads to the expression of ICAM-1 and VCAM-1 that mediates cell adhesion (Schweitzer et al., 1997) and previous studies have indeed shown the presence of VCAM-1 in the red pulp of the spleen (Dutta et al., 2015; Tada, Inoue, Widayati, & Fukuta, 2008). Further immuno-histological studies will be required to explore specifically VCAM-1 mediated endothelial-sickle RBC adhesion within the human spleen.

Impaired RBC mechanical properties was analyzed using ISCs as a surrogate marker of severely impaired RBC deformability (Liu et al., 1993). In SCA, repeated HbS polymerization results in circulating dense red cells constituted not only of sickled cells but also of irregularly

shaped cells. ISCs are of short life span, correlate with hemolysis *in vivo*, and contribute to the pathophysiology of vaso-occlusion (Goodman, 2004). We recently showed that ISCs were poorly deformable and prone to blocking capillaries *in vitro* (Lizarralde Irigorri et al., 2018). Because of their lack of deformability, we hypothesized that ISCs get trapped in the filtering beds of the red pulp, notably at the inter-endothelial slits barrier. We show here that ISCs are indeed present in the circulation at a very young age, and significantly increase with time, similarly to %HJB-RBCs. Furthermore, we show that the %ISCs correlates with splenic uptake indicating that impaired deformability negatively impacts the splenic filtration function.

Because ASS is the most life-threatening splenic complication in infants with SCA and is probably the extreme acute expression of spleen dysfunction, we analyzed specifically infants who experienced ASS and compared them to a selected subgroup of the cohort who remained asymptomatic throughout the follow-up. Here we demonstrate that ASS causes further splenic dysfunction, as illustrated by the increase of %HJB-RBCs in those who experienced ASS, an unsurprising yet so far undemonstrated finding. Regarding determinants of ASS, while keeping in mind the small number of events, we found no correlation between increased RBC adhesion properties and the occurrence of this event. Conversely, %ISCs was significantly elevated at 3-6 months in infants who later experienced ASS, a finding suggesting that ISCs, and hence decreased deformability, may be an important contributor to ASS. Trapping of ISCs may cause a decreased outflow, favoring further sickling and ultimately ASS. Further studies on larger samples shall be required to comfort these findings.

In conclusion, our study demonstrates that flow cytometry analysis of %HJB-RBCs alone may accurately reflect spleen filtration function in very young SCA children. Using such analysis together with spleen scintigraphy we show that splenic loss of function is present very early in life at 3-6 months of age in SCA infants, further declines and is unrelated to spleen volume. Hyposplenism results from both RBC increased adhesive properties and, critically, loss of

deformability. ISCs are additionally a potential contributor to ASS, which in turn results in further loss of splenic function.

PATIENTS & METHODS

Patients and blood samples

Infants diagnosed with SCA following neonatal screening were enrolled in a multi-center prospective study on prognostic factors in sickle cell anemia (ClinicalTrials.gov: NCT01207037) between September 2010 and March 2013 described in Brousse et al., 2018 (Brousse et al., 2018). Inclusion criteria were: 1) SS or S-β° sickle genotype; 2) Age less than 6 months; 3) No prior episode of ASS. At each study visit, complete clinical work up and blood sampling were performed and relevant medical events were recorded. Patients were followed with scheduled visits planned at enrolment (3 and/or 6 months), 12, 18 and 24 months. All received standard age-appropriate care for SCA, however none were treated with hydroxyurea in accordance to national treatment guidelines during the study period. No child was lost to follow up. The protocol was approved by the ethics committee “Comité pour la Protection des Personnes Ile de France II” and by the French agency for security of health products (AFSSAPS). ASS was defined by the sudden enlargement of spleen (>2cm compared to basal) with a decrease of Hb level (>2 g/dl compared to previous measurement) and reticulocytes >100 000/mm³. Asymptomatic patients were defined as patients who did not experience any ASS, vaso-occlusive crisis (VOC), transfusion or hospitalization for SCD-related events during the follow up period up to 24 months of age.

At each visit, blood analysis for routine and SCA specific biomarkers was performed as described elsewhere (Brousse et al., 2018). In addition, RBCs reserved in ID-CellStab (Biorad) were cryopreserved in the Centre National de Référence pour les Groupes Sanguins (CNRGS). Blood samples from 7 healthy adult donors obtained from the Etablissement Français du Sang (EFS) were used as negative control.

In this cohort of 57 patients, HJB-RBCs and ISCs quantification was performed in 45 patients for whom sufficient sample volumes were available at two different time points (3-6 and 18 months) and who had not been transfused in the prior 2 months (Figure I.4). However, 7 of

these infants were transfused at some point during the follow up. Adhesion assays were performed in 15 randomly selected non-transfused patients for whom samples were available at all time points for longitudinal analysis.

Splenic scintigraphy was initially part of the systematic splenic exploration in all infants enrolled in the study but following parental reluctance, an amendment to the protocol was agreed upon, and spleen scintigraphy exploration became optional. Transfusion was not an exclusion criterion. It was performed in 25 patients at the first time point (3-6 months), 17 of whom underwent a sequential exploration at 18 months. The subgroup in whom splenic scintigraphy was performed was therefore based on parental acceptance and technical possibility (e.g. adequate venous access). Of note this subgroup did not differ from the rest of the cohort in terms of baseline clinical, biological or splenic characteristics (data not shown). Among the 25 patients who underwent a spleen scintigraphy, 7 were transfused at some point during the course of the study, 2 of which after splenic scintigraphy.

HJB-RBCs quantification

Sample preparation

Blood samples were collected using EDTA tubes and centrifuged at 1500 rpm for 5 min. Ten μ l of the RBC pellet were washed twice with 1 ml of buffer (PBS, 0.5% BSA) by centrifugation at 1500 rpm for 5 min at room temperature. RBCs were suspended in 1 ml of buffer, 80 μ l of the suspension were added to 120 μ l of buffer, and Hoechst 33342 (Life Technologies) is added at a final concentration of 40 μ g/ml and incubated for 5 min at room temperature.

Imaging Flow Cytometry assay

Samples were acquired with the ImageStream[®]x Mark II Imaging Flow Cytometer (IFC) (Merck Millipore) using the 405 laser. Analysis was performed using the IDEAS 6.2 software. The Hoechst-positive population was gated with reference to a negative tube. To quantify the HJB-containing RBCs we developed a mask using the Modulation feature (a feature measuring

the intensity range of an image normalized between 0 and 1) and the H Entropy feature (a texture feature used to determine if pixel values in an image follow a pattern or are randomly distributed). The above features were chosen due to their ability to distinguish significantly the specific HJB-containing RBCs population from the non-specific staining. As shown in Supplementary Figure 1A, using the H Entropy Mean_M07_Hoechst on the x-axis and Modulation_Morphology (M07, Hoechst)_Hoechst on the y-axis, we set up the coordinates of the gate as: 3.356 - 5.9 on the X-axis and 0.38 - 0.456 on the Y-axis.

Flow Cytometry assay

Samples were prepared in the same manner as in the previous paragraph and acquired with a BD FACSCanto II Flow Cytometer using the 405 laser. 50,000 events were acquired for each sample using the DIVA software. Analysis was performed using the FCS Express 6 Flow Research Edition software (De Novo Software).

Blood smears and May-Grünwald-Giemsa staining

A drop of blood was placed on one end of a glass slide and dispersed over the slide's length using a coverslip. The blood smears were fixed with methanol for 30 seconds at room temperature and stained with May-Grünwald-Giemsa staining (1/10 dilution in PBS) for 20 min. The slides were then washed with deionized water and left to dry. Photos were taken using an upright microscope (Leica DM6000 B) with a 20x/0,4 HCX PL FLUOTAR, equipped with a DFC300 FX color camera. HJB-containing RBCs were quantified using the ImageJ software.

Spleen scintigraphy

Spleen/liver scintigraphy, using heat-denatured ^{99m}Tc labeled RBCs, was performed in a subgroup of patients at two different time points (6 and 18 months) as previously described.(Owunwanne, Halkar, Al-Rasheed, Abubacker, & Abdel-Dayem, 1988). Spleen scintigraphy with heated autologous red cells measures primarily the filtrative capacity of the splenic red pulp because heated RBCs are poorly deformable and therefore get trapped in the splenic microvasculature,(Adekile et al., 1996; Klausner et al., 1975) as opposed to spleen scintigraphy with colloids which measures the phagocytic function of the spleen.(Adekile et al., 1996) Radionuclide images were taken of the posterior, left lateral, and anterior views of the spleen. Splenic uptake was compared with that of the liver and expressed in a semi quantitative percentage: 0-25% (lowest splenic uptake); 25-50; 50-75%; 75-100%; 100-150% (highest splenic uptake) (Figure 11). Spleen volume was calculated using computed tomography. Spleen volume was estimated after 1.5 hour of tomography acquisition.

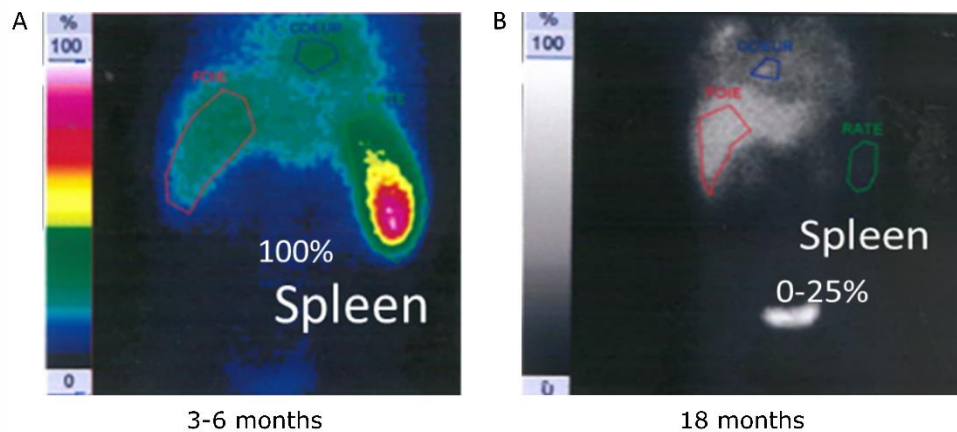


Figure 11: **Spleen/liver scintigraphy, using heat-denatured ^{99m}Tc labeled RBCs.** Images from a spleen/liver scintigraphy using heat-denatured ^{99m}Tc labeled RBCs performed in the same SCA infant at (A) 3-6 months with a splenic uptake of 100-150% and (B) 18 months with a splenic uptake of 0-25%.

Quantification of Irreversibly Sickled Cells (ISCs)

The percentage of irreversible sickle cells (ISCs) was determined using an Imagestream ISX MkII flow cytometer (Amnis Corp, EMD Millipore). Two μl of packed RBCs were suspended in 200 μl of ID-CellStab (Biorad) and 50,000 events were acquired. Irreversibly sickled cells (ISCs) were quantified using the IDEAS software (version 6.2) based on an analysis published by Van Beers et al (van Beers et al., 2014). Using features of morphology and shape, we set up a new refined analysis to measure ISCs. As shown in Figure 12, using the Raw Min Pixel_MC Ch01 on the x-axis and Modulation_Object (M01,Ch01, Tight) on the y-axis, we set up the coordinates of the gate as: 378.69 - 650.631 on the X-axis and 0.082 – 0.339 on the Y-axis.

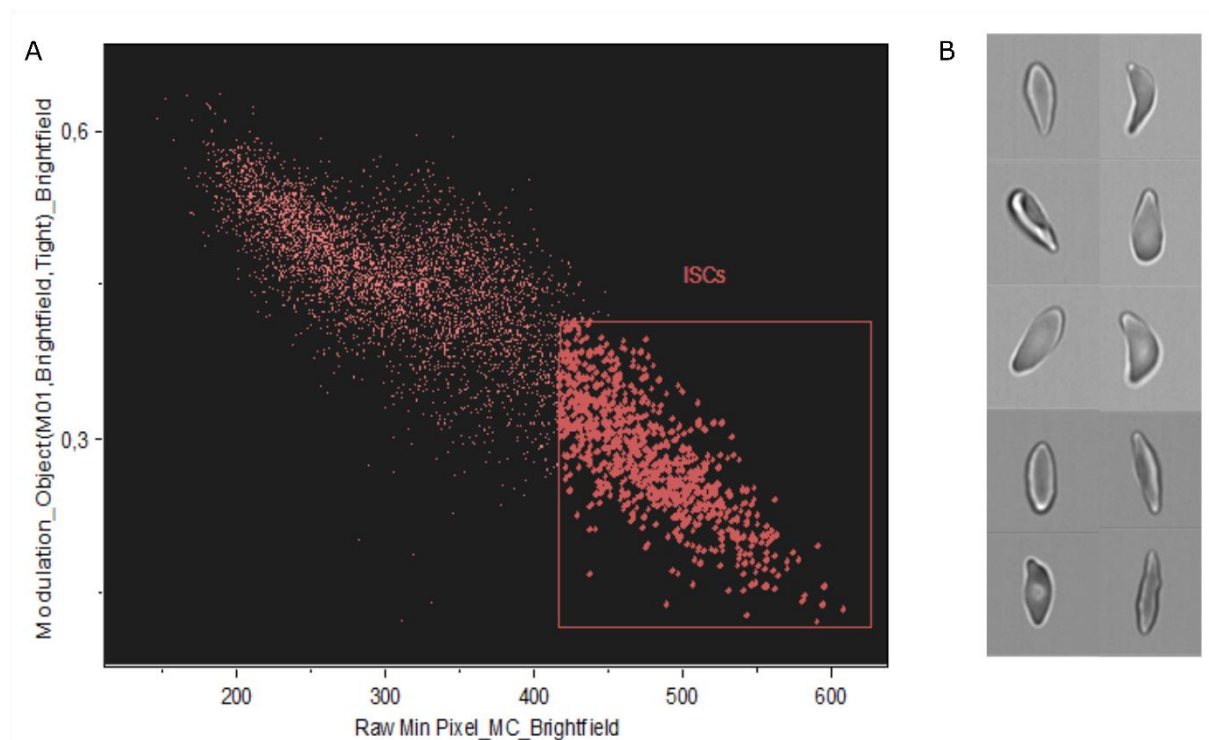


Figure 12: **Quantification of irreversibly sickled cells using imaging flow cytometry.** (A) Gating of ISCs in an SCA blood sample using imaging flow cytometry. (B) images of irreversibly sickled cells (ISCs) typical of the population present in the ISCs gating.

Flow cytometry analysis

Blood samples were washed 3 times with PBS and 5 μl of RBC pellet was suspended in 5 mL of PBS supplemented with 0.2% BSA. The mouse monoclonal primary antibody was prepared

as follows: CD239 (F241 clone, INTS) was prepared at a dilution of 1/10. Washed RBC suspensions (80 μ l) were incubated with 20 μ l of the allocated primary antibody for 60 min at room temperature. The samples were then washed twice with PBS 0.2% BSA followed by the addition of an anti-mouse PE-conjugated secondary antibody (Beckton Dickinson) at a dilution factor of 1/100. The secondary antibody was incubated for 45 min in the dark at room temperature. After 2 washes with PBS 0.2% BSA, 200 μ l of Retic-Count™ (Becton Dickinson) were added to each sample. After an incubation of 30 min the samples were analyzed using a BD FACScanto II flow cytometer (Becton Dickinson) and FACSDiva software (Version 6.1.3).

Flow adhesion assays

Red blood cell adhesion to TrHBMEC monolayers or to immobilized laminin 521 (Biolamina AB, Sundbyberg, Sweden) was determined under physiological flow conditions using Vena8 Endothelial+ biochips (internal channel dimensions: length 20 mm, width 0.8 mm, height 0.12 mm) and ExiGo nanopumps (Cellix Ltd, Dublin, Ireland).

Culture of TrHBMECs in Vena8 Endothelial+ biochips

For each experiment, TrHBMECs were cultured in 4 channels of a Vena8 Endothelial+ biochip for a period of 48 hours before performing the adhesion assay. The channels of the chip were coated with 0.2% gelatin and placed in the incubator (37°C) for 20 min before the addition of the cell suspension. The cell suspension was prepared at a concentration of 8×10^6 cells/mL in complete medium. After perfusion of TrHBMECs in the channels the biochip was incubated for 1.5 hour at 37°C 5% CO₂ to allow cell attachment and spreading. The channels were then connected to the Kima pump to ensure medium renewal during the 48h of culture. The medium circulation rate through the channels was as follows: a circulating phase at 300 μ l/min for 30 seconds followed by a 2-hour static phase. The circulation was monitored by the iKima application. After 24 hours of culture, TNF α (100 U/mL) was added to the media to activate the endothelial cells during 24 hours.

Coating of channels with laminin

Laminin 521 (5 ng/ μ l) solutions were added to the channels of a Vena8 Endothelial+ biochip. The biochip was placed in a humid box at 4°C overnight. Prior to the adhesion experiments laminin coated channels were saturated with hanks solution supplemented with 5% BSA for 2 hours.

Preparation of blood samples

Red blood cells were washed 3 times with PBS by centrifugation at 300 g for 5 min. Cell suspensions in Hanks buffer supplemented with 0.4% BSA were adjusted at 15×10^7 cells/mL or 5×10^7 cells/mL for adhesion assays on TrHBMECs or laminin respectively.

Adhesion assays under flow conditions

Adhesion assays were performed at the Dynamic Adhesion Platform (Institut National de la Transfusion Sanguine, Paris). Four blood suspensions were perfused in parallel at a shear stress of 0.5 dyn/cm² for 5 min (laminin) or 0.2 dyn/cm² for 10 min (TrHBMECs) using the ExiGo nanopumps, and 5-minutes washouts were performed with Hanks buffer supplemented with 0.4% BSA at 0.5, 1, 2, 3, 5 and 7 dyn/cm². After each wash, adherent cells were counted in 5 representative areas along the centerline of each channel using the AxioObserver Z1 microscope and AxioVision 4 analysis software (Carl Zeiss, Le Pecq, France). Images of the same 5 areas were obtained throughout each experiment using the “Mark and Find” module of AxioVision analysis software. Quantification of adherent cells was done by the ImageJ software (Image Processing and Analysis in Java).

Immunoprecipitation and Western blot analyses

RBCs were lysed for 45 min at 4°C with lysis buffer (Tris 20mM, NaCl 150 mM, EDTA 5mM, Triton x100 1% and Azide 0.02%). After centrifugation at 15000 rpm for 15 min at 4°C supernatants were incubated with 2 μ l of goat serum and 15 μ l of protein A sepharose (PAS) (Amersham Biosciences) in a preclearing step of 3 hours at 4°C. After centrifugation at 5000

rpm for 5 min at 4°C supernatants were incubated with the mouse monoclonal anti-Lu/BCAM antibody (clone F241) and 15 µl of PAS overnight at 4°C. After centrifugation the beads were washed 5 times with lysis buffer and the proteins eluted in Laemmli buffer at 100°C for 5 min. Proteins were electrophoresed through 8% SDS-polyacrylamide gel and electroblotted to a nitrocellulose membrane. The membrane was blocked in TBS 1x, 0.1% tween 20, 5% BSA (TBS-T-B) and probed with rabbit polyclonal anti-PhosphoLu antibody (1:10000 dilution in TBS-T-B). This was followed by anti-rabbit antibody conjugated to horseradish peroxidase (1:2000 dilution in TBS-T-B). The signal was revealed using the chemiluminescent detection assay (ECL; GE Healthcare Life Sciences) and images were captured using the Chemidoc (BIORAD). The membranes were then probed with biotinylated anti-Lu antibody (R&D Systems) (1:10000 dilution in TBS-T-B), which was followed by HRP-conjugated streptavidine (Amersham International) incubation (1:2000 dilution in 1x TBS containing 0.05% tween 20) and revealed with ECL (GE Healthcare Life Sciences). The quantification of the proteins was achieved using Quantity One Software (Biorad).

Statistics

Data were analyzed by two-tailed Wilcoxon test or paired Wilcoxon test as appropriate. Association between quantitative variables was assessed using Spearman correlation test. GraphPad Prism 7.00 and R software were used. * $p < 0.05$, ** $p < 0.01$, *** $p < 0.001$ and **** $p < 0.0001$ were considered significant.

*CHAPTER II: New Insights into the
Expression and Cellular Distribution of
HbF, and the Effect of Hydroxycarbamide*

RESULTS

Fetal hemoglobin (HbF) is a modulator of disease severity as it inhibits HbS polymerization. Therefore, determining the percentage of F-cells with significant HbF concentrations using an accurate and simple method is of major interest in SCD, both for clinical and research purposes. In this part of the project, we first used a microfluidic approach to analyze the effect of HbF content in protecting red cells from mechanical stress and hemolysis. The design and fabrication of the microfluidic device is detailed in our publication in *Lab on a Chip* which is also found in the Appendix on page 189 (DOI: 10.1039/c8lc00637g), these aspects will therefore not be further discussed in the chapter.

In this chapter, we analyzed HbF intracellular concentration using imaging flow cytometry and defined 3 populations of F-cells based on HbF content: Low, Medium and High F-cells. We analyzed the distribution of these subpopulations in young infants, untreated patients and patients treated with hydroxycarbamide, and studied the effect of HbF on the ability to generate ISCs and to protect from mechanical stress.

Early survival advantage of F-cells during erythroid maturation

In SCD, F-cells have a survival advantage in the circulation over RBCs with no HbF (Franco et al., 2006). This feature can be evidenced by the increase in the fraction of F-cells (or enrichment of F-cells) during erythroid maturation i.e. between the reticulocyte and the mature RBC stages within one blood sample. In SCD patients, reticulocytes exit the bone marrow at an immature stage, as a consequence of marrow hyper stimulation by peripheral hemolysis. We investigated the distribution of HbF across 3 different maturation stages, ranging from immature to mature RBCs: R1 reticulocytes (CD71⁺RNA⁺), R2 reticulocytes (CD71⁻RNA⁺) and mature RBCs (CD71⁻RNA⁻). Cells were fixed, permeabilized to allow entry of PE-conjugated anti-HbF antibody and analyzed by flow cytometry. First, we confirmed enrichment of F-cells between the reticulocyte and mature stages as %F-cells was higher in mature RBCs

than in reticulocytes for each patient considered individually (Figure 1A and 1B). When assessing F-cells within the reticulocyte population, we also found enrichment between the R1 and the R2 stages (Figure 1C), suggesting that reticulocytes are prone to hemolysis few minutes or hours after exiting the bone marrow.

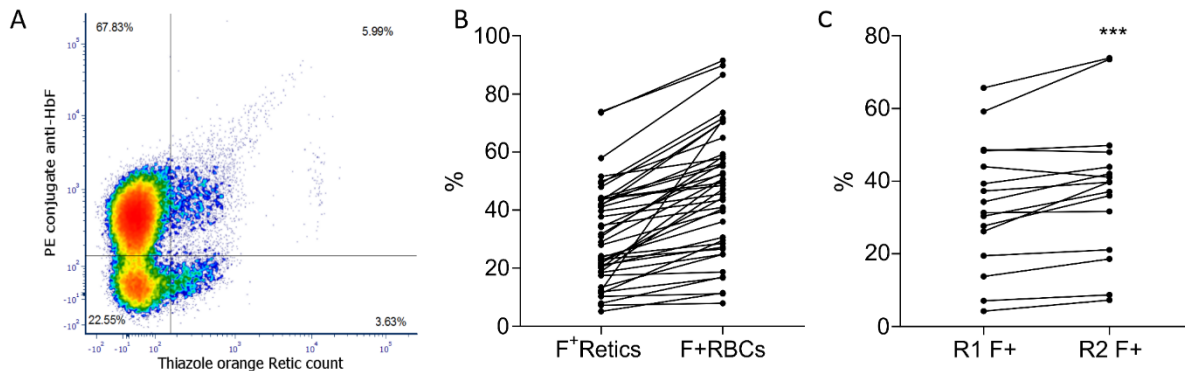


Figure 1: HbF in reticulocytes and mature RBCs. (A) Flow cytometry dot plot representing RBCs stained for HbF (Y axis) and a reticulocyte marker (X axis). (B) Percentage of HbF-positive cells in reticulocytes and mature RBCs of 42 SCD patients. (C) Percentage of HbF-positive cells in young reticulocytes (R1 - CD71⁺) and older reticulocytes (R2 - CD71⁻) of 16 SCD patients. Wilcoxon paired test ** $p < 0.01$, *** $p < 0.0001$.

High, medium and low % of HbF within F-cells in non-treated patients

We estimated the expression level of HbF within the F-cell (HbF containing cells) population by measuring the mean fluorescence intensity (MFI) by flow cytometry (Figure 2A). We found a wide distribution of the MFI across patients (Figure 2B) indicating that HbF has different expression levels within F-cells. To further explore the expression level of HbF within the F-cell population, we set up a measurement method based on imaging flow cytometry that takes into account both the intensity of the fluorescent signal and the cell size, thus reflecting HbF intracellular concentration. Using this method, we divided F-cells into 3 subpopulations depending on HbF intracellular expression level: Low, Medium and High F-cells (Figure 2C and D). We determined the percentage of each subpopulation in 36 untreated SCD patients and found a wide distribution within the 3 subpopulations among all patients (Figure 2E). More

importantly Low F-cells were predominant compared to Medium and High F-cells (Figure 2E), indicating that while HbF is distributed in a high number of cells, only a small fraction of F-cells contain high amounts of HbF. To validate our gating method and challenge our conclusion, we assessed the presence of irreversibly sickled cells (ISCs) within the 3 subpopulations as an *in vivo* marker of low HbF expression level (Serjeant et al., 1978), since HbF interferes with polymerization and hence sickling. We evidenced ISCs in both non-F and F-cells subpopulations (Figure 2F), with decreasing percentages according to the F content. The absence of ISCs in the High F-cell subpopulation and the high levels of ISCs in the Low F-cell subpopulation (Figure 2F) suggested that HbF needs to reach a possibly high threshold level to be protective against sickling and hence prevent ISCs to be produced.

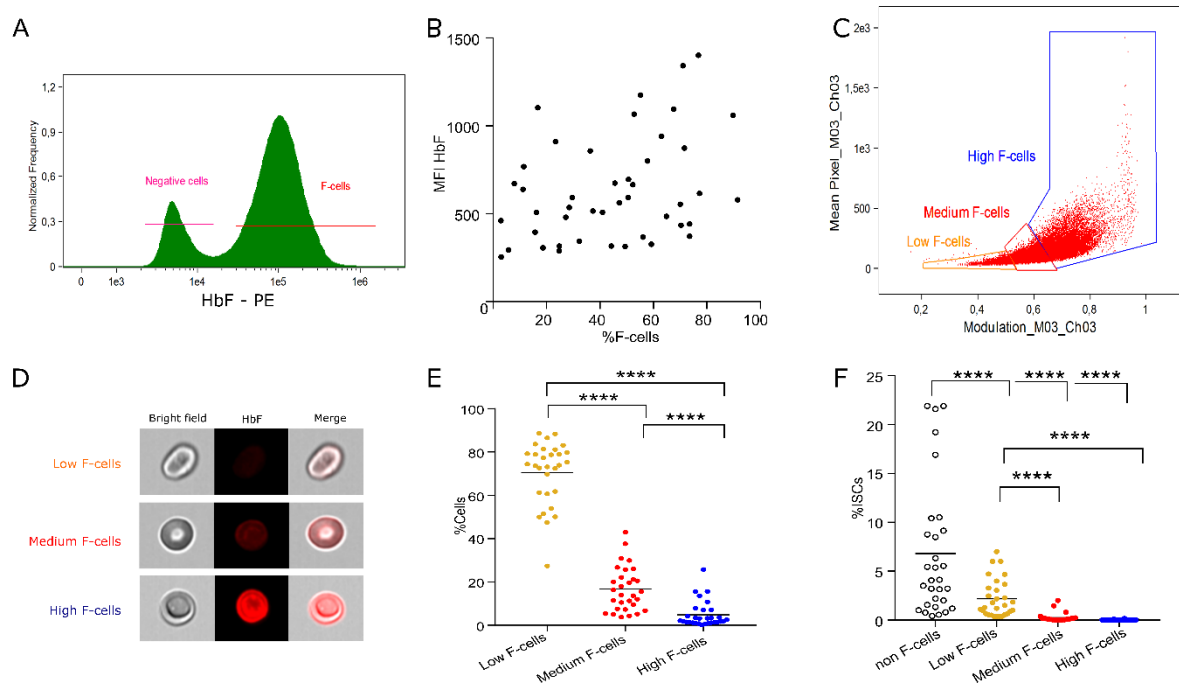


Figure 2: Expression and cellular distribution of HbF in non-treated red cells. (A) Flow cytometry histograms representing the expression of HbF in SS RBCs. (B) Correlation between the %HbF and the mean fluorescence intensity (MFI) of F-cells ($n=45$, $R^2=0.127$). (C) Imaging flow cytometry (IFC) dot plot representing the three populations of F-cells: Low, Medium and High F-cells. (D) Images of Low, Medium and High F-cells obtained by IFC. (E) Distribution of the percentage of Low, Medium and High F-cells within total RBCs of 30 non-treated SCD patients. (F) %ISCs in non-F-cells, Low, Medium and High F-cells ($n=30$). Wilcoxon paired test. Mann-Whitney test, **** $p<0.0001$.

F-cells with low levels of HbF are lysed upon mechanical challenge

Using a microfluidic biochip in which flowing RBCs were challenged mechanically in 10 consecutive 5 μm x 5 μm channels, we have recently shown that F-cells resist better to lysis than non-F-cells (Figure 3A and B) (Lizarralde Irigorri et al., 2018). A typical assay consisted in perfusing RBC suspensions in the biochip and measuring free hemoglobin and %F-cells at the entry (Input) and the exit (Output) of the device. We further performed assays with 9 blood samples from homozygous SS patients and measured the % of Low and High F-cells before and after perfusion in the biochip. As expected, perfusion of RBC suspensions in the biochip led to hemolysis, with an increase of free hemoglobin concentration in the Output and an enrichment in F-cells (Figure 3C and D). Specifically, there was less Low F-cells and more High F-cells in the Output than in the Input (Figure 3E and F) indicating that Low F-cells were preferably hemolyzed upon mechanical stress, in these conditions. We also demonstrated that hemolysis of F-cells occurs *in vivo* with the presence of free HbF in SCD patients' plasma (Lizarralde Irigorri et al., 2018).

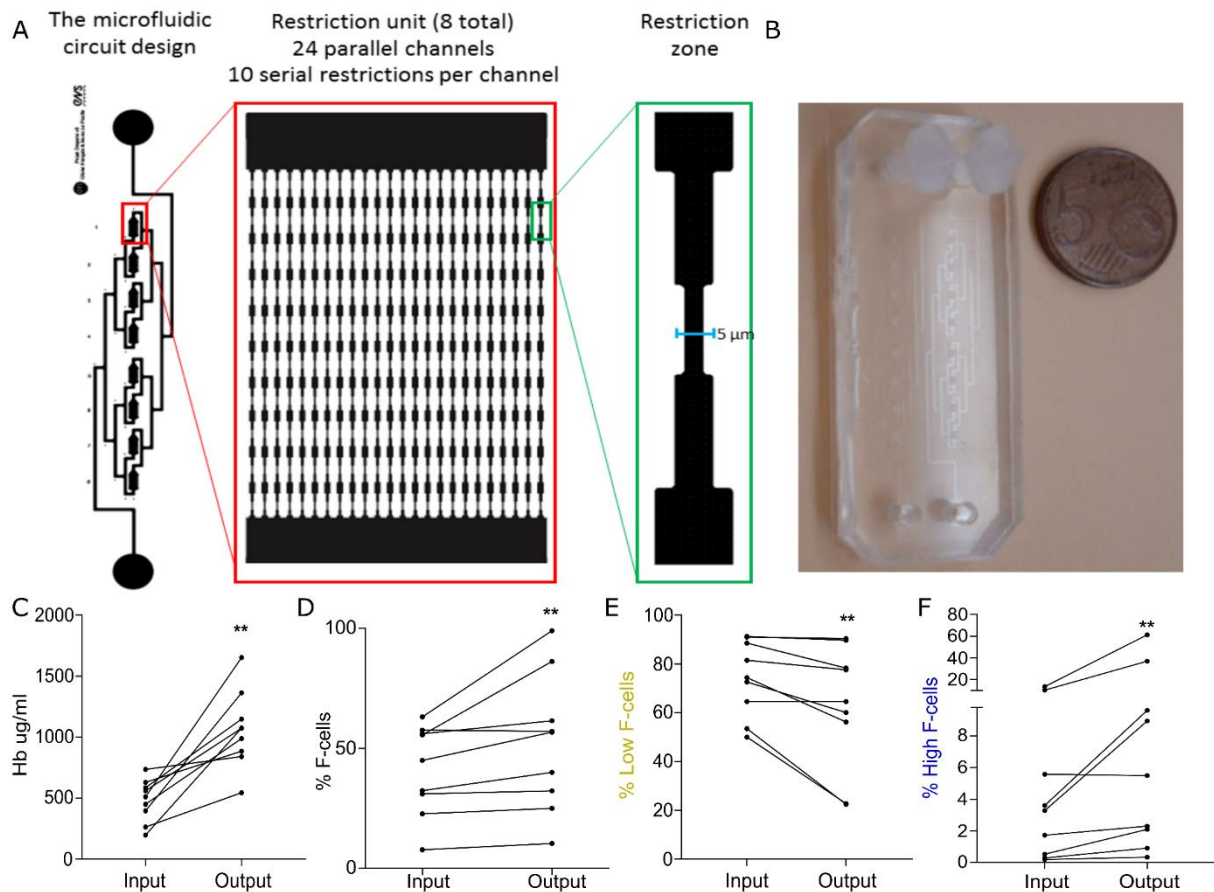


Figure 3: **The microfluidic biochip.** (A) Each microfluidic circuit (*top left panel*) is composed of 8 restriction units of 24 parallel channels with 10 serial restrictions of 5 µm in each channel. (B) The PDMS biochip with 2 independent circuits. (C) Free hemoglobin in the supernatant of RBC suspensions before and after mechanical stress of SS RBCs (n=9). Percentage of (D) F-cells (E) Low F-cells and (F) High F-cells before and after mechanical stress of SS RBCs (n=9). ** $p < 0.01$. Wilcoxon paired test.

HbF expression and distribution in infancy

We investigated HbF expression and distribution within RBCs in a longitudinal manner in a cohort of SCD infants between the age of 3-6 and 18 months. As expected, %HbF and %F-cells decreased from 3-6 than to 18 months (Figure 4A and B) in relation with the progressive decrease of γ gamma globin expression and the increase of β globin. We determined the % of Low, Medium and High F-cells in total RBCs and found a wide distribution at both time points, with Low F-cells representing the largest fraction (Figure 4C), indicating that the majority of F-cells had relatively small amounts of HbF. There was a significant decrease with time of

Medium and High F-cells in total blood at 18 months (Figure 4C). Within the F-cell population only, we found the same decrease of Medium and High F-cells at 18 months and in addition an increase of Low F-cells resulting in an altogether different HbF distribution at 18 months, with an increasing proportion of cells having small amounts of HbF, as observed in older patients (Figure 4D).

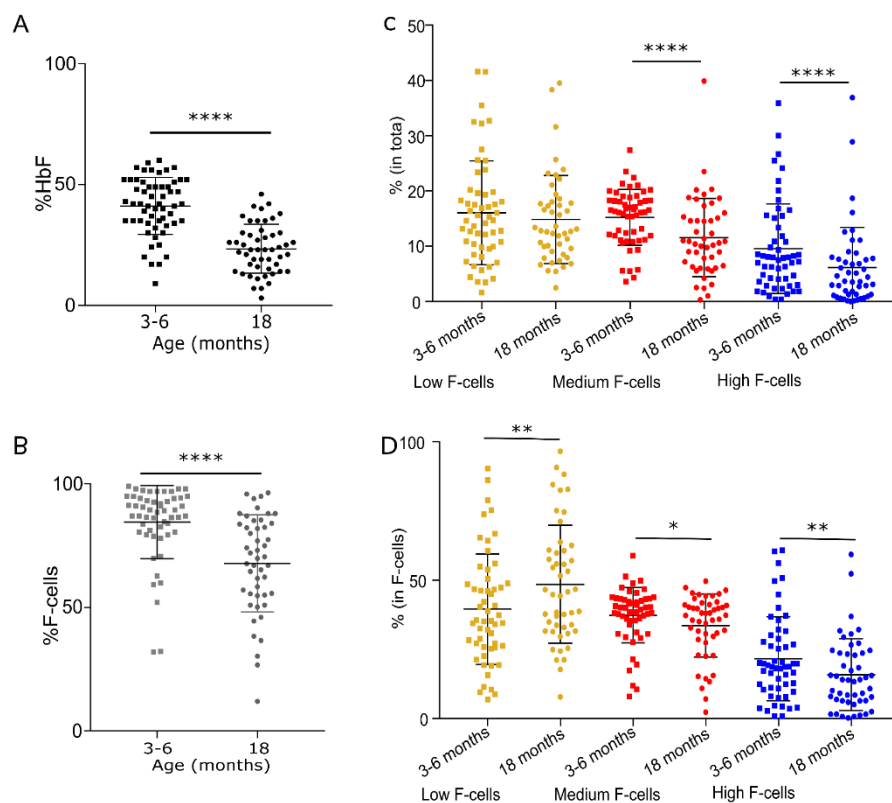


Figure 4: **F-cells distribution in SCD children.** Percentage of (A) HbF and (B) F-cells measured at 3-6 and 18 months in 50 SCA children. Percentage of Low, Medium and High F-cells in (C) total RBC population and in the (D) F-cell population measured in 47 SCD children at 3-6 and 18 months. * $p < 0.05$, ** $p < 0.01$, **** $p < 0.0001$. Wilcoxon paired test.

Impact of HC on HbF expression and cellular distribution

We studied the effect of HC on the expression and distribution of HbF in RBCs using the same imaging flow cytometry method. We analyzed HbF expression in a longitudinal manner in 10 homozygous patients before and after a minimal period of 7 months after HC treatment initiation at an average dosage of 20-25mg/kg/day. As expected, %HbF, as measured by HPLC,

and %F-cells were increased following treatment (Figure 5A and B). The effect of HC also translated into lower levels of ISCs during treatment (Figure 5C). Assessing the cellular distribution of HbF, we found an inverted profile regarding the Low, Medium and High subpopulations, with higher percentages of High than Low F-cells following treatment (Figure 5D). Investigating the distribution of Low and High F-cells within the F-cell population, we observed a systematic increase of %High F-cells for all patients and a decrease of %Low F-cells (Figure 5D). Regarding the distribution of HbF in the total RBC population, we observed a decrease in Low F-cells in the majority of the patients (Figure 5E). Note that the 4 patients who showed an increase in Low F-cells are those with the lowest HbF levels recorded before the start of HC treatment. Altogether, this indicates that HC increases both the percentage of cells expressing HbF and the intracellular concentration of HbF in these cells.

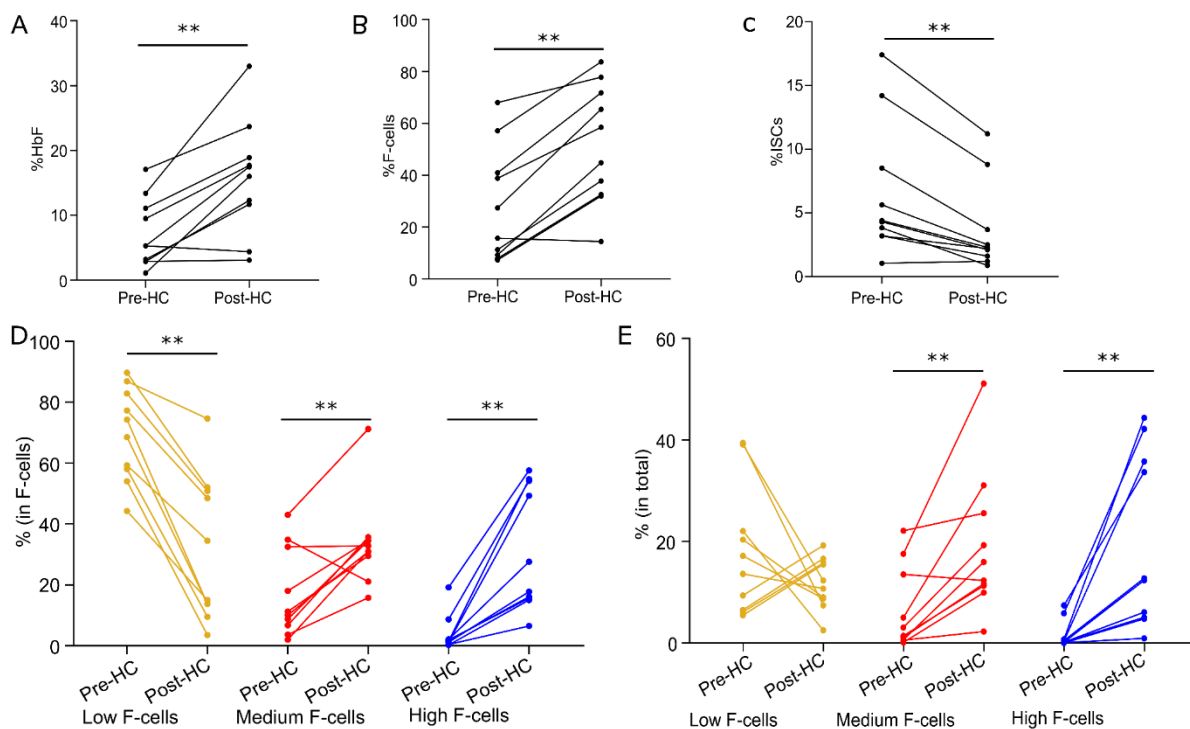


Figure 5: Effect of HC on HbF distribution. The percentage of (A) HbF, (B) F-cells and (C) ISCs pre and post HC treatment. The percentage of Low, Medium and High F-cells pre and post HC treatment in (D) the F-cell population and (E) total RBC population. (n=10). ** $p < 0.01$. Wilcoxon paired test.

Effect of HC on RBC mechanical properties

To gain insight into the effect of HC treatment on the mechanical properties of RBCs we performed microfluidic assays with RBCs from HC-treated patients. Significant levels of hemolysis were found to occur during the assays for all patients (Figure 6A) but unexpectedly there was no enrichment of F-cells (Figure 6B), indicating that under HC treatment, mechanical stress does not preferentially induce hemolysis of the non-F population.

To further explore the mechanism underlying this observation, we hypothesized that under HC treatment, non-F-cells might be more resistant to shear stress because of improved deformability following better hydration, reflected by greater MCV (from 76 fl to 92 fl), a hypothesis already stated by Orringer et al (Orringer et al., 1991). HC is known to increase the mean corpuscular volume (MCV) of RBCs, which is believed to be subsequent to the increase of %F-cells in the circulation, which have a bigger MCV (Wiles & Howard, 2009). However, there are no specific analyses of the size and morphology of F and non-F-cells previously published. To evaluate RBC volume, we relied on imaging flow cytometry, using the projected surface area (PSA) feature, by gating only circular RBCs facing the camera. First, we measured PSA of F and non-F-cells before HC treatment and confirmed that F-cells were larger than non-F-cells in all 10 patients (Figure 6C and D). There was an increase in the PSA of both F and non-F-cells under HC treatment, (Figure 6E) with non-F-cells reaching levels similar to those of F-cells and control RBCs (Figure 6F). These data indicated that HC treatment increases cell volume of RBCs regardless of HbF expression, with positive impact on cell shape and morphology and possibly deformability. This was further supported by showing that %ISCs within the non-F-cell population was lower during HC treatment than before (Figure 6G).

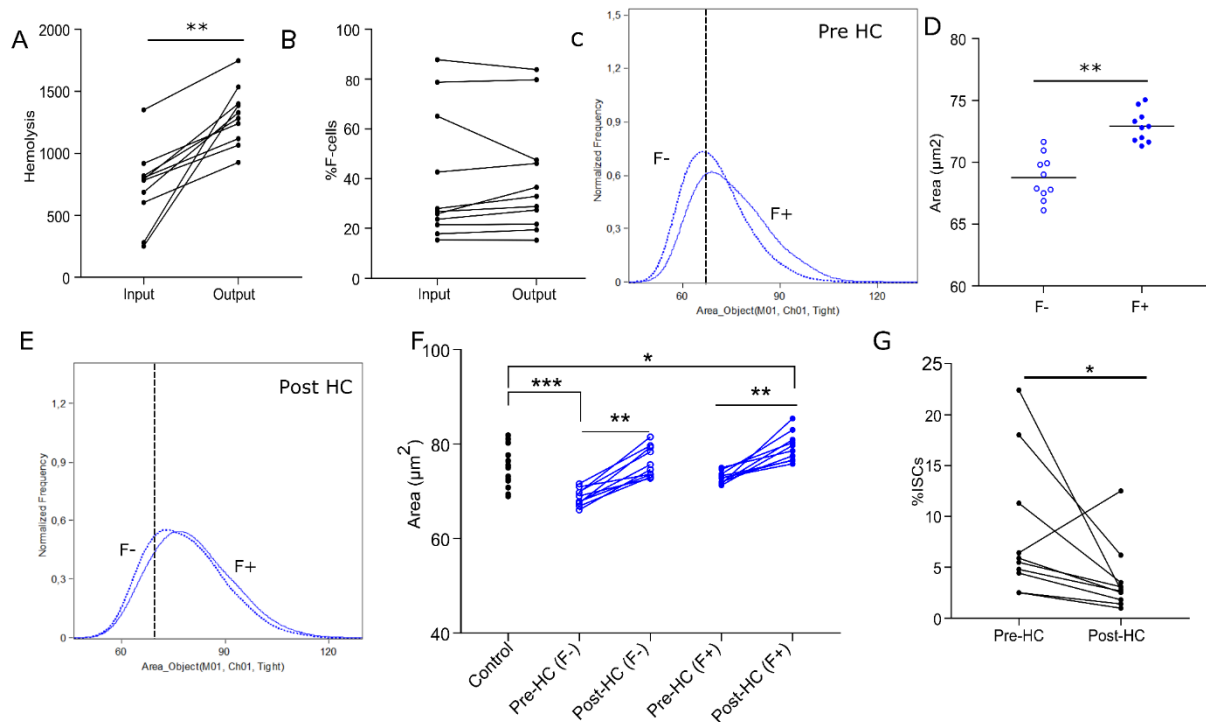


Figure 6: Effect of HC on RBC volume. (A) Free hemoglobin in the supernatant of RBC suspensions before and after mechanical stress of HC treated SS RBCs (n=10). (B) Percentage F-cells before and after mechanical stress of SS RBCs (n=10). (C) A histogram representation of the surface area distribution measured by imaging flow cytometry of non-F and F-cells before HC treatment for one patient. (D) Surface area of non-F and F-cells before HC treatment in 10 patients. (E) A histogram representation of the surface area of non-F and F-cells after HC treatment in one patient. (F) Surface area of non-F and F-cells before and after HC treatment in 10 patients and 15 control. (G) Percentages of ISCs in the non-F cell population before and after HC treatment in 10 patients. * $p < 0.05$, ** $p < 0.01$, *** $p < 0.001$. Wilcoxon paired test. Mann-Whitney test.

Relationship between %HbF and %F-cells according to age or HC treatment

To explore the relationship between total amounts of HbF and its cellular distribution, we plotted %HbF measured by HPLC against %F-cells determined by flow cytometry. There was a linear regression between both parameters in all patient categories but with different R^2 values indicating a different evolution of HbF cellular distribution according to age. More precisely, the values showed an important scattering at 3-6 months as compared to 18 months, which was in turn more scattered than in children > 4 years. This difference was reflected by a poor value of R^2 at 3-6 months (0.23), which increased at 18 months (0.45) and tended to one in older children (0.88) as well as in HC-treated patients (0.8) (Figure 7), demonstrating that %HbF is

a good indicator of HbF cellular distribution in older children and patients treated with HC as it is sufficient to predict %F-cells. Conversely, in infants at 3-6 months of age, %F-cells poorly predict %HbF likely because most patients show a pan distribution of HbF, as the globin switch is only just beginning.

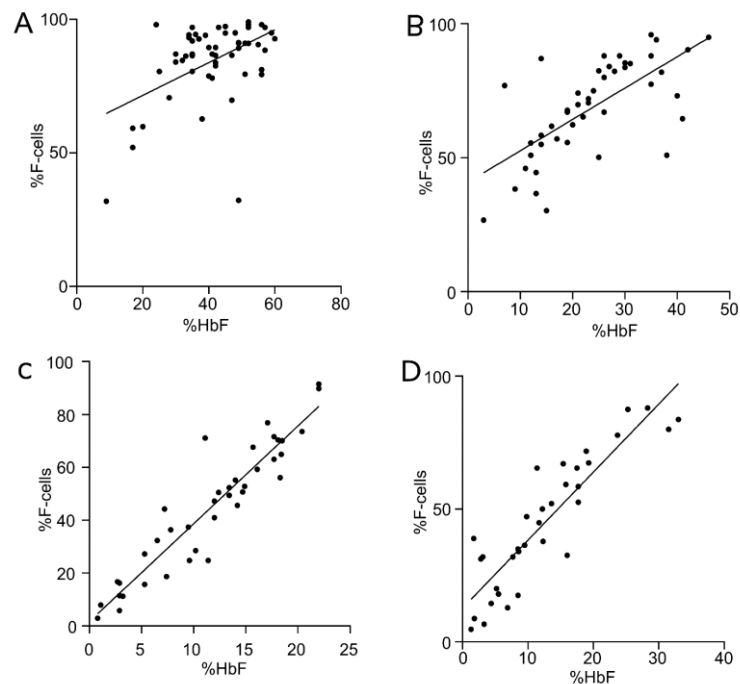


Figure 7: **HbF correlation with F-cells.** A linear regression plot of %HbF and %F-cells in (A) 3-6 months (n=54), (B) 18 months (n=54), (C) >4 years non-treated (n=38) and (D) HC-treated patients (n=38). Linear Regression.

Given the role of intracellular levels of HbF in protecting RBCs from lysis, we then compared the different categories of F-cell populations in relation with %HbF. In infants and non-treated patients, total %High F-cells was not correlated with %HbF indicating that %HbF measured by HPLC does not reflect the proportion of circulating cells with high amounts of HbF in these patients (Figure 8A-C).

Conversely, in HC-treated patients %High F-cells was correlated with %HbF (Figure 8D), indicating that under HC, %High F-cells is a great contributor to %HbF measured by HPLC. Note that, while Low F-cells correlated with %HbF in non-treated patients, no correlation was

observed in the HC-treated cohort. The latter indicating that %HbF measured by HPLC reflects different F-cell populations in non-treated and HC-treated patients, Low and High F-cells respectively.

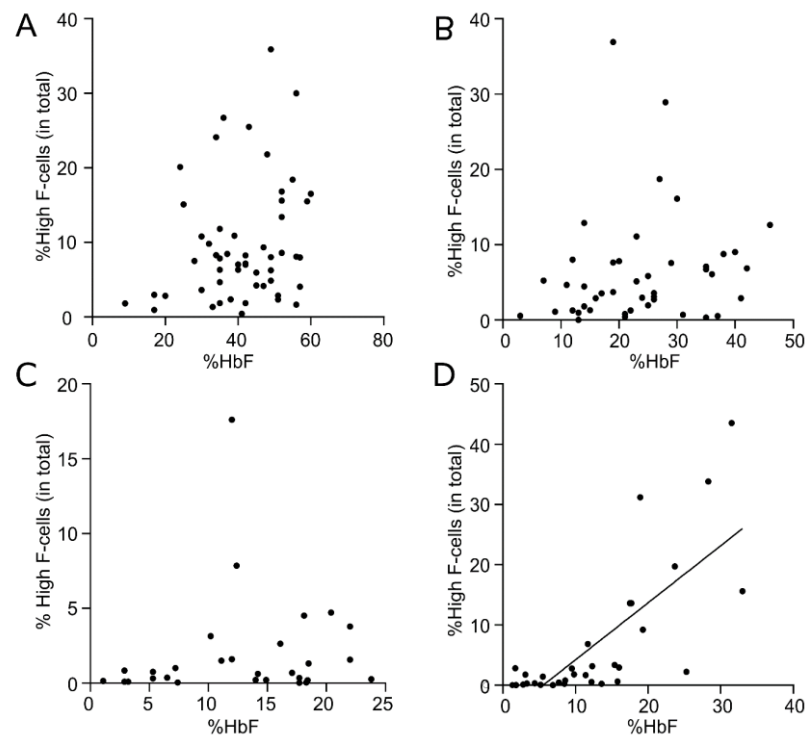


Figure 8: **HbF correlation with High F-cells.** A linear regression plot of %HbF and %High F-cells (in total RBCs) in (A) 3-6 months (n=54), (B) 18 months (n=54), (C) >4 years non-treated (n=30) and (D) HC-treated patients (n=30). Linear Regression.

Effect of HC treatment on the distribution of High and Low F-cells

We similarly investigated the correlation between HbF and Low and High F-cells within the F-cell population in treated patients (unknown dosage). We found that HbF has a negative correlation with %Low F-cells and a positive correlation with %High F-cells, altogether illustrating how HC changes the distribution of HbF in F-cells (Figure 9A and B). To further confirm the effect of HC on HbF distribution in circulating RBCs, we performed a curve fitting for both subpopulations. We obtained a second order polynomial fit for Low F-cells and HbF,

with an equation of $f(x)=4.242+0.8224x-0.0275x^2$ for the mean of the distribution assuming normal distributed noise (Figure 9C). For the relationship between High F-cells and HbF a second order polynomial curve was also obtained for the mean with the equation of $f(x)=-0.7348+0.08962x+0.02731x^2$ (Figure 9D).

A plot was then extracted for each curve (Figure 9E and F). At HbF levels of 13.76%, the %Low F-cells starts to decrease, concomitantly with an increase of %High F-cells (Figure 9E and F). These results showed that under 13.76% of HbF the main effect of HC is an increase of %Low F-cells, with very low amounts of High F-cells in the circulation (mean: 1.25%). They also suggest that %HbF of 13.76% could be considered as a target value above which significant amounts of F-cells with high amounts of HbF are present in the circulation.

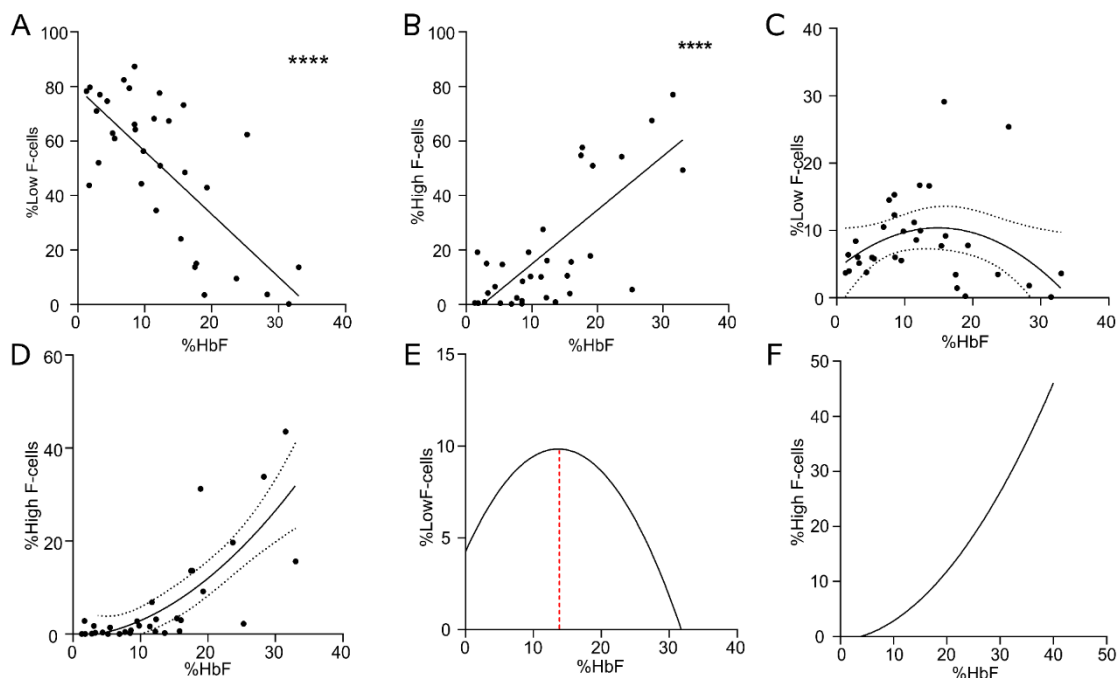


Figure 9: **Cellular distribution of HbF during HC treatment.** Linear regression between HbF and (A) Low F-cells and (B) High F-cells within the F-cell population in HC treated patients (n=34). A second order polynomial fit for HbF and (C) Low F-cells and (D) High F-cells. A function plot of HbF with respect to (E) Low F-cells and (F) High F-cells. **** $p<0.0001$.

To test the effect of this cut-off value regarding biological parameters, we divided the HC-treated population in two groups according to the %HbF cutoff of 13.76%. We found slight but not significant increase of hematocrit and total hemoglobin concentration in the group of patients with >13.76% HbF associated with a slight decrease in percentage reticulocytes and total bilirubin. Interestingly, however, in patients with %HbF >13.76% there was a higher %F-reticulocytes and F-cells together with less ISCs indicating that HC-treated patients with >13.76%, despite non-significant differences in hematological parameters, may have beneficial clinical effects (i.e. less sickling) than those with <13.76% HbF (Figure 10A-C).

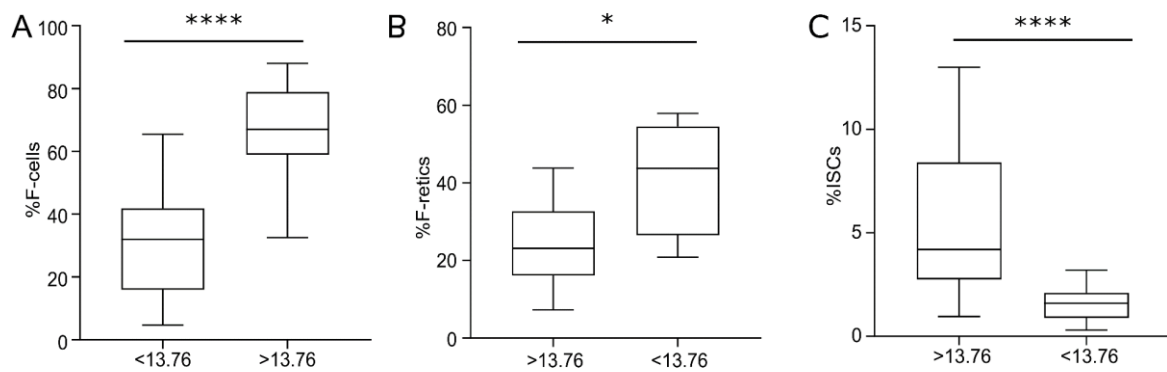


Figure 10: **HbF and ISCs during HC treatment.** A graph representing the percentage of (A) F-cells, (B) F-reticulocytes and (C) ISCs in two groups of HC-treated patients, group1: HbF <13.76 (n=21) and group 2: HbF >13.76 (n=17). Mann-Whitney unpaired test. * $p < 0.05$, **** $p < 0.0001$.

DISCUSSION

HbF expression in sickle RBCs has been reported by several studies to positively improve red cell survival (Franco et al., 2006). These *in vivo* studies showed that the survival of non-F-cells is about 2 weeks for most SCD patients versus about 6 weeks for F-cells (Franco et al., 1998), but did not explore the specific mechanism by which HbF expression was beneficial. Our results support these findings and further extend them by highlighting the role of HbF content and distribution in protecting red cells from hemolysis secondary to mechanical stress, including in immature reticulocytes. Altogether, our results emphasize the protective role of HbF against mechanical hemolysis during sickle red cell maturation in the circulation.

Using a microfluidics device, we demonstrated a specific decrease of Low F-cells after mechanical stress indicating that a subpopulation of F-cells which contain a low amount of HbF undergoes lysis, in line with a prior demonstration that a minimal threshold of HbF should be reached to protect RBCs from destruction (Maier-Redelsperger et al., 1998). *In vivo*, this was illustrated by our data showing that free hemoglobin in SCD patients' plasma is mainly composed of HbS, with very small amounts of HbF and that the HbF/HbS ratio in RBC lysates is significantly greater than in the plasma, as measured by HPLC. (Lizarralde Iragorri et al., 2018). The microfluidic data regarding High F-cells further validated our gating strategy and suggested that the High F-cells population expresses significant amounts of HbF that may fall within the previously reported protective range of 9-12 pg/cell (Maier-Redelsperger et al., 1994), given the absence of irreversibly sickled cells (ISCs) in the High F-cells population, while significant amounts were found in the Low F-cells population.

Using a longitudinal cohort, we showed that HC is not only able to increase HbF and % F-cells, i.e. induce an altogether higher amount of HbF, but also to modify HbF distribution by significantly increasing High F-cells and decreasing Low F-cells. Thus, HC treatment changes the cellular distribution of HbF. This effect translates into a decrease in ISCs levels in the circulation, including among the non F-cell population. Further exploring this finding, we

showed that HC treatment increases the volume of all cells in the circulation, regardless of their HbF content, including non-F cells. This confirms a possibly additional beneficial effect of HC through an increase in volume and potentially improved hydration of all cells. Our results confirm the hypothesis postulated by Orringer et al. in 1991, that the effect of HC on cell volume might be independent of HbF increase in the cells (Orringer et al., 1991). Ultimately, an increase of cell volume would translate into improved deformability as indirectly suggested by the absence of enrichment of F-cells following mechanical shear stress using our microfluidics device.

HPLC is used in clinical practice to monitor %HbF in patients treated with HC. The predictive value of %HbF is however poor because it does not reflect the cellular distribution of HbF within cells. Here, we showed that %HbF and %F-cells were tightly correlated in SCD patients >5 years with no HC treatment, meaning that %F-cells can be predicted with good confidence from %HbF. However, there was no correlation between %High F-cells and %HbF or %F-cells in these non-treated patients, indicating that none of these 2 parameters can predict the proportion of High F-cells in the circulation. Indeed, 2 patients with similar %HbF and close %F-cells can have very different proportions of High F-cells in the circulation. Conversely, in treated patients, as HbF levels start to increase more cells become High F-cells and are thus possibly better protected in the circulation.

Regarding SCD infants, we have previously shown that HbF measured by HPLC at 3-6 months is a predictive marker of severe outcomes up to 2 years of age (Brousse et al., 2018). Nevertheless, the lack of correlation between HbF and High F-cells at this age can be explained by the high content of HbF in almost all cells. Altogether, when the HbF level is high as in infants, High F-cells are expected to be very abundant, whereas when the HbF level decreases its distribution becomes critical as it can differ between patients. Monitoring both the quantity

of total HbF and the percentage of Low and High F-cells are therefore both important after the age of 2, when HbF levels start to decrease.

In order to better understand the changes of distribution of HbF within cells in the HC treated population, we modelled our results with a curve fitting for Low and High F-cells. Altogether, we observed that at an HbF value of 13.76% (HPLC), the Low F-cell population starts to decrease while the High F-cell population starts to increase. Our finding is in accordance with the concept of a threshold value as shown in the seminal clinical study by Platt et al. that demonstrated improved survival in patients with HbF levels higher than 8.6%. Likewise, simulations performed by Steinberg et al., suggested that at HbF levels lower than 5% , very few F-cells are protected while at HbF levels higher than 10% more protected cells are present (Platt et al., 1994; Platt et al., 1994; Steinberg, Chui, Dover, Sebastiani, & Alsultan, 2014).

This study gives new insights into the role of the mechanical dimension as a critical contributing factor to hemolytic anemia in SCD. It also highlights that HbF exerts its protective role *in vivo*, showing evidence that high HbF levels protect RBCs from hemolysis upon mechanical stress. This study altogether explores the beneficial effect of HbF on red cell protection against mechanical hemolysis, a potential major contributor of anemia in SCD patients. More specifically, we show that if a critical amount of HbF at a single cell level is necessary to exert this protection, yet under HC treatment a globally positive impact is achieved on the whole red cell population, including non F-cells. Finally, we show the potential role of High F-cells as a more precise marker of HC efficacy, and potentially clinical marker of decreased severity.

PATIENTS & METHODS

Patients

The study was conducted in accordance with the Declaration of Helsinki and was approved by the Regional Ethics Committee (n°3215 CPP Ile de France III). Blood samples were recovered from blood tubes drawn for medical care after written informed consent. Blood samples were collected on ethylenediaminetetraacetic acid (EDTA) from patients with sickle cell anemia (SS and Sbeta° genotypes), and from healthy donors (Etablissement Français du Sang).

Flow Cytometry and Imaging Flow Cytometry

HbF staining and analysis

Three μ l of RBCs were fixed in with 2.7% formaldehyde, 0.1% glutaraldehyde, PBS 1x for 15 min. After 2 washes with PBS, RBCs were permeabilized in 0.1 M Octyl β -D-Glucopyranoside for 15 min and saturated in PBS, 1% BSA, 0.2% goat serum for 30 min. The RBC pellet was suspended in 60 μ l of saturation solution and 10 μ l of this suspension were incubated with 5 μ l of PE-conjugated HbF antibody (Life Technologies), with or without 5 μ l of APC-conjugated CD71 antibody (Invitrogen), for 20 min. RBCs were washed and suspended in 200 μ l of BD Retic-Count™ (thiazole orange) reagent. After 30 min of incubation, cells were analyzed using a BD FACScanto II flow cytometer (BD Biosciences) and acquired using the Diva software version 8 (BD Biosciences). Data was analyzed using FCS Express 6 software (DeNovo Software).

Samples were also analyzed using the Imagestream ISX MkII flow cytometer (Amnis Corp, EMD Millipore) and the INSPIRE software version 99.4.437.0. Acquired data was analyzed using IDEAS software version 6.2 (Amnis Corp, EMD Millipore).

Irreversibly Sickled Cells Quantification

The percentage of irreversible sickle cells (ISCs) was determined using an Imagestream ISX MkII flow cytometer (Amnis Corp, EMD Millipore). Two μ l of packed RBCs were suspended

in 200 μ l of ID-CellStab (Biorad) and 50,000 events were acquired. Irreversibly sickled cells (ISCs) were quantified using the IDEAS software (version 6.2) based on an analysis published by Van Beers et al.¹⁸ Using features of morphology and shape, we set up a new refined analysis to measure ISCs. As shown in our publication found in the Appendix on page 189, using the Raw Min Pixel_MC Ch01 on the x-axis and Modulation_Object (M01,Ch01,Tight) on the y-axis, we set up the coordinates of the gate as: 378.69 - 650.631 on the X-axis and 0.082 – 0.339 on the Y-axis (Lizarralde Iragorri et al., 2018).

Hemolysis and HbF measurements

Free hemoglobin concentrations were determined using the Drabkin's reagent (Sigma - Aldrich). Briefly, 7.5 μ l of each RBC suspension supernatant were incubated with 17.5 μ l of Drabkin's solution for 30 min in the dark. Absorbance was then measured by Nanodrop 2000 (Thermo Scientific) at 540 nm and the free hemoglobin concentration was determined using a standard curve obtained with known concentrations of free AA or SS hemoglobin (Sigma - Aldrich). The percentage of hemolysis, representing the percentage of lysed RBCs in each sample, was determined using a standard curve obtained with hemoglobin concentration in total lysates of fixed RBCs amounts.

Standard curve: The standard curve was done following the supplier instructions. A 2 mg/ml AA and SS hemoglobin solutions were prepared. Serial dilutions from these hemoglobin solutions were prepared [80, 200, 400, 600 mg/ml]. Then 7.5 μ l of each dilution was incubated with 17.5 μ l of Drabkin's solution for 30 minutes in the dark. The absorbance was read at 540 nm by Nanodrop 2000 (Thermo Scientific) and then a calibration curve of absorbance values versus hemoglobin concentration (mg/ml) was plotted. A curve, passing through the origin, was obtained and used to calculate the hemoglobin amount in the collected samples.

Statistics

Data was analyzed by Man-Whitney or Wilcoxon test as required. Correlation (Pearson's correlation coefficient), linear regression and second order polynomial curves were generated using the GraphPad Prism 7.00 software. * $p < 0.05$, ** $p < 0.01$, *** $p < 0.001$ and **** $p < 0.0001$ were considered significant.

With respect to the functions, the Graphpad software was used to find the best fit for the functions shown in Figure II.9 C-F. Graph pad inferred the degree of the polynomial from data using a nested models approach, together with likelihood ratio tests to select the most appropriate model. This showed that a linear model was significantly worse at explaining the data while higher order polynomials (third order or higher) did not improve the fit significantly over the second order model.

*CHAPTER III: Anti-apoptotic Role of
Fetal Hemoglobin During Human Terminal
Erythroid Differentiation Regulates
Ineffective Erythropoiesis in Sickle Cell
Disease*

RESULTS

While ineffective erythropoiesis has long been recognized to be a key contributor to anemia in thalassemia, its role in anemia of sickle cell disease (SCD) has not been critically explored. Ineffective erythropoiesis has been suggested to be a feature of SCD based on studies of mixed chimerism in a small cohort of transplanted patients with severe sickle phenotype.

In this chapter, using both *in vivo* and *in vitro* derived human erythroblasts we assessed the extent of ineffective erythropoiesis in SCD patients. We focused on the terminal phase of erythroid differentiation and addressed the impact of bone marrow hypoxia on HbS polymerization and subsequent cell death of differentiating erythroblasts, in relation with HbF expression.

Cell death during the terminal stages of erythroid differentiation in bone marrow of SCD patients

Bone marrow aspirates were obtained from 3 controls and 3 SCD patients. Cells were stained for surface markers GPA, CD49d and Band 3 and analyzed by flow cytometry. Differentiating erythroblasts were determined using the CD49d and Band 3 double staining pattern within the GPA⁺ population (Figure 1A, B), as previously described (Hu et al., 2013). Imaging flow cytometry was used to confirm homogeneity of each gated population using features of size, morphology and nuclear size and polarization (Figure 1C). We quantified the cells at the early basophilic (EB), late basophilic (LB), polychromatic and orthochromatic stages. Considering the GPA positive population as 100%, the mean percentages of EB, LB, polychromatic and orthochromatic cells in the control samples (Figure 1A) were 3.71%, 8.39%, 14.8% and 27%, respectively (Figure 1D), confirming a single cell division without cell loss separating two successive development stages. For SCD samples (Figure 1B), percentages were 5.45%, 10.61%, 19.28% and 25% (Figure 1D), indicating loss of cell doubling between the

polychromatic and orthochromatic stages (1.3 ± 0.08 vs. 1.9 ± 0.29 for control, Figure 1E) and implying cell death between these 2 stages in a significant proportion of erythroblasts.

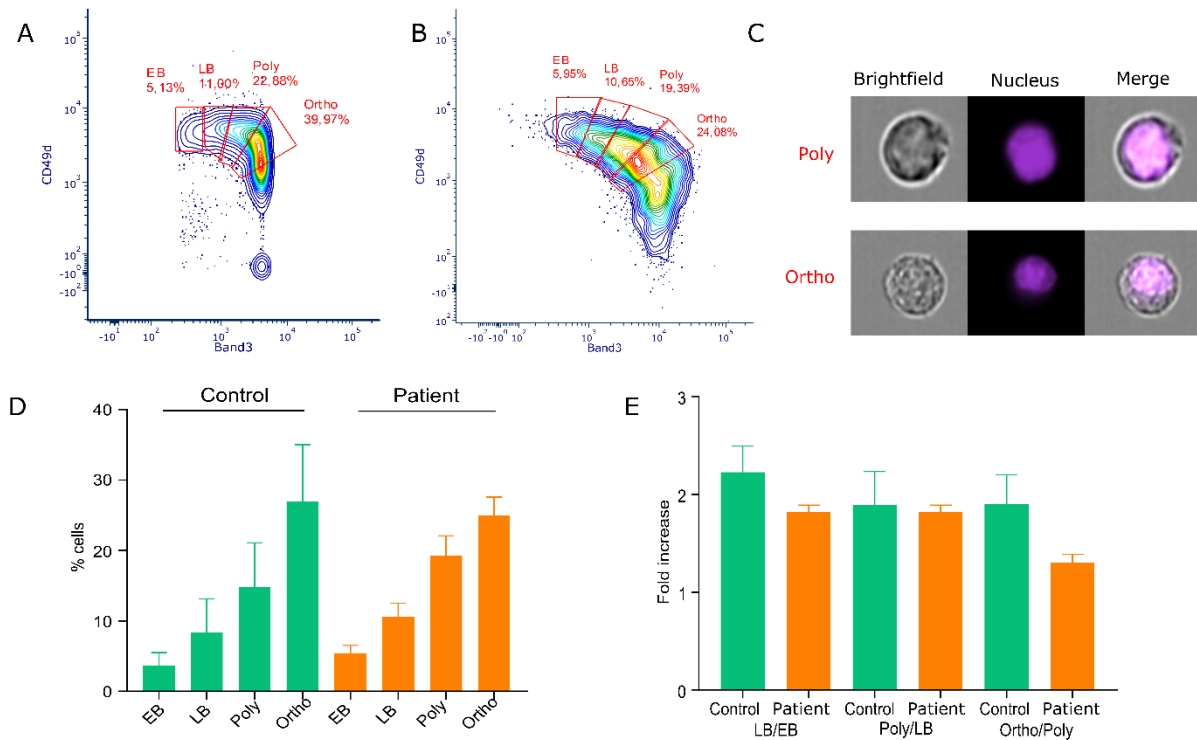


Figure 1: Analysis of human terminal erythroid differentiation *in vivo*. A contour plot representing the distribution of GPA-positive cells with respect to Band 3 (x-axis) and CD49d (y-axis) from human bone marrow samples of (A) control and (B) SCD patient. (C) Images obtained using imaging flow cytometry from the gating of polychromatic (Poly) and orthochromatic (Ortho) erythroblasts. Nucleus was stained with Hoechst. (D) Percentages of cells at the early basophilic (EB), late basophilic (LB), polychromatic (Poly) and orthochromatic (Ortho) stages in 3 bone marrow samples of controls (green) and SCD patients (orange). (E) The fold increase of cells between the EB and LB (LB/EB), LB and Poly (Poly/LB), Poly and Ortho (Ortho/Poly) stages in 3 controls and 3 SCD patients.

Hypoxia-induced cell death during *in vitro* terminal erythroid differentiation

The bone marrow environment is known to be hypoxic (Mohyeldin et al., 2010; Yeo et al., 2018). As hypoxia induces HbS polymerization, we hypothesized that cell death may occur *in vivo* because of HbS polymer formation in the late stages of differentiation with high hemoglobin cytoplasmic concentration. To test our hypothesis, we performed *in vitro* erythroid differentiation using CD34⁺ cells isolated from SCD patients and from healthy donors. A 2-

phase erythroid differentiation protocol was used and cultures were performed at two different oxygen conditions starting at day 3 of the second phase, at which time hemoglobin synthesis is markedly increased: normoxia and partial hypoxia (5% O₂) (Figure 2). There was no difference in the general waterfall pattern of erythroid differentiation of control erythroblasts between normoxia and hypoxia (Figure 3A), although hypoxia translated into a higher but not statistically significant increase in proliferation rate (Figure 3B). Under normoxia, SCD differentiation showed a mild acceleration till day 9 as compared to control (Figure 3A), with a proliferation rate that was negatively impacted by hypoxia (Figure 3B). Under both oxygen conditions, cell proliferation was significantly higher in the control than in the SCD cultures, starting from day 7 and at day 9 (Figure 3B). Of note, enucleation rate, measured at day 11 of culture, was higher for control than SCD erythroblasts (Figure 3C). In addition, enucleation rate was improved under hypoxia for control erythroblasts while it was diminished for SCD cells, indicating a negative impact of hypoxia on this critical maturation step in the SCD context.

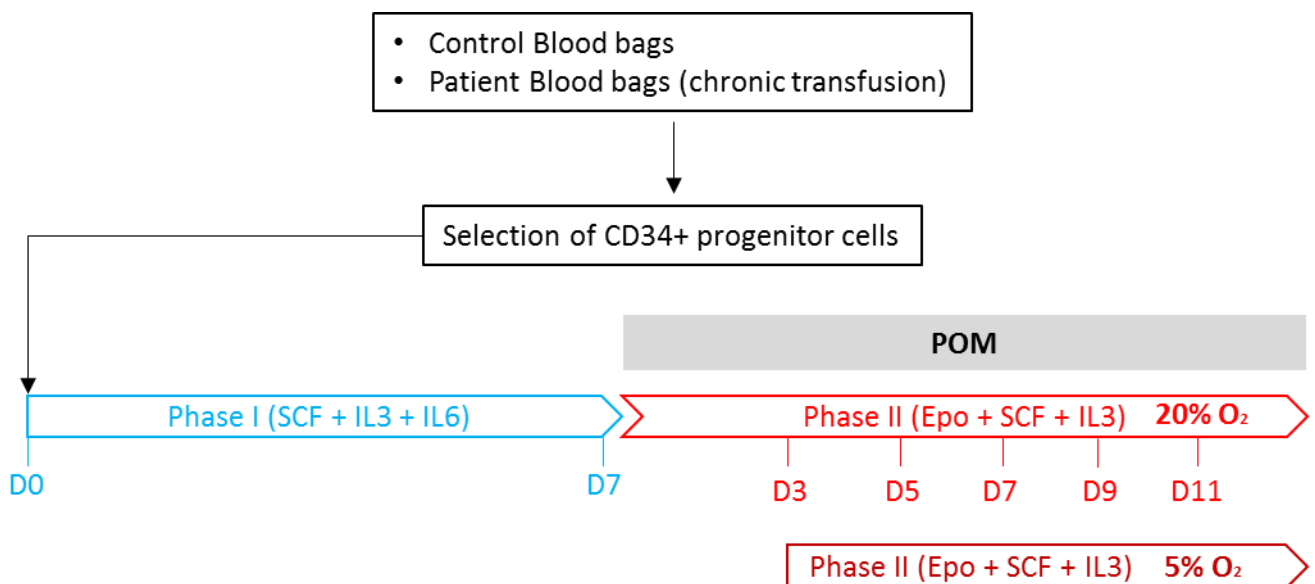


Figure 2: **Work flow of erythroid differentiation experiments.**

To assess if the decrease in proliferation in SCD was due to cell death, we measured the percentage of apoptotic cells in the cultures by staining for annexin V⁺ cells (Figure 3D). This percentage of annexin V⁺ cells was higher in SCD than in control cultures for both oxygen conditions at days 7, 9 and 11 (Figure 3E). Furthermore, apoptosis levels of SCD cells were higher under hypoxia than under normoxia at days 7 and 9 while no differences were noted for control cells (Figure 3E). There was no difference in the extent of apoptosis for SCD erythroblasts at day 11 under either oxygen conditions, indicating that cells that survived following day 9 of culture were not impacted by hypoxia. MGG staining showed that control cells were predominantly at the polychromatic and orthochromatic stages at day 7, with significant amounts of enucleated cells at day 9 (Figure 3F). Erythroid differentiation of SCD cells was delayed as compared to control (Figure 3F), confirming the flow cytometry data (Figure 3A). These results were in accordance with the cell loss in SCD observed between the polychromatic and orthochromatic stages *in vivo* (Figure 1). This validated our choice of 5% O₂ to mimic hypoxia in bone marrow and indicated that hypoxic conditions during the terminal differentiation stages induce cell death in SCD cells only.

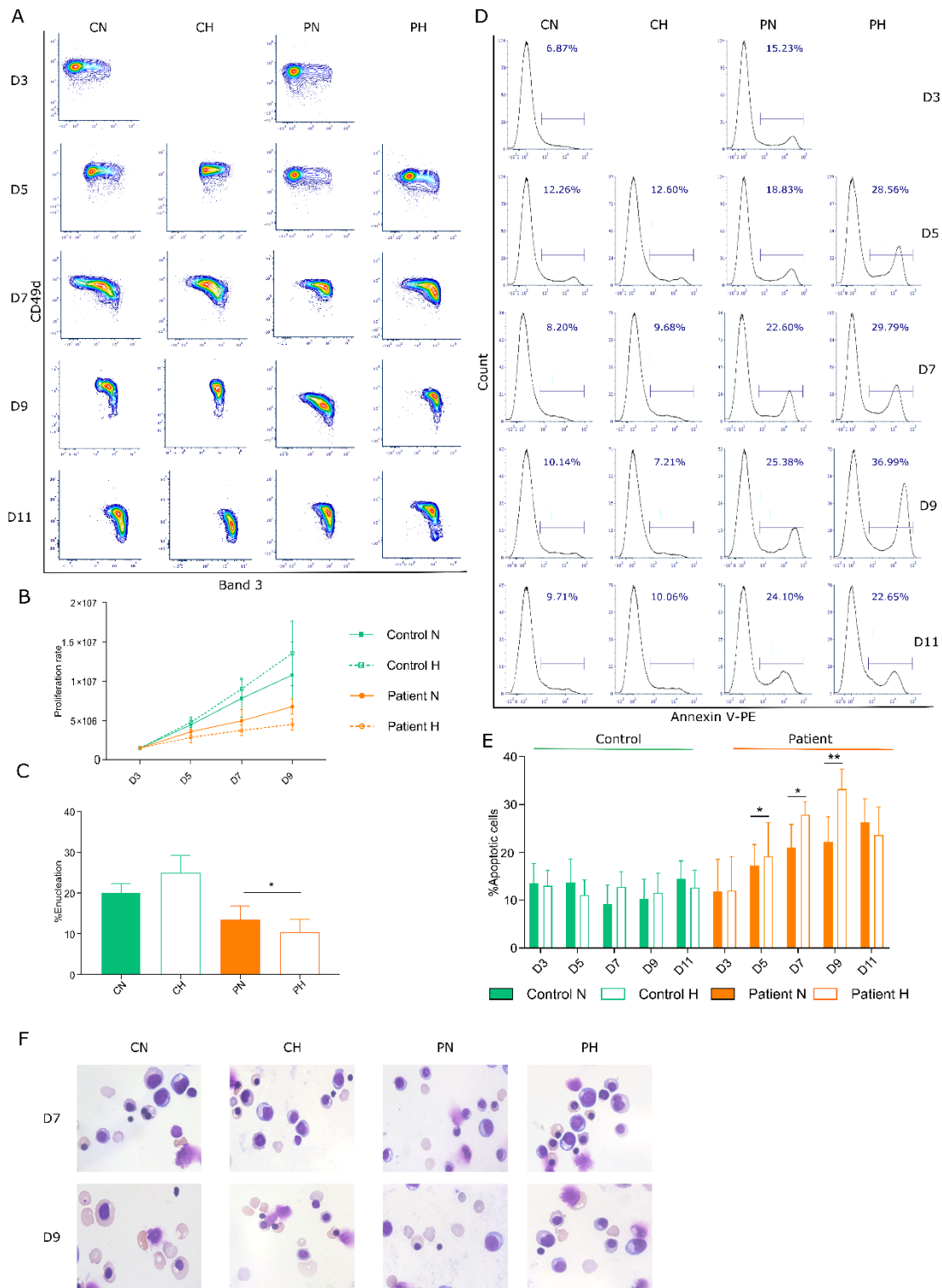


Figure 3: Cell proliferation and apoptosis during terminal erythroid differentiation *in vitro* under normoxia and partial hypoxia. (A) A contour plot representing the distribution of GPA-positive cells with respect to the expression of Band 3 (x-axis) and CD49d (y-axis) at day 3, 5, 7, 9 and 11 of phase II in control erythroid precursors under normoxia (CN) or hypoxia (CH), and in patient erythroid precursors under normoxia (PN) or hypoxia (PH). (B) Proliferation rate of erythroid precursors at day 3, 5, 7 and 9 in control (n = 4) and patient (n = 6) under normoxia (N) and hypoxia (H). (C) Percentage of enucleation measured at day 11. (D) Flow cytometry plots showing percentage of apoptotic cells (Annexin V-positive cells) measured at day 3, 5, 7, 9 and 11. (E) Percentage of apoptotic cells in control (n = 4) and patients (n = 6) under normoxia (N) and hypoxia (H). (F) MGG staining images of erythroid precursors at day 7 and 9 of phase II. * $p < 0.05$, ** $p < 0.01$, *** $p < 0.001$; Wilcoxon paired test (C and E).

F-cells are enriched during SCD erythroid differentiation

Using flow cytometry, we measured the percentage of cells expressing HbF (F-cells) during *in vitro* differentiation (Figure 4A). Under both normoxia and hypoxia, higher percentages of F-cells (%F-cells) were observed for SCD cells than for control, at days 5, 7, 9 and 11 (Figure 4A, B). Interestingly, there was no difference of %F-cells between normoxia and hypoxia for control cells, while for SCD %F-cells was higher under hypoxia than under normoxia (Figure 4A, B). Taken together with the apoptosis data, these findings imply that F-cells were positively selected under hypoxia. This inference was supported by the finding of higher percentages of dead cells within the non-F-cell population as compared to the F-cell population for SCD cells, whereas these percentages were similar between both cell populations in the control (Figure 4C, D).

To further explore this finding, we measured the percentage of F-cells in the bone marrow of SCD patients during terminal erythroid differentiation. There was a significant increase in %F-cells between the polychromatic ($18.24\% \pm 1.77$) and orthochromatic stages ($30.82\% \pm 4.49$) (Figure 4E, F), concomitant with the cell loss observed between these stages (Figure 1D, E). Taken together, our data show preferential survival of F-cells during erythroid differentiation both *in vitro* and *in vivo* and support our hypothesis for an anti-apoptotic role of HbF during *in vivo* erythropoiesis in SCD.

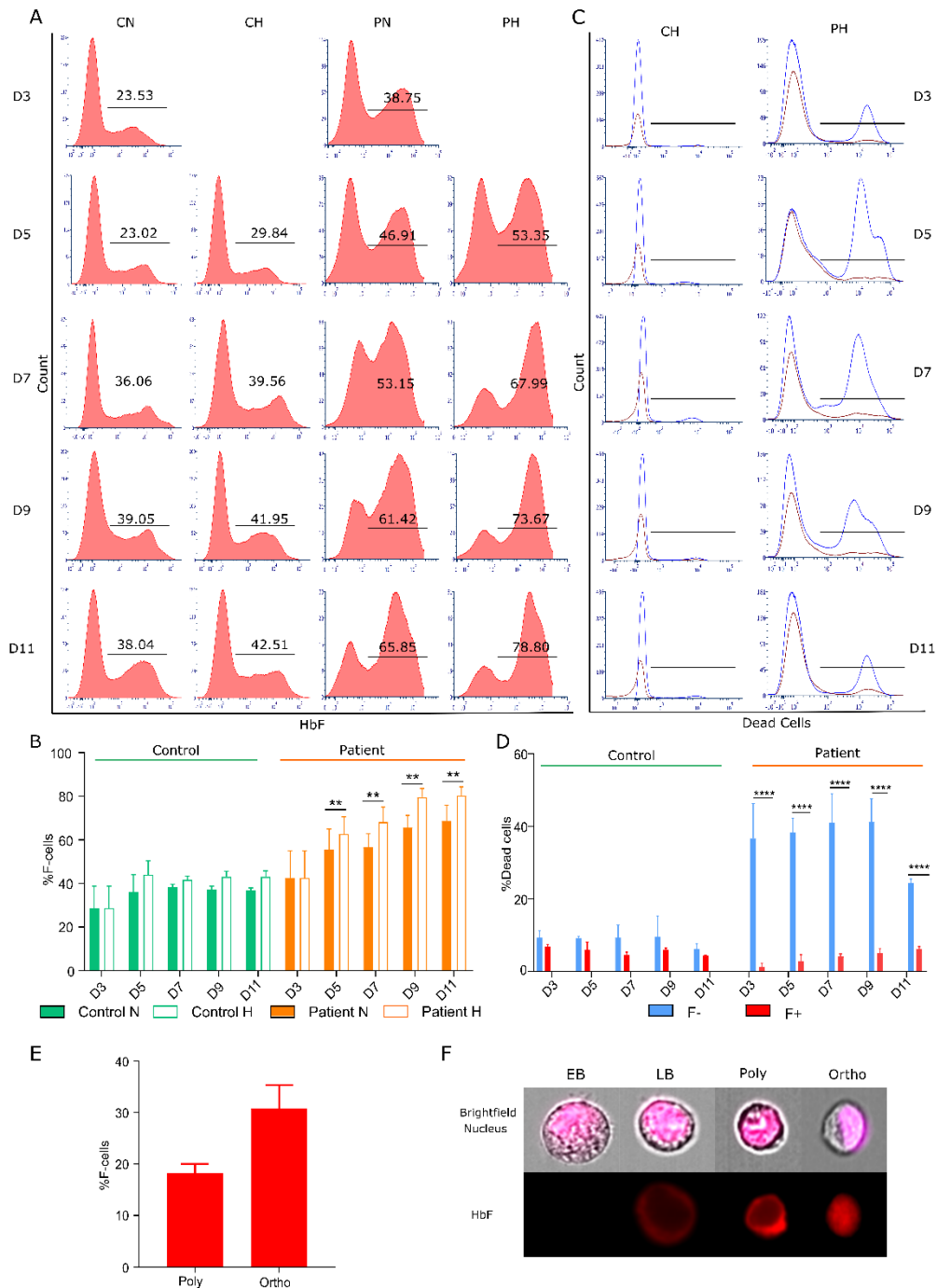


Figure 4: Distribution of erythroid precursors expressing HbF *in vivo* and *in vitro*. (A) Flow cytometry plots showing the percentage of F-cells at day 3, 5, 7, 9 and 11 of phase II in control erythroid precursors under normoxia (CN) or hypoxia (CH), and in patient erythroid precursors under normoxia (PN) or hypoxia (PH). (B) Percentage of F-cells measured at day 3, 5, 7, 9, and 11 of phase II in control (n = 4) and patient cells (n = 6) under normoxia (N) and hypoxia (H). (C) Flow cytometry plots showing dead cells in non-F (F-) (blue curve) and F-cells (F+) (red curve) of control (CH) and patient (PH) cells under hypoxia. (D) Percentage of dead cells measured in the F- and F+ subpopulations for control and patient cells under hypoxia. (E) Percentage of F-cells *in vivo* in the polychromatic (Poly) and orthochromatic (Ortho) subpopulations of the patient bone marrow samples (n=3). (F) Imaging flow cytometry images of early basophilic (EB), late basophilic (LB), polychromatic (Poly) and orthochromatic (Ortho) precursors. Upper images are a merge of brightfield and nucleus, lower images are for HbF staining (red). * $p < 0.05$, ** $p < 0.01$, *** $p < 0.001$, **** $p < 0.0001$; Wilcoxon paired test (B and D).

HSP70 is sequestered in the cytoplasm of non-F-cells

As cytoplasmic sequestration of the chaperone protein HSP70 by α globin aggregates is associated with cell death during erythropoiesis in β -thalassemia major (Arlet et al., 2014), we investigated if apoptosis of SCD erythroblasts might be due to cytoplasmic trapping of HSP70 by HbS polymers. We performed Western blot analyses to quantify HSP70 in the cytoplasmic and nuclear extracts of erythroblasts at day 7 of phase II of culture (Figure 5A). The nucleus/cytoplasm (N/C) ratio of HSP70 was lower under hypoxia than under normoxia for SCD cells, while no difference was observed between both conditions for control cells (Figure 5B). Under normoxia the ratio was also lower for SCD cells than control cells (Figure 5B) indicating mislocalization of HSP70 under these conditions. This result suggests altered subcellular localization of HSP70 in SCD cells, with lower amounts in the nucleus and higher in the cytoplasm when compared to control cells. This imbalance is further exacerbated at 5% O₂, indicating HSP70 trapping in the cytoplasm of SCD cells under hypoxia.

To further explore the molecular mechanism of cytoplasmic trapping of HSP70, we performed immunofluorescence assays using confocal microscopy and found co-localization of HSP70 and hemoglobin in both control and SCD cells (Figure 5C). We used Pearson's correlation coefficient to assess the degree of co-localization and found no difference between both cell types (data not shown), probably because of the high abundance of hemoglobin in the cytoplasm and also due to the optical resolution (Pawley JB., 2006) of a laser scanning confocal microscope (theoretical lateral resolution of approx. 200nm with a 63x/1.4NA lens). To overcome this limitation, we performed proximity ligation assays (PLA), that show fluorescent spots when two proteins are at a distance <40 nm¹⁵. Using this method, we detected SCD cells with fluorescent spots (PLA⁺) under both normoxic and hypoxic conditions (Figure 5D) that we quantified using imaging flow cytometry (Figure 5E). The percentage of PLA⁺ cells was higher in SCD than control cells for both normoxic and hypoxic conditions at days 5 (not

shown) and 7 (Figure 5F), indicating proximity between HSP70 and HbS but not HbA. Moreover, there were more PLA⁺ SCD cells under hypoxia than normoxia (Figure 5F), with a higher mean fluorescence intensity (data not shown), indicating that hypoxia induces the formation of more HbS-HSP70 complexes that could account for cytoplasmic retention of HSP70.

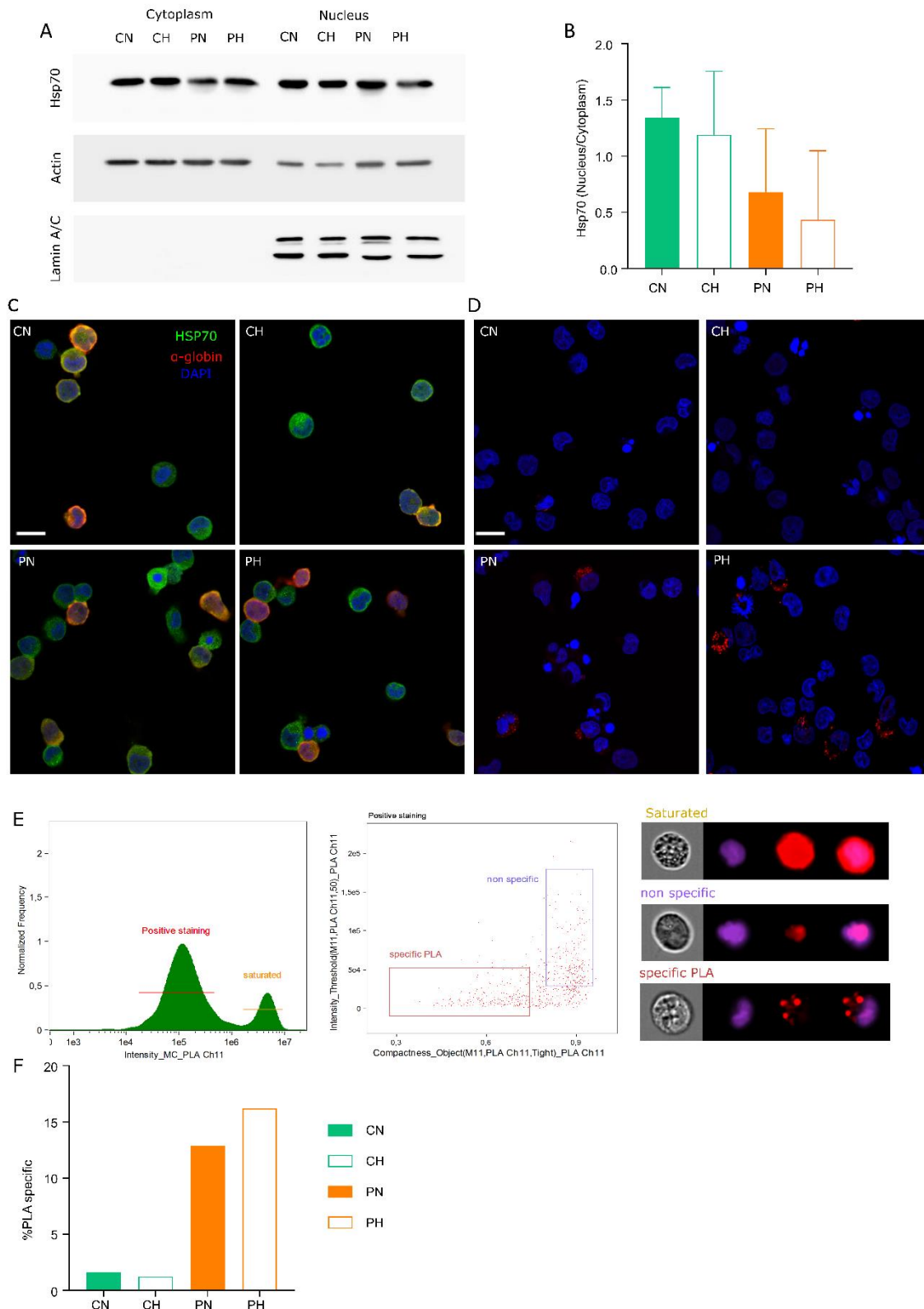


Figure 5: HSP70 cytoplasmic and nuclear distribution, and colocalization with α -globin. (A) Western blot analysis of protein cytoplasmic and nuclear extracts of erythroid precursors at day 7 of phase II from control normoxia (CN), control hypoxia (CH), patient normoxia (PN) and patient hypoxia (PH). (B) Quantification of HSP70 nucleus/cytoplasm ratio from (A) ($n=3$). (C) Confocal microscopy images of erythroid precursors at day 7 of phase II from CN, CH, PN and PH showing colocalization (in yellow) of HSP70 (green) and α -globin (red); nucleus is in blue ($n=3$); scale bar represents 10 μ m. (D) Proximity Ligation Assay between HSP70 and α -globin at day 7 of phase II. Red spots indicate

proximity (<40 nm) between both proteins. Spots were observed in PN and PH cultures, while no spots were seen in CN and CH. A representative image of each culture is shown (n=3); scale bar represents 10 μm . (E) (Left) A histogram representing the intensity of APC signal generated by PLA, a gating of positive staining and saturated staining is indicated. (Middle) A dot plot representing an analysis mask using the compactness feature (x-axis) and intensity feature (y-axis) to discriminate between PLA specific staining and non-specific staining. (Right) Representative images of each gate. (F) Percentage of cells with a PLA-specific staining (in a total of 7000 cells) in one representative experiment for CN, CH, PN and PH erythroid precursors at day 7 of phase II.

The small differences seen in the Western-blot results between normoxic and hypoxic conditions of patient cells (Figure 4A, B) was most probably due to the fact that the starting material was a mix of F and non-F-cells and the relatively small increase in %F-cells induced by hypoxia (11.5% increase at D7, Figure 3B). This is supported by the small difference between both conditions in the PLA assays (Figure 4F). To overcome this hurdle, we used imaging flow cytometry to investigate HSP70 localization specifically in F-cells and non-F-cells. We further explored HSP70 trapping in the cytoplasm by investigating its localization in F-cells and non-F-cells by imaging flow cytometry. Using morphological parameters, specifically nuclear and cytoplasmic surface areas, we set up an analysis template to discriminate between the basophilic, polychromatic and orthochromatic erythroblasts in the GPA positive population (Figure 6A). The gating strategy was adapted from a previously described analysis performed on mouse cells (Kalfa & McGrath, 2018) (Table 1). Note that for our analysis only Hoechst positive cells with high GPA expression were taken into consideration thus eliminating both reticulocytes and proerythroblasts. As expected, the basophilic erythroblasts had the largest cytoplasm and nucleus areas, followed by the polychromatic and then the orthochromatic erythroblasts (Figure 6B-D).

Table 1: X and Y coordinates defining the gating of the Basophilic, Polychromatic and Orthochromatic erythroblasts using imaging flow cytometry.

Gate	X-coordinates	Y-coordinates
Orthochromatic E	35.942	73.813
	22.81	66.918
	18.608	45.436
	31.447	18.915
	53.539	15.467
	69.823	26.341
Polychromatic E	53.802	78.322
	90.046	34.297
	71.398	27.402
	36.993	74.078
Basophilic E	54.59	80.709
	90.572	35.092
	121.826	34.949
	145.201	59.226
	148.352	83.891
	143.625	110.412
	135.22	128.976
	109.219	133.22
	87.945	123.407
	73.5	115.716
59.055	93.704	

The distribution of HSP70 in each subpopulation was investigated for non-F-cells and F-cells by measuring the intensity of HSP70 in the nuclear and cytoplasmic compartments and by calculating the nucleus/cytoplasm (N/C) ratio. In the hypoxic culture at day 7, we observed a higher nuclear intensity of HSP70 in the F-cells as compared to non-F-cells of SCD polychromatic and orthochromatic cells, while there was no difference in control cells (Figure 6E-G). The N/C ratio of HSP70 was also significantly higher in the F-cells of both populations (Figure 6H), confirming the Western-blot findings (Figure 5A). In control cultures no difference in the HSP70 N/C ratio was observed between F-cells and non-F-cells in both polychromatic and orthochromatic erythroblasts (Figure 6I). More specifically, this ratio was not different from the ratio observed for SCD F-cells (Figure 6I), indicating that HSP70 trapping in the cytoplasmic compartment of non-F-cells is specific for SCD erythroblasts.

Although there was no significant difference of HSP70 N/C ratio between SCD F-cells and control, this ratio showed a wide distribution in SCD F-cells. We hypothesized that this heterogeneity might be linked to the intracellular levels of HbF in these cells. Using an analysis mask that quantifies the amount of HbF per cell, we classified F-cells as Low and High F-cells, depending on the intracellular expression level of HbF (Figure 6J). This mask uses the feature of modulation which measures the range intensity of a specific staining in an image; two gates were identified using this analysis, the Low F-cells (with a cut-off of 0.74 for the modulation feature) and High F-cells (with a cut-off of 0.85 for the modulation feature). We found that HSP70 N/C ratio was higher in High than in Low F-cells (Figure 6K), indicating that the amounts of HSP70 trapped in the cytoplasm was inversely correlated with the cytoplasmic content of HbF and suggesting that high amounts of HbF would be needed for a complete protection against apoptosis. This inference was supported by our findings showing lower percentages of Low F-cells in SCD cultures as compared to control, as well as lower percentages of SCD Low F-cells under hypoxic than normoxic conditions (Figure 6L). On the other hand, the percentage of High F-cells was significantly higher in SCD erythroblasts as compared to control, with even higher percentages under hypoxia (Figure 6L). Note that no difference in the percentage of Low or High F-cells was observed between hypoxia and normoxia for control cells (Figure 6L), indicating that the differences observed for SCD cells were not due to hypoxia-induced γ globin gene expression but rather to differential cell death related to HbF expression levels. To gain better insight into the relation between HbF expression level and HSP70 localization, we divided the F-cell population into 7 subpopulations (Figure 7A) and plotted the HSP70 N/C ratio values against the HbF intensity per F-cell. The fitted curve was hyperbolic (Figure 7B), reaching a plateau of HSP70 N/C ratio at a modulation mask value of ~ 800 indicating normalization of HSP70 nuclear localization at this HbF level.

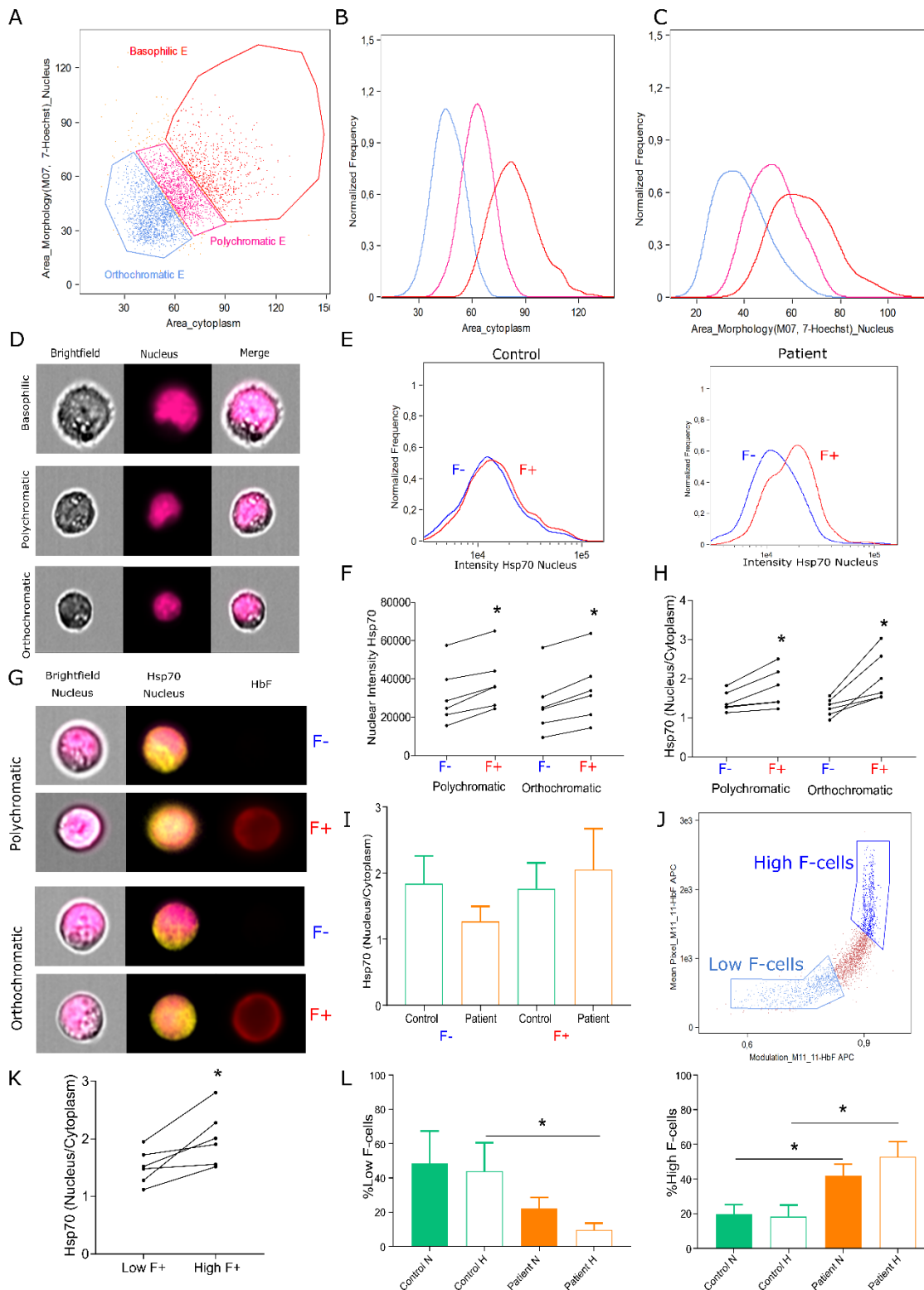


Figure 6: HSP70 cytoplasmic and nuclear distribution in F- and F+ cells using imaging flow cytometry. (A) A dot plot representing the area of the cytoplasm (x-axis) and the area of the nucleus (y-axis) of GPA-high erythroblasts. The dot plot shows the gating of the basophilic, polychromatic and orthochromatic erythroblasts. A histogram representing the area of the cytoplasm (B) and of the nucleus (C) for the 3 subpopulations (basophilic: red, polychromatic: pink and orthochromatic: blue). (D) Images of each subpopulation obtained by imaging flow cytometry. (E) Distribution of the nuclear intensity of HSP70 at day 7 of phase II in the F- and F+ subpopulations of control (left) and patient (right) cells under hypoxia. (F) Nuclear intensity of HSP70 in F- and F+ polychromatic and orthochromatic

erythroblasts at day 7 of phase II (n=6). (G) Images of polychromatic and orthochromatic patient erythroblasts representing HSP70 in yellow, HbF in red and the nucleus in purple. (H) HSP70 nucleus/cytoplasm ratio in F- and F+ polychromatic and orthochromatic patient erythroblasts at day 7 of phase II (n=6). (I) HSP70 nucleus/cytoplasm ratio in F- and F+ orthochromatic cells of control (n=3) and SCD samples (n = 6) at day 7 of phase II under hypoxia. (J) A dot plot representing the modulation mask of HbF (x-axis) and mean pixel HbF values (y-axis) used to discriminate between Low and High F-cells. (K) HSP70 nucleus/cytoplasm ratio in Low and High F-cells of patients' orthochromatic erythroblasts at day 7 of phase II under hypoxia (n=6). (L) Percentage of Low F-cells (left) and High F-cells (right) in control (n=3) and patient (n=6) cells at normoxia and hypoxia at day 7 of phase II. * $p < 0.05$. Wilcoxon paired test (F, H, K) and Mann-Whitney unpaired test (L).

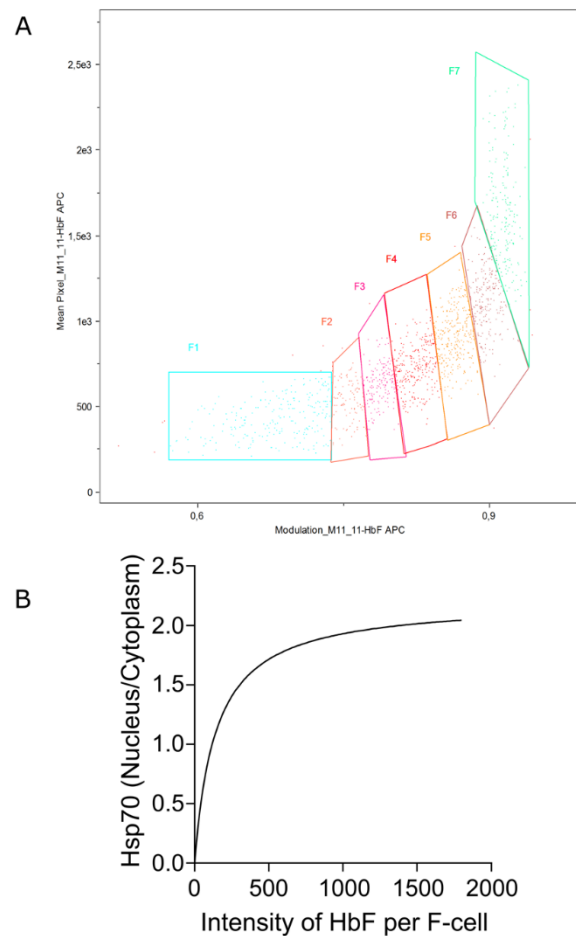


Figure 7: **Relation between HbF intensity and HSP70 N/C ratio in F-cells using imaging flow cytometry.** (A) A dot plot representing the modulation mask of HbF (x-axis) and mean pixel HbF values (y-axis) used to gate 7 cell subpopulations from Low to High F-cells. (B) Nonlinear hyperbola curve between HSP70 N/C ratio and HbF intensity per F-cell.

Induction of HbF by pomalidomide protects against cell death

To confirm the anti-apoptotic role of HbF in SCD erythroblasts we induced its expression *in vitro* using pomalidomide (POM), an immunomodulatory drug previously shown to induce HbF during erythropoiesis (Dulmovits et al., 2016; Moutouh-de Parseval et al., 2008), and determined if higher HbF levels could rescue the cells from apoptosis.

As we were interested in monitoring the stages during which hemoglobin is synthesized, POM was added at day 1 of phase II of culture. As expected, POM-treated SCD cultures showed higher percentages of F-cells than non-treated ones, reaching a mean of 62% in normoxia and 79% in hypoxia at D7 of phase II, compared to 43% and 63.5%, respectively (Figure 8A, B). HbF induction by POM was associated with significantly lower apoptosis levels as compared to non-treated cultures under both hypoxia and normoxia (Figure 8C, D) resulting in improved proliferation rates in both conditions (Figure 8E). Moreover, there was no significant difference in the proliferation rate and the apoptosis levels between normoxic and hypoxic conditions of POM-treated cells indicating that the higher F-cell levels under hypoxia were not due to cell enrichment subsequent to a loss of non-F-cells. To gain further insight into the effect of POM on HbF induction we assessed the distribution of HbF within the F-cell population using imaging flow cytometry. We found less Low F-cells and more High F-cells in the presence of POM (Figure 8F) indicating that POM has a central effect increasing both the percentage of cells expressing HbF and HbF levels within each F-cell. Finally, and as expected, higher percentages of F-cells in the presence of POM were associated with decreased percentages of PLA-positive cells (data not shown), indicating re-localization of HSP70 to the nucleus in these conditions.

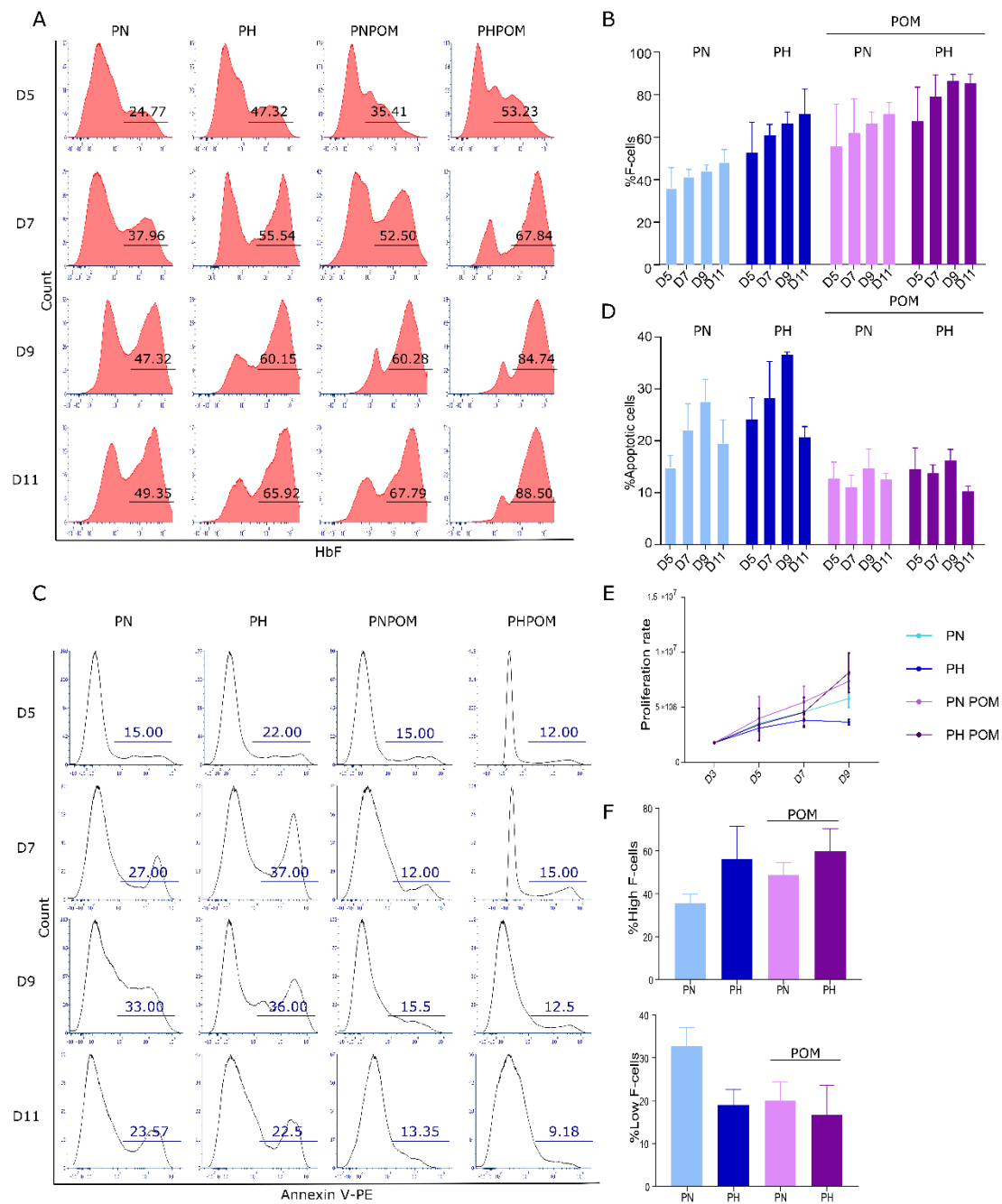


Figure 8: Effect of pomalidomide on terminal erythroid differentiation of SCD erythroblasts. (A) Flow cytometry plots showing the percentage of F-cells at day 5, 7, 9 and 11 of phase II in patient erythroblasts under normoxia (PN), hypoxia (PH), normoxia with POM (PNP) and hypoxia with POM (PHP). (B) Percentage of F-cells in PN, PNP, PH and PHP measured at day 5, 7, 9 and 11 (n=3). (C) Flow cytometry plots showing percentage of Annexin V-positive cells at day 5, 7, 9 and 11 of PN, PH, PNP and PHP. (D) Percentage of apoptotic cells measured by flow cytometry in PN, PH, PNP and PHP at day 5, 7, 9 and 11 (n=3). (E) Proliferation curves of the 4 different culture conditions: PN, PH, PNP and PHP. (F) Percentage of High F-cells (left) and Low F-cells (right) of erythroblasts at day 7 of phase II in cultures non-treated and treated with POM.

DISCUSSION

Ineffective erythropoiesis has been previously suggested to be a feature of SCD (Blouin et al., 1999; Finch, Lee, & Leonard, 1982; Hasegawa et al., 1998; Wu, C. J. et al., 2005) but it has not been critically evaluated and demonstrated. Our present findings provide direct evidence of ineffective erythropoiesis in SCD patients, with significant cell death occurring at the late stages of terminal differentiation *in vivo*.

Among previous reports, the study by Wu and collaborators has highlighted abnormalities during erythropoiesis of transplanted SCD patients by showing intramedullary loss of SCD erythroblasts with progressive maturation (Wu, C. J. et al., 2005). Their results showing relative enrichment of donor erythroid precursors at the onset of hemoglobinization are in accordance with our results showing significant cell death between the polychromatic and the orthochromatic stages, stages at which cellular HbS concentration reaches sufficiently high levels to form polymers under partial hypoxia. Our *in vivo* data document the occurrence of ineffective erythropoiesis in non-transplanted SCD patients, in the absence of conditioning and exogenous donor-related factors that can impact the hematopoietic niche and interfere with the survival of patient's erythroblasts.

Our findings also revealed a new role for HbF in SCD by showing that it protects a subpopulation of differentiating erythroblasts from apoptosis, both *in vivo* and *in vitro*. HbF is a known modulator of disease severity in SCD as it inhibits HbS polymerization at the molecular level, preventing or attenuating RBC sickling and alleviating disease complications (Powars, Weiss, Chan, & Schroeder, 1984; Sewchand, Johnson, & Meiselman, 1983). In healthy adults, HbF accounts for less than 1% of total hemoglobin and is restricted to a small subset of RBCs (2%) called F-cells (Boyer et al., 1975; Wood, W. G. et al., 1975). In SCD, the expression of HbF is higher than in healthy individuals and varies considerably among patients. Although the reasons of this increased expression of HbF are not completely elucidated, stress erythropoiesis and preferential survival of F-cells in the circulation are well-documented

contributing factors (Dover et al., 1978; Franco et al., 2006; Stamatoyannopoulos et al., 1985). Our findings imply that high HbF levels not only increase survival of circulating red cells but also play a role in the preferential survival of erythroblasts under physiologically relevant hypoxic conditions in the bone marrow.

Pomalidomide (CC-4047) is an FDA-approved third-generation immunomodulatory drug, developed to achieve increased antimyeloma activity with reduced side effects compared with thalidomide (Bartlett, Dredge, & Dalglish, 2004; Dimopoulos, Richardson, Moreau, & Anderson, 2015; McCurdy & Lacy, 2013). It has recently been shown to induce HbF expression *in vitro* in human CD34⁺ progenitor cells (Moutouh-de Parseval et al., 2008), and *in vivo* in the Townes' knockout humanized SCD mouse model (Meiler et al., 2011), and to exert this effect by a transcriptional reprogramming of erythroid progenitors (Dulmovits et al., 2016). Our findings clearly showed that *in vitro* induction of HbF by POM rescues SCD erythroblasts from cell death and improves their differentiation and suggest that POM may improve erythropoiesis in SCD patients, which is in accordance with the study showing improved efficiency of erythropoiesis *in vivo* in SCD mice treated with POM (Meiler et al., 2011).

From a mechanistic perspective, our data suggest that apoptosis of non-F-cells is due to the sequestration of HSP70 in the cytoplasm. HSP70 is a chaperone protein that plays an important role during erythropoiesis by protecting GATA-1 from cleavage by caspase-3 in the presence of Epo (Ribeil et al., 2007). Its cytoplasmic sequestration within α globin aggregates was demonstrated in erythroblasts of patients with β thalassemia major (β -TM) (Arlet et al., 2014). Similar to β -TM, SCD erythroblasts showed increased apoptosis under normoxia as compared to control, but only starting from day 7 of culture when there is significant increase in globin synthesis. However, hypoxia induced significant cell death in these cells after only 2 days of incubation suggesting the involvement of HbS polymerization in this phenomenon as no such death was seen in control. In contrast to β -TM where HSP70 can be trapped in the cytoplasm

as soon as α globin chains are expressed, the molecular event that initiates such trapping in SCD, i.e. HbS polymerization, occurs only in cells with high cellular concentration of HbS, required for polymer formation. This is in accordance with the absence of cell death in the early stages during which the intracellular concentration of hemoglobin is low. We showed that low levels of HbF are less protective against cell death, probably because they are not sufficiently effective in inhibiting HbS polymerization because intracellular HbF concentration needs to reach a minimal threshold to exert its protective polymer-inhibiting effect as reported in circulating RBCs (Noguchi et al., 1983). Nevertheless, we show that physiologic hypoxia does not lead to exclusive selection of F-cells, as significant amounts of cells with no HbF still complete terminal erythroid differentiation both *in vitro* and *in vivo*. Further investigations are needed to finely address the biological mechanisms underlying this observation and the commitment of erythroid progenitors to the F lineage in SCD.

Finally, our study brings to light the importance of applying partial hypoxia during the second phase of erythroid differentiation *in vitro* in order to mimic the SCD *in vivo* conditions. To our opinion, this parameter together with the proliferation rate and the percentage of apoptotic cells during the differentiation stages are a critical triptic that should be considered for the studies exploring the beneficial impact of therapeutic approaches targeting HbS polymerization in SCD such as HbF induction (Antoniani et al., 2018; McArthur et al., 2019; Paikari & Sheehan, 2018), anti-sickling molecules such as Voxelotor (Vichinsky et al., 2019) or gene therapy aiming at expressing a therapeutic β globin (Ribeil et al., 2017). Our findings suggest that such strategies, initially designed to improve red cell survival in the circulation, would also positively impact erythropoiesis and bone marrow cellularity.

In summary, our study supports the occurrence of ineffective erythropoiesis in SCD and suggests that its specific targeting by therapeutic strategies will have significant clinical benefits. Most importantly, it shows that HbF has a dual beneficial effect in SCD by conferring

a preferential survival of F-cells in the circulation and by decreasing ineffective erythropoiesis. These findings thus bring new insights into the role of HbF in modulating clinical severity of anemia in SCD by both regulating red cell production and red cell destruction.

MATERIALS & METHODS

Biological samples

The study was conducted according to the declaration of Helsinki with approval from a medical ethics committee (GR-Ex/PPP-DC2016-2618/CNILMR01). Blood bags from SCD patients enrolled in an exchange transfusion program, bone marrow aspirates from 3 SCD patients undergoing surgery and bone marrow tissues from 3 non-anemic donors undergoing hip/sternum surgery, were obtained after informed consent, from Necker-Enfants Malades Hospital (Paris, France) and the North Shore-LIJ Health System (New York, USA) under institutional review board (IRB) approval. Control blood bags from healthy donors were obtained from the Etablissement Français du Sang (EFS).

Antibodies and fluorescent dyes

BV421-conjugated anti-glycophorin A (GPA), APC-conjugated anti-CD49d, FITC- or PE-conjugated anti-HbF, APC-conjugated CD36 mouse monoclonal antibodies were obtained from BD Biosciences. The PE-conjugated anti-Band 3 mouse monoclonal antibody (PE-BRIC6) was obtained from Bristol Institute for Transfusion Sciences. FITC-conjugated anti-HSP70, anti-Lamin A/C and anti- α hemoglobin mouse monoclonal antibodies were obtained from Santa Cruz. Hoechst33342 was obtained from Life Technologies; Hoechst34580, Fixable viability stain 780 (FVS), 7-Aminoactinomycin D (7AAD) and PE-conjugated Annexin V were obtained from BD Biosciences. Rabbit anti-Hsp70/Hsp72 polyclonal antibody was obtained from Enzo Lifesciences. Mouse HRP anti-actin monoclonal antibody was obtained from Santa Cruz. Anti-rabbit and anti-mouse IgG, HRP-linked secondary antibodies were purchased from Cell Signaling. Goat anti-rabbit Alexa 633 and Alexa 488 secondary antibodies were obtained from Invitrogen. DAPI Fluoromount – G mounting media was obtained from Southern Biotech.

In vitro differentiation of human erythroid progenitors

Peripheral blood mononuclear cells were isolated from blood samples after pancoll fractionation (PAN Biotech). CD34⁺ cells were then isolated by a magnetic sorting system (Miltenyi Biotec CD34 Progenitor cell isolation kit) following the supplier protocol. CD34⁺ cells were placed in an *in vitro* two-phase liquid culture system, as previously described (Fibach et al., 1989; Reihani et al., 2016). During the first phase, cells were expanded for 7 days in a medium containing 100 ng/ml of human recombinant (hr) interleukin (IL)-6 (Miltenyi Biotec), 10 ng/ml of hr IL-3 (Miltenyl Biotec) and 50 ng/ml hr stem cell factor (SCF) (Miltenyi Biotec) in Iscove's Modified Dulbecco's Medium IMDM (Gibco) supplemented with 15% BIT 9500 (Stem Cell Technologies), 100 U/ml Penicillin Streptomycin (Gibco) and 2 mM L-Glutamine (Gibco). On day 7, cells were harvested and cultured for 11 days with the second phase medium [10 ng/ml hr IL-3, 50 ng/ml hr SCF, and 2 U/ml of erythropoietin (EPO)]. At day 3 of phase II, cell suspensions were split into 2 and one half was cultured under partial hypoxia (5% O₂) until day 11 while the other was cultured at normoxia. Cells were diluted at 5x10⁵ cells/ml at day 3, 5, 7, 9 and 11 of phase II.

For cultures treated with pomalidomide, cells were incubated with 1 μM pomalidomide (Sigma - Aldrich) as previously described (Dulmovits et al., 2016), starting from the day 1 of phase II.

Imaging Flow Cytometry analysis of human bone marrow samples

Bone marrow samples were processed as previously described (Hu et al., 2013). For bone marrow samples from SCD patients, mononuclear cells were fixed with PBS 1% formaldehyde (Sigma - Aldrich), 0.025% glutaraldehyde (Sigma - Aldrich) for 15 min, washed twice with PBS, permeabilized with 0.1 M Octyl β-D-Glucopyranoside (Sigma - Aldrich) for 15 min and saturated in PBS, 1% BSA, 2% goat serum for 30 min. Cells were then stained for GPA, CD49d, Band 3 and HbF for 30 min in the dark. Cells stained with the isotype control antibodies were used as a negative control. Compensation was performed using BD Biosciences compensation

beads following the supplier instructions. Samples were then analyzed using the Imagestream ISX MkII flow cytometer (Amnis Corp, EMD Millipore) and the INSPIRE software version 99.4.437.0. Acquired data was analyzed using IDEAS software version 6.2 (Amnis Corp, EMD Millipore).

Flow cytometry

For all the following stainings, cells were analyzed using a BD FACScanto II flow cytometer (BD Biosciences) and acquired using the Diva software version 8 (BD Biosciences). Data was analyzed using FCS Express 6 software (DeNovo Software).

Surface marker staining

In vitro cultured cells were stained for surface expression of GPA, Band 3 and CD49d at day 3, 5, 7, 9 and 11. Briefly, 10^5 cells were suspended in 20 μ l of PBS supplemented with 0.5% of bovine serum albumin (BSA), incubated with fluorescence-conjugated antibodies for 30 min in the dark, washed twice with PBS, 0.5% BSA before incubation with 7AAD for 5 min prior to analysis.

Enucleation analysis

Cells (10^5) were washed once with PBS, stained with 1 μ g/ml Hoechst34580 for 45 min at 37°C, washed twice with PBS, 0.5% BSA and incubated with anti-CD36 antibody for 30 min in the dark. Cells were then washed twice with PBS, 0.5% BSA and analyzed.

Apoptotic cells

Cells were stained with PE-conjugated Annexin V to measure the percentage of apoptotic cells. Briefly, 10^5 cells were washed once with Annexin buffer, resuspended in 25 μ l of the same buffer and stained with 2.5 μ l of PE-conjugated Annexin V for 20 min in the dark. Samples were then diluted with 200 μ l of Annexin buffer prior to analysis.

HbF and HSP70 staining

Cells were stained with a fixable viability stain (FVS) at a dilution of 1/1000 for 20 min in the dark, washed twice with PBS then fixed with 1% formaldehyde, 0.025% glutaraldehyde in PBS for 15 min. Cells were then washed twice with PBS, permeabilized in 0.1 M Octyl β -D-Glucopyranoside for 15 min and saturated in PBS, 1% BSA, 2% goat serum for 30 min. Cells were then stained with anti-HbF and/or anti-HSP70 and anti-GPA antibodies for 30 min in the dark, washed twice and analyzed. Hoechst33342 nucleus dye was added before analyzing the cells with imaging flow cytometry.

Cytospin

Cytospin was performed using 10^5 cells. Cells were washed twice with PBS and spun on slides using the Cytospin 2 centrifuge (Shandon). Slides were stained with May-Grunwald-Giemsa (MGG) following manufacturer's instructions (Sigma - Aldrich). Slides were then washed with deionized water and left to dry. Slides were covered by a coverslip using the EUKITT classic (O. Kindler ORSA Tech). Cells were imaged using an inverted microscope (Leica DM6000 B) with a 20x/0.4 HCX PL FLUOTAR, equipped with a DFC300 FX color camera. Analysis was performed using the ImageJ software.

Cell fractionation and Western blot

Cytoplasmic and nuclear protein fractions were extracted from erythroblasts at day 7 of phase II using the NE-PER nuclear and cytoplasmic kit (Thermo Scientific). Ten μ g of nuclear and cytoplasmic proteins were analyzed by SDS-PAGE, using 10% polyacrylamide gels, followed by immunoblotting. The antibodies used were rabbit anti-HSP70, mouse anti-actin and mouse anti-lamin A/C as a control for the nuclear extract. Proteins were revealed using ECL clarity (Biorad) and the Chemidoc MP imaging system (Biorad). Analysis was performed using Image Lab (Biorad).

Confocal Microscopy and Proximity Ligation Assay

Cells (10^5) from day 7 of phase II were washed and fixed with 1% formaldehyde, 0.025% glutaraldehyde for 15 min, treated with 50 mM NH_4Cl (Sigma - Aldrich) for 10 min and washed twice with PBS. Cells were then permeabilized with 1% β -D-glucopyranoside (Sigma - Aldrich) for 15 min, incubated with a saturation solution (1% BSA and 2% goat serum) overnight then with rabbit anti-Hsp70/72 and mouse anti- α hemoglobin (sc-514378 Santa Cruz) for 1 hour at room temperature. After 3 washes with PBS, cells were incubated with goat anti-rabbit Alexa 633 and goat anti-mouse Alexa 488 for 45 min at room temperature, or the PLA secondary antibodies (see below). After a final washing step, cells were spun onto slides and mounted with DAPI. Acquisition was made on LSM700 Zeiss confocal microscope using Zen software. Analysis was performed using Fiji (Schindelin et al., 2012). Fields were selected with respect to cell size, as the smallest cells are the most differentiated. DAPI positive staining was used to define the nuclear region of interest (ROI) and α -globin staining was used to identify the cytoplasmic region. ROI masks were then applied using image calculator to eliminate the nuclear region. Colocalization was quantified using JACoP plugin to calculate the Pearson's correlation coefficient (Bolte & Cordelieres, 2006). Thirty cells were analyzed per experiment. Proximity ligation assay was performed using the Duolink flow PLA Detection Kit – FarRed (Sigma - Aldrich). Cells were incubated with oligonucleotide-conjugated secondary antibodies (PLA probe PLUS anti-mouse and PLA probe MINUS anti-rabbit) for 1 hour at room temperature. Ligation and amplification steps were performed according to the manufacturer's guidelines. For imaging flow cytometry, all incubations were performed with cells in Eppendorf tubes.

Statistics

Statistical analyses were performed with GraphPad Prism (version 7). The data was analyzed using the Mann-Whitney unpaired test and Wilcoxon paired test, as indicated in the figure legends.

CONCLUSIONS & PERSPECTIVES

First, this work has brought new insights into spleen function and the role of fetal hemoglobin in sickle cell disease. Our study in a cohort of infants demonstrates that flow cytometry analysis of %HJB-RBCs alone may accurately reflect spleen filtration function in very young SCA children. We also show that splenic loss of function is present very early in life at 3-6 months of age in SCA infants, further declines and is unrelated to spleen volume. Moreover, hyposplenism results from both RBC increased adhesive properties and, critically, loss of deformability. We also highlighted that ISCs are a potential contributor to ASS, which in turn results in further loss of splenic function.

The second part of this work presents an original approach to determine HbF distribution per cell. Using our innovative microfluidics device, we show that a critical amount of HbF per cell is essential to protect RBCs from hemolysis by mechanical stress. Our longitudinal cohort of patients treated with HC shows that HC has a global positive impact on red cells, by not only increasing HbF content but also by increasing the volume of all RBCs independently of HbF. We moreover show that High F-cells are a more precise marker of HC efficacy and can be considered as a potential clinical marker for disease severity.

In the last part of this thesis, we show for the first time clear evidence of ineffective erythropoiesis in SCD and reveal a new role of HbF during terminal erythropoiesis protecting erythroblasts from apoptosis. Erythroblast cell death was associated with the sequestration of HSP70 in the cytoplasm and was reverted when HbF was induced in these cells. These findings imply that beneficial effects on anemic phenotype by increased HbF levels is not only due to increased life span of circulating sickle cells but also to decreased ineffective erythropoiesis.

In conclusion, my thesis shows that HbF has an additional beneficial effect in SCD by not only conferring a preferential survival of F-cells in the circulation but also by decreasing ineffective erythropoiesis. Importantly, it suggests that the so termed “delayed” hemoglobin switch in SCD

might be partly due to an enrichment in F-erythroblasts during terminal erythroid differentiation occurring very early in infancy, shortly after birth.

My work opens new perspectives in the SCD field:

First, it would be interesting to perform longitudinal prospective studies to evaluate our newly proposed markers, i.e. ISC and High F-cells in relation with disease severity in children and adults with SCD.

Second, our results on HbF distribution both in circulating RBCs and in late erythroblasts point to the percentage of F-reticulocytes, particularly F-R1, and to the expression level of HbF in these cells, as a potential marker of ineffective erythropoiesis in SCD. A longitudinal study has recently started in the laboratory to assess the kinetics of F-reticulocytes in SCD children and adults over a 2-year period, together with markers of anemia such as percentage and absolute count of reticulocytes, hematocrit and hemoglobin levels.

Finally, there are several fundamental research perspectives to further explore erythroid differentiation in SCD as well as reticulocyte maturation. This includes the study of enucleation and organelle sorting in relation with bone marrow hypoxia and the generation of stress reticulocytes with a specific protein content. Furthermore, the high levels of erythroblast apoptosis that we have measured *in vivo* might impact the erythroblastic island and it would be interesting to assess the function and phenotype of the central macrophage in these patients.

BIBLIOGRAPHY

References

- Adekile, A. D., McKie, K. M., Adeodu, O. O., Sulzer, A. J., Liu, J. S., McKie, V. C., . . . Akenzua, G. I. (1993). Spleen in sickle cell anemia: Comparative studies of nigerian and U.S. patients. *American Journal of Hematology*, 42(3), 316-321.
- Adekile, A. D., Owunwanne, A., Al-Za'abi, K., Haider, M. Z., Tuli, M., & Al-Mohannadi, S. (2002). Temporal sequence of splenic dysfunction in sickle cell disease. *American Journal of Hematology*, 69(1), 23-27. doi:10.1002/ajh.10010 [pii]
- Adekile, A. D., Tuli, M., Haider, M. Z., Al-Zaabi, K., Mohannadi, S., & Owunwanne, A. (1996). Influence of alpha-thalassemia trait on spleen function in sickle cell anemia patients with high HbF. *American Journal of Hematology*, 53(1), 1-5. doi:10.1002/(SICI)1096-8652(199609)53:13.0.CO;2-V [pii]
- Airede, A. I. (1992). Acute splenic sequestration in a five-week-old infant with sickle cell disease. *The Journal of Pediatrics*, 120(1), 160.
- Almeida, C. B., Scheiermann, C., Jang, J. E., Prophete, C., Costa, F. F., Conran, N., & Frenette, P. S. (2012). Hydroxyurea and a cGMP-amplifying agent have immediate benefits on acute vaso-occlusive events in sickle cell disease mice. *Blood*, 120(14), 2879-2888. doi:10.1182/blood-2012-02-409524 [doi]
- Alsultan, A., Alabdulaali, M. K., Griffin, P. J., Alsuliman, A. M., Ghabbour, H. A., Sebastiani, P., . . . Steinberg, M. H. (2014). Sickle cell disease in saudi arabia: The phenotype in adults with the arab-indian haplotype is not benign. *British Journal of Haematology*, 164(4), 597-604. doi:10.1111/bjh.12650 [doi]

- Antoniani, C., Meneghini, V., Lattanzi, A., Felix, T., Romano, O., Magrin, E., . . . Miccio, A. (2018). Induction of fetal hemoglobin synthesis by CRISPR/Cas9-mediated editing of the human beta-globin locus. *Blood*, *131*(17), 1960-1973. doi:10.1182/blood-2017-10-811505 [doi]
- Arlet, J. B., Dussiot, M., Moura, I. C., Hermine, O., & Courtois, G. (2016). Novel players in beta-thalassemia dyserythropoiesis and new therapeutic strategies. *Current Opinion in Hematology*, *23*(3), 181-188. doi:10.1097/MOH.0000000000000231 [doi]
- Arlet, J. B., Ribeil, J. A., Guillem, F., Negre, O., Hazoume, A., Marcion, G., . . . Courtois, G. (2014). HSP70 sequestration by free alpha-globin promotes ineffective erythropoiesis in beta-thalassaemia. *Nature*, *514*(7521), 242-246. doi:10.1038/nature13614 [doi]
- Bakanay, S. M., Dainer, E., Clair, B., Adekile, A., Daitch, L., Wells, L., . . . Kutlar, A. (2005). Mortality in sickle cell patients on hydroxyurea therapy. *Blood*, *105*(2), 545-547. doi:10.1182/blood-2004-01-0322 [doi]
- Bartlett, J. B., Dredge, K., & Dalglish, A. G. (2004). The evolution of thalidomide and its IMiD derivatives as anticancer agents. *Nature Reviews.Cancer*, *4*(4), 314-322. doi:10.1038/nrc1323 [doi]
- Bartolucci, P., Chaar, V., Picot, J., Bachir, D., Habibi, A., Fauroux, C., . . . El Nemer, W. (2010). Decreased sickle red blood cell adhesion to laminin by hydroxyurea is associated with inhibition of lu/BCAM protein phosphorylation. *Blood*, *116*(12), 2152-2159. doi:10.1182/blood-2009-12-257444 [doi]
- Bernaudin, F., Socie, G., Kuentz, M., Chevret, S., Duval, M., Bertrand, Y., . . . SFGM-TC. (2007). Long-term results of related myeloablative stem-cell transplantation to cure sickle cell disease. *Blood*, *110*(7), 2749-2756. doi:10.1182/blood-2007-03-079665 [pii]
- Bessis, M. C., & Breton-Gorius, J. (1962). Iron metabolism in the bone marrow as seen by electron microscopy: A critical review. *Blood*, *19*, 635-663.

- Blouin, M. J., De Paepe, M. E., & Trudel, M. (1999). Altered hematopoiesis in murine sickle cell disease. *Blood*, *94*(4), 1451-1459.
- Boehm, D., Mazurier, C., Giarratana, M. C., Darghouth, D., Faussat, A. M., Harmand, L., & Douay, L. (2013). Caspase-3 is involved in the signalling in erythroid differentiation by targeting late progenitors. *PLoS One*, *8*(5), e62303. doi:10.1371/journal.pone.0062303 [doi]
- Bolte, S., & Cordelières, F. P. (2006). A guided tour into subcellular colocalization analysis in light microscopy. *Journal of Microscopy*, *224*(Pt 3), 213-232. doi:JMI1706 [pii]
- Booth, C., Inusa, B., & Obaro, S. K. (2010). Infection in sickle cell disease: A review. *International Journal of Infectious Diseases : IJID : Official Publication of the International Society for Infectious Diseases*, *14*(1), e2-e12. doi:10.1016/j.ijid.2009.03.010 [doi]
- Bowdler, A. J. (2002). *The complete spleen: Structure, function, and clinical disorders*. Totowa, N.J.: Humana Press. Retrieved from <http://www.loc.gov/catdir/enhancements/fy0825/2001039716-d.html>; <http://www.loc.gov/catdir/enhancements/fy0825/2001039716-t.html>
- Boyer, S. H., Belding, T. K., Margolet, L., & Noyes, A. N. (1975). Fetal hemoglobin restriction to a few erythrocytes (F cells) in normal human adults. *Science (New York, N.Y.)*, *188*(4186), 361-363. doi:10.1126/science.804182 [doi]
- Boyer, S. H., Margolet, L., Boyer, M. L., Huisman, T. H., Schroeder, W. A., Wood, W. G., . . . Cartner, R. (1977). Inheritance of F cell frequency in heterocellular hereditary persistence of fetal hemoglobin: An example of allelic exclusion. *American Journal of Human Genetics*, *29*(3), 256-271.
- Brousse, V., Buffet, P., & Rees, D. (2014). The spleen and sickle cell disease: The sick(led) spleen. *British Journal of Haematology*, *166*(2), 165-176. doi:10.1111/bjh.12950 [doi]

- Brousse, V., Colin, Y., Pereira, C., Arnaud, C., Odievre, M. H., Boutemy, A., . . . El Nemer, W. (2014). Erythroid adhesion molecules in sickle cell anaemia infants: Insights into early pathophysiology. *EBioMedicine*, 2(2), 154-157. doi:10.1016/j.ebiom.2014.12.006 [doi]
- Brousse, V., El Hoss, S., Bouazza, N., Arnaud, C., Bernaudin, F., Pellegrino, B., . . . De Montalembert, M. (2018). Prognostic factors of disease severity in infants with sickle cell anemia: A comprehensive longitudinal cohort study. *American Journal of Hematology*, doi:10.1002/ajh.25260 [doi]
- Brousse, V., Elie, C., Benkerrou, M., Odievre, M. H., Lesprit, E., Bernaudin, F., . . . de Montalembert, M. (2012). Acute splenic sequestration crisis in sickle cell disease: Cohort study of 190 paediatric patients. *British Journal of Haematology*, 156(5), 643-648. doi:10.1111/j.1365-2141.2011.08999.x [doi]
- Brown, A. K., Sleeper, L. A., Miller, S. T., Pegelow, C. H., Gill, F. M., & Waclawiw, M. A. (1994). Reference values and hematologic changes from birth to 5 years in patients with sickle cell disease. cooperative study of sickle cell disease. *Archives of Pediatrics & Adolescent Medicine*, 148(8), 796-804.
- Broxmeyer, H. E. (2013). Erythropoietin: Multiple targets, actions, and modifying influences for biological and clinical consideration. *The Journal of Experimental Medicine*, 210(2), 205-208. doi:10.1084/jem.20122760 [doi]
- Brugnara, C., Bunn, H. F., & Tosteson, D. C. (1986). Regulation of erythrocyte cation and water content in sickle cell anemia. *Science (New York, N.Y.)*, 232(4748), 388-390. doi:10.1126/science.3961486 [doi]
- Buffet, P. A., Milon, G., Brousse, V., Correas, J. M., Dousset, B., Couvelard, A., . . . David, P. H. (2006). Ex vivo perfusion of human spleens maintains clearing and processing functions. *Blood*, 107(9), 3745-3752. doi:2005-10-4094 [pii]

- Bunn, H. F. (2013). Erythropoietin. *Cold Spring Harbor Perspectives in Medicine*, 3(3), a011619. doi:10.1101/cshperspect.a011619 [doi]
- Cameron, P. U., Jones, P., Gorniak, M., Dunster, K., Paul, E., Lewin, S., . . . Spelman, D. (2011). Splenectomy associated changes in IgM memory B cells in an adult spleen registry cohort. *PLoS One*, 6(8), e23164. doi:10.1371/journal.pone.0023164 [doi]
- Campbell-Lee, S. A., Gvozdan, K., Choi, K. M., Chen, Y. F., Saraf, S. L., Hsu, L. L., . . . Triulzi, D. J. (2018). Red blood cell alloimmunization in sickle cell disease: Assessment of transfusion protocols during two time periods. *Transfusion*, 58(7), 1588-1596. doi:10.1111/trf.14588 [doi]
- Casper, J. T., Koethe, S., Rodey, G. E., & Thatcher, L. G. (1976). A new method for studying splenic reticuloendothelial dysfunction in sickle cell disease patients and its clinical application: A brief report. *Blood*, 47(2), 183-188.
- Cavazzana, M., Antoniani, C., & Miccio, A. (2017). Gene therapy for beta-hemoglobinopathies. *Molecular Therapy : The Journal of the American Society of Gene Therapy*, 25(5), 1142-1154. doi:S1525-0016(17)30123-5 [pii]
- Cavazzana, M., Ribeil, J. A., Lagresle-Peyrou, C., & Andre-Schmutz, I. (2017). Gene therapy with hematopoietic stem cells: The diseased bone marrow's point of view. *Stem Cells and Development*, 26(2), 71-76. doi:10.1089/scd.2016.0230 [doi]
- Chasis, J. A., & Mohandas, N. (2008). Erythroblastic islands: Niches for erythropoiesis. *Blood*, 112(3), 470-478. doi:10.1182/blood-2008-03-077883 [doi]
- Chen, M. C., Zhou, B., Zhang, K., Yuan, Y. C., Un, F., Hu, S., . . . Yen, Y. (2015). The novel ribonucleotide reductase inhibitor COH29 inhibits DNA repair in vitro. *Molecular Pharmacology*, 87(6), 996-1005. doi:10.1124/mol.114.094987 [doi]

- Chen, M. J., Li, Y., De Obaldia, M. E., Yang, Q., Yzaguirre, A. D., Yamada-Inagawa, T., . . . Speck, N. A. (2011). Erythroid/myeloid progenitors and hematopoietic stem cells originate from distinct populations of endothelial cells. *Cell Stem Cell*, 9(6), 541-552. doi:10.1016/j.stem.2011.10.003 [doi]
- Chopra, R., Al-Mulhim, A. R., & Al-Baharani, A. T. (2005). Fibrocongestive splenomegaly in sickle cell disease: A distinct clinicopathological entity in the eastern province of Saudi Arabia. *American Journal of Hematology*, 79(3), 180-186. doi:10.1002/ajh.20380 [doi]
- Couque, N., Girard, D., Ducrocq, R., Boizeau, P., Haouari, Z., Missud, F., . . . Benkerrou, M. (2016). Improvement of medical care in a cohort of newborns with sickle-cell disease in North Paris: Impact of national guidelines. *British Journal of Haematology*, 173(6), 927-937. doi:10.1111/bjh.14015 [doi]
- de Jong, K., Larkin, S. K., Styles, L. A., Bookchin, R. M., & Kuypers, F. A. (2001). Characterization of the phosphatidylserine-exposing subpopulation of sickle cells. *Blood*, 98(3), 860-867. doi:10.1182/blood.v98.3.860 [doi]
- Dimopoulos, M. A., Richardson, P. G., Moreau, P., & Anderson, K. C. (2015). Current treatment landscape for relapsed and/or refractory multiple myeloma. *Nature Reviews Clinical Oncology*, 12(1), 42-54. doi:10.1038/nrclinonc.2014.200 [doi]
- Dover, G. J., Boyer, S. H., Charache, S., & Heintzelman, K. (1978). Individual variation in the production and survival of F cells in sickle-cell disease. *The New England Journal of Medicine*, 299(26), 1428-1435. doi:10.1056/NEJM197812282992603 [doi]
- Dulmovits, B. M., Appiah-Kubi, A. O., Papoin, J., Hale, J., He, M., Al-Abed, Y., . . . Blanc, L. (2016). Pomalidomide reverses gamma-globin silencing through the transcriptional reprogramming of adult hematopoietic progenitors. *Blood*, 127(11), 1481-1492. doi:10.1182/blood-2015-09-667923 [doi]

- Dutta, P., Hoyer, F. F., Grigoryeva, L. S., Sager, H. B., Leuschner, F., Courties, G., . . . Nahrendorf, M. (2015). Macrophages retain hematopoietic stem cells in the spleen via VCAM-1. *The Journal of Experimental Medicine*, 212(4), 497-512. doi:10.1084/jem.20141642 [doi]
- Ehrlich, C. P., Papanicolaou, N., Treves, S., Hurwitz, R. A., & Richards, P. (1982). Splenic scintigraphy using tc-99m-labeled heat-denatured red blood cells in pediatric patients: Concise communication. *Journal of Nuclear Medicine : Official Publication, Society of Nuclear Medicine*, 23(3), 209-213.
- El Hoss, S., & Brousse, V. (2019). Considering the spleen in sickle cell disease. *Expert Review of Hematology*, , 1-11. doi:10.1080/17474086.2019.1627192 [doi]
- El Nemer, W., Colin, Y., Bauvy, C., Codogno, P., Fraser, R. H., Cartron, J. P., & Le Van Kim, C. L. (1999). Isoforms of the lutheran/basal cell adhesion molecule glycoprotein are differentially delivered in polarized epithelial cells. mapping of the basolateral sorting signal to a cytoplasmic di-leucine motif. *The Journal of Biological Chemistry*, 274(45), 31903-31908.
- El Nemer, W., Gane, P., Colin, Y., Bony, V., Rahuel, C., Galacteros, F., . . . Le Van Kim, C. (1998). The lutheran blood group glycoproteins, the erythroid receptors for laminin, are adhesion molecules. *The Journal of Biological Chemistry*, 273(27), 16686-16693.
- Embury, S. H., Clark, M. R., Monroy, G., & Mohandas, N. (1984). Concurrent sickle cell anemia and alpha-thalassemia. effect on pathological properties of sickle erythrocytes. *The Journal of Clinical Investigation*, 73(1), 116-123. doi:10.1172/JCI111181 [doi]
- Emond, A. M., Collis, R., Darvill, D., Higgs, D. R., Maude, G. H., & Serjeant, G. R. (1985). Acute splenic sequestration in homozygous sickle cell disease: Natural history and management. *The Journal of Pediatrics*, 107(2), 201-206. doi:S0022-3476(85)80125-6 [pii]

- Fabry, M. E., Mears, J. G., Patel, P., Schaefer-Rego, K., Carmichael, L. D., Martinez, G., & Nagel, R. L. (1984). Dense cells in sickle cell anemia: The effects of gene interaction. *Blood*, *64*(5), 1042-1046.
- Fibach, E., Manor, D., Oppenheim, A., & Rachmilewitz, E. A. (1989). Proliferation and maturation of human erythroid progenitors in liquid culture. *Blood*, *73*(1), 100-103.
- Finch, C. A., Lee, M. Y., & Leonard, J. M. (1982). Continuous RBC transfusions in a patient with sickle cell disease. *Archives of Internal Medicine*, *142*(2), 279-282.
- Franco, R. S., Lohmann, J., Silberstein, E. B., Mayfield-Pratt, G., Palascak, M., Nemeth, T. A., . . . Rucknagel, D. L. (1998). Time-dependent changes in the density and hemoglobin F content of biotin-labeled sickle cells. *The Journal of Clinical Investigation*, *101*(12), 2730-2740.
doi:10.1172/JCI2484 [doi]
- Franco, R. S., Yasin, Z., Palascak, M. B., Ciralo, P., Joiner, C. H., & Rucknagel, D. L. (2006). The effect of fetal hemoglobin on the survival characteristics of sickle cells. *Blood*, *108*(3), 1073-1076. doi:108/3/1073 [pii]
- Frenette, P. S. (2002). Sickle cell vaso-occlusion: Multistep and multicellular paradigm. *Current Opinion in Hematology*, *9*(2), 101-106.
- Galanello, R., Sanna, S., Perseu, L., Sollaino, M. C., Satta, S., Lai, M. E., . . . Cao, A. (2009). Amelioration of sardinian beta0 thalassemia by genetic modifiers. *Blood*, *114*(18), 3935-3937.
doi:10.1182/blood-2009-04-217901 [doi]
- Gale, H. I., Bobbitt, C. A., Setty, B. N., Sprinz, P. G., Doros, G., Williams, D. D., . . . Castro-Aragon, I. (2016). Expected sonographic appearance of the spleen in children and young adults with sickle cell disease: An update. *Journal of Ultrasound in Medicine : Official Journal of the American Institute of Ultrasound in Medicine*, *35*(8), 1735-1745. doi:10.7863/ultra.15.09023 [doi]

- Ganz, T. (2012). Macrophages and systemic iron homeostasis. *Journal of Innate Immunity*, 4(5-6), 446-453. doi:10.1159/000336423 [doi]
- Gaston, M. H., Verter, J. I., Woods, G., Pegelow, C., Kelleher, J., Presbury, G., . . . Lobel, J. S. (1986). Prophylaxis with oral penicillin in children with sickle cell anemia. A randomized trial. *The New England Journal of Medicine*, 314(25), 1593-1599. doi:10.1056/NEJM198606193142501 [doi]
- Giarratana, M. C., Rouard, H., Dumont, A., Kiger, L., Safeukui, I., Le Penec, P. Y., . . . Douay, L. (2011). Proof of principle for transfusion of in vitro-generated red blood cells. *Blood*, 118(19), 5071-5079. doi:10.1182/blood-2011-06-362038 [doi]
- Gifford, S. C., Derganc, J., Shevkoplyas, S. S., Yoshida, T., & Bitensky, M. W. (2006). A detailed study of time-dependent changes in human red blood cells: From reticulocyte maturation to erythrocyte senescence. *British Journal of Haematology*, 135(3), 395-404. doi:BJH6279 [pii]
- Gluckman, E., Cappelli, B., Bernaudin, F., Labopin, M., Volt, F., Carreras, J., . . . Eurocord, the Pediatric Working Party of the European Society for Blood and Marrow Transplantation, and the Center for International Blood and Marrow Transplant Research. (2017). Sickle cell disease: An international survey of results of HLA-identical sibling hematopoietic stem cell transplantation. *Blood*, 129(11), 1548-1556. doi:10.1182/blood-2016-10-745711 [doi]
- Goodman, S. R. (2004). The irreversibly sickled cell: A perspective. *Cellular and Molecular Biology (Noisy-Le-Grand, France)*, 50(1), 53-58.
- Granick, S., & Levere, R. D. (1964). Heme synthesis in erythroid cells. *Progress in Hematology*, 4, 1-47.
- Grasso, J. A., Sullivan, A. L., & Sullivan, L. W. (1975). Ultrastructural studies of the bone marrow in sickle cell anaemia. I. the structure of sickled erythrocytes and reticulocytes and their phagocytic destruction. *British Journal of Haematology*, 31(2), 135-148.

- Gregoli, P. A., & Bondurant, M. C. (1999). Function of caspases in regulating apoptosis caused by erythropoietin deprivation in erythroid progenitors. *Journal of Cellular Physiology*, 178(2), 133-143. doi:10.1002/(SICI)1097-4652(199902)178:23.0.CO;2-5 [pii]
- Gregory, C. J., & Eaves, A. C. (1977). Human marrow cells capable of erythropoietic differentiation in vitro: Definition of three erythroid colony responses. *Blood*, 49(6), 855-864.
- Groom, A. C., Schmidt, E. E., & MacDonald, I. C. (1991). Microcirculatory pathways and blood flow in spleen: New insights from washout kinetics, corrosion casts, and quantitative intravital videomicroscopy. *Scanning Microscopy*, 5(1), 159-73; discussion 173-4.
- Grosse, S. D., Odame, I., Atrash, H. K., Amendah, D. D., Piel, F. B., & Williams, T. N. (2011). Sickle cell disease in africa: A neglected cause of early childhood mortality. *American Journal of Preventive Medicine*, 41(6 Suppl 4), S398-405. doi:10.1016/j.amepre.2011.09.013 [doi]
- Habara, A., & Steinberg, M. H. (2016). Minireview: Genetic basis of heterogeneity and severity in sickle cell disease. *Experimental Biology and Medicine (Maywood, N.J.)*, 241(7), 689-696. doi:10.1177/1535370216636726 [doi]
- Harrod, V. L., Howard, T. A., Zimmerman, S. A., Dertinger, S. D., & Ware, R. E. (2007). Quantitative analysis of howell-jolly bodies in children with sickle cell disease. *Experimental Hematology*, 35(2), 179-183. doi:S0301-472X(06)00602-3 [pii]
- Hasegawa, S., Rodgers, G. P., Dwyer, N., Noguchi, C. T., Blanchette-Mackie, E. J., Uyesaka, N., . . . Fibach, E. (1998). Sickling of nucleated erythroid precursors from patients with sickle cell anemia. *Experimental Hematology*, 26(4), 314-319.
- Herrick, J. B. (2001). Peculiar elongated and sickle-shaped red blood corpuscles in a case of severe anemia. 1910. *The Yale Journal of Biology and Medicine*, 74(3), 179-184.

- Higgs, D. R., Aldridge, B. E., Lamb, J., Clegg, J. B., Weatherall, D. J., Hayes, R. J., . . . Serjeant, G. R. (1982). The interaction of alpha-thalassemia and homozygous sickle-cell disease. *The New England Journal of Medicine*, *306*(24), 1441-1446. doi:10.1056/NEJM198206173062402 [doi]
- Hoban, M. D., Orkin, S. H., & Bauer, D. E. (2016). Genetic treatment of a molecular disorder: Gene therapy approaches to sickle cell disease. *Blood*, *127*(7), 839-848. doi:10.1182/blood-2015-09-618587 [doi]
- Hu, J., Liu, J., Xue, F., Halverson, G., Reid, M., Guo, A., . . . An, X. (2013). Isolation and functional characterization of human erythroblasts at distinct stages: Implications for understanding of normal and disordered erythropoiesis in vivo. *Blood*, *121*(16), 3246-3253. doi:10.1182/blood-2013-01-476390 [doi]
- Imagawa, S., Yamamoto, M., & Miura, Y. (1997). Negative regulation of the erythropoietin gene expression by the GATA transcription factors. *Blood*, *89*(4), 1430-1439.
- Ingram, V. M. (1956). A specific chemical difference between the globins of normal human and sickle-cell anaemia haemoglobin. *Nature*, *178*(4537), 792-794. doi:10.1038/178792a0 [doi]
- John, A. B., Ramlal, A., Jackson, H., Maude, G. H., Sharma, A. W., & Serjeant, G. R. (1984). Prevention of pneumococcal infection in children with homozygous sickle cell disease. *British Medical Journal (Clinical Research Ed.)*, *288*(6430), 1567-1570. doi:10.1136/bmj.288.6430.1567 [doi]
- Jones, S., Duncan, E. R., Thomas, N., Walters, J., Dick, M. C., Height, S. E., . . . Rees, D. C. (2005). Windy weather and low humidity are associated with an increased number of hospital admissions for acute pain and sickle cell disease in an urban environment with a maritime temperate climate. *British Journal of Haematology*, *131*(4), 530-533. doi:BJH5799 [pii]

- Kalfa, T., & McGrath, K. E. (2018). Analysis of erythropoiesis using imaging flow cytometry. *Methods in Molecular Biology (Clifton, N.J.)*, 1698, 175-192. doi:10.1007/978-1-4939-7428-3_10 [doi]
- Kan, Y. W., & Nathan, D. G. (1968). Beta thalassemia trait: Detection at birth. *Science (New York, N.Y.)*, 161(3841), 589-590. doi:10.1126/science.161.3841.589 [doi]
- Kan, Y. W., & Nathan, D. G. (1970). Mild thalassemia: The result of interactions of alpha and beta thalassemia genes. *The Journal of Clinical Investigation*, 49(4), 635-642. doi:10.1172/JCI106274 [doi]
- Kar, B. C., Satapathy, R. K., Kulozik, A. E., Kulozik, M., Sirr, S., Serjeant, B. E., & Serjeant, G. R. (1986). Sickle cell disease in orissa state, india. *Lancet (London, England)*, 2(8517), 1198-1201. doi:S0140-6736(86)92205-1 [pii]
- Kato, G. J., Gladwin, M. T., & Steinberg, M. H. (2007). Deconstructing sickle cell disease: Reappraisal of the role of hemolysis in the development of clinical subphenotypes. *Blood Reviews*, 21(1), 37-47. doi:S0268-960X(06)00041-5 [pii]
- Kato, G. J., Piel, F. B., Reid, C. D., Gaston, M. H., Ohene-Frempong, K., Krishnamurti, L., . . . Vichinsky, E. P. (2018). Sickle cell disease. *Nature Reviews.Disease Primers*, 4, 18010. doi:10.1038/nrdp.2018.10 [doi]
- Kaul, D. K., Fabry, M. E., & Nagel, R. L. (1996). The pathophysiology of vascular obstruction in the sickle syndromes. *Blood Reviews*, 10(1), 29-44. doi:S0268-960X(96)90018-1 [pii]
- Khemani, K., Katoch, D., & Krishnamurti, L. (2019). Curative therapies for sickle cell disease. *The Ochsner Journal*, 19(2), 131-137. doi:10.31486/toj.18.0044 [doi]

- Kiel, M. J., He, S., Ashkenazi, R., Gentry, S. N., Teta, M., Kushner, J. A., . . . Morrison, S. J. (2007). Haematopoietic stem cells do not asymmetrically segregate chromosomes or retain BrdU. *Nature*, *449*(7159), 238-242. doi:nature06115 [pii]
- Kinney, T. R., Helms, R. W., O'Branski, E. E., Ohene-Frempong, K., Wang, W., Daeschner, C., . . . Ware, R. E. (1999). Safety of hydroxyurea in children with sickle cell anemia: Results of the HUG-KIDS study, a phase I/II trial. pediatric hydroxyurea group. *Blood*, *94*(5), 1550-1554.
- Klausner, M. A., Hirsch, L. J., Leblond, P. F., Chamberlain, J. K., Klemperer, M. R., & Segel, G. B. (1975). Contrasting splenic mechanisms in the blood clearance of red blood cells and colloidal particles. *Blood*, *46*(6), 965-976.
- Krauss, S. W., Lo, A. J., Short, S. A., Koury, M. J., Mohandas, N., & Chasis, J. A. (2005). Nuclear substructure reorganization during late-stage erythropoiesis is selective and does not involve caspase cleavage of major nuclear substructural proteins. *Blood*, *106*(6), 2200-2205. doi:2005-04-1357 [pii]
- Labie, D., & Elion, J. (1999). Molecular and cellular pathophysiology of sickle cell anemia. [Physiopathologie moléculaire et cellulaire de la drepanocytose] *Pathologie-Biologie*, *47*(1), 7-12.
- Lane, P. A., O'Connell, J. L., Lear, J. L., Rogers, Z. R., Woods, G. M., Hassell, K. L., . . . Buchanan, G. R. (1995). Functional asplenia in hemoglobin SC disease. *Blood*, *85*(8), 2238-2244.
- Lee, S. H., Crocker, P. R., Westaby, S., Key, N., Mason, D. Y., Gordon, S., & Weatherall, D. J. (1988). Isolation and immunocytochemical characterization of human bone marrow stromal macrophages in hemopoietic clusters. *The Journal of Experimental Medicine*, *168*(3), 1193-1198. doi:10.1084/jem.168.3.1193 [doi]

- Lettre, G., & Bauer, D. E. (2016). Fetal haemoglobin in sickle-cell disease: From genetic epidemiology to new therapeutic strategies. *Lancet (London, England)*, *387*(10037), 2554-2564. doi:10.1016/S0140-6736(15)01341-0 [doi]
- Lettre, G., Sankaran, V. G., Bezerra, M. A., Araujo, A. S., Uda, M., Sanna, S., . . . Orkin, S. H. (2008). DNA polymorphisms at the BCL11A, HBS1L-MYB, and beta-globin loci associate with fetal hemoglobin levels and pain crises in sickle cell disease. *Proceedings of the National Academy of Sciences of the United States of America*, *105*(33), 11869-11874. doi:10.1073/pnas.0804799105 [doi]
- Liu, S. C., Derick, L. H., & Palek, J. (1993). Dependence of the permanent deformation of red blood cell membranes on spectrin dimer-tetramer equilibrium: Implication for permanent membrane deformation of irreversibly sickled cells. *Blood*, *81*(2), 522-528.
- Lizarralde Irigorri, M. A., El Hoss, S., Brousse, V., Lefevre, S. D., Dussiot, M., Xu, T., . . . El Nemer, W. (2018). A microfluidic approach to study the effect of mechanical stress on erythrocytes in sickle cell disease. *Lab on a Chip*, *18*(19), 2975-2984. doi:10.1039/c8lc00637g [doi]
- Lux, S. E., John, K. M., & Karnovsky, M. J. (1976). Irreversible deformation of the spectrin-actin lattice in irreversibly sickled cells. *The Journal of Clinical Investigation*, *58*(4), 955-963. doi:10.1172/JCI108549 [doi]
- Maier-Redelsperger, M., Elion, J., & Girot, R. (1998). F reticulocytes assay: A method to evaluate fetal hemoglobin production. *Hemoglobin*, *22*(5-6), 419-425.
- Maier-Redelsperger, M., Noguchi, C. T., de Montalembert, M., Rodgers, G. P., Schechter, A. N., Gourbil, A., . . . Peltier, J. Y. (1994). Variation in fetal hemoglobin parameters and predicted hemoglobin S polymerization in sickle cell children in the first two years of life: Parisian prospective study on sickle cell disease. *Blood*, *84*(9), 3182-3188.

- Manwani, D., & Frenette, P. S. (2013). Vaso-occlusion in sickle cell disease: Pathophysiology and novel targeted therapies. *Blood*, *122*(24), 3892-3898. doi:10.1182/blood-2013-05-498311 [doi]
- Mburu, J., & Odame, I. (2019). Sickle cell disease: Reducing the global disease burden. *International Journal of Laboratory Hematology*, *41 Suppl 1*, 82-88. doi:10.1111/ijlh.13023 [doi]
- McArthur, J. G., Svenstrup, N., Chen, C., Fricot, A., Carvalho, C., Nguyen, J., . . . Maciel, T. T. (2019). A novel, highly potent and selective phosphodiesterase-9 inhibitor for the treatment of sickle cell disease. *Haematologica*, doi:haematol.2018.213462 [pii]
- McCarville, M. B., Luo, Z., Huang, X., Rees, R. C., Rogers, Z. R., Miller, S. T., . . . BABY HUG Investigators. (2011). Abdominal ultrasound with scintigraphic and clinical correlates in infants with sickle cell anemia: Baseline data from the BABY HUG trial. *AJR.American Journal of Roentgenology*, *196*(6), 1399-1404. doi:10.2214/AJR.10.4664 [doi]
- McCurdy, A. R., & Lacy, M. Q. (2013). Pomalidomide and its clinical potential for relapsed or refractory multiple myeloma: An update for the hematologist. *Therapeutic Advances in Hematology*, *4*(3), 211-216. doi:10.1177/2040620713480155 [doi]
- McGrath, K. E., Frame, J. M., Fromm, G. J., Koniski, A. D., Kingsley, P. D., Little, J., . . . Palis, J. (2011). A transient definitive erythroid lineage with unique regulation of the beta-globin locus in the mammalian embryo. *Blood*, *117*(17), 4600-4608. doi:10.1182/blood-2010-12-325357 [doi]
- Mebius, R. E., & Kraal, G. (2005). Structure and function of the spleen. *Nature Reviews.Immunology*, *5*(8), 606-616. doi:nri1669 [pii]
- Meiler, S. E., Wade, M., Kutlar, F., Yerigenahally, S. D., Xue, Y., Moutouh-de Parseval, L. A., . . . Kutlar, A. (2011). Pomalidomide augments fetal hemoglobin production without the myelosuppressive effects of hydroxyurea in transgenic sickle cell mice. *Blood*, *118*(4), 1109-1112. doi:10.1182/blood-2010-11-319137 [doi]

- Menzel, S., Garner, C., Gut, I., Matsuda, F., Yamaguchi, M., Heath, S., . . . Thein, S. L. (2007). A QTL influencing F cell production maps to a gene encoding a zinc-finger protein on chromosome 2p15. *Nature Genetics*, *39*(10), 1197-1199. doi:ng2108 [pii]
- Mohyeldin, A., Garzon-Muvdi, T., & Quinones-Hinojosa, A. (2010). Oxygen in stem cell biology: A critical component of the stem cell niche. *Cell Stem Cell*, *7*(2), 150-161. doi:10.1016/j.stem.2010.07.007 [doi]
- Moriguchi, T., & Yamamoto, M. (2014). A regulatory network governing Gata1 and Gata2 gene transcription orchestrates erythroid lineage differentiation. *International Journal of Hematology*, *100*(5), 417-424. doi:10.1007/s12185-014-1568-0 [doi]
- Moutouh-de Parseval, L. A., Verhelle, D., Glezer, E., Jensen-Pergakes, K., Ferguson, G. D., Corral, L. G., . . . Chan, K. (2008). Pomalidomide and lenalidomide regulate erythropoiesis and fetal hemoglobin production in human CD34+ cells. *The Journal of Clinical Investigation*, *118*(1), 248-258. doi:10.1172/JCI32322 [doi]
- Nandakumar, S. K., Ulirsch, J. C., & Sankaran, V. G. (2016). Advances in understanding erythropoiesis: Evolving perspectives. *British Journal of Haematology*, *173*(2), 206-218. doi:10.1111/bjh.13938 [doi]
- Naymagon, L., Pendurti, G., & Billett, H. H. (2015). Acute splenic sequestration crisis in adult sickle cell disease: A report of 16 cases. *Hemoglobin*, *39*(6), 375-379. doi:10.3109/03630269.2015.1072550 [doi]
- Nemati, M., Hajalioghli, P., Jahed, S., Behzadmehr, R., Rafeey, M., & Fouladi, D. F. (2016). Normal values of spleen length and volume: An ultrasonographic study in children. *Ultrasound in Medicine & Biology*, *42*(8), 1771-1778. doi:10.1016/j.ultrasmedbio.2016.03.005 [doi]

- Neubauer, H., Cumano, A., Muller, M., Wu, H., Huffstadt, U., & Pfeffer, K. (1998). Jak2 deficiency defines an essential developmental checkpoint in definitive hematopoiesis. *Cell*, *93*(3), 397-409. doi:S0092-8674(00)81168-X [pii]
- Noguchi, C. T., Rodgers, G. P., Serjeant, G., & Schechter, A. N. (1988). Levels of fetal hemoglobin necessary for treatment of sickle cell disease. *The New England Journal of Medicine*, *318*(2), 96-99. doi:10.1056/NEJM198801143180207 [doi]
- Noguchi, C. T., Torchia, D. A., & Schechter, A. N. (1983). Intracellular polymerization of sickle hemoglobin. effects of cell heterogeneity. *The Journal of Clinical Investigation*, *72*(3), 846-852. doi:10.1172/JCI111055 [doi]
- Odievre, M. H., Verger, E., Silva-Pinto, A. C., & Elion, J. (2011). Pathophysiological insights in sickle cell disease. *The Indian Journal of Medical Research*, *134*, 532-537. doi:IndianJMedRes_2011_134_4_532_89895 [pii]
- Orkin, S. H. (2000). Diversification of haematopoietic stem cells to specific lineages. *Nature Reviews Genetics*, *1*(1), 57-64. doi:10.1038/35049577 [doi]
- Orringer, E. P., Blythe, D. S., Johnson, A. E., Phillips, G., Jr, Dover, G. J., & Parker, J. C. (1991). Effects of hydroxyurea on hemoglobin F and water content in the red blood cells of dogs and of patients with sickle cell anemia. *Blood*, *78*(1), 212-216.
- Owunwanne, A., Halkar, R., Al-Rasheed, A., Abubacker, K. C., & Abdel-Dayem, H. (1988). Radionuclide imaging of the spleen with heat denatured technetium-99m RBC when the splenic reticuloendothelial system seems impaired. *Journal of Nuclear Medicine : Official Publication, Society of Nuclear Medicine*, *29*(3), 320-323.
- Padmos, M. A., Roberts, G. T., Sackey, K., Kulozik, A., Bail, S., Morris, J. S., . . . Serjeant, G. R. (1991). Two different forms of homozygous sickle cell disease occur in Saudi Arabia. *British Journal of Haematology*, *79*(1), 93-98.

- Paikari, A., & Sheehan, V. A. (2018). Fetal haemoglobin induction in sickle cell disease. *British Journal of Haematology*, *180*(2), 189-200. doi:10.1111/bjh.15021 [doi]
- Palis, J. (2008). Ontogeny of erythropoiesis. *Current Opinion in Hematology*, *15*(3), 155-161. doi:10.1097/MOH.0b013e3282f97ae1 [doi]
- Parganas, E., Wang, D., Stravopodis, D., Topham, D. J., Marine, J. C., Teglund, S., . . . Ihle, J. N. (1998). Jak2 is essential for signaling through a variety of cytokine receptors. *Cell*, *93*(3), 385-395. doi:S0092-8674(00)81167-8 [pii]
- Pauling, L., & Itano, H. A. (1949). Sickle cell anemia a molecular disease. *Science (New York, N.Y.)*, *110*(2865), 543-548. doi:10.1126/science.110.2865.543 [doi]
- Pawley JB. (2006). Handbook of biological confocal microscopy.(Springer US, New York, NY,)
- Pearson, H. A., Spencer, R. P., & Cornelius, E. A. (1969a). Functional asplenia in sickle-cell anemia. *The New England Journal of Medicine*, *281*(17), 923-926. doi:10.1056/NEJM196910232811703 [doi]
- Pearson, H. A., Spencer, R. P., & Cornelius, E. A. (1969b). Functional asplenia in sickle-cell anemia. *The New England Journal of Medicine*, *281*(17), 923-926. doi:10.1056/NEJM196910232811703 [doi]
- Piel, F. B., Hay, S. I., Gupta, S., Weatherall, D. J., & Williams, T. N. (2013). Global burden of sickle cell anaemia in children under five, 2010-2050: Modelling based on demographics, excess mortality, and interventions. *PLoS Medicine*, *10*(7), e1001484. doi:10.1371/journal.pmed.1001484 [doi]
- Piel, F. B., Rees, D. C., & Williams, T. N. (2014). Managing the burden of sickle-cell disease in africa. *The Lancet.Haematology*, *1*(1), e11-2. doi:10.1016/S2352-3026(14)70017-1 [doi]

- Piel, F. B., Steinberg, M. H., & Rees, D. C. (2017). Sickle cell disease. *The New England Journal of Medicine*, 377(3), 305. doi:10.1056/NEJMc1706325 [doi]
- Platt, O. S., Brambilla, D. J., Rosse, W. F., Milner, P. F., Castro, O., Steinberg, M. H., & Klug, P. P. (1994). Mortality in sickle cell disease. life expectancy and risk factors for early death. *The New England Journal of Medicine*, 330(23), 1639-1644. doi:10.1056/NEJM199406093302303 [doi]
- Potts, K. S., Sargeant, T. J., Markham, J. F., Shi, W., Biben, C., Josefsson, E. C., . . . Taoudi, S. (2014). A lineage of diploid platelet-forming cells precedes polyploid megakaryocyte formation in the mouse embryo. *Blood*, 124(17), 2725-2729. doi:10.1182/blood-2014-02-559468 [doi]
- Powars, D. R., Weiss, J. N., Chan, L. S., & Schroeder, W. A. (1984). Is there a threshold level of fetal hemoglobin that ameliorates morbidity in sickle cell anemia? *Blood*, 63(4), 921-926.
- Powell, R. W., Levine, G. L., Yang, Y. M., & Mankad, V. N. (1992). Acute splenic sequestration crisis in sickle cell disease: Early detection and treatment. *Journal of Pediatric Surgery*, 27(2), 215-8; discussion 218-9. doi:0022-3468(92)90315-X [pii]
- Quinn, C. T., Rogers, Z. R., McCavit, T. L., & Buchanan, G. R. (2010). Improved survival of children and adolescents with sickle cell disease. *Blood*, 115(17), 3447-3452. doi:10.1182/blood-2009-07-233700 [doi]
- Ramakrishnan, M., Moisi, J. C., Klugman, K. P., Iglesias, J. M., Grant, L. R., Mpoudi-Etame, M., & Levine, O. S. (2010). Increased risk of invasive bacterial infections in african people with sickle-cell disease: A systematic review and meta-analysis. *The Lancet.Infectious Diseases*, 10(5), 329-337. doi:10.1016/S1473-3099(10)70055-4 [doi]
- Redwood, A. M., Williams, E. M., Desal, P., & Serjeant, G. R. (1976). Climate and painful crisis of sickle-cell disease in jamaica. *British Medical Journal*, 1(6001), 66-68. doi:10.1136/bmj.1.6001.66 [doi]

- Rees, D. C., Williams, T. N., & Gladwin, M. T. (2010). Sickle-cell disease. *Lancet (London, England)*, 376(9757), 2018-2031. doi:10.1016/S0140-6736(10)61029-X [doi]
- Reihani, N., Arlet, J. B., Dussiot, M., de Villemeur, T. B., Belmatoug, N., Rose, C., . . . Franco, M. (2016). Unexpected macrophage-independent dyserythropoiesis in gaucher disease. *Haematologica*, 101(12), 1489-1498. doi:haematol.2016.147546 [pii]
- Ribeil, J. A., Arlet, J. B., Dussiot, M., Moura, I. C., Courtois, G., & Hermine, O. (2013). Ineffective erythropoiesis in beta -thalassemia. *TheScientificWorldJournal*, 2013, 394295. doi:10.1155/2013/394295 [doi]
- Ribeil, J. A., Hacein-Bey-Abina, S., Payen, E., Magnani, A., Semeraro, M., Magrin, E., . . . Cavazzana, M. (2017). Gene therapy in a patient with sickle cell disease. *The New England Journal of Medicine*, 376(9), 848-855. doi:10.1056/NEJMoa1609677 [doi]
- Ribeil, J. A., Zermati, Y., Vandekerckhove, J., Cathelin, S., Kersual, J., Dussiot, M., . . . Hermine, O. (2007). Hsp70 regulates erythropoiesis by preventing caspase-3-mediated cleavage of GATA-1. *Nature*, 445(7123), 102-105. doi:nature05378 [pii]
- Rivella, S. (2009). Ineffective erythropoiesis and thalassemias. *Current Opinion in Hematology*, 16(3), 187-194. doi:10.1097/MOH.0b013e32832990a4 [doi]
- Rogers, D. W., Serjeant, B. E., & Serjeant, G. R. (1982). Early rise in the "pitted" red cell count as a guide to susceptibility to infection in childhood sickle cell anaemia. *Archives of Disease in Childhood*, 57(5), 338-342.
- Rogers, D. W., Vaidya, S., & Serjeant, G. R. (1978). Early splenomegaly in homozygous sickle-cell disease: An indicator of susceptibility to infection. *Lancet (London, England)*, 2(8097), 963-965. doi:S0140-6736(78)92527-8 [pii]

- Rogers, Z. R., Wang, W. C., Luo, Z., Iyer, R. V., Shalaby-Rana, E., Dertinger, S. D., . . . BABY HUG. (2011). Biomarkers of splenic function in infants with sickle cell anemia: Baseline data from the BABY HUG trial. *Blood*, *117*(9), 2614-2617. doi:10.1182/blood-2010-04-278747 [doi]
- Romana, M., Connes, P., & Key, N. S. (2018). Microparticles in sickle cell disease. *Clinical Hemorheology and Microcirculation*, *68*(2-3), 319-329. doi:10.3233/CH-189014 [doi]
- Rosse, W. F., Gallagher, D., Kinney, T. R., Castro, O., Dosik, H., Moohr, J., . . . Levy, P. S. (1990). Transfusion and alloimmunization in sickle cell disease. the cooperative study of sickle cell disease. *Blood*, *76*(7), 1431-1437.
- Safeukui, I., Correias, J. M., Brousse, V., Hirt, D., Deplaine, G., Mule, S., . . . Buffet, P. A. (2008). Retention of plasmodium falciparum ring-infected erythrocytes in the slow, open microcirculation of the human spleen. *Blood*, *112*(6), 2520-2528. doi:10.1182/blood-2008-03-146779 [doi]
- Sankaran, V. G., Joshi, M., Agrawal, A., Schmitz-Abe, K., Towne, M. C., Marinakis, N., . . . Agrawal, P. B. (2013). Rare complete loss of function provides insight into a pleiotropic genome-wide association study locus. *Blood*, *122*(23), 3845-3847. doi:10.1182/blood-2013-09-528315 [doi]
- Sankaran, V. G., Menne, T. F., Xu, J., Akie, T. E., Lettre, G., Van Handel, B., . . . Orkin, S. H. (2008). Human fetal hemoglobin expression is regulated by the developmental stage-specific repressor BCL11A. *Science (New York, N.Y.)*, *322*(5909), 1839-1842. doi:10.1126/science.1165409 [doi]
- Sankaran, V. G., & Nathan, D. G. (2010). Reversing the hemoglobin switch. *The New England Journal of Medicine*, *363*(23), 2258-2260. doi:10.1056/NEJMcibr1010767 [doi]
- Sankaran, V. G., & Orkin, S. H. (2013). The switch from fetal to adult hemoglobin. *Cold Spring Harbor Perspectives in Medicine*, *3*(1), a011643. doi:10.1101/cshperspect.a011643 [doi]

- Schindelin, J., Arganda-Carreras, I., Frise, E., Kaynig, V., Longair, M., Pietzsch, T., . . . Cardona, A. (2012). Fiji: An open-source platform for biological-image analysis. *Nature Methods*, 9(7), 676-682. doi:10.1038/nmeth.2019 [doi]
- Schweitzer, K. M., Vicart, P., Delouis, C., Paulin, D., Drager, A. M., Langenhuijsen, M. M., & Weksler, B. B. (1997). Characterization of a newly established human bone marrow endothelial cell line: Distinct adhesive properties for hematopoietic progenitors compared with human umbilical vein endothelial cells. *Laboratory Investigation; a Journal of Technical Methods and Pathology*, 76(1), 25-36.
- Sears, D. A., & Udden, M. M. (2012). Howell-jolly bodies: A brief historical review. *The American Journal of the Medical Sciences*, 343(5), 407-409. doi:10.1097/MAJ.0b013e31823020d1 [doi]
- Seki, M., & Shirasawa, H. (1965). Role of the reticular cells during maturation process of the erythroblast. 3. the fate of phagocytized nucleus. *Acta Pathologica Japonica*, 15(4), 387-405.
- Serjeant, G. R., Serjeant, B. E., Desai, P., Mason, K. P., Sewell, A., & England, J. M. (1978). The determinants of irreversibly sickled cells in homozygous sickle cell disease. *British Journal of Haematology*, 40(3), 431-438.
- Serjeant, G. R., Serjeant, B. E., & Mason, K. (1977). Heterocellular hereditary persistence of fetal haemoglobin and homozygous sickle-cell disease. *Lancet (London, England)*, 1(8015), 795-796. doi:10.1016/s0140-6736(77)92976-2 [doi]
- Severn, C. E., & Toye, A. M. (2017). The challenge of growing enough reticulocytes for transfusion. Paper presented at the Copenhagen Denmark. , 13(1) 80-86. doi:<https://doi.org/10.1111/voxs.12374> Retrieved from <https://onlinelibrary.wiley.com/doi/full/10.1111/voxs.12374>
- Sewchand, L. S., Johnson, C. S., & Meiselman, H. J. (1983). The effect of fetal hemoglobin on the sickling dynamics of SS erythrocytes. *Blood Cells*, 9(1), 147-166.

- Singhal, A., Thomas, P., Kearney, T., Venugopal, S., & Serjeant, G. (1995). Acceleration in linear growth after splenectomy for hypersplenism in homozygous sickle cell disease. *Archives of Disease in Childhood*, 72(3), 227-229. doi:10.1136/adc.72.3.227 [doi]
- Skutelsky, E., & Danon, D. (1972). On the expulsion of the erythroid nucleus and its phagocytosis. *The Anatomical Record*, 173(1), 123-126. doi:10.1002/ar.1091730111 [doi]
- Solier, S., Fontenay, M., Vainchenker, W., Droin, N., & Solary, E. (2017). Non-apoptotic functions of caspases in myeloid cell differentiation. *Cell Death and Differentiation*, 24(8), 1337-1347. doi:10.1038/cdd.2017.19 [doi]
- Stamatoyannopoulos, G., Veith, R., Galanello, R., & Papayannopoulou, T. (1985). Hb F production in stressed erythropoiesis: Observations and kinetic models. *Annals of the New York Academy of Sciences*, 445, 188-197. doi:10.1111/j.1749-6632.1985.tb17188.x [doi]
- Steinberg, M. H. (2008). Sickle cell anemia, the first molecular disease: Overview of molecular etiology, pathophysiology, and therapeutic approaches. *TheScientificWorldJournal*, 8, 1295-1324. doi:10.1100/tsw.2008.157 [doi]
- Steinberg, M. H., Barton, F., Castro, O., Pegelow, C. H., Ballas, S. K., Kutlar, A., . . . Terrin, M. (2003). Effect of hydroxyurea on mortality and morbidity in adult sickle cell anemia: Risks and benefits up to 9 years of treatment. *Jama*, 289(13), 1645-1651. doi:10.1001/jama.289.13.1645 [doi]
- Steinberg, M. H., Chui, D. H., Dover, G. J., Sebastiani, P., & Alsultan, A. (2014). Fetal hemoglobin in sickle cell anemia: A glass half full? *Blood*, 123(4), 481-485. doi:10.1182/blood-2013-09-528067 [doi]
- Steiniger, B., Barth, P., & Hellinger, A. (2001). The perifollicular and marginal zones of the human splenic white pulp : Do fibroblasts guide lymphocyte immigration? *The American Journal of Pathology*, 159(2), 501-512. doi:S0002-9440(10)61722-1 [pii]

- Steiniger, B., Bette, M., & Schwarzbach, H. (2011). The open microcirculation in human spleens: A three-dimensional approach. *The Journal of Histochemistry and Cytochemistry : Official Journal of the Histochemistry Society*, 59(6), 639-648. doi:10.1369/0022155411408315 [doi]
- Steiniger, B. S. (2015). Human spleen microanatomy: Why mice do not suffice. *Immunology*, 145(3), 334-346. doi:10.1111/imm.12469 [doi]
- Stuart, M. J., & Nagel, R. L. (2004). Sickle-cell disease. *Lancet (London, England)*, 364(9442), 1343-1360. doi:S0140673604171924 [pii]
- Tada, T., Inoue, N., Widayati, D. T., & Fukuta, K. (2008). Role of MAdCAM-1 and its ligand on the homing of transplanted hematopoietic cells in irradiated mice. *Experimental Animals*, 57(4), 347-356. doi:JST.JSTAGE/expanim/57.347 [pii]
- Tanavde, V. M., Malehorn, M. T., Lumkul, R., Gao, Z., Wingard, J., Garrett, E. S., & Civin, C. I. (2002). Human stem-progenitor cells from neonatal cord blood have greater hematopoietic expansion capacity than those from mobilized adult blood. *Experimental Hematology*, 30(7), 816-823. doi:S0301472X02008184 [pii]
- Telfer, P., Coen, P., Chakravorty, S., Wilkey, O., Evans, J., Newell, H., . . . Kirkham, F. (2007). Clinical outcomes in children with sickle cell disease living in england: A neonatal cohort in east london. *Haematologica*, 92(7), 905-912.
- Thein, S. L., Menzel, S., Peng, X., Best, S., Jiang, J., Close, J., . . . Lathrop, M. (2007). Intergenic variants of HBS1L-MYB are responsible for a major quantitative trait locus on chromosome 6q23 influencing fetal hemoglobin levels in adults. *Proceedings of the National Academy of Sciences of the United States of America*, 104(27), 11346-11351. doi:0611393104 [pii]
- Thompson, A. A., Walters, M. C., Kwiatkowski, J., Rasko, J. E. J., Ribeil, J. A., Hongeng, S., . . . Cavazzana, M. (2018). Gene therapy in patients with transfusion-dependent beta-thalassemia. *The New England Journal of Medicine*, 378(16), 1479-1493. doi:10.1056/NEJMoa1705342 [doi]

- Topley, J. M., Rogers, D. W., Stevens, M. C., & Serjeant, G. R. (1981). Acute splenic sequestration and hypersplenism in the first five years in homozygous sickle cell disease. *Archives of Disease in Childhood*, 56(10), 765-769. doi:10.1136/adc.56.10.765 [doi]
- Turhan, A., Weiss, L. A., Mohandas, N., Coller, B. S., & Frenette, P. S. (2002). Primary role for adherent leukocytes in sickle cell vascular occlusion: A new paradigm. *Proceedings of the National Academy of Sciences of the United States of America*, 99(5), 3047-3051. doi:10.1073/pnas.052522799 [doi]
- Udani, M., Zen, Q., Cottman, M., Leonard, N., Jefferson, S., Daymont, C., . . . Telen, M. J. (1998). Basal cell adhesion molecule/lutheran protein. the receptor critical for sickle cell adhesion to laminin. *The Journal of Clinical Investigation*, 101(11), 2550-2558. doi:10.1172/JCI1204 [doi]
- van Beers, E. J., Samsel, L., Mendelsohn, L., Saiyed, R., Fertrin, K. Y., Brantner, C. A., . . . Kato, G. J. (2014). Imaging flow cytometry for automated detection of hypoxia-induced erythrocyte shape change in sickle cell disease. *American Journal of Hematology*, 89(6), 598-603. doi:10.1002/ajh.23699 [doi]
- Vichinsky, E., Hoppe, C. C., Ataga, K. I., Ware, R. E., Nduba, V., El-Beshlawy, A., . . . HOPE Trial Investigators. (2019). A phase 3 randomized trial of voxelotor in sickle cell disease. *The New England Journal of Medicine*, doi:10.1056/NEJMoa1903212 [doi]
- Walterspiel, J. N., Rutledge, J. C., & Bartlett, B. L. (1984). Fatal acute splenic sequestration at 4 months of age. *Pediatrics*, 73(4), 507-508.
- Wang, W. C., Wynn, L. W., Rogers, Z. R., Scott, J. P., Lane, P. A., & Ware, R. E. (2001). A two-year pilot trial of hydroxyurea in very young children with sickle-cell anemia. *The Journal of Pediatrics*, 139(6), 790-796. doi:S0022-3476(01)91580-X [pii]
- Ware, R. E., & Aygun, B. (2009). Advances in the use of hydroxyurea. *Hematology.American Society of Hematology.Education Program*, , 62-69. doi:10.1182/asheducation-2009.1.62 [doi]

- Weatherall, D., Hofman, K., Rodgers, G., Ruffin, J., & Hrynkow, S. (2005). A case for developing north-south partnerships for research in sickle cell disease. *Blood*, *105*(3), 921-923. doi:2004-06-2404 [pii]
- Weller, S., Braun, M. C., Tan, B. K., Rosenwald, A., Cordier, C., Conley, M. E., . . . Weill, J. C. (2004). Human blood IgM "memory" B cells are circulating splenic marginal zone B cells harboring a prediversified immunoglobulin repertoire. *Blood*, *104*(12), 3647-3654. doi:10.1182/blood-2004-01-0346 [doi]
- Wiles, N., & Howard, J. (2009). Role of hydroxycarbamide in prevention of complications in patients with sickle cell disease. *Therapeutics and Clinical Risk Management*, *5*, 745-755. doi:10.2147/tcrm.s4769 [doi]
- Wojchowski, D. M., Sathyanarayana, P., & Dev, A. (2010). Erythropoietin receptor response circuits. *Current Opinion in Hematology*, *17*(3), 169-176. doi:10.1097/MOH.0b013e328338008b [doi]
- Wood, K. C., Hsu, L. L., & Gladwin, M. T. (2008). Sickle cell disease vasculopathy: A state of nitric oxide resistance. *Free Radical Biology & Medicine*, *44*(8), 1506-1528. doi:10.1016/j.freeradbiomed.2008.01.008 [doi]
- Wood, W. G., Stamatoyannopoulos, G., Lim, G., & Nute, P. E. (1975). F-cells in the adult: Normal values and levels in individuals with hereditary and acquired elevations of hb F. *Blood*, *46*(5), 671-682.
- Wu, C. J., Krishnamurti, L., Kutok, J. L., Biernacki, M., Rogers, S., Zhang, W., . . . Ritz, J. (2005). Evidence for ineffective erythropoiesis in severe sickle cell disease. *Blood*, *106*(10), 3639-3645. doi:2005-04-1376 [pii]
- Wu, H., Liu, X., Jaenisch, R., & Lodish, H. F. (1995). Generation of committed erythroid BFU-E and CFU-E progenitors does not require erythropoietin or the erythropoietin receptor. *Cell*, *83*(1), 59-67. doi:0092-8674(95)90234-1 [pii]

- Yeo, J. H., Cosgriff, M. P., & Fraser, S. T. (2018). Analyzing the formation, morphology, and integrity of erythroblastic islands. *Methods in Molecular Biology (Clifton, N.J.)*, 1698, 133-152.
doi:10.1007/978-1-4939-7428-3_8 [doi]
- Yoder, M. C. (2014). Inducing definitive hematopoiesis in a dish. *Nature Biotechnology*, 32(6), 539-541. doi:10.1038/nbt.2929 [doi]
- Zhang, D., Xu, C., Manwani, D., & Frenette, P. S. (2016). Neutrophils, platelets, and inflammatory pathways at the nexus of sickle cell disease pathophysiology. *Blood*, 127(7), 801-809.
doi:10.1182/blood-2015-09-618538 [doi]
- Zivot, A., Lipton, J. M., Narla, A., & Blanc, L. (2018). Erythropoiesis: Insights into pathophysiology and treatments in 2017. *Molecular Medicine (Cambridge, Mass.)*, 24(1), 11-018-0011-z.
doi:10.1186/s10020-018-0011-z [doi]

APPENDIX

Article 1

LETTERS TO THE EDITOR

A novel non-invasive method to measure splenic filtration function in humans

The detection of red cells with Howell-Jolly bodies and liver-spleen scintigraphy scanning are the currently used methods to assess splenic filtration function. The former is time-consuming, user-dependent and quantitative. The latter is semi-quantitative but uses radioactive material in an invasive, laborious manner. Here, we developed an automated, high-throughput, non-invasive and low-cost method to measure splenic filtration function accurately using flow cytometry.

Loss of splenic function results in short- and long-term potentially life-threatening complications including susceptibility to infections by encapsulated bacteria and thromboembolic events.^{1,2} Increasing evidence points to the need to preserve splenic function in various situations such as post-traumatic spleen injury, pancreatic neoplasia and hemolytic anemias. Adequate measurements of the residual function of the spleen are, therefore, crucial.

Howell-Jolly bodies (HJB) are 1 μm DNA inclusion bodies that are the consequence of cytogenetic damage. In healthy individuals, HJB-containing red blood cells (RBC) are found at very low frequency as HJB are cleared efficiently by the spleen. The spleen is a distinctive adapted lymphoid organ that serves as the largest filter of blood in the human body. The spleen comprises two critical structures: (i) the white pulp, containing the immune effector cells and (ii) the red pulp, composed of splenic sinuses and pulp cords that form a filtering structural entity.³ RBC flowing in the pulp cords are forced to deform and squeeze through narrow inter-endothelial slits in order to enter the venous circulation. During this process intracellular inclusions, such as HJB or parasites, are removed from the RBC, a phenomenon known as pitting.^{4,5} Identification of HJB in the circulation consequently serves as an indicator of altered splenic filtration function.^{6,7}

To date, the gold standard for assessing splenic function remains liver-spleen scintigraphy scanning. This technique provides a qualitative and/or semi-quantitative measurement of splenic function by evaluating the

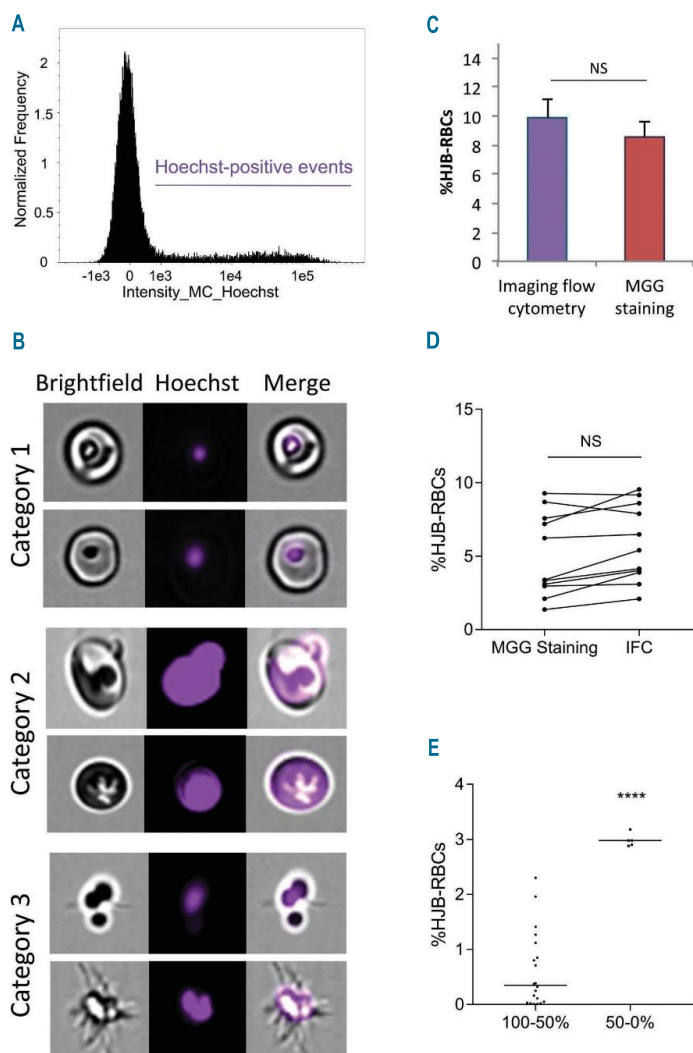


Figure 1. Detecting Howell-Jolly bodies using imaging flow cytometry. (A) Histogram representing the intensity of Hoechst staining in a splenectomized individual. (B) Images from imaging flow cytometry distinguishing three categories of cells: (i) RBC with HJB-like spots, (ii) RBC bound to Hoechst-positive particles and (iii) Hoechst-positive particles. (C, D) Graphs representing the percentage of HJB-RBC determined by the classical blood smear technique and imaging flow cytometry in (C) 10 splenectomized individuals (unpaired *t* test, $P=0.07$) and (D) 11 adults with sickle cell disease (Wilcoxon test, $P=0.057$) (NS: non-significant). (E) Graphical representation of the percentage of HJB-RBC determined by imaging flow cytometry in 20 patients with a splenic uptake of 100-50% and seven patients with a splenic uptake of 50-0% (Mann-Whitney test, $P<0.0001$). MGG: May-Grunwald Giemsa, IFC: imaging flow cytometry.

LETTERS TO THE EDITOR

splenic uptake of either heat-denatured RBC or nano-colloids, labeled with technetium-99m.⁸ Although these techniques have proven reliable, they are time-consuming, invasive and not readily available. The classically used method for assessing splenic dysfunction is, therefore, quantification of HJB-containing RBC by May-Grünwald Giemsa staining on blood smears. The percentage of HJB-containing RBC is evaluated by counting 100-200 RBC under the microscope; the result is delivered as %HJB, a percentage higher than 1% reflecting loss of splenic function. This method is user-dependent and may be faulty because of the small number of counted cells. Another similar, commonly used method is to count "pitted" erythrocytes by interference contrast microscopy.⁹ Splenic dysfunction does, however, occur gradually in many pathological conditions and is not accurately evaluated by a binary "filters/does not filter" state. A flow cytometry-based method using propidium iodide as a DNA dye to measure micronucleated reticulocytes was reported in 1996¹⁰ and later used in clinical studies to quantify HJB-containing RBC.^{11,12} As propidium iodide also stains RNA that is present in young RBC (reticulocytes), this method requires an efficient RNA digestion step to be accurate. In addition to issues

regarding partial digestion, reticulocytes, which represent 0.5-1% of circulating RBC in healthy individuals, can reach high percentages in pathological situations such as hemolytic anemias, including sickle cell disease (SCD) and hereditary spherocytosis, which increases the risk of including significant numbers of false-positive events.

Here, we developed a simple non-invasive high-throughput technique based on flow cytometry to specifically detect HJB-containing RBC and precisely quantify their percentage in the circulation. To do so, we used blood samples from splenectomized individuals, patients with SCD, and healthy donors. SCD is an autosomal recessive disease during which spleen injury occurs early in life due to vaso-occlusion caused by RBC sickling secondary to the polymerization of a mutated hemoglobin (HbS).¹³ The splenic dysfunction is associated with considerable morbidity and mortality¹⁴, including life-threatening acute splenic sequestration and an increased risk of infections. In SCD, the onset of spleen dysfunction occurs within the first years of life¹⁵ with the function decreasing thereafter to a state of complete loss, called auto-splenectomy.

In our method, we stained the HJB using Hoechst dye

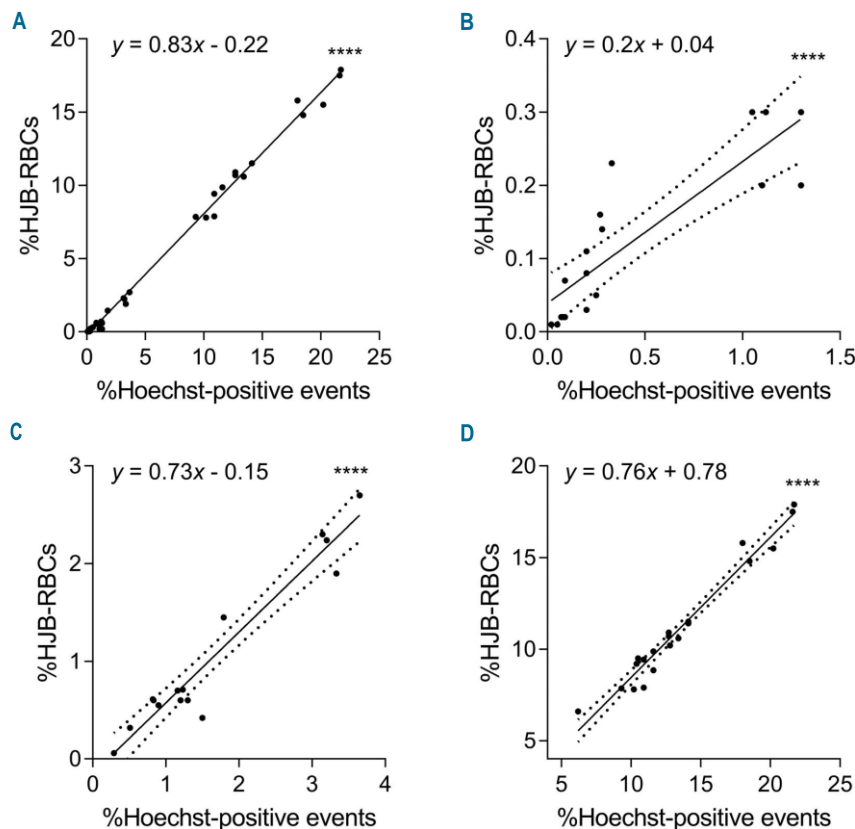


Figure 2. Relationship between %Hoechst-positive events and %HJB-RBC. (A) Linear regression relationship between %Hoechst-positive events (x) and %HJB-RBC (y) in 53 blood samples ($y = 0.83x - 0.22$). (B-D) Refinement of the linear regression according to three cut-offs of %Hoechst-positive events: (B) <0.5% (n=18) ($y = 0.2x + 0.04$), (C) 0.5-3.5% (n=14) ($y = 0.73x - 0.15$), and (D) >3.5% (n=21) ($y = 0.76x + 0.78$). Correlation (Pearson correlation coefficient) and linear regression, $P < 0.0001$.

as this does not bind to RNA molecules. First, we used blood samples from splenectomized individuals to detect significant amounts of HJB-containing RBC (HJB-RBC). After removal of the buffy coat, the RBC were washed and incubated for 5 min in phosphate-buffered saline with Hoechst at 0.2%. RBC were analyzed with a standard flow cytometer and percentages of Hoechst-positive events were determined (*Online Supplementary Table S1, Online Supplementary Methods*). As the results indicated high percentages of Hoechst-positive RBC, we repeated this experiment using seven blood samples from healthy donors. All samples showed percentages higher than 1% (*Online Supplementary Table S1*) suggesting the presence of significant numbers of false-positive events. For further characterization, we used imaging flow cytometry and analyzed Hoechst-positive events in 50,000 RBC (Figure 1A,B). We could distinguish three categories: (i) RBC with HJB-like spots, (ii) RBC bound to Hoechst-positive particles and (iii) Hoechst-positive particles (Figure 1B). The Hoechst-positive particles were considered non-specific events, i.e. DNA released after lysis of neutrophils during the preparation steps, and were excluded using a combination of masks (*Online Supplementary Figure S1A*). This strategy markedly reduced the percentage of Hoechst-positive events in all blood samples (*Online Supplementary Table S1*) and all corresponding pictures thereafter showed RBC with HJB-like spots.

To validate this method, we compared the results with those obtained with classical May-Grünwald Giemsa staining in ten splenectomized individuals. HJB-RBC were counted manually within a total of 3,000 RBC (*Online Supplementary Figure S1B*). The results confirmed a robust correlation and therefore efficient gating and mask parameters to exclude false-positive events (Figure 1C). This was also the case when comparing both methods using blood samples from 11 adult patients with SCD (P1-P11) (Figure 1D).

We thereafter applied our imaging flow cytometry method to evaluate the percentage of HJB-RBC (%HJB-RBC) in 25 very young SCD children (P12-P36; age range, 6-12 months) who underwent technetium-99m RBC splenic scintigraphy. Patients were divided into two groups according to their splenic uptake percentage: (100%-50%) and (50%-0%). The two groups displayed marked differences, with the (100%-50%) and (50%-0%) groups showing medians of 0.35% and 2.98% HJB-RBC, respectively (Figure 1E).

Because imaging flow cytometry is not a readily available technology, we aimed at refining the standard flow cytometry method in order to allow accurate evaluation of %HJB-RBC. We determined %HJB-RBC by flow cytometry in the group of 53 individuals with various degrees of splenic function (36 SCD patients, 10 splenectomized individuals and 7 non-splenectomized healthy donors). The percentage of total Hoechst-positive events, determined by standard flow cytometry, was plotted against the percentage of HJB-containing RBC determined by imaging flow cytometry (*Online Supplementary Table S1*). We observed a robust linear regression between both parameters (Figure 2A), with the following equation: $y = 0.83x - 0.22$, where y is the %HJB-RBC and x the % of Hoechst-positive events generated by flow cytometry. We further refined this equation by dividing the 53 samples into three groups and generated three equations based on three cut-offs of Hoechst-positive events: $< 0.5\%$, $0.5-3\%$ and $> 3\%$ (Figure 2B-D).

Monitoring spleen function has been neglected

because the methods used are labor-intensive, such as counting pitted or HJB-positive RBC, or invasive, such as liver-spleen scintigraphy scanning. Here, we describe an automated, non-invasive technique for the sensitive detection and evaluation of splenic filtration dysfunction. In contrast to the previously published flow cytometry technique, our method does not require cell fixation, RNA digestion steps or sample shipment. Our technique is simple and straightforward to implement in medical centers equipped with standard flow cytometers, thereby offering splenic function tests routinely. Such tests would be of great interest and might significantly affect the management and follow-up of patients with pathologies characterized by splenic injury, including SCD, thalassemia, red cell membrane disorders, celiac disease and cancer during chemotherapy. For instance, implementing our method in the early follow-up of children with SCD would play an important role in monitoring their infectious risk, a life-threatening consequence of this disease.

Sara El Hoss,^{1,2,3} Michaël Dussiot,⁴ Olivier Renaud,^{5,6,7,8} Valentine Brousse^{*1,2,3,9} and Wassim El Nemer^{*1,2,3}.

¹Biologie Intégrée du Globule Rouge UMR_S1134, Inserm, Univ. Paris Diderot, Sorbonne Paris Cité, Univ. de la Réunion, Univ. des Antilles; ²Institut National de la Transfusion Sanguine, Paris; ³Laboratoire d'Excellence GR-Ex, Paris; ⁴INSERM UMR1163, CNRS ERL8254, Laboratoire d'excellence GR-Ex, Université René-Descartes, Imagine Institute, Paris; ⁵Institut Curie, Paris Sciences et Lettres Research University, Paris; ⁶U934, Institut National de la Santé et de la Recherche Médicale, Paris; ⁷UMR3215, Centre National de la Recherche Scientifique, Paris; ⁸Cell and Tissue Imaging Facility (PICT-IBiSA), Institut Curie, Paris and ⁹Service de Pédiatrie Générale, Hôpital Necker-Enfants Malades, Centre de Référence de la Drépanocytose, AP-HP, Paris, France

*VB and WEN contributed equally to this work.

Acknowledgments: we thank Dr Thierry Peyrard and Ms. Dominique Gien, Sirandou Tounkara and Eliane Véra at the Centre National de Référence pour les Groupes Sanguins for the management of blood samples, and Dr Arnaud Chene for his valuable help in performing MGG staining. This work was supported by the Institut National de la Santé et de la Recherche Médicale (Inserm), the Institut National de la Transfusion Sanguine and the Laboratory of Excellence GR-Ex, reference ANR-11-LABX-0051; GR-Ex is funded by the program "Investissements d'avenir" of the French National Research Agency, reference ANR-11-IDEX-0005-02. We acknowledge the PICT-IBiSA (Paris, France), member of the French National Research Infrastructure France-BioImaging (ANR-10-INBS-04), for microscopy experiments.

Funding: Sara El Hoss was funded by the Ministère de l'Enseignement Supérieur et de la Recherche (Ecole Doctorale BioSPC) and received financial support from the "Club du Globule Rouge et du Fer".

Correspondence: wassim.el-nemer@inserm.fr
doi:10.3324/haematol.2018.188920

Information on authorship, contributions, and financial & other disclosures was provided by the authors and is available with the online version of this article at www.haematologica.org.

References

- Kristinsson SY, Gridley G, Hoover RN, Check D, Landgren O. Long-term risks after splenectomy among 8,149 cancer-free American veterans: a cohort study with up to 27 years follow-up. *Haematologica*. 2014;99(2):392-398.
- Lin JN, Lin CL, Lin MC, et al. Increased risk of hemorrhagic and ischemic strokes in patients with splenic injury and splenectomy: a nationwide cohort study. *Medicine (Baltimore)*.

LETTERS TO THE EDITOR

- 2015;94(35):e1458.
1. Mebius RE, Kraal G. Structure and function of the spleen. *Nat Rev Immunol.* 2005;5(8):606-616.
 2. Buffet PA, Safeukui I, Deplaine G, et al. The pathogenesis of *Plasmodium falciparum* malaria in humans: insights from splenic physiology. *Blood.* 2011;117(2):381-392.
 3. Spencer RP, Pearson HA. The spleen as a hematological organ. *Semin Nucl Med.* 1975;5(1):95-102.
 4. Pearson HA, Spencer RP, Cornelius EA. Functional asplenia in sickle-cell anemia. *N Engl J Med.* 1969;281(17):923-926.
 5. Brousse V, Buffet P, Rees D. The spleen and sickle cell disease: the sick(led) spleen. *Br J Haematol.* 2014;166(2):165-176.
 6. Ehrlich CP, Papanicolaou N, Treves S, Hurwitz RA, Richards P. Splenic scintigraphy using Tc-99m-labeled heat-denatured red blood cells in pediatric patients: concise communication. *J Nucl Med.* 1982;23(3):209-213.
 7. Casper JT, Koethe S, Rodey GE, Thatcher LG. A new method for studying splenic reticuloendothelial dysfunction in sickle cell disease patients and its clinical application: a brief report. *Blood.* 1976;47(2):183-188.
 8. Dertinger SD, Torous DK, Tometsko KR. Simple and reliable enumeration of micronucleated reticulocytes with a single-laser flow cytometer. *Mutat Res.* 1996;371(3-4):283-292.
 9. Harrod VL, Howard TA, Zimmerman SA, Dertinger SD, Ware RE. Quantitative analysis of Howell-Jolly bodies in children with sickle cell disease. *Exp Hematol.* 2007;35(2):179-183.
 10. Rogers ZR, Wang WC, Luo Z, et al. Biomarkers of splenic function in infants with sickle cell anemia: baseline data from the BABY HUG Trial. *Blood.* 2011;117(9):2614-2617.
 11. Pauling L, Itano HA, et al. Sickle cell anemia, a molecular disease. *Science.* 1949;109(2835):443.
 12. Ware RE, de Montalembert M, Tshilolo L, Abboud MR. Sickle cell disease. *Lancet.* 2017;390(10091):311-323.
 13. Pearson HA, Gallagher D, Chilcote R, et al. Developmental pattern of splenic dysfunction in sickle cell disorders. *Pediatrics.* 1985;76(3):392-397.

Article 2

Received: 12 August 2018 | Accepted: 15 August 2018

DOI: 10.1002/ajh.25260



RESEARCH ARTICLE

Prognostic factors of disease severity in infants with sickle cell anemia: A comprehensive longitudinal cohort study

Valentine Brousse^{1,2} | Sara El Hoss² | Naïm Bouazza^{3,4} | Cécile Arnaud⁵ |
 Françoise Bernaudin⁵ | Béatrice Pellegrino⁶ | Corinne Guitton⁷ |
 Marie-Hélène Odièvre-Montanié⁸ | David Mames⁹ | Chantal Brouzes¹⁰ |
 Véronique Picard¹¹ | Thao Nguyen-Khoa¹⁰ | Catia Pereira² | Claudine Lapoumériou² |
 Serge Pissard¹² | Kate Gardner^{13,14} | Stephan Menzel¹³ | Caroline Le Van Kim² |
 Yves Colin-Aronovicz² | Pierre Buffet² | Narla Mohandas¹⁵ | Caroline Elie³ |
 Micheline Maier-Redelsperger⁹ | Wassim El Nemer² | Mariane de Montalembert¹

¹Service de Pédiatrie et Maladies Infectieuses, Hôpital Universitaire Necker-Enfants Malades, Paris, France²UMR_S 1134 Biologie Intégrée du Globule Rouge, Université Sorbonne Paris Cité/Université Paris Diderot/INSERM/INTS/Laboratoire d'Excellence GR-Ex, Paris, France³Unité de Recherche Clinique/Centre d'investigation clinique Paris Descartes Necker-Cochin, Assistance Publique-Hôpitaux de Paris, Paris, France⁴Université Paris Descartes, EA7323, Sorbonne Paris Cité, Paris, France⁵Service de Pédiatrie, Centre Hospitalier Intercommunal de Créteil, Créteil, France⁶Service de Pédiatrie, Centre Hospitalier Poissy-Saint Germain, Poissy, France⁷Service de Pédiatrie, Hôpital Universitaire Kremlin-Bicêtre, Le Kremlin-Bicêtre, France⁸Service de Pédiatrie, Hôpital Universitaire Armand Trousseau, Paris, France⁹Laboratoire d'Hématologie, Hôpital Universitaire Tenon, Paris, France¹⁰Laboratoires d'Hématologie et de Biochimie, Hôpital Universitaire Necker-Enfants Malades, Paris, France¹¹Laboratoire d'Hématologie, Hôpital Universitaire Kremlin Bicêtre, Le Kremlin Bicêtre, France¹²Laboratoire de Biochimie Génétique, Hôpital Universitaire Henri Mondor, Créteil, France¹³King's College London, Division of Cancer Studies, London, UK¹⁴King's College Hospital NHS Foundation Trust, London, UK¹⁵Red Cell Physiology Laboratory, New York Blood Center, New York, New York

Correspondence

Valentine Brousse, Service de Pédiatrie et Maladies Infectieuses, Hôpital Universitaire Necker-Enfants Malades, Paris, France, 149 rue de Sèvres, 75015 Paris, France, Email: valentine.brousse@aphp.fr

Funding information

"Investissements d'avenir" of the French National Research Agency, Grant/Award Number: ANR-11-IDEX-0005-02; Laboratory of Excellence GR-Ex, Grant/Award Number: ANR-11-LABX-0051; Département de la Recherche Clinique et du Développement de l'Assistance Publique-Hôpitaux de Paris; French Ministry of Health, Grant/Award Number: P071228.

Abstract

In order to identify very early prognostic factors that can provide insights into subsequent clinical complications, we performed a comprehensive longitudinal multi-center cohort study on 57 infants with sickle cell anemia (55 SS; 2 Sβ⁰) during the first 2 years of life (ClinicalTrials.gov: NCT01207037). Time to first occurrence of a severe clinical event—acute splenic sequestration (ASS), vaso-occlusive (VOC) event requiring hospitalization, transfusion requirement, conditional/ abnormal cerebral velocities, or death—was used as a composite endpoint. Infants were recruited at a mean age of 4.4 T1 months. Median follow-up was 19.4 months.

During the study period, 38.6% of infants experienced ≥1 severe event: 14% ASS, 22.8% ≥ 1 VOC (median age: 13.4 and 12.8 months, respectively) and 33.3% required transfusion. Of note, 77% of the cohort was hospitalized, with febrile illness being the leading cause for admission. Univariate analysis of various biomarkers measured at enrollment showed that fetal hemoglobin

(HbF) was the strongest prognostic factor of subsequent severe outcome. Other biomarkers measured at enrolment including absolute neutrophil or reticulocyte counts, expression of erythroid adhesion markers, % of dense red cells, cellular deformability or γ -globin genetic variants, failed to be associated with severe clinical outcome. Multivariate analysis demonstrated that higher Hb concentration and HbF level are two independent protective factors (adjusted HRs (95% CI) 0.27 (0.11-0.73) and 0.16 (0.06-0.43), respectively). These findings imply that early measurement of HbF and Hb levels can identify infants at high risk for subsequent severe complications, who might maximally benefit from early disease modifying treatments.

1 | INTRODUCTION

Sickle cell anemia (SCA), although a long described monogenic disorder, remains a severe disease with an unpredictable course. The first months of life are a time with a low incidence of complications, a state attributable to the sustained level of protective fetal hemoglobin (HbF). HbF has a pivotal anti-polymerization effect on the mutant hemoglobin (HbS). As the physiological switch from HbF to HbS progresses, increased polymerization of HbS occurs, resulting in multiple and inter related downstream effects: vaso occlusion, hemolysis, inflammation, increased cell adhesion, endothelial dysfunction and decreased function of NO. These changes are likely to play a role in the observed marked variability in the manifestations of both acute complications and progressive organ damage in infants as they age.

In high-income countries, generalized neonatal screening has led to a drastic decline in SCA-related mortality in very young children through the implementation of penicillin prophylaxis, immunization, parental education, cerebral vasculopathy screening and improved medical care¹. Yet, complications such as acute splenic sequestration (ASS), dactylitis, acute anemia, acute chest syndrome (ACS), severe invasive infection, and central nervous system injury remain prevalent and unpredictable².

Numerous studies have attempted to define biomarkers associated with disease severity or clinical outcomes with a predominant focus on adults and/or using either a retrospective or cross-sectional study design³. Many of these studies were performed before the implementation of newborn screening and of prophylactic programs. Furthermore, the studies employed a wide variability in the definition of clinical severity and of outcomes. Indeed, contradictory results have been found regarding diverse markers of severity, such as the predictive value of HbF. In fact, validated prognostic markers are still lacking for identification of children at high risk, particularly in early infancy⁴. Need for such identification is becoming increasingly important as more therapeutic and curative options are being developed^{5, 6}. The goal of the present longitudinal study was to identify clinical, biological or genetic parameters early in infancy, before the onset of complications that could predict severe outcomes in the first 2 years of life. An additional objective was to describe longitudinally the natural history and the evolution of specific biomarkers in a cohort of SCA newborns by regular and frequent monitoring during the first 2 years of life.

2 | METHODS

2.1 | Study design and subjects

A prospective study (ClinicalTrials.gov: NCT01207037) was set up at five participating centers. The primary objective was to determine prognostic factors predicting severe SCA-related events within first 2 years of life in SCA infants. Inclusion criteria were: (1) SS or S- β^0 sickle genotype; (2) Age less than 6 months; (3) No prior episode of ASS. Due to the exploratory nature of the study, no sample size was predetermined, but a target number of 60 infants was established, based on the expected number of SCA newborns referred to these centers during the inclusion period (around 120 newborns) and an estimated 50% acceptance rate. The study was offered to all infants meeting the inclusion criteria in the participating centers during the inclusion period.

After informed consent was obtained, patients in the study were followed with scheduled visits planned at enrolment (3 and/or 6 months), 12, 18 and up to 24 months. All received standard age-appropriate care for SCA, with no modification of access to care or medication in relation with the study⁷. The protocol was approved by the ethics committee "Comité pour la Protection des Personnes Ile de France II" and by the French agency for security of health products (AFSSAPS).

2.1.1 | Endpoints and monitoring

At each study visit, complete clinical work up and blood sampling were performed and relevant medical events were recorded. Time to occurrence of first severe SCA-related event was used as a primary composite endpoint. A severe SCA-related event was defined as the occurrence of either ASS, vaso-occlusive complications (VOC) requiring hospitalization (including either painful episodes and/or acute chest syndrome (ACS)), blood transfusion, conditional or abnormal trans cranial Doppler (TCD) or death. We did not include stroke because the occurrence of stroke before age 2 in a cohort screened at birth is an exceptionally rare event. ASS was defined as a sudden increase of a palpable spleen size (>2 cm compared to basal) measured below the costal margin, with a decrease of Hb level >2 g/dL compared to previous measurement). Parents were taught to watch for signs of anemia and to palpate the spleen. In case of pallor, fatigue or a palpable spleen, parents were advised to refer to clinical staff, as recommended⁷.

A VOC event was defined as pain in the extremities, back, abdomen, chest, or head for which no other explanation could be found. Pain medication based on paracetamol and non-steroid anti-inflammatory drugs was given at home as recommended. No opioid medication is available for infants outside hospital, following French legislation. ACS was defined as a new pulmonary infiltrate and at least three of the following findings: chest pain, temperature elevation above 38.5°C, tachypnea, wheezing or cough⁸. Conditional or abnormal velocities on imaging TCD were defined by Time Averaged Mean Maximal Velocities >170 or 200 cm/s respectively in the middle cerebral artery or internal carotid⁹. Experienced pediatricians using a standardized preformat for each study visit collected all clinical data.

For each patient, complete blood counts and erythrocyte indices were determined using an Advia 120 Hematology System (SIEMENS, Germany). Dense cells were defined by MCHC >41 g/dL for both reticulocytes and mature red blood cells.¹⁰

Red cell deformability was assessed by osmotic gradient ektacytometry (Technicon) as previously described¹¹. The deformability Index (DI) is a measure of cellular deformability. The 0 min point in hypo-osmolar region of the curve corresponds to the osmolarity at which 50% of the red blood cells hemolyse and reflects the surface area to volume ratio. A right shift in O min indicates a decrease in surface area to volume ratio, that is, increasing values indicate decreased area to volume ratio. The O⁰, the osmolarity in the hyper-osmolar region of the curve at which DI value is 50% of the DI max, reflects the hydration state of the red cells¹². A left shift in O⁰ (lower values) indicates a decrease in cell volume accompanied by a rise in internal viscosity. HbF percentage was quantified by high performance ion-exchange liquid chromatography (HPLC) VARIANTnbs system (BioRad Laboratories, Marnes La Coquette, France). Known and previously described erythroid adhesion markers¹³ (CD239: Lu-BCAM, CD36, CD242: ICAM4, CD49d: α 4 β 1, CD44, CD47, CD58: LFA3, CD99, CD108, CD147, CD151) were analyzed by flow cytometry on samples stored at -196°C at the Centre National de Référence pour les Groupes Sanguins, Paris. Genetic analysis was performed as follows: following DNA extraction (Flexigen DNA kit, ref: 51206, Qiagen GmbH, 40724 Hilden, Germany), beta globin locus and haplotypes were analyzed¹⁴¹⁵. Beta globin haplotypes (Senegal, Benin, Central African Republic, Cameroon, and Atypical) were determined and categorized as previously published¹⁶. Favorable haplotypes were defined as Sen/Sen, Ben/Sen, Cam/Sen or Sen/Atyp; unfavorable haplotypes as Car/Car, Cam/Car, Car/Atyp or Ben/Car; while other haplotypes were categorized as intermediate. The most frequent deletional form of alpha thalassaemia (3.7) was characterized as previously described¹⁷. Regarding the genetic component of HbF production, the three major HbF genetic loci (HMIP-2A, BCL11A, Xmn1-HGB2)¹⁸ regulating HbF production and the recently defined genetic score of HbF in sickle cell disease (HbF)¹⁹ were analyzed in terms of effects of HbF production on clinical outcomes. F positive red blood cells (F-cells) were analyzed by flow cytometry and Imaging Flow cytometry, using a PE-conjugated HbF antibody (Life Technologies). Samples were processed using a BD FACS Canto II (BD Biosciences) and analysis was performed using DIVA software (BD Biosciences). Samples were also processed using ImageStreamX Mark II Imaging Flow Cytometer and analyzed using IDEAS 6.2 software.

1.1 | Statistical analysis

Data are presented as median [interquartile range] for all quantitative variables and with proportions for categorical variables. Time to first occurrence of a severe SCA-related event was used as a composite endpoint. Severe outcomes throughout the follow-up were visualized with the use of Kaplan-Meier curves, using the log-rank test to compare two groups. Patients lost to follow-up were censored at the date of last contact. Multivariate cox regression analysis was performed with the Cox regression model and Hazard Ratios (HRs) were calculated with 95% Confidence Interval (CI). The proportional hazards assumption of the Cox regression models was tested and assessed with the Schoenfeld residuals for each variable. Post hoc analyses were further used to investigate on significant threshold values. Longitudinal comparisons of SCA-related biomarkers between inclusion and 24 months of age were assessed using Wilcoxon signed-rank tests for paired data. All statistical tests were two-tailed and a p value of less than 0.05 was considered significant. Analyses of secondary endpoints were not adjusted for multiple comparisons, and should be interpreted as exploratory. All tests were performed using the R software (R development Core Team. A language and environment for statistical computing. Available from: <http://www.R-project.org>) version 3.3.2.

2 | RESULTS

2.1 | Study participants

Between December 2010 and March 2013, 114 children with a neonatal diagnosis of SCA were referred to five investigating centres in the Paris area. A total of 57 infants (SS $n = 55$; S β^0 $n = 2$; 54.4% males) were included in the study and followed for a median of 19.4 months (range 3.1-23.2). Two infants dropped out at 6 months because parents withdrew their consent and two were lost to follow up at 6.6 and 7.9 months respectively.

3.2 | Patient characteristics at inclusion

Major clinical, genetic and biological characteristics at inclusion are summarized in Table 1 and Supporting Information Table 1.

Median age at inclusion was 4.4 months [3.4-5.2]. A history of a medical event was reported in 9 (16%), including prior hospitalization in 5 (8.5%). Only one event however was related to SCA (dactylitis), other events were infectious (bronchiolitis $n = 2$; isolated fever $n = 1$, diarrhea $n = 1$). Growth parameters were normal: 6.6 kg [5.8-7.6], 61.5 cm [60.2-65] and no child had a Z score < 2 SD for body mass index for age. None had a palpable spleen and clinical examination was unremarkable.

Eighteen patients (32.1%) had coexisting heterozygous α -thalassaemia due to the deletional variant $\alpha^{-3.7}$. A balanced distribution of β -globin haplotype categories was found with around 1/3 of patients in each of the favorable, unfavorable and intermediate categories. Percentage of F+ cells and HbF% or concentration correlated strongly with each other (data not shown). Likewise, the genetic HbF score showed a good correlation with HbF measures ($\rho = 0.46$,

TABLE 1 Main clinical and biological characteristics at enrollment

Age (months) median [IQR]	4.4 [3.4-5.2]
Sex ratio (M/F) %	54.4
Genotype <i>n</i> (%)	
SS	55 (96.5)
Sβ ^o	2 (3.5)
Hemoglobin (g/dL)	9.2 [8.4-9.9]
Mean cell volume (MCV) (fl)	72 [67-75.5]
Mean hemoglobin content (MHC) (pg/cell)	25.4 [23.5-26.6]
Mean corpuscular hemoglobin concentration (MCHC) (g/dL)	35.3 [34.5-35.8]
Platelets (× 10 ⁹ /L)	395 [341.5-518]
Absolute leucocyte count (× 10 ⁹ /L)	8.9 [7.8-10.8]
Absolute neutrophil count (× 10 ⁹ /L)	1.8 [1.5-2.3]
Absolute lymphocyte count (× 10 ⁹ /L)	6.2 [4.9-7.8]
Absolute reticulocyte count (× 10 ⁹ /L)	133 [99.2-199.2]
HbF (g/dL)	3.8 [3-4.7]
HbF (%)	42 [35-50.5]
Total F-cells (%)	88.8 [80.7-94.2]
g (HbF) score	2.2 (1.9-2.6)
Maximum elongation index	0.4 [0.4-0.4]
O min (mOs/kg)	104 [94-113.5]
O ^h or hyper (mOs/kg)	306 [295.5-316]
Total dense cells (%)	22.7 [17-28.6]
Dense mature cells (%)	23.6 [17.6-30.9]
Dense reticulocytes (%)	10.2 [7.5-14.2]

g (HbF): genetic score for HbF;

$P = 0.001$ with BCL11-A rs 1427407 as the major determinant (data not shown).

There was an early alteration of deformability parameters (low DI, O min and O^h) in this young cohort, when compared to normal controls¹² and a substantially elevated % of both the dense reticulocyte and mature red cell subpopulations. A specific profile of expression of erythroid markers on reticulocytes and mature red cells was noted and is detailed in the paragraph "Analysis of longitudinal data".

3.3 | Clinical course in infancy

Altogether, 22 (38.6%) patients developed at least one severe SCA-related outcome. Figure 1 Panel A shows the Kaplan Meier estimate of the 24-month event-free rate, which was 54.4% (95% CI, 39.7 to 74.5%). Figure 1 Panels B and C show the 24-month ASS-free and VOC-free rates, respectively. VOC events occurred in 13 infants (22.8%) during the course of the study, at a median age of 12.8 months [11.5-16.7] for the first episode, with 6 experiencing >2 episodes. Regarding ASS, 8 (14%) infants experienced at least one episode, at a median age of 13.4 months [9.7-14.3] and five of which experienced one recurrence during the study period. None had more than two episodes but four were regularly transfused after the second episode according to our protocol²⁰. Regarding transfusion, 19 infants (33.3%) required at least one transfusion with 10 (17.6%) requiring more than two, including the four children on a regular transfusion program for the prevention of ASS. Only one infant presented a conditional TCD before 2 years of age, none had an abnormal TCD nor experienced a

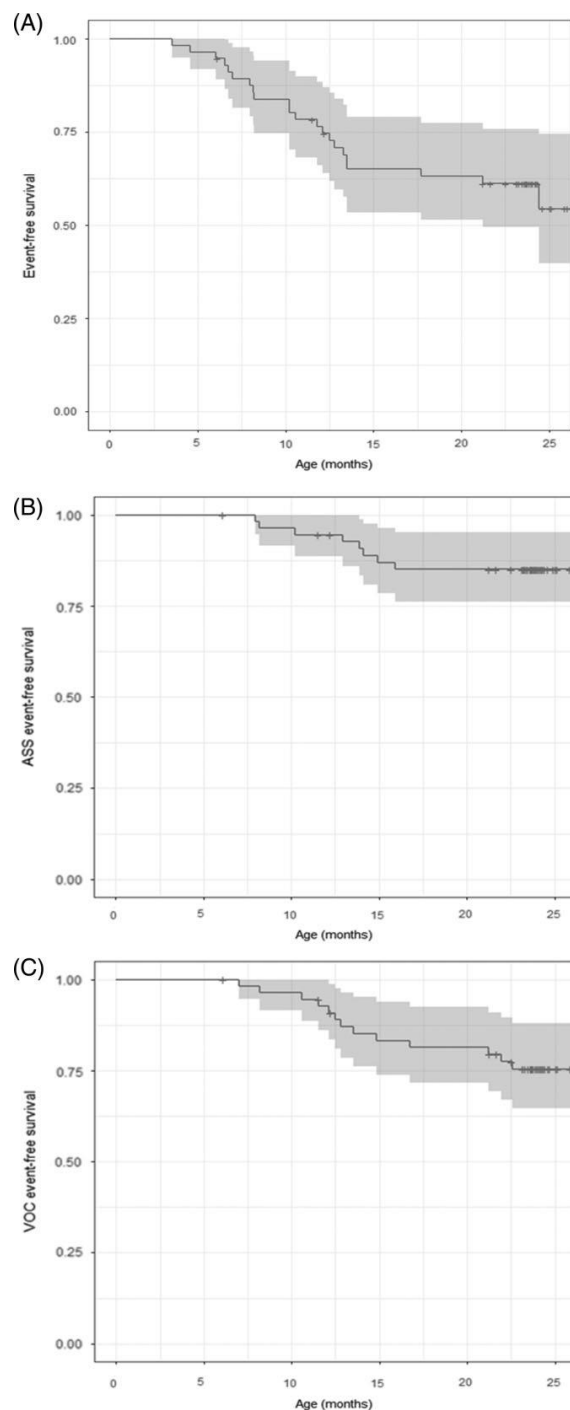


FIGURE 1 Kaplan-Meier event-free survival curve with 95% confidence interval (area). (A) Time to first occurrence of one of the following event was used as a composite endpoint: Acute splenic sequestration, vaso-occlusive event requiring hospitalization, transfusion, conditional or abnormal TCD. (B) Time to first occurrence of acute splenic sequestration (ASS) (C) time to first occurrence of vaso-occlusive (VOC) event

stroke. No infant experienced ACS. No infant died. No infant was started on hydroxycarbamide, in line with European authorization licensing the drug in SCA for only children over 2 years.

The first severe SCA-related event in the cohort occurred at a median age of 10.4 months (3.5-24.4). It was a VOC event for eight infants (36.4%), an ASS for 3 (13.6%) and a transfusion requirement for 11 (50%).

During the course of the study, 44 (77%) infants required 157 hospital admissions. Median number of hospitalizations was two (range 1-12) per child with 32 (72.7%) experiencing more than one event. Of note, first cause of admission was a febrile illness in 31 infants (63 cases), with a median of 2 (range 1-8) hospitalizations per child but no invasive pneumococcal infection was noted. A focal infection (ie, pyelonephritis, pulmonary infection, gastro intestinal infection) was reported in 15 cases. In the remaining 48 cases, febrile illness was attributed to a viral cause (in four cases with an identified virus and presumably viral in the remaining cases). VOC and ASS-related admissions involved 19 patients (38 cases) with a median number of hospitalizations of 2 (range 1-6). Hospitalization with anemia as the only cause of admission was reported in 10 cases. The remaining causes of admission included general pediatric reasons mostly unrelated to SCA (intussusception, inguinal hernia, low weight gain, other).

3.3 | Early prognostic factors of disease severity

Clinical, genetic and biological parameters at enrollment (4 months) were analyzed for their prognostic value and the results are summarized in Table 2:

When combining all severe outcomes, univariate analysis of data at enrollment showed that the most powerful protective factor was increased HbF levels, whether in % or concentration ($P < 0.001$) or F-cells % ($P < 0.05$). Furthermore, protective thresholds of HbF levels were identified: HbF% $> 33.5\%$ on enrollment, the hazard ratio (95% CI) for an adverse event was 0.24 (0.09-0.58) ($P < 0.001$), and HbF concentration > 2.8 g/dL (HR (95% CI) = 0.11 (0.04-0.27), $P < 0.001$). Likewise, high percentage of F-cells was protective with a threshold of 80% positive cells. Factors negatively influencing outcome were a low level of Hb ($P < 0.001$), high MCV ($P = 0.027$), low MCHC ($P = 0.014$) and unfavorable β -globin haplotypes (Car/Car; Ben/Car) ($P = 0.017$). Of note, Hb and MCHC were expectedly interrelated.

In a multivariate analysis, Hb level > 8 g/dL and HbF $> 33.5\%$ proved to be two independent protective prognostic factors against a SCA-related severe event (adjusted HRs (95%CI) 0.27 (0.11-0.73) and 0.16 [0.06-0.43], respectively, Figure 2). Although absolute reticulocyte count (ARC) was inversely correlated to Hb concentration ($\rho = -0.55$, $P < 0.001$) and to HbF % ($\rho = -0.40$, $P = 0.003$), it was not predictive of a severe outcome. Likewise, absolute neutrophil count, level of expression of potentially important erythroid adhesion markers (CD36, CD 239: Lu/B-CAM, CD242: ICAM-4/LW), % of dense red cells, or deformability parameters failed to predict overall severity in this very young cohort.

3.4.1 | Early prognostic factors of ASS

Univariate analysis showed that higher HbF (whether in % or concentration) was the strongest protective parameters for ASS ($P < 0.001$) with a significant threshold of 33.5% or 2.8 g/dL, respectively.

TABLE 2 Univariate analysis of potential prognostic markers at 4 months of a SCA-related severe event occurring before 2 years: ASS, vaso-occlusive event (VOC or ACS), transfusion, conditional or abnormal velocities and death

	HR (95% CI)	P value
Hemoglobin (g/dL)	0.49 (0.33-0.74)	$P < 0.001$
Mean cell volume (MCV) (fl) (MCV) (fl)	1.09 (1.01-1.17)	$P = 0.027$
Mean Hemoglobin content (MHC) (pg/cell)	1.14 (0.94-1.38)	$P = 0.17$
Mean corpuscular hemoglobin concentration (MCHC) (g/dL)	0.71 (0.55-0.93)	$P = 0.0026$
Platelets ($\times 10^9$ /L)	1 (0.9-1)	$P = 0.99$
Absolute leucocyte count ($\times 10^9$ /L)	1.07 (0.94-1.22)	$P = 0.32$
Absolute neutrophil count ($\times 10^9$ /L)	1.18 (0.73-1.9)	$P = 0.48$
Absolute lymphocyte count ($\times 10^9$ /L)	0.98 (0.92-1.05)	$P = 0.60$
Absolute reticulocyte count ($\times 10^9$ /L)	1 (0.99-1.01)	$P = 0.07$
HbF (%)	0.93 (0.9-0.97)	$P < 0.0001$
HbF (g/dL)	0.33 (0.17-0.63)	$P < 0.0001$
F-cells	0.97 (0.95-0.99)	$P = 0.031$
HbF genetic score	0.18 (0.01-1.89)	$P = 0.15$
Maximum elongation index	1.32 (0.59-2.91) ¹	$P = 0.49$
O ³ or hyper (mOs/kg)	1.01 (0.99-1.04)	$P = 0.22$
O min (mOs/kg)	1 (0.98-1.02)	$P = 0.95$
Total dense cells (%)	1 (0.96-1.04)	$P = 0.93$
Dense mature cells (%)	1 (0.97-1.04)	$P = 0.82$
Dense reticulocytes (%)	0.98 (0.92-1.04)	$P = 0.55$
Unfavorable haplotype	4.73 (1.31-17.1)	$P = 0.017$

CI confidence interval; ¹HR for 0.1-unit increase. Unfavorable haplotype: Cam/Car; Car/Car; Car/Ben; Car/Atyp.

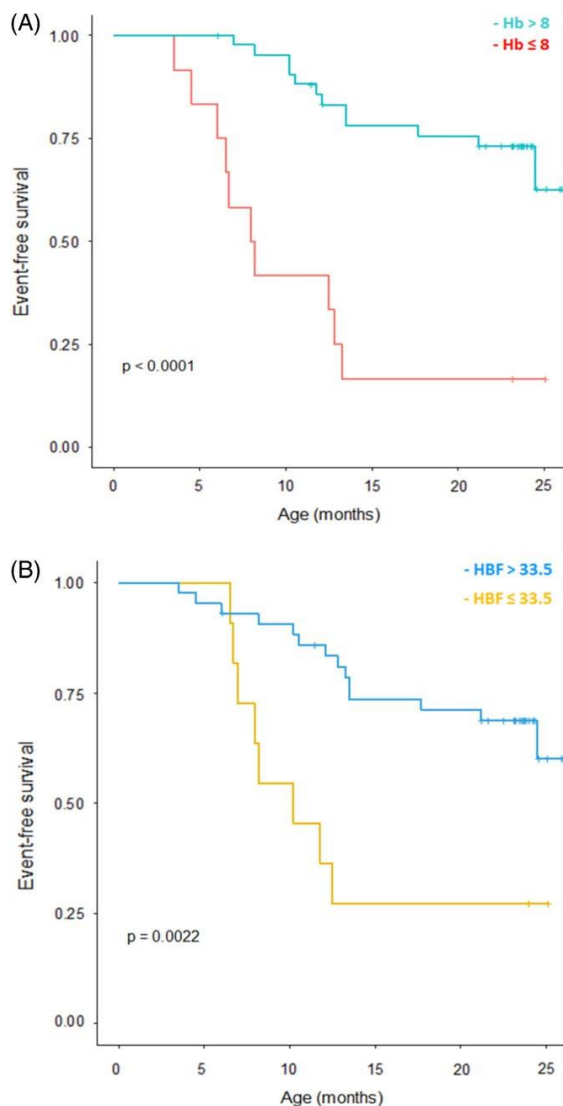


FIGURE 2 Kaplan-Meier event-free survival curves. (A) Survival curve by Hb concentration below (red) or above (blue) the threshold value of 8 g/dL. (B) Survival curve by HbF level below (yellow) or above (blue) the threshold value of 33.5%. *P*-value is derived from log-rank test [Color figure can be viewed at wileyonlinelibrary.com]

Likewise, higher percentage of F-cells protected from the occurrence of ASS ($P = 0.003$). There was no association between the genetic score for HbF and the occurrence of ASS. Importantly, other biomarkers including ARC, % dense red cells (whether mature red cells or dense reticulocytes), ektacytometry parameters, percentage of expression of adhesion markers failed to be specific prognostic factors for ASS. Likewise, co inheritance of α -thalassemia or β -globin haplotype category did not influence the occurrence of ASS.

3.4.1 | Early prognostic factors for VOC events

Regarding VOC events, univariate analysis of data at inclusion showed that low Hb level (<8 g/dL), and % high dense cells correlated with the

occurrence of a VOC event ($P = 0.004$ and 0.018 , respectively). Conversely HbF levels at 4 months (whether in %, concentration or F-cells %) were not predictive. Likewise, the HbF genetic score did not influence VOC outcome.

3.5 | Analysis of longitudinal data

3.5.1 | Clinical data

During the first 2 years of life, SCA infants, regardless of disease severity, demonstrated normal growth with only one child displaying a Z score for BMI < -3 SD at 24 months. The proportion of infants with splenomegaly increased during the time frame of the study with none of the infants having a palpable enlarged spleen at enrollment. However, 10 patients (20%) had an enlarged spleen at 2 years of age and at least 19 patients (33.3%) experienced palpable splenomegaly at some point during the study period.

3.5.2 | Biological data

The present study allowed us to establish longitudinal trends for conventional and SCA-specific laboratory parameters during the first 2 years of life (Supporting Information Tables 2 and 3). Comparison of parameters at entry and exit yielded expected marked differences, illustrating the highly dynamic changes occurring during this time frame, notably regarding absolute neutrophils and reticulocyte counts. At 3-6 months, reticulocytes exhibited a specific profile of expression of erythroid adhesion markers, as previously reported¹³, with an increased expression of Lu-BCAM on reticulocytes. By age 2, the ratio of Lu-BCAM positive reticulocytes, that is, the % of positive cells among total reticulocytes did not increase. In contrast the numbers of Lu-BCAM expressing mature red cells increased significantly, as well as the mean fluorescence intensity (MFI), reflecting the maturation of Lu-BCAM positive reticulocytes into mature cells with time (Supporting Information Table 3). The expression of other known erythroid adhesion markers on reticulocytes increased over time, mainly because of an increase in the reticulocyte count (Supporting Information). The fraction of dense cells as well as deformability parameters remained unchanged during the study period. HbF % (or concentration) steadily decreased over time and reached a mean level of 21% at 24 months of age.

4 | DISCUSSION

Despite many attempts and numerous reported studies over the last three decades, early, robust and validated prognostic factors are still lacking in SCA⁴. The absence of conclusive data relates in part to the highly complex pathophysiology of SCA but also to important disparities in design, inclusion criteria, age at sampling and definition of clinical severity used in the different studies. Furthermore, constant improvement in early diagnosis, management and preventive strategies makes it difficult to compare the findings from the diverse previously reported studies. The primary objective of our study was therefore to enroll very young infants before the occurrence of clinical events to analyze prospectively the predictive value of clinical

features and relevant biomarkers that can account in subsequent complications.

Because the strategies for clinical management of SCA have drastically changed over the years²¹, we chose severity end points to reflect the current burden of SCA in the context of a well-developed health care system. For instance, as families are educated to treat moderate pain at home, we chose to measure painful events requiring hospitalization, thereby capturing episodes of severe pain causing substantial morbidity. In contrast to previous studies, the prospective and longitudinal design of the present study in conjunction with enrollment of infants at a very young age (4 months) and the comprehensive examination of biomarkers *before* the occurrence of complications enabled us to obtain robust predictive data in spite of the relatively small size of our study cohort. There is no reason to believe that this cohort might differ from the general SCA population, as there was no benefit from the study (no additional access to medication or medical care).

Over 20 years ago, Platt et al. concluded that a high level of HbF in adults and older children predicted improved survival in SCA patients and was probably a reliable childhood forecaster of adult life expectancy²². In fact, despite the very well established beneficial effect of an elevated HbF level in SCA, no study has previously prospectively demonstrated its protective value when measured in infants. In the present study, among all the potentially relevant parameters that were analyzed, HbF level (whether in total percentage or concentration or F-cells) measured around 4 months of age was indeed the most robust predictive factor of a severe SCA-related outcome in the first 2 years of life, extending the observations of Platt into infancy. Moreover, a significant protective threshold value of HbF at 4 months was identified (33.5%, 2.8 g/dL, or 80% F-cells, respectively). This finding in our young cohort contrasts with those in the study by Miller²³, in which no such predictive value for HbF was shown, possibly because measurements were performed later (in the second year of life), clinical outcomes studied were different (including nonhospitalized pain) and preventive strategies for cerebrovascular disease and pneumococcal infections had not been implemented.

We sought to decipher the protective role of HbF by looking at the genetic determination of HbF production. As expected, all HbF-related measures (F-cells and HbF %) were highly correlated and were consistently predictive. Although known genetic variants only account for 10–20% of HbF production²⁴, in infants it might be expected that most of the variation in HbF levels is caused by genetic factors, with relatively less variation due to acquired and environmental factors. We therefore tested a previously validated score *g*(HbF), representing the genetic component of % HbF¹⁹. A very strong correlation with HbF production after 6 months of age was noted. Interestingly, the major (and only) contributor to such correlation was the BCL11A rs1427407 variant. However, the score failed to have a prognostic value for severe clinical outcomes as did, predictably, each of the variants analyzed, including BCL11A rs1427407. The lack of correlation of this genetic score with clinical outcomes in our cohort may relate to the differences in genetic background and age of the cohorts in which the score was initially validated, and additional genetic determinants may be of importance. However, this result also strongly

suggests that nongenetic determinants of HbF are important in modulating clinical severity, even in very young children. Thus, although genetic loci can strongly influence phenotypic expression of SCA, their accuracy for predicting clinical severity in individuals is not reliable and results cannot be extrapolated easily across cohorts of diverse origins. In contrast, we demonstrate that a readily available and cost-effective measurement of HbF at 4 months of age may be of important clinical relevance.

Importantly, other previously reported biomarkers, notably the ARC²⁵, leucocyte counts²³, Lu-BCAM expression²⁶ and more generally adhesion molecules failed to provide prognostically significant insights in our study. Regarding reticulocyte and leucocyte counts, differences in study design might account for these discrepancies^{27,28}. Regarding adhesion molecules, the reason for not being able to document such effects in the present study may be related to the fact that our measurements were performed at 4 months of age, before these biomarkers are fully expressed. Their predictive value may therefore be of importance for complications occurring later in life. Another explanation could be that the expression of adhesion molecules does not accurately reflect their adhesion activity, which would be more adequately analyzed by functional adhesion experiments. We are aware of the relatively small size of our cohort and the limited period of observation that may also explain such discrepancy. However we want to emphasize the power of our longitudinal prospective study to provide accurate prognostic data, in contrast to correlative studies that are based on cross sectional or retrospective design, and as such, do not allow the determination of a prognostic value. While the latter have yielded valuable insights into pathophysiological pathways, clinical relevance is not easily evidenced nor replicated³.

Reference hematological values for SCD infants from the Cooperative Study of Sickle Cell Disease cohort was published a number of years ago²⁹. Our study significantly extends this data set with longitudinal examination of novel biological determinants including the expression profile of adhesion molecules, cell density and deformability parameters, on both reticulocytes and mature red cells. The very early enrolment and the longitudinal design of this study enabled us to obtain comprehensive insights into the clinical and biological changes occurring in the first 2 years of life, in relation to clinical outcome. At enrolment, infants displayed mild anemia (Hb 9.3 ± 1.3 g/dL), in association with high levels of dense red cells (22%), remarkably impaired deformability parameters and a sub population of reticulocytes displaying a specific profile of adhesion molecules expression. Thereafter, the most remarkable changes that occurred were the significant increase of neutrophils and reticulocytes. Surprisingly, Hb concentration remained rather stable possibly because HbF percentage or concentration whilst decreasing remained at a fairly high level at 24 months (21%)

SCA remains a severe disease. Contrasting with the absence of mortality, there was a high disease burden, illustrated by both the number of hospital admissions and the occurrence of severe SCA-related events during infancy. By 2 years of age, 44 (77%) infants of the cohort had required at least one hospitalization. In contrast to some other geographical settings, participation in studies in France is not expected to increase access to hospital or medication, because

there is free healthcare access to all. These high figures therefore should not be influenced by the fact that these infants were in a study and families more cautious. Notwithstanding hospital admissions, when specifically considering SCA-related events, 22 (38.6%) babies had experienced at least one severe event by 24 months. This data is consistent with the hospitalization rate reported in the nontreated arm of the BABY HUG trial³⁰. In contrast, no ACS was reported in our cohort as opposed to 27 events, a discrepancy possibly related to the older age of the BABY HUG cohort (mean age at enrollment: 13.5 T2-8 months) with ACS occurring at a median age of 27 months (12-39). Altogether, these results demonstrate the persistently high and early burden of SCA in very young children screened at birth and followed up in a socio economically privileged setting.

Screening tools to select patients at high risk for complications remains a challenge in SCA management. Our study demonstrates the ability of HbF measured in the first months of life to robustly predict disease severity. Following the BABY HUG trial³¹, hydroxycarbamide, which increases HbF level, was recommended for all SCA infants starting at 9 months of age, regardless of clinical severity³². Our data also argues for an early use of HbF inducing agents as a disease modifying treatment because a very large fraction of SCA infants will experience a severe complication in the first 2 years of age, because red cells are markedly abnormal by the age of 4 months, and because a low level of HbF is a strong marker of short-term severity.

ACKNOWLEDGMENTS

We are very thankful to Thierry Peyrard, Dominique Gien, Eliane Vera and Sirandou Tounkara at the Centre National de Référence pour les Groupes Sanguins for the management of blood samples. We wish to thank Geneviève Milon and Peter David for their early and continuous input and support. We are also very thankful to David Rees for his support. This study was funded by a research grant from the French Ministry of Health (PHRC 2007, P071228) and sponsored by the Département de la Recherche Clinique et du Développement de l'Assistance Publique-Hôpitaux de Paris. The study was supported by grants from Laboratory of Excellence GR-Ex, reference ANR-11-LABX-0051. The labex GR-Ex is funded by the program "Investissements d'avenir" of the French National Research Agency, reference ANR-11-IDEX-0005-02.

ORCID

Valentine Brousse  <http://orcid.org/0000-0002-4984-754X>

Wassim El Nemer  <http://orcid.org/0000-0001-8184-427X>

REFERENCES

- Couque N, Girard D, Ducrocq R, et al. Improvement of medical care in a cohort of newborns with sickle-cell disease in North Paris: impact of national guidelines. *Br J Haematol*. 2016;173(6):927-937.
- Ware RE, de Montalembert M, Tshilolo L, Abboud MR. Sickle cell disease. *Lancet*. 2017;390:311-323.
- Rees DC, Gibson JS. Biomarkers in sickle cell disease. *Br J Haematol*. 2012;156(4):433-445.
- Meier ER, Fasano RM, Levett PR. A systematic review of the literature for severity predictors in children with sickle cell anemia. *Blood Cells Mol Dis*. 2017;65:86-94.
- de Montalembert M, Brousse V, Chakravorty S, et al. Are the risks of treatment to cure a child with severe sickle cell disease too high? *BMJ*. 2017;359:j5250.
- Ataga KI, Kutlar A, Kanter J. Crizanlizumab in sickle cell disease. *N Engl J Med*. 2017;376(18):1796.
- Syndromes drepanocytaires de l'enfant et de l'adolescent. Haute Autorité de Santé https://www.has-sante.fr/portail/upload/docs/application/pdf/2010-04/ald_10_pnds_drepano_enfant_web.pdf; 2010.
- Vichinsky EP, Styles LA, Colangelo LH, Wright EC, Castro O, Nickerson B. Acute chest syndrome in sickle cell disease: clinical presentation and course. Cooperative study of sickle cell disease. *Blood*. 1997;89(5):1787-1792.
- Adams RJ, Brambilla DJ, Granger S, et al. Stroke and conversion to high risk in children screened with transcranial Doppler ultrasound during the STOP study. *Blood*. 2004;103(10):3689-3694.
- Maier-Redelsperger M, Flahault A, Neonato MG, Girot R, Labie D. Automated analysis of mature red blood cells and reticulocytes in SS and SC disease. *Blood Cells Mol Dis*. 2004;33(1):15-24.
- Clark MR, Mohandas N, Shohet SB. Osmotic gradient ektacytometry: comprehensive characterization of red cell volume and surface maintenance. *Blood*. 1983;61(5):899-910.
- Da Costa L, Suner L, Galimand J, et al. Diagnostic tool for red blood cell membrane disorders: assessment of a new generation ektacytometer. *Blood Cells Mol Dis*. 2016;56(1):9-22.
- Brousse V, Colin Y, Pereira C, et al. Erythroid adhesion molecules in sickle cell Anaemia infants: insights into early pathophysiology. *EBio-Medicine*. 2015;2(2):154-157.
- Pissard S, Beuzard Y. A potential regulatory region for the expression of fetal hemoglobin in sickle cell disease. *Blood*. 1994;84(1):331-338.
- Costa C, Pissard S, Girodon E, Huot D, Goossens M. A one-step real-time PCR assay for rapid prenatal diagnosis of sickle cell disease and detection of maternal contamination. *Mol Diagn*. 2003;7(1):45-48.
- Sheehan VA, Luo Z, Flanagan JM, et al. Genetic modifiers of sickle cell anemia in the BABY HUG cohort: influence on laboratory and clinical phenotypes. *Am J Hematol*. 2013;88(7):571-576.
- Dode C, Krishnamoorthy R, Lamb J, Rochette J. Rapid analysis of -alpha 3.7 thalassaemia and alpha alpha alpha anti 3.7 triplication by enzymatic amplification analysis. *Br J Haematol*. 1993;83(1):105-111.
- Makani J, Menzel S, Nkya S, et al. Genetics of fetal hemoglobin in Tanzanian and British patients with sickle cell anemia. *Blood*. 2011;117(4):1390-1392.
- Gardner K, Fulford T, Silver N, et al. G(HbF): a genetic model of fetal hemoglobin in sickle cell disease. *Blood Adv*. 2018;2(3):235-239.
- Brousse V, Buffet P, Rees D. The spleen and sickle cell disease: the sick(led) spleen. *Br J Haematol*. 2014;166(2):165-176.
- Telfer P, Coen P, Chakravorty S, et al. Clinical outcomes in children with sickle cell disease living in England: a neonatal cohort in East London. *Haematologica*. 2007;92(7):905-912.
- Platt OS, Brambilla DJ, Rosse WF, et al. Mortality in sickle cell disease. Life expectancy and risk factors for early death. *N Engl J Med*. 1994;330(23):1639-1644.
- Miller ST, Sleeper LA, Pegelow CH, et al. Prediction of adverse outcomes in children with sickle cell disease. *N Engl J Med*. 2000;342(2):83-89.
- Thein SL. Genetic association studies in beta-hemoglobinopathies. *Hematology Am Soc Hematol Educ Program*. 2013;2013:354-361.
- Meier ER, Fasano RM, Estrada M, He J, Luban NL, McCarter R. Early Reticulocytosis and anemia are associated with abnormal and conditional Transcranial Doppler velocities in children with sickle cell anemia. *J Pediatr*. 2016;169:227-31 e1.
- Picot J, Goudot C, Berkenou J, et al. Flow cytometry analyses reveal association between Lu/BCAM adhesion molecule and osteonecrosis in sickle cell disease. *Am J Hematol*. 2014;89(1):115-117.

1. Meier ER, Byrnes C, Lee YT, et al. Increased reticulocytosis during infancy is associated with increased hospitalizations in sickle cell anemia patients during the first three years of life. *PLoS One*. 2013;8(8): e70794.
2. Quinn CT, Lee NJ, Shull EP, Ahmad N, Rogers ZR, Buchanan GR. Prediction of adverse outcomes in children with sickle cell anemia: a study of the Dallas newborn cohort. *Blood*. 2008;111(2):544-548.
3. Brown AK, Sleeper LA, Miller ST, Pegelow CH, Gill FM, Waclawiw MA. Reference values and hematologic changes from birth to 5 years in patients with sickle cell disease. Cooperative study of sickle cell disease. *Arch Pediatr Adolesc Med*. 1994;148(8):796-804.
4. Thornburg CD, Files BA, Luo Z, et al. Impact of hydroxyurea on clinical events in the BABY HUG trial. *Blood*. 2012;120(22):4304-4310. quiz 448.
5. Wang WC, Ware RE, Miller ST, et al. Hydroxycarbamide in very young children with sickle-cell anaemia: a multicentre, randomised, controlled trial (BABY HUG). *Lancet*. 2011;377(9778):1663-1672.
6. Yawn BP, Buchanan GR, Afenyi-Annan AN, et al. Management of sickle cell disease: summary of the 2014 evidence-based report by expert panel members. *JAMA*. 2014;312(10):1033-1048.

SUPPORTING INFORMATION

Additional supporting information may be found online in the Supporting Information section at the end of the article.

How to cite this article: Brousse V, El Hoss S, Bouazza N, et al. Prognostic factors of disease severity in infants with sickle cell anemia: A comprehensive longitudinal cohort study. *Am J Hematol*. 2018;93:1411-1419. <https://doi.org/10.1002/ajh.25260>

Article 3



Journal Name

ARTICLE

A microfluidic approach to study the effect of mechanical stress on erythrocytes in sickle cell disease

Received 00th January 20xx,
Accepted 00th January 20xx

DOI: 10.1039/x0xx00000x

www.rsc.org/

Maria Alejandra Lizarralde Iragorri^{a,b,c}, Sara El Hoss^{a,b,c}, Valentine Brousse^{a,b,c,d}, Sophie D Lefevre^{a,b,c}, Michael Dussiot^e, Tieying Xu^f, Alexander Rodrigo Ferreira^g, Yann Lamarre^g, Ana Cristina Silva Pinto^g, Simone Kashima^g, Claudine Lapoumroulie^{a,b,c}, Dimas Tadeu Covas^{g,h}, Caroline Le Van Kim^{a,b,c}, Yves Colin^{a,b,c}, Jacques Elion^{a,b,c}, Olivier Françaisⁱ, Bruno Le Pioufle^f, Wassim El Nemer^{a,b,c†}

The human red blood cell is a biconcave disc of 6-8 x 2 μm that is highly elastic. This capacity to deform enables it to stretch while circulating through narrow capillaries to ensure its main function of gas exchange. Red cell shape and deformability are altered in membrane disorders because of defects in skeletal or membrane proteins affecting protein-protein interactions. Red cell properties are also altered in other pathologies such as sickle cell disease. Sickle cell disease is a genetic hereditary disorder caused by a single point mutation in the β-globin gene generating sickle haemoglobin (HbS). Hypoxia drives HbS polymerization that is responsible for red cell sickling and reduced deformability. The main clinical features of sickle cell disease are vaso-occlusive crises and haemolytic anaemia. Foetal haemoglobin (HbF) inhibits HbS polymerization and positively impacts red cell survival in the circulation but the mechanism through which it exerts this action is not fully characterized. In this study, we designed a microfluidic biochip mimicking the dimensions of human capillaries to measure the impact of repeated mechanical stress on the survival of red cells at the single cell scale under controlled pressure. We show that mechanical stress is a critical parameter underlying intravascular haemolysis in sickle cell disease and that high intracellular levels of HbF protect against lysis. The biochip is a promising tool to address red cell deformability in pathological situations and to screen for molecules positively impacting this parameter in order to improve red cell survival in the circulation.

Introduction

Red blood cells (RBCs) have traditionally been viewed as simple haemoglobin bags that transport oxygen. Behind this simplicity an intricate setting of protein complexes, transporters, enzymes and intrinsic mechanical properties play a major role to insure the essential function of gas exchange. At rest, the human RBC is a discocyte of a regular and uniform biconcave shape with an average diameter of 6-8 μm and a thickness of 2 μm. It repeatedly deforms in the circulation as it squeezes through narrow capillaries whose diameter can be

smaller than its own.¹ This high elasticity and aptitude to deform is made possible by horizontal and vertical protein interactions within an intricate network of skeletal and membrane proteins including spectrin and the Band3 complex.² The horizontal interactions involve spectrin heterodimer self-association and are crucial for the stability of the skeleton, while the vertical interactions anchor the skeleton to the lipid bilayer stabilising the RBC membrane. Impaired protein association or loss of interaction leads to hereditary membrane disorders such as hereditary elliptocytosis and hereditary spherocytosis, in which the RBC shape and deformability are altered.³

Altered RBC deformability is a major determinant of impaired perfusion, increased blood viscosity, and obstruction of microvessels. RBC deformability might be affected by several factors including cell geometry, cell shape, rheological properties of the cell membrane, and cytoplasmic viscosity related to the intracellular haemoglobin concentration.⁴⁻⁶ Several of these parameters are altered in sickle cell disease (SCD), an autosomal recessive disorder caused by a single mutation in the 6th codon of the β globin gene resulting in the expression of an abnormal haemoglobin that polymerizes under hypoxic conditions driving RBC sickling.⁷ Dehydration and sickling alter the RBC shape, which decreases cell deformability and increases rigidity, resulting in significant

^a Biologie Intégrée du Globule Rouge UMR_S1134, Inserm, Univ. Paris Diderot, Sorbonne Paris Cité, Univ. de la Réunion, Univ. des Antilles

^b Institut National de la Transfusion Sanguine, F-75015 Paris, France

^c Laboratoire d'Excellence GR-Ex, Paris, France

^d Service de Pédiatrie Générale, Hôpital Necker-Enfants Malades, Centre de Référence de la Drépanocytose, AP-HP, Paris

^e Université Sorbonne Paris Cité, Université Paris Descartes, Inserm, CNRS, Institut Imagine, Laboratory of Cellular and Molecular Mechanisms of Hematological Disorders and Therapeutic Implications, Laboratoire d'Excellence GR-Ex

^f ENS Paris-Saclay, CNRS Institut d'Alembert, SATIE, Univ. Paris Saclay, France

^g Center for Cell-based Therapy/Hemocentro de Ribeirão Preto, São Paulo, Brazil

^h Ribeirão Preto Medical School, University of São Paulo, Ribeirão Preto, São Paulo, Brazil

ⁱ ESIEE-Paris, ESYCOM EA2552, University Paris-Est, Noisy Le Grand, France

[†] These authors contributed equally to this work.

Correspondence: Wassim El Nemer, Inserm, UMR_S 1134, INTS, 6 rue Alexandre Cabanel, 75015 Paris, France, E-mail: wassim.el-nemer@inserm.fr; Phone: +33144493071; Fax: +33143065019.

ARTICLE

untoward implications on blood rheology and microcirculatory flow.⁸⁻¹² SCD is characterized by a haemolytic anaemia in which intravascular haemolysis takes place. Disappearance of sickle RBCs in the circulation can be either because of haemolysis, due to mechanical forces, or of removal by macrophages because of phosphatidylserine exposure at the cell surface due to elevated levels of oxidative stress and sickling-induced phospholipid disorganisation.¹³⁻¹⁵

In this study, we designed a microfluidic biochip to specifically address the role of mechanical stress in sickle RBC haemolysis. We validated the biochip as a good tool to evaluate RBC resistance to lysis upon repeated mechanical stress exerted on flowing RBCs. The biochip is a promising tool to address RBC deformability in pathological situations such as red cell membrane disorders or infectious diseases and to screen for molecules with beneficial effect on RBC elasticity in sickle cell disease and other pathologies where RBC deformability is altered.

Experimental

The microfluidic biochip

The fabrication process

A microfluidic device containing a network of microchannels with serial restrictions was designed with the aim of mimicking the mechanical stress exerted on RBCs in the microcirculation. The chip was designed as a circuit containing 8 units mounted in parallel. Each unit is composed of 24 parallel channels (Figure 1A). Each channel is 5 μm high and combines 10 serial restrictions of 5 μm separated by 20 and 30 μm -wide areas to allow RBC relaxation (Figure 1A, B). The microfluidic device was made of polydimethylsiloxane (PDMS, Sylgard), a silicone elastomer, using standard microfabrication and molding techniques.¹⁶ A master mold containing 3 microfluidic chips, each composed of 2 independent circuits, was made (Figure 1C).

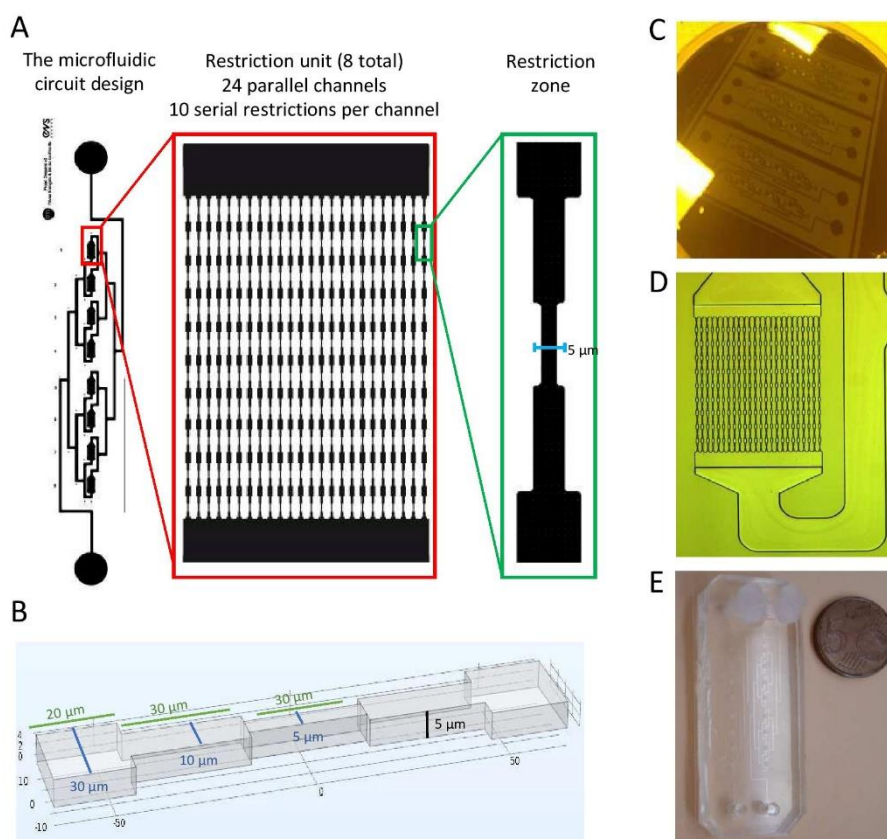


Fig. 1 The microfluidic biochip: design and fabrication. (A) Each microfluidic circuit (top left panel) is composed of 8 restriction units of 24 parallel channels with 10 serial restrictions of 5 μm in each channel. (B) 3D representation of a restriction zone with dimensions. (C) SU-8 mold showing the pattern of 3 identical biochips; the biochip is mounted to work in duplicate, with 2 independent circuits as in (A). (D) Microscopy image of a restriction unit from the SU-8 mold taken to control the dimensions of all channels. (E) The PDMS biochip with 2 independent circuits.

Journal Name

ARTICLE

The mold was fabricated by the micro-patterning of two successive SU-8 photoresist layers (Microchem, Newton, MA) above a 4 inches Silicon wafer used as a supporting substrate. The following process was achieved: i) A first layer of SU-8-2005, with uniform thickness of 5 μm was spincoated (3000 rpm, 30 s) above the Silicon wafer, baked (2 min, 95°C), exposed to UV (105 mJ/cm^2) through a chromium mask (Toppan-Photomask), and post-exposure baked prior to development (5 min, 95°C). This layer defines the geometry of the microchannel networks including the fluidic restrictions mimicking the microcirculation; ii) A second thicker SU-8 layer was then patterned (thickness of 30 μm , obtained by the spincoating of SU-8 2025 (3000 rpm, 30 s), baking (10 min, 95°C), UV illumination (150 mJ/cm^2), post-expose baking (10 min, 95°C), and developing. This layer defines the geometry of the fluidic access, which requires a larger section in order to reduce the hydrodynamic resistance and subsequently the filling time of the device. Hard baking of this 2-level SU-8 mold was finally achieved (30 min, 175°C). The dimensions of the channels within the SU-8 mold were controlled by microscopy measurements (Figure 1D). After validating the sizes, the mold was used for the casting of PDMS (poured on the mold with a 10:1 ratio, and finally baked at 75°C for 2h). Access through-holes were punched on the PDMS chip, for insertion of Luer (TM) connections with the flow controller. The PDMS device finally obtained, with open channels formed on one of its faces, was covalently bound to a microscope cover slide using O_2 plasma activation and bonding (30 W, 300 mT, 20 s) for sealing (Figure 1E).

Perfusion of red blood cell suspensions

The chip was designed for a mean rate of 100 $\mu\text{l}/\text{h}$ under 100 mbar of pressure. An MFCSTM-EZ microfluidic flow control system (Fluigent) was used to regulate the flow pressure in the microfluidic biochip. The biochip was connected to the pump by 1.6 mm silicone tubing and male luer connectors and mounted on the stage of an inverted AxioObserver Z1 microscope (Zeiss) coupled with a Phantom Miro M 320S high-speed camera, following the experimental setting in Figure 2A. For each assay, 60 μl of RBC suspensions at 30% haematocrit were loaded in the Input well of the biochip and perfused at a constant pressure of 350 mBar for 20 min. 30% haematocrit, and not normal haematocrit (38-54%), was used in order to mimic physiological conditions of patients with SCD, as these patients suffer severe haemolytic anaemia. At 350 mbar the theoretical shear stress exerted on RBCs is of 0.95, 1.76 and 5.51 Pa at the centreline of the 30, 10 and 5 μm sections, respectively (Figure 2B). The theoretical velocity in the same zones is of 11.96, 25.63 and 53.98 mm/s, respectively (Figure 2C). The pressure of 350 mBar was used to decrease the experimental running time to 20 min and was validated after assaying haemolysis versus pressure at 100, 350 and 700 mbar. RBCs were collected at the Output well and centrifuged at 200xg for 3 minutes at room temperature in parallel with RBCs from the initial suspension (Input). The supernatant was collected and free haemoglobin concentrations were measured using Drabkin's reagent as described in the following paragraph.

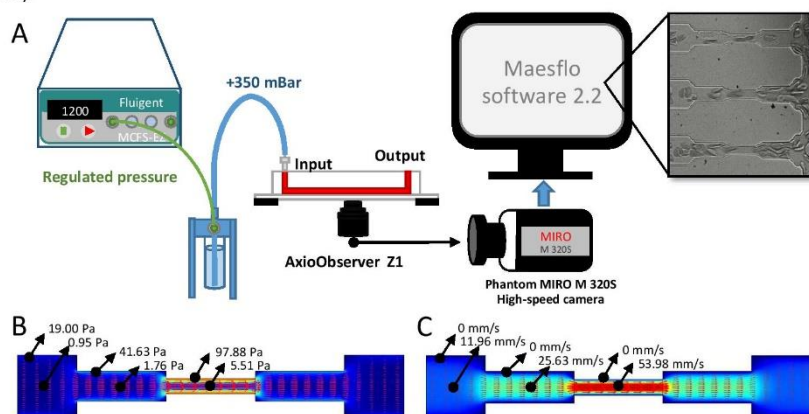


Fig. 2 (A) Experimental setup. The microfluidic device is mounted on the stage of an inverted microscope equipped with a Phantom MIRO M 320S high-speed video camera. Sixty μl of red blood cell suspension at 30% hematocrit are loaded in a male luer connector at the input well and the cells are pushed through the circuit during 20 min at 350 mBar using a Fluigent MFCS-EZ pump with positive pressure. Frame sequences are taken throughout the experiment using the high-speed camera and analysed with the Phantom Camera Control software (PCC) v2.2. Red blood cells are collected at the output well for further analyses. (B,C) Graphic representation of (B) the shear stress exerted on flowing red blood cells and (C) the velocity with respect to the channel width (ConsolTM finite element simulation).

Journal Name

ARTICLE

Haemolysis and HbF measurements

Free haemoglobin concentrations were determined using the Drabkin's reagent (Sigma-Aldrich). Absorbance was measured by Nanodrop 2000 (Thermo Scientific) at 540 nm and concentrations were determined using standard curves obtained with known concentrations of control (HbA) or sickle (HbS) haemoglobin (Sigma-Aldrich).

HbF and HbS levels were measured by cation-exchange high performance liquid chromatography (VARIANT™ II Hemoglobin Testing System, Bio-rad) in RBC lysates (5 µl of total blood in 1000 µl of reagent) and plasma (500 µl of plasma in 500 µl of reagent).

Blood fractionation using Percoll density gradients

Whole blood was fractionated as previously described,¹⁷ using 3 Percoll gradient layers with densities of 1.076, 1.096 and 1.11. Mean cell volume in each subpopulation was measured by the CASY cell counter (OLS).

Flow cytometry and imaging flow cytometry

Three µl of RBCs were fixed in 1% formaldehyde, 0.025% glutaraldehyde, PBS 1x for 15 min. After 2 washes with PBS, RBCs were permeabilized in 0.1 M Octyl β-D-Glucopyranoside for 15 min and saturated in PBS, 1% BSA, 2% goat serum for 30 min. The RBC pellet was suspended in 60 µl of saturation solution and 10 µl of this suspension were incubated with 5 µl of PE-conjugated HbF antibody (Life Technologies), with or without 5 µl of APC-conjugated CD71 antibody (Invitrogen), for 20 min. RBCs were washed and suspended in 200 µl of BD Retic-Count™ (thiazole orange) reagent for 30 min. Fixed, permeabilized and unstained RBCs of each blood sample were used as negative control. Samples were processed using a BD FACS Canto II (BD Biosciences) and analysis was performed using DIVA software (BD Biosciences).

The percentage of irreversible sickle cells (ISCs) was determined using an Imagestream IX MkII flow cytometer (Amnis Corp, EMD Millipore). Two µl of packed RBCs were suspended in 200 µl of ID-CellStab (Biorad) and 50,000 events were acquired. Irreversibly sickled cells (ISCs) were quantified using the IDEAS software (version 6.2) based on an analysis published by Van Beers et al.¹⁸ Using features of morphology and shape, we set up a new refined analysis to measure ISCs. As shown in Figure 1, using the Raw Min Pixel_MC Ch01 on the x-axis and Modulation_Object (M01,Ch01,Tight) on the y-axis, we set up the coordinates of the gate as: 378.69 - 650.631 on the X-axis and 0.082 - 0.339 on the Y-axis.

In vitro sickling assay

RBC sickling was monitored by time-lapse microscopy at increasing hypoxia stages: 20, 10, 5 and 0% O₂, as described.¹⁹

Statistics

Data was analyzed by two-tailed Mann-Whitney or Wilcoxon test, and one-way ANOVA test using the GraphPad Prism 7.00 software. *P ≤ 0.05, **P ≤ 0.01, ***P ≤ 0.001 and ****P ≤ 0.0001 were considered significant

Patients

The study was conducted in accordance with the Declaration of Helsinki and was approved by the Regional Ethics Committee (n°3215 CPP Ile de France III). Blood samples were recovered from blood tubes drawn for medical care after written informed consent. Blood samples were collected on ethylenediaminetetraacetic acid (EDTA) from patients with sickle cell anaemia (SS and Sbeta° genotypes), and from healthy donors (Etablissement Français du Sang, EFS). Blood samples from a total of 62 patients (25 females and 37 males; median age: 8 years [Min-Max: 2-53 years]) and 12 healthy donors (age range: 18-70, as per EFS criteria) were used in this study. Patients were not transfused and were not treated by hydroxyurea. All experiments were performed with fresh blood samples, within 2 hours after blood was drawn.

Results and discussion**Validation of the microfluidic biochip with red cells from healthy donors and patients with sickle cell disease**

We designed the microfluidic biochip to apply repetitive mechanical constraints on flowing RBCs in order to mimic the stress exerted in the microcirculation and thus challenge RBC deformability and elasticity. The device was designed to allow each perfused RBC to flow in a single channel and undergo a maximum of 10 successive mechanical squeezing constraints, depending on whether it resists haemolysis or not, before exiting the channel.

To evaluate if the biochip had the minimal stringency to induce haemolysis, we tested it with control blood (AA). Twelve independent RBC suspensions at haematocrit 30% were perfused for 20 min at 350 mBar (Video 1). Blood suspensions were collected at the output well and free haemoglobin was measured in the supernatant after centrifugation. Free haemoglobin concentrations were slightly but significantly higher in the output than in the input (before perfusion) suspensions (Figure 3A), indicating that the biochip was a good tool to exert mechanical forces on flowing RBCs. This

haemolysis was probably due to the preferential loss of old RBCs, as these cells are known to be poorly deformable following surface area loss and cell volume decrease during their ageing process, after more than 100 days in the circulation after exiting the bone marrow.^{20, 21}

We tested the performance of sickle RBCs in the biochip using blood samples from 23 SCD patients (Video 2). There was a significant increase of free haemoglobin in the output suspension as compared to input (Figure 3A). Haemolysis was greater in the SCD than in the control samples (Figure 3B), indicating that SS RBCs are more fragile than AA RBCs. This result further validated the biochip as a good tool to investigate RBC resistance to lysis under repeated mechanical constraints in a pathological context. They suggest that intravascular haemolysis in SCD patients might be partially driven by mechanical forces that disrupt the integrity of circulating RBCs thus contributing to anaemia in this disease.

Impact of mechanical stress on sickle red blood cell subpopulations

Irreversibly sickled cells (ISCs) are a hallmark of SCD resulting from HbS polymerisation and the presence of HbS fibres in the cytoplasm. They are poorly deformable, dehydrated and of short lifespan as compared to non-sickled RBCs.²² To determine the impact of mechanical stress on ISCs, we determined their percentage before and after perfusion in the biochip. This quantification was made using imaging flow cytometry by optimising an automated method based on morphological and shape features¹⁸ (Figure 3C). We determined the percentage of ISCs (%ISCs) in the input and output suspensions of 13 SCD blood samples (Figure 3D). We

observed a significant decrease in the output, indicating that ISCs are more prone to lysis upon mechanical stress than other RBC populations and suggesting that their shortened lifespan in vivo is most probably due to mechanical stress-induced haemolysis. Another possibility for this decreased percentage is a preferential blockade or skimming in the capillaries. This was probably not the case because this would have caused a significant jamming and subsequent blockade of the microfluidic circuit, which had not occurred in any of the 13 assays.

To exclude this possibility and further investigate the mechanical properties of RBC subpopulations we performed similar assays using low density (LD) and high density (HD) SS RBCs obtained after Percoll density fractionation. Blood samples from 9 SCD patients were fractionated and LD and HD suspensions were perfused in parallel in the biochips. As expected, both subpopulations showed high haemolysis levels when compared to control AA blood (Figure 3B). The haemolysis level in the HD fraction was 2-fold higher than in the LD fraction (Figure 3B, E) indicating that HD RBCs are stiffer, less deformable and more prone to haemolysis than LD RBCs, as they resist less to mechanical constraints. This was in accordance with the morphology analysis that showed higher amounts of ISCs in the HD than in the LD fraction (Figure 3F). In addition to the haemolysis levels, we monitored the cell behaviour in the flow and found that HD RBCs were more prone to blocking the channels than LD RBCs (Figure 3G and Videos 3&4). The blocking of the channels was partial for the majority of HD samples tested, but total obstruction of the biochip occurred for 2 out of 9 samples.

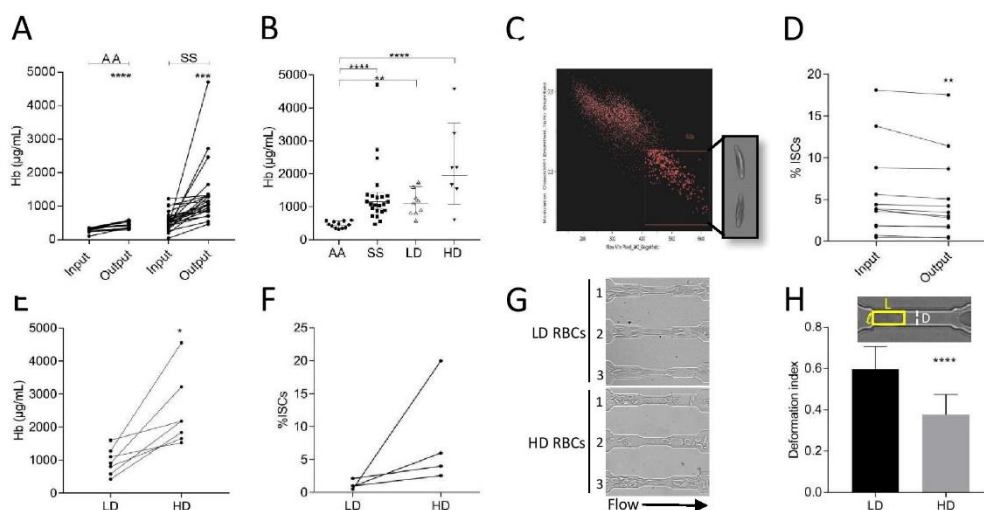


Fig. 3 (A) Free haemoglobin in the supernatant of RBC suspensions before and after mechanical stress of AA ($n = 12$) and SS RBCs ($n = 23$); Wilcoxon paired test **** $P < 0.0001$, *** $P < 0.001$. (B) Free haemoglobin after mechanical stress of 12 AA, 23 SS, 9 LD and 7 HD RBC samples; ANOVA; ** $P < 0.01$, **** $P < 0.0001$. (C) *Left panel*: Gating of irreversibly sickled cells (ISCs) in an SCD blood sample using imaging flow cytometry; *right panel*: images of two ISCs. (D) Percentage of ISCs before and after mechanical stress ($n = 12$). (E) Free haemoglobin and (F) %ISCs after mechanical stress of 7 (E) and 4 (F) paired LD and HD RBC samples. (G) Snapshots of LD and HD RBCs flowing through the microfluidic channels. *Left panel*: LD RBCs flowing through three channels. *Right panel*: HD RBCs flowing through channel 3 while channels 1 and 2 are blocked. For live imaging see videos 3&4. (H) Deformation index of LD and HD RBCs ($L/I/D$) normalized with respect to the mean cell volume in each subpopulation.

Journal Name

ARTICLE

To further confirm the difference of deformability between both cell types we measured the deformation index (DI) of RBCs as described by Tomaiuolo and collaborators.²³ The cell deformation index (measured as the ratio between the long side and the short side of a bounding box enclosing the RBC body, normalized with respect to capillary diameter) was determined at the last portion of the 5 μm section, before the cell exited to the 10 μm section (Figure 3H). As RBCs from SCD patients are heterogeneous in shape and volume because of sickling and dehydration, we focused on RBCs with similar morphology in both subpopulations, i.e. biconcave and round RBCs. In addition, as LD RBCs are bigger than HD RBCs we normalized the DI with respect to the mean cell volume in each subpopulation measured by a cell counter. The DI of HD RBCs was significantly lower than that of LD RBCs (Figure 3H), confirming that HD RBCs are stiffer and less deformable than LD RBCs. This is in good agreement with results from the literature showing decreased DI after *in vitro*-induced rigidity of RBCs treated with glutaraldehyde.²³

Interestingly, and contrary to what we had expected, we did not see a systematic blockade of the capillaries by ISCs. As a matter of fact, we observed that as the velocity increases, most of the ISCs align horizontally along the centreline of the channel, which allows them to flow through the restriction zone without the need to deform, as the capillary section is bigger than their own (Figure 4A and Video 5). This horizontal alignment under high velocity conditions is expected and in agreement with results from the literature showing similar alignment of biconcave RBCs with increasing shear rates.²⁴ In some cases, although the ISCs were not aligned horizontally, probably because of a pressure and velocity drop in the channel, they were able to flow through the restriction zone by bending and they recovered their initial shape at the exit (Figure 4B and Video 6). These original observations indicate that despite their documented decreased deformability a proportion of ISCs are able of limited flexibility that allows them to bend in order to flow through narrow capillaries. The percentage of ISCs that flew by aligning horizontally was much higher than the percentage of those that bended in the channel (70.5 \pm 2.8 versus 29.5 \pm 2.8). Altogether, these observations are in accordance with the presence of significant levels of ISCs in blood samples; such levels would not be detected if the ISCs were skimmed after systematic blockade at the entry of micro-capillaries *in vivo*. ISCs exhibit a heterogeneous morphology. Their percentage and shape are influenced by several factors related to modulators of intracellular HbS concentrations such as HbF expression, co-inheritance of α -thalassaemia and hydration. Our microfluidic device would be a very good tool to specifically address the

variability of the mechanical properties of these cells under flow conditions within a blood sample and among patients.

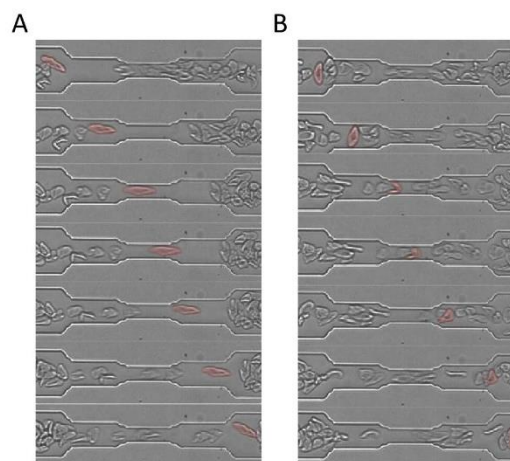


Fig. 4 Irreversibly sickled cells flowing through the microfluidic device. (A) ISC aligning horizontally along the centreline of the channel and flowing through the restriction without deformation. (B) ISC facing the restriction and bending to flow through. After exiting the restriction the ISC recovers slowly its initial shape. For live imaging see videos 5 and 6.

Impact of foetal haemoglobin expression on resistance to lysis of sickle red blood cells

Expression and distribution of foetal haemoglobin in sickle red blood cells

Foetal haemoglobin (HbF) is capable of inhibiting sickle haemoglobin (HbS) polymerization at the molecular level, preventing or attenuating RBC sickling and partially alleviating disease complications.^{25, 26} HbF is the predominant haemoglobin during gestation and is composed of two α and two γ globin chains.²⁷ Slightly before birth, HbF is substituted by adult haemoglobin (HbA) during a process called foetal-to-adult haemoglobin switch that is finely controlled by transcription factors at the β -globin locus.²⁷ In healthy adults HbF accounts for less than 1% of total hemoglobin²⁸ and is restricted to a small subset of RBCs (2%) called F-cells.²⁹⁻³¹ In SCD the expression of HbF is higher than in healthy individuals and varies considerably among patients. It has been shown that F-cells survive longer in the circulation than non-F-cells.^{32, 33} This preferential survival of F-cells is supported by studies showing that the percentage of mature F-cells is higher than that of reticulocytes (young RBCs) expressing HbF within the same SCD patient.^{34, 35}

To determine whether the protective role of HbF is due to improved deformability of the cells we monitored the survival of F-cells in our microfluidic device. Before performing these experiments we set up the HbF-staining method using flow cytometry. HbF was detected using a specific anti-human HbF antibody and reticulocytes were stained using an RNA dye (Figure 5A). As a matter of fact, reticulocytes exiting the bone marrow contain residual but detectable levels of RNA that are lost during maturation. First, we confirmed the preferential survival of reticulocytes expressing HbF (F⁺Retics) in 8 SCD by showing that the percentage of F⁺Retics was lower than the percentage of F⁺RBCs (%F⁺RBCs) for all patients (Figure 5B). We further validated our HbF staining to ensure that it was reflecting the distribution of HbF by assessing the percentage of ISC8 in 30 SCD blood samples. As expected, there was an inverse correlation between %ISC8 and %F⁺RBCs (Figure 5C), which is a direct effect of the anti-sickling effect of HbF.

Foetal haemoglobin expression protects sickle red cells from increased density and from lysis upon repeated mechanical stress

We assessed the impact of HbF expression on RBC resistance to mechanical stress by measuring the percentage of F⁺RBCs in our microfluidic device. The %F⁺RBCs was higher in the output than in the input suspensions for all samples, indicating that haemolysis targets the F⁻RBC subpopulation (Figure 5D). There was also a significant increase of the mean fluorescence intensity (MFI) of the F⁺RBCs in the output suspension (Figure 5E) suggesting the loss of RBCs with low levels of HbF and indicating that minimal amounts are needed for HbF to exert its protective effect under repeated mechanical stress. To address this hypothesis in vivo, we measured the percentage of HbF within free haemoglobin in the plasma of SCD patients

using HPLC. Plasma from 7 patients was analysed, together with total RBC lysates. The HbF/HbS ratio in the plasma was much lower than in RBC lysates in all patients (Figure 5F), indicating that F⁺RBCs are protected against intravascular haemolysis in vivo. In accordance with our results obtained with the microfluidic biochip, the presence of low amounts of HbF in the plasma suggests that some F⁺RBCs, most probably those with low amounts of HbF, still encounter lysis in vivo. These RBCs most probably contain less than 9 pg of HbF per cell as 9–12 pg of intracellular HbF were suggested to be protective from sickling.³⁵

To further explore the role of HbF we measured the %F⁺RBCs in the LD and HD subpopulations. We found higher levels in the LD than in the HD RBCs for all samples (Figure 6A) suggesting that the lower levels of haemolysis of LD RBCs were probably due to a higher proportion of %F⁺RBCs in this subpopulation. In addition, we estimated the HbF expression level in both populations, as reflected by the mean fluorescence intensity of F⁺RBCs, and it was higher in the LD subpopulation (Figure 6B), further supporting our microfluidic results and indicating that high levels of HbF are protective against increased RBC density.

To confirm the physiological relevance of HbF expression in these cells we performed in vitro sickling assays under controlled oxygen atmosphere (Figure 6C). As expected, and because HbF is an anti-sickling haemoglobin, the percentage of sickled cells at 5% O₂ was inversely correlated to the percentage of F⁺RBCs in total blood (Figure 6D). The percentage of sickled cells was much lower in the LD than in the HD subpopulations for all samples (Figure 6E), indicating less HbS polymerisation in LD RBCs and confirming the levels of F⁺RBCs measured for these subpopulations.

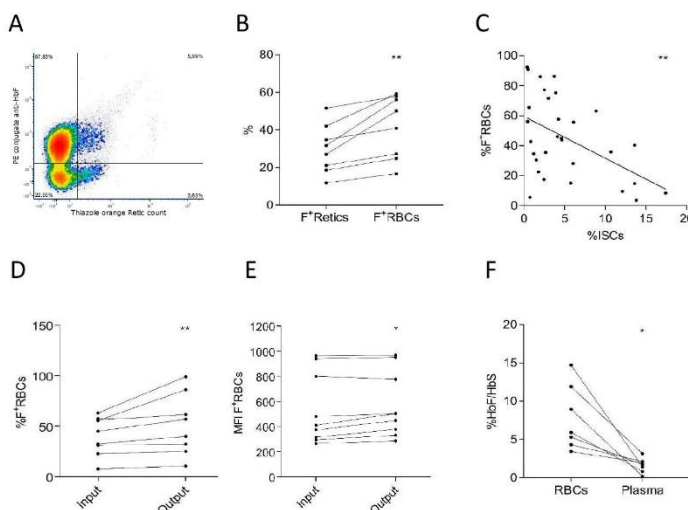


Fig. 5 Role of HbF in RBC resistance to lysis. (A) Flow cytometry dot plot representing RBCs stained for HbF (Y axis) and a reticulocyte marker (X axis). (B) Percentage of HbF-positive cells in reticulocytes and mature RBCs of 8 SCD patients. (C) Inverse correlation between the %ISC8 and the %F⁺RBCs ($n = 30$, $**P < 0.01$). (D) Percentage and (E) MFI of F⁺RBCs before and after mechanical stress. (F) Percentage of HbF/HbS in RBC lysates and plasma of 7 SCD patients, as measured by HPLC. (B,D-F) Wilcoxon paired test, $*P < 0.05$, $**P < 0.01$.

Journal Name

ARTICLE

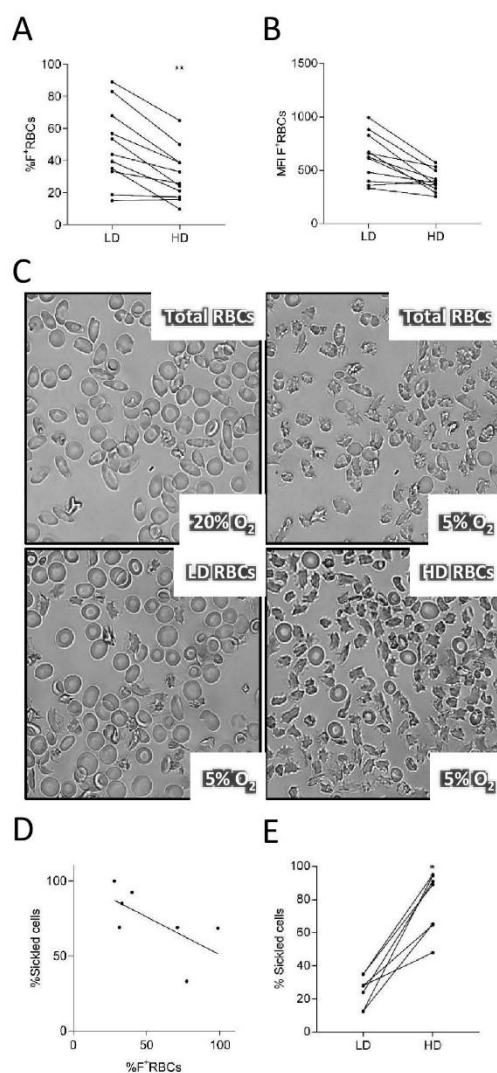


Fig. 6 HbF in sickle RBC subpopulations. (A) Percentage and (B) mean fluorescence intensity of F⁺RBCs in the LD and HD subpopulations ($n = 11$; Wilcoxon paired test, $**P < 0.01$). (C) Upper panels: microscopy images of SS RBCs at 20% oxygen (normoxia) and 5% oxygen (hypoxia); lower panels: microscopy images of low density (LD) and high density (HD) RBCs from an SCD patient at 5% oxygen (hypoxia). (D) Inverse correlation between the percentage of F⁺RBCs and the percentage of sickled cells at 5% oxygen ($n = 7$). (E) Percentage of sickled cells in the LD and HD subpopulations at 5% oxygen ($n = 7$; Wilcoxon paired test, $*P < 0.05$).

Conclusions

Our microfluidic device shows the importance of the mechanical parameter in sickle RBC destruction and the pivotal role of HbF in protecting these cells against lysis. HbF expression in sickle RBCs has been reported by several studies as positively impacting cell survival; our study demonstrates that this protective role is partially exerted by conferring to RBCs the ability of resisting lysis upon repeated mechanical stress. This resistance indicates that HbF expression preserves RBC elasticity and deformability, which is most probably a direct effect of its anti-sickling function.

In vivo studies have shown that the survival of non-F-cells is about 2 weeks for most SCD patients, whereas F cells survive about 6 weeks.³³ Our results are in accordance with these findings and further extend them by highlighting the role of mechanical stress as an important factor that negatively impacts survival of non-F-cells. This is supported by our results

obtained in vivo showing that free haemoglobin in SCD patients plasma is mainly composed of HbS, with very small amounts of HbF. This indicates the preferential targeting of the non-F-cell population by intravascular haemolysis. Furthermore, the presence of low amounts of HbF in the plasma indicates that a subpopulation of F-cells still undergoes lysis, which supports the fact that a minimal threshold of HbF should be reached to protect RBCs from destruction.³⁵

Our results with fractionated blood gave insightful information reflecting the impact of HbF expression on RBC properties in vivo. We showed that F⁺RBCs had a preferential segregation to the LD population indicating that HbF protects against the formation of dense cells in the circulation. However, F⁺RBCs were still detected in the HD population, with high percentages in some patients, indicating that the presence of HbF was not sufficient to protect RBCs from shifting to the dense fraction either because its intracellular levels are not high enough, as discussed above, or because of factors that are independent from sickling such as cell dehydration.^{36, 37}

Moreover, we showed that the HD population contained more ISCs and presented a higher in vitro sickling rate than the LD population, which is in accordance with the lower percentage of F⁺RBCs in this population. Our microfluidic data showed that HD RBCs were less resistant to lysis than LD RBCs and had a lower deformation index, indicating loss of cell elasticity with increased density. More importantly, we showed that in addition to their increased lysis rate, HD RBCs were more prone to obstructing the microfluidic device, supporting the two-step model of the vaso-occlusive crisis in which adhesion of deformable RBCs^{38, 39} or leukocytes^{40, 41} reduces effective lumen-diameter of post-capillary venules promoting selective

Lab on a Chip Accepted Manuscript

trapping of dense RBCs in the areas of adhesion.⁴² Such phenomenon was also observed in our experiments, as we were able to see leukocytes adhering to the capillary wall in a 10 μm section reducing the luminal diameter and blocking an irreversibly sickled RBC in the capillary (Video 7).

Vaso-occlusive crisis has been investigated in vitro with microfluidic approaches using different types of biomimetic devices. These devices addressed several parameters including RBC deformability, cellular interactions with coated proteins or cultured endothelial monolayers, and capillary dimensions, with or without implementing gas exchange chambers to mimic hypoxic conditions.⁴³⁻⁴⁸ The main objective of our microfluidic device was not to mimic the vaso-occlusive crisis but to exert repeated mechanical stress on flowing RBCs in capillaries with physiologically relevant dimensions (5 x 5 μm sections). Thanks to its highly parallelized design, our device allows processing 60 μl of blood suspension in 20 min at 350 mBar, which was enough for our subsequent haemolysis and flow cytometry analyses. Although the fact of pushing the cells through 10 serial restrictions within a short time does not mimic physiological conditions, the design has the advantage of exerting homogeneous and identical mechanical forces at the single cell level on all flowing RBCs, which cannot be achieved by other techniques such as vortexing or centrifuging RBC suspensions. Our microfluidic biochip is a good tool to address the impact of mechanical stress on RBC resistance to lysis, and to mimic circulatory jamming as it was blocked in two assays with HD RBCs. The impact of hypoxia and oxygenation on those parameters will be addressed by coupling our device to a gas exchange layer.

The biochip developed in this study provides a tool of simple use to address biological questions related to red cell elasticity and ability to resist lysis upon mechanical stress. In addition to these parameters, the biochip might be useful for studies exploring the interplay between mechanotransduction and the regulation of red cell volume to address the role of mechanosensors such as Piezo in pathophysiology.^{49, 50} Using the biochip in the context of SCD gave new insights into the role of the mechanical dimension as a critical contributing factor to anaemia in this pathology. Finally, our study validates the microfluidic device as a good tool for drug screening strategies aiming at developing new therapies to improve red cell deformability and resistance to lysis in pathological contexts.

Conflicts of interest

There are no conflicts to declare.

Acknowledgements

We thank Mr Leonardo Molina Cancino for technical support during his internship. The work was supported by the Institut National de la Santé et de la Recherche Médicale (Inserm), the Institut National de la Transfusion Sanguine, the Laboratory of Excellence GR-Ex, reference ANR-11-LABX-0051, the

Laboratory of Excellence LaSIPS (ANR-10-LABX-0040-Lasips), and FAPESP grant for Center for Cell-based Therapy (CTC 2013/08135-2). GR-Ex is funded by the program "Investissements d'avenir" of the French National Research Agency, reference ANR-11-IDEX-0005-02. Sara El Hoss and Maria Alejandra Lizarralde Iragorri were funded by the Ministère de l'Enseignement Supérieur et de la Recherche (Ecole Doctorale BioSPC); they received financial support from: Club du Globule Rouge et du Fer and Société Française d'Hématologie.

Author contributions

MALI and SEH conducted experiments, acquired and analyzed data and wrote the manuscript, VB provided blood samples and clinical data, analyzed and discussed data, MD and ARF conducted experiments, acquired and analyzed data, SDL, TX and CL conducted experiments, YL analyzed data, ACSP provided blood samples and clinical data, SK supervised experiments, analyzed data and edited the manuscript, DTC, CLVK, YC and JE edited the manuscript, OF and BLP conducted experiments, provided reagents and wrote the manuscript, WEN designed research, analyzed data and wrote the manuscript.

References

1. N. Mohandas, M. R. Clark, M. S. Jacobs and S. B. Shoheit, *J Clin Invest*, 1980, **66**, 563-573.
2. S. E. t. Lux, *Blood*, 2016, **127**, 187-199.
3. J. Narla and N. Mohandas, *Int J Lab Hematol*, 2017, **39 Suppl 1**, 47-52.
4. Y. Alapan, Y. Matsuyama, J. A. Little and U. A. Gurkan, *Technology (Singap World Sci)*, 2016, **4**, 71-79.
5. J. G. Dobbe, M. R. Hardeman, G. J. Streekstra, J. Strackee, C. Ince and C. A. Grimbergen, *Blood Cells Mol Dis*, 2002, **28**, 373-384.
6. M. Rabaj, J. A. Detterich, R. B. Wenby, T. M. Hernandez, K. Toth, H. J. Meiselman and J. C. Wood, *Biorheology*, 2014, **51**, 159-170.
7. L. Pauling, H. A. Itano and et al., *Science*, 1949, **109**, 443.
8. G. A. Barabino, M. O. Platt and D. K. Kaul, *Annu Rev Biomed Eng*, 2010, **12**, 345-367.
9. P. Connes, T. Alexy, J. Detterich, M. Romana, M. D. Hardy-Dessources and S. K. Ballas, *Blood Rev*, 2016, **30**, 111-118.
10. F. B. Piel, M. H. Steinberg and D. C. Rees, *N Engl J Med*, 2017, **376**, 1561-1573.
11. M. J. Stuart and R. L. Nagel, *Lancet*, 2004, **364**, 1343-1360.
12. R. E. Ware, M. de Montalembert, L. Tshilolo and M. R. Abboud, *Lancet*, 2017, DOI: 10.1016/S0140-6736(17)30193-9.
13. B. Lubin, D. Chiu, B. Roelofsen and L. L. Van Deenen, *Prog Clin Biol Res*, 1981, **56**, 171-193.
14. E. Marva and R. P. Hebbel, *Blood*, 1994, **83**, 242-249.
15. S. Voskou, M. Aslan, P. Fanis, M. Phylactides and M. Kleanthous, *Redox Biol*, 2015, **6**, 226-239.
16. J. C. McDonald and G. M. Whitesides, *Acc Chem Res*, 2002, **35**, 491-499.
17. P. Bartolucci, V. Chaar, J. Picot, D. Bachir, A. Habibi, C. Fauroux, F. Galacteros, Y. Colin, C. Le Van Kim and W. El Nemer, *Blood*, 2010, **116**, 2152-2159.

ARTICLE

Journal Name

18. E. J. van Beers, L. Samsel, L. Mendelsohn, R. Saiyed, K. Y. Fertrin, C. A. Brantner, M. P. Daniels, J. Nichols, J. P. McCoy and G. J. Kato, *Am J Hematol*, 2014, **89**, 598-603.
19. J. A. Ribell, S. Hacein-Bey-Abina, E. Payen, A. Magnani, M. Semeraro, E. Magrin, L. Caccavelli, B. Neven, P. Bourget, W. El Nemer, P. Bartolucci, L. Weber, H. Puy, J. F. Meritet, D. Grevent, Y. Beuzard, S. Chretien, T. Lefebvre, R. W. Ross, O. Negre, G. Veres, L. Sandler, S. Soni, M. de Montalembert, S. Blanche, P. Leboulch and M. Cavazzana, *N Engl J Med*, 2017, **376**, 848-855.
20. G. J. Bosman, J. M. Werre, F. L. Willekens and V. M. Novotny, *Transfus Med*, 2008, **18**, 335-347.
21. N. Mohandas and W. Groner, *Ann N Y Acad Sci*, 1989, **554**, 217-224.
22. S. R. Goodman, *Cell Mol Biol (Noisy-le-grand)*, 2004, **50**, 53-58.
23. G. Tomaiuolo, L. Lanotte, R. D'Apolito, A. Cassinese and S. Guido, *Med Eng Phys*, 2016, **38**, 11-16.
24. J. Dupire, M. Socol and A. Viallat, *Proc Natl Acad Sci U S A*, 2012, **109**, 20808-20813.
25. D. R. Powars, J. N. Weiss, L. S. Chan and W. A. Schroeder, *Blood*, 1984, **63**, 921-926.
26. L. S. Sewchand, C. S. Johnson and H. J. Meiselman, *Blood Cells*, 1983, **9**, 147-166.
27. V. G. Sankaran, J. Xu and S. H. Orkin, *Br J Haematol*, 2010, **149**, 181-194.
28. S. H. Boyer, L. Margolet, M. L. Boyer, T. H. Huisman, W. A. Schroeder, W. G. Wood, D. J. Weatherall, J. B. Clegg and R. Cartner, *Am J Hum Genet*, 1977, **29**, 256-271.
29. S. H. Boyer, T. K. Belding, L. Margolet and A. N. Noyes, *Science*, 1975, **188**, 361-363.
30. S. H. Boyer, T. K. Belding, L. Margolte, A. N. Noyes, P. J. Burke and W. R. Bell, *Johns Hopkins Med J*, 1975, **137**, 105-115.
31. W. G. Wood, G. Stamatoyannopoulos, G. Lim and P. E. Nute, *Blood*, 1975, **46**, 671-682.
32. G. J. Dover, S. H. Boyer, S. Charache and K. Heintzelman, *N Engl J Med*, 1978, **299**, 1428-1435.
33. R. S. Franco, J. Lohmann, E. B. Silberstein, G. Mayfield-Pratt, M. Palascak, T. A. Nemeth, C. H. Joiner, M. Weiner and D. L. Rucknagel, *J Clin Invest*, 1998, **101**, 2730-2740.
34. R. S. Franco, Z. Yasin, M. B. Palascak, P. Ciraolo, C. H. Joiner and D. L. Rucknagel, *Blood*, 2006, **108**, 1073-1076.
35. M. Maier-Redelsperger, C. T. Noguchi, M. de Montalembert, G. P. Rodgers, A. N. Schechter, A. Gourbil, D. Blanchard, J. P. Jais, R. Ducrocq, J. Y. Peltier and et al., *Blood*, 1994, **84**, 3182-3188.
36. C. Brugnara, H. F. Bunn and D. C. Tosteson, *Science*, 1986, **232**, 388-390.
37. C. Brugnara, T. Van Ha and D. C. Tosteson, *Blood*, 1989, **74**, 487-495.
38. D. K. Kaul, M. E. Fabry and R. L. Nagel, *Blood*, 1986, **68**, 1162-1166.
39. D. K. Kaul, M. E. Fabry and R. L. Nagel, *Proc Natl Acad Sci U S A*, 1989, **86**, 3356-3360.
40. D. K. Kaul and R. P. Hebbel, *J Clin Invest*, 2000, **106**, 411-420.
41. A. Turhan, L. A. Weiss, N. Mohandas, B. S. Collier and P. S. Frenette, *Proc Natl Acad Sci U S A*, 2002, **99**, 3047-3051.
42. D. K. Kaul and M. E. Fabry, *Microcirculation*, 2004, **11**, 153-165.
43. V. M. Dominical, D. M. Vital, F. O'Dowd, S. T. Saad, F. F. Costa and N. Conran, *Exp Hematol*, 2015, **43**, 223-228.
44. E. Du, M. Diez-Silva, G. J. Kato, M. Dao and S. Suresh, *Proc Natl Acad Sci U S A*, 2015, **112**, 1422-1427.
45. J. M. Higgins, D. T. Eddington, S. N. Bhatia and L. Mahadevan, *Proc Natl Acad Sci U S A*, 2007, **104**, 20496-20500.
46. D. J. Quinn, I. Pivkin, S. Y. Wong, K. H. Chiam, M. Dao, G. E. Karniadakis and S. Suresh, *Ann Biomed Eng*, 2011, **39**, 1041-1050.
47. M. Tsai, A. Kita, J. Leach, R. Rounsevell, J. N. Huang, J. Moake, R. E. Ware, D. A. Fletcher and W. A. Lam, *J Clin Invest*, 2012, **122**, 408-418.
48. D. K. Wood, A. Soriano, L. Mahadevan, J. M. Higgins and S. N. Bhatia, *Sci Transl Med*, 2012, **4**, 123ra126.
49. S. N. Bagriantsev, E. O. Gracheva and P. G. Gallagher, *J Biol Chem*, 2014, **289**, 31673-31681.
50. P. G. Gallagher, *Curr Opin Hematol*, 2013, **20**, 201-207.

Article 4

Insights into determinants of spleen injury in sickle cell anemia

Sara El Hoss,¹⁻³ Sylvie Cochet,¹⁻³ Mickaël Marin,¹⁻³ Claudine Lapoumériou,¹⁻³ Michael Dussiot,⁴ Naïm Bouazza,^{5,6} Caroline Elie,^{5,6} Mariane de Montalembert,^{3,7} Cécile Arnaud,⁸ Corinne Guitton,⁹ Béatrice Pellegrino,¹⁰ Marie Hélène Odièvre,¹¹ Frédérique Moati,¹² Caroline Le Van Kim,¹⁻³ Yves Colin Aronovicz,¹⁻³ Wassim El Nemer,^{1-3,*} and Valentine Brousse^{1-3,7,*}

¹Biologie Intégrée du Globule Rouge, Unité Mixte de Recherche S1134, INSERM, Université Paris Diderot, Sorbonne Paris Cité, Université de la Réunion, Université des Antilles, Paris France; ²Institut National de la Transfusion Sanguine, Paris, France; ³Laboratoire d'Excellence GR-Ex, Paris, France; ⁴Université Sorbonne Paris Cité, Université Paris Descartes, INSERM, Centre National de la Recherche Scientifique, Institut Imagine, Laboratory of Cellular and Molecular Mechanisms of Hematological Disorders and Therapeutic Implications, Laboratoire d'Excellence GR-Ex, Paris, France; ⁵Unité de Recherche Clinique/Centre d'Investigation Clinique Paris Descartes Necker-Cochin, Assistance Publique-Hôpitaux de Paris, Paris, France; ⁶Université Paris Descartes, EA7323, Sorbonne Paris Cité, Paris, France; ⁷Service de Pédiatrie Générale, Hôpital Necker-Enfants Malades, Centre de Référence de la Drépanocytose, Assistance Publique-Hôpitaux de Paris, Paris, France; ⁸Service de Pédiatrie, Centre Hospitalier Intercommunal de Créteil, Créteil, France; ⁹Service de Pédiatrie, Hôpital Universitaire Kremlin-Bicêtre, Le Kremlin Bicêtre, France; ¹⁰Service de Pédiatrie, Centre Hospitalier Poissy-Saint Germain, Poissy, France; ¹¹Service de Pédiatrie, Hôpital Universitaire Armand Trousseau, Paris, France; and ¹²Service de Médecine Nucléaire, Hôpital Universitaire Kremlin Bicêtre, Le Kremlin Bicêtre, France

Key Points

- Spleen filtration function is altered in infants with SCA as early as 3-6 months of age.
- Both impaired deformability and increased adhesion of sickle RBCs play a key role in splenic loss of function.

Spleen dysfunction is central to morbidity and mortality in children with sickle cell anemia (SCA). The initiation and determinants of spleen injury, including acute splenic sequestration (ASS) have not been established. We investigated splenic function longitudinally in a cohort of 57 infants with SCA enrolled at 3 to 6 months of age and followed up to 24 months of age and explored the respective contribution of decreased red blood cell (RBC) deformability and increased RBC adhesion on splenic injury, including ASS. Spleen function was evaluated by sequential ^{99m}Tc heated RBC spleen scintigraphy and high-throughput quantification of RBCs with Howell-Jolly bodies (HJBs). At 6 and 18 months of age, spleen filtration function was decreased in 32% and 50% of infants, respectively, whereas the median %HJB-RBCs rose significantly (from 0.3% to 0.74%). An excellent correlation was established between %HJB-RBCs and spleen scintigraphy results. RBC adhesion to laminin and endothelial cells increased with time. Adhesion to endothelial cells negatively correlated with splenic function. Irreversibly sickled cells (ISCs), used as a surrogate marker of impaired deformability, were detected at enrollment and increased significantly at 18 months. % ISCs correlated positively with %HJB-RBCs and negatively with splenic uptake, indicating a relationship between their presence in the circulation and splenic dysfunction. In the subgroup of 8 infants who subsequently experienced ASS, %ISCs at enrollment were significantly higher compared with the asymptomatic group, suggesting a major role of impaired deformability in ASS. Higher levels of %HJB-RBCs were observed after the occurrence of ASS, demonstrating its negative impact on splenic function.

Introduction

Splenic dysfunction is central to morbidity and mortality in children with sickle cell anemia (SCA). The spleen is morphologically and functionally normal at birth, but when the rise of the mutated hemoglobin (HbS) allows Hb polymerization to occur, it is inferred that sickling-related injury takes place in the spleen and results in progressive or acute ischemia. The spleen is indeed the first organ to be clinically symptomatic during the course of the disease in early infancy.^{1,2} Although early therapeutic intervention

Submitted 5 March 2019; accepted 23 May 2019. DOI 10.1182/bloodadvances.2019000106.

*V.B. and W.E.N. contributed equally to this work.

The full-text version of this article contains a data supplement.

© 2019 by The American Society of Hematology

(hydroxyurea, hematopoietic stem cell therapy, and blood transfusion programs) may allow a variable degree of reversal of spleen loss of function,³⁻⁵ ultimately, repeated spleen injury leads to the fibrosis of the organ, a loss also referred to as autosplenectomy.

Altogether, splenic clinical manifestations in children with SCA include acute splenic sequestration (ASS), splenomegaly, chronic sequestration (or hypersplenism), and spleen atrophy. All these complications remain somewhat unpredictable and furthermore may combine with a variable degree of loss of function, with no clear relationship between the size of the spleen and its function. ASS, defined by the sudden enlargement of the spleen with an acute drop in Hb level of >2 g/dL, is a major life-threatening event in infancy, occurring in 10% to 30% of infants with SCA, with 75% of first cases occurring at <2 years of age.⁶ Little is known about determinants or predictive factors of ASS and their specific impact on spleen function. By contrast, splenic loss of immune and filtering functions, central to pneumococcal defense in childhood, is a well-described phenomenon associated with an increased risk of death in the absence of prophylaxis or treatment.^{7,8}

The spleen allows efficient filtering and clearance of senescent or infected red blood cells (RBCs) and bacterial antigens.⁹ The red pulp of the spleen filters the blood and is composed of cords and venous sinuses. It is known to be the major source of mononuclear phagocytic cells involved in the filtering function of the organ. In the splenic cords, RBCs circulate freely in direct contact with spleen resident cells, macrophages and endothelial cells lining the splenic sinuses,⁹ which remove senescent or abnormal cells and contribute to the pitting mechanism, a process that clears nuclear remnants or parasites from the RBCs before they recirculate.^{10,11} This circulation in the red pulp is therefore termed "open" and is also slow, because of a high hematocrit of $\sim 60\%$, which favors cell-cell interaction.¹² In order to join the venous circulation, RBCs flowing through the red pulp must pass through interendothelial slits (1-3 μm wide) that line the sinuses. Within this ultimate checkpoint, RBCs that are not deformable are trapped. Altogether, if the filtering function of the spleen is altered, the clearance of nuclear remnants fails, and they are found in circulating RBCs as Howell-Jolly bodies (HJB-RBCs).

At least 2 major characteristics of sickle RBCs—namely, impaired deformability and increased adhesion—may play an important role in splenic injury, notably ASS. Impaired deformability of sickled RBCs promotes their becoming trapped during their circulation, particularly upstream of the narrow interendothelial slits.⁶ Likewise, increased RBC adhesion may contribute to the congestion of the red pulp through prolonged RBC interactions with cellular and matrix components. Such abnormal interactions could involve the erythroid adhesion marker Lu/BCAM (CD239; Lutheran/basal cell-adhesion molecule), whose expression is increased on reticulocytes of infants with SCA as early as 3 to 6 months of age¹³ and whose ligand is laminin,¹⁴ a major component of the spleen's extracellular matrix.¹⁵

Our study's primary objective was to evaluate the initiation of spleen loss of function in a cohort of SCA infants enrolled very early in life (3-6 months of age) and thereafter longitudinally followed up to 24 months of age. Specifically, we measured splenic function sequentially using flow cytometry-based measurements of HJB-RBCs, coupled with ^{99m}Tc heated RBC spleen scintigraphy. Our secondary objective was to explore determinants of spleen injury focusing

on impaired deformability and increased adhesion properties of sickle RBCs as potential major contributors. We therefore chose to measure, at enrollment and thereafter longitudinally, the usual SCA biomarkers and, more specifically, irreversibly sickled cells (ISCs) as a surrogate marker of RBC deformability and the expression of the adhesion marker Lu/BCAM and its functional activity, in relation to spleen injury, notably ASS.

Methods

Patients and blood samples

Infants diagnosed with SCA following neonatal screening were enrolled in a multicenter prospective study on prognostic factors in SCA (ClinicalTrials.gov: NCT01207037) from September 2010 through March 2013, described in Brousse et al.¹⁶ Inclusion criteria were (1) SS or S- β^0 sickle genotype, (2) age <6 months, and (3) no prior episode of ASS. At each study visit, complete clinical workup and blood sampling were performed, and relevant medical events were recorded. Patients were followed up with scheduled visits planned at enrollment (3 and/or 6 months), 12, 18, and 24 months. All received standard age-appropriate care for SCA; however, none was treated with hydroxyurea, in accordance with national treatment guidelines during the study period. No child was lost to follow-up. The protocol was approved by the ethics committee (Comité pour la Protection des Personnes Ile de France II) and by the French agency for security of health products (Agence Française de Sécurité Sanitaire des Produits de Santé). ASS was defined by the sudden enlargement of the spleen (>2 cm compared with basal) with a decrease in Hb level (>2 g/dL, compared with the previous measurement) and reticulocytes >100 000/mm³. Asymptomatic patients were defined as patients who did not experience any ASS, vaso-occlusive crisis, transfusion, or hospitalization for sickle cell disease (SCD)-related events during the follow-up period up to 24 months of age.

At each visit, blood analysis for routine and SCA-specific biomarkers was performed as described elsewhere.¹⁶ In addition, RBCs reserved in ID-CellStab (Bio-Rad) were cryopreserved in the Centre National de Référence pour les Groupes Sanguins. Blood samples from 7 healthy adult donors obtained from the Etablissement Français du Sang were used as negative controls.

In this cohort of 57 patients, HJB-RBCs and ISCs quantification was performed in 45 patients for whom sufficient sample volumes were available at 2 different time points (3-6 and 18 months) and who had not been transfused in the prior 2 months (supplemental Figure 1). However, 7 of these infants were transfused at some point during the follow-up. Adhesion assays were performed in 15 randomly selected nontransfused patients for whom samples were available at all time points for longitudinal analysis.

Spleen scintigraphy was initially part of the systematic splenic exploration in all infants enrolled in the study but, in response to parental reluctance, an amendment to the protocol was agreed upon, and spleen scintigraphy exploration became optional. Transfusion was not an exclusion criterion. It was performed in 25 patients at the first time point (3-6 months), 17 of whom underwent a sequential exploration at 18 months of age. The subgroup in whom spleen scintigraphy was performed was therefore based on parental acceptance and technical possibility (eg, adequate venous access). Of note, this subgroup did not differ from the rest of the cohort in terms of baseline clinical, biological, or splenic characteristics (data

not shown). Among the 25 patients who underwent a spleen scintigraphy, 7 were transfused at some point during the course of the study, 2 after spleen scintigraphy.

Quantification of HJBs

Quantification of %HJB-RBCs was performed by using imaging flow cytometry (IFC), as previously described.¹⁷ Briefly, 10 μ L of the RBC pellet was suspended in 1 mL of buffer (phosphate buffered saline; 0.5% bovine serum albumin), 80 μ L of the suspension was added to 120 μ L of buffer, and Hoechst 33342 (Life Technologies) was added at a final concentration of 40 μ g/mL and incubated for 5 minutes at room temperature. Importantly, this HJB-RBCs quantification technique can also be applied using a classic flow cytometer. Classic May-Grünwald Giemsa smears were performed in parallel for comparison purposes.

Quantification of ISCs

ISCs, a subpopulation of dense cells with marked decreased deformability, were quantified using an IFC-based method.¹⁸ Briefly, 2 μ L of packed RBCs were suspended in 200 μ L of ID-CellStab (Bio-Rad) and 50 000 events were acquired using ImageStream X Mark II Imaging Flow Cytometer. ISCs were quantified using IDEAS (version 6.2). We optimized an analysis based on morphological and shape features,¹⁹ to finely evaluate the percentage of ISCs in blood samples, as previously described.²⁰

Flow cytometry analysis

Expression of CD239/Lu/BCAM was quantified, as previously described.¹³ Samples were analyzed by flow cytometry with a BD FACScanto II flow cytometer (Becton Dickinson) and FACSDiva software (version 6.1.3).

Adhesion assays

RBC adhesion to immobilized laminin 521 (Biolamina, AB) and transformed human bone marrow endothelial cell (TrHBMEC) monolayers was determined under physiological flow conditions, using Vena8 Endothelial+ biochips (internal channel dimensions: length, 20 mm; width, 0.8 mm; and height, 0.12 mm) and ExiGo nanopumps (Cellix), as described.²¹⁻²³ TrHBMECs were pretreated with tumor necrosis factor- α (100 U/mL) 24 hours before adhesion experiments. Adhesion experiments were performed at the 4 time points in 15 patients with characteristics comparable to the rest of the cohort.

Phosphorylation assays

Evaluation of the activated state of the Lu/BCAM long isoform Lu was performed through phosphorylation assays. In brief, RBCs were lysed for 45 minutes at 4°C with lysis buffer (Tris, 20 mM; NaCl, 150 mM; EDTA, 5 mM; and Triton X100, 1%). Phosphorylation of Lu/BCAM was performed after immunoprecipitation with a specific anti-Phospho-Lu antibody (Institut National de la Transfusion Sanguine). The quantification of the proteins was achieved using Quantity One Software (Bio-Rad).

Spleen scintigraphy

Spleen/liver scintigraphy, using heat-denatured ^{99m}Tc-labeled RBCs, was performed as previously described.²⁴ Spleen scintigraphy with heated autologous red cells measures primarily the filtration capacity of the splenic red pulp because heated RBCs are poorly deformable and therefore get trapped in the splenic

microvasculature.^{25,26} Radionuclide images were taken of the posterior, left lateral, and anterior views of the spleen. Splenic uptake was compared with that of the liver and expressed in a semiquantitative percentage using a computational method: 0% to 25% (lowest splenic uptake), 25% to 50%, 50% to 75%, 75% to 100%, and 100% to 150% (highest splenic uptake).

Splenic volume was calculated by computed tomography and was estimated after 1.5 hours of tomography acquisition.

Statistics

Data were analyzed by 2-tailed Wilcoxon test or paired Wilcoxon test, as appropriate. The association between quantitative variables was assessed with the Spearman correlation test. GraphPad Prism, version 7.00, and R software were used. $P \leq .05$ was considered significant.

Results

Very early loss of splenic function and subsequent further decline with time

Spleen function was assessed with both a high-throughput cytometry method for HJB-RBC counts and ^{99m}Tc heated RBC scintigraphy at 2 time points (3-6 and 18 months of age) in a cohort of 57 infants (SS, $n = 55$; S- β^0 , $n = 2$; 54.4% males). At enrollment (median age, 6 months; range, 2.8-8), median fetal Hb (HbF) level was 42% (range, 35%-50.5%), as previously reported.¹⁶ Supplemental Figure 1 explains the exploration of spleen function performed on this cohort.

The median %HJB-RBCs in 45 patients at enrollment was low (0.3%; range, 0.01%-2.9%) and comparable to that in an adult healthy control group, albeit with a different distribution range (0.3%; range, 0.01%-0.6%; $n = 7$; $P = .93$; Figure 1A; supplemental Table 1).

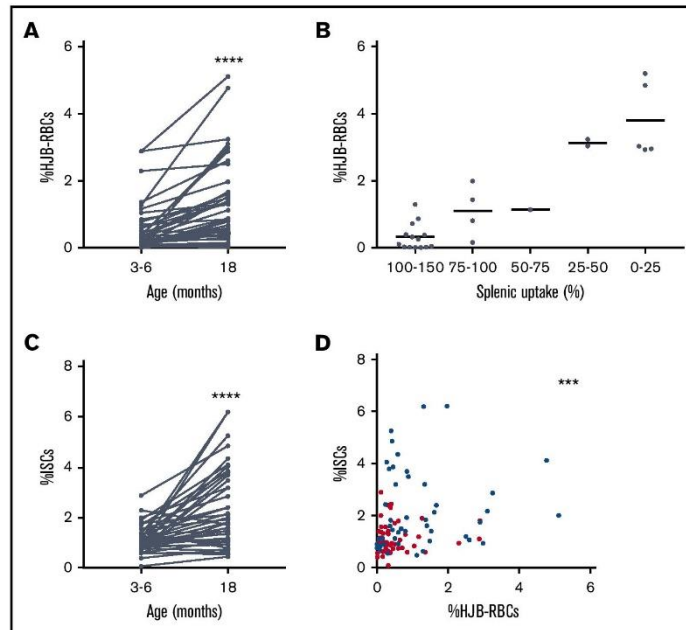
HJB-RBCs counts by classic May-Grünwald Giemsa blood smears were only slightly elevated in a very small proportion of patients and did not allow further interpretation by lack of sensitivity.

Spleen scintigraphy with ^{99m}Tc heated RBCs was performed in a subgroup of 25 patients (with characteristics comparable to the rest of the cohort; data not shown) at a median age of 6.2 months (range, 4.9-8.0). Splenic uptake was normal in 17 cases (68%) and decreased in 8 (32%; Table 1). All scans were qualified as homogenous. Median splenic volume was 45 mL (range, 0-100), an increase compared with that of healthy age-matched controls (median, 21 mL; range, 14-42).²⁷ Only 28% of the patients had a splenic volume within the 5th to 95th percentiles of age-matched healthy controls. There was no predictive value between routine laboratory parameters, including RBC parameters (Hb, mean corpuscular volume, and mean corpuscular hemoglobin concentration), hemolysis markers, %HbF measured at enrollment, and the result of spleen scans at this age (supplemental Table 2).

Between enrollment and 18 months of age, the median %HJB-RBCs increased significantly (from 0.3% to 0.74%; range, 0.01-5.11) illustrating the expected decline in splenic function with time. Of note, excluding the patients who were transfused during follow-up ($n = 7$) did not yield any significant changes in the results. Spleen scintigraphy performed sequentially in 17 patients at a median age of 18.3 months (range, 16.6-19.5) showed a decreased splenic uptake in 7 patients (41.7%) and a stable scan in 9 (53%), further

Figure 1. HJB-RBCs and ISCs in children with SCA.

(A) %HJB-RBCs determined by IFC in 45 children at 3 to 6 and 18 months. **** $P < .0001$, Wilcoxon paired test. (B) Distribution of %HJB-RBCs with respect to splenic uptake as measured by ^{99m}Tc heated RBCs spleen scintigraphy. Splenic uptake of 100% to 150% ($n = 15$), 75% to 100% ($n = 4$), 50% to 75% ($n = 1$), 25% to 50% ($n = 2$), and 0% to 25% ($n = 5$). (C) %ISCs determined by IFC in 45 children at 3 to 6 and 18 months. **** $P < .0001$, Wilcoxon paired test. (D) Spearman correlation between %ISCs and %HJB-RBCs at 3 to 6 (red dots) and 18 months (blue dots). $n = 99$; $R^2 = 0.69$; *** $P < .001$.



illustrating the decline of function with age, except for 1 patient who had an unexpected increase in splenic uptake (Table 1). Altogether, there was no evidence of a significant positive effect of transfusion on spleen scintigraphy results (data not shown).

At 18 months of age, the median splenic volume was 70 mL (range, 0-115), an increase compared with the 31 mL (range, 10.59-65.4) in healthy controls. At this time point, only 17% of the patients had a splenic volume within the 5th to 95th percentiles of age-matched healthy controls.²⁷ Whereas 56% had an increased volume, 28% had a decreased volume. There was no correlation between splenic uptake and volume, altogether or independently, at each time point. Similarly, there was no correlation between %HJB-RBCs and splenic volume, demonstrating that volume is not predictive of splenic function. Importantly, at all time points, a significant correlation was found between %HJB-RBCs and splenic uptake (Figure 1B; $R^2 = 0.69$; $P < .0001$).

Impaired deformability of RBCs increases with time and impacts splenic function

At enrollment, ISCs were found in the circulation (median, 0.96%; range, 0.08% to 2.9%; $n = 45$) and increased significantly at 18 months of age (1.71%; range, 0.47-6.21; Figure 1C; supplemental Table 1), similar to %HJB-RBCs (Figure 1A). Pooling of all time point measurements showed a positive correlation between %ISCs and %HJB-RBCs (Figure 1D), suggesting a relationship between altered RBC deformability and splenic loss of function. As expected, there was a positive correlation between %ISCs and the splenic uptake measured by scintigraphy ($R^2 = 0.3$; *** $P = .0005$; supplemental Figure 2A). Because HbF modulates

the polymerization of HbS and hence RBC deformability,²⁸ we looked at the relationship between ISCs and HbF and found a significant correlation ($R^2 = 0.16$; *** $P < .0001$; supplemental Figure 2B).

RBC adhesion increases with time in young infants and plays a role in loss of splenic function

RBC adhesive properties were investigated in a subgroup of 15 infants by first performing adhesion assays on tumor necrosis factor- α -activated endothelial cells. RBCs were adherent at 3 to

Table 1. Spleen function at 3-6 and 18 months of age in children with SCA, as measured by ^{99m}Tc -heated RBC spleen scintigraphy (splenic uptake) and %HJB-RBCs

Age, mo	Splenic uptake, %	Patients, n (%)	%HJB-RBCs, median (range)
3-6	100-150	17 (68)	0.32 (0.01-1.27)
	75-100	3 (12)	0.16, 0.3 and 1.96
	50-75	1 (4)	ND
	25-50	2 (8)	0.05 and 3.18
	0-25	2 (8)	2.88 and 2.9
18	100-150	9 (50)	0.07 (0.01-1.3)
	75-100	2 (11.1)	0.8 and 1.41
	50-75	1 (5.6)	1.12
	25-50	2 (11.1)	2.98*
	0-25	4 (22.2)	4.77 (1.37-5.11)

ND, not determined.

*Only 1 blood sample was processed.

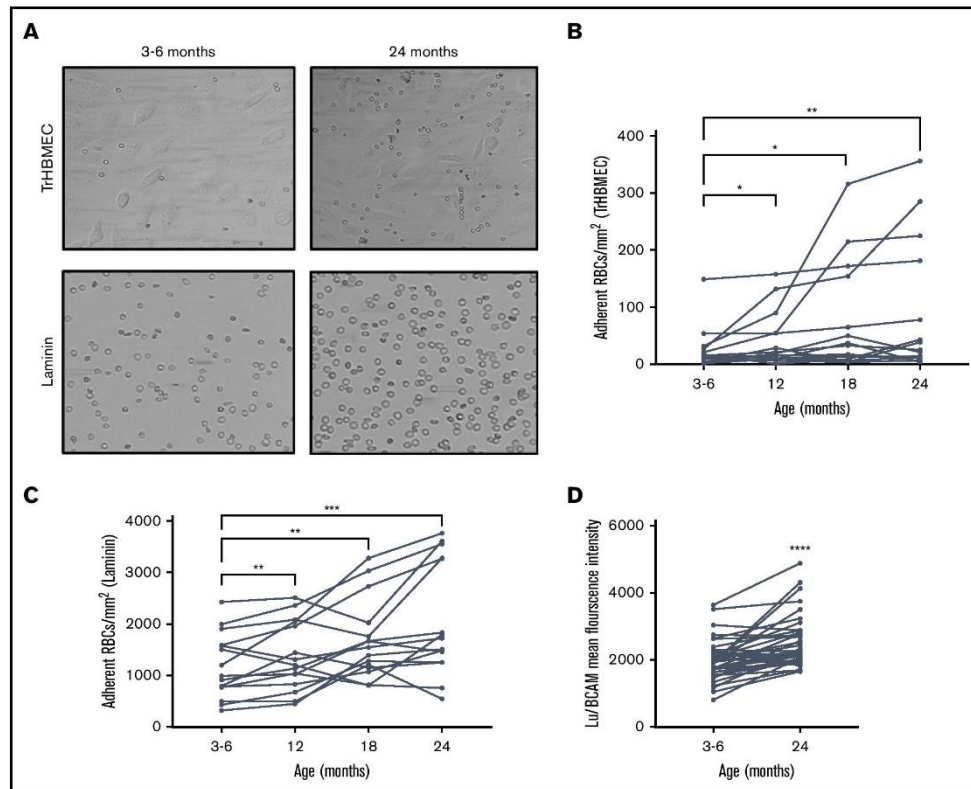


Figure 2. Lu/BCAM expression and mediated RBC adhesion. (A) Microscopic images of RBCs adhering to TrHBMEC monolayers and laminin 521-coated micro-channels at 3 to 6 and 24 months. Original magnification $\times 20$. (B-C) The amount of adherent RBCs/mm² on TrHBMEC-coated channels ($n = 15$) (B) and laminin-coated channels ($n = 15$) (C) at 3 to 6, 12, 18, and 24 months. * $P < .05$, ** $P < .005$, *** $P < .001$, Wilcoxon test. (D) Mean fluorescence intensity of Lu/BCAM on mature RBCs. **** $P < .0001$, Wilcoxon test.

6 months of age, with a significant progressive increase of the adhesion level at 12, 18, and 24 months (Figure 2A-B), indicating an early triggering of the RBC adhesive phenotype and subsequent increase during the first 2 years of life.

We then focused on the erythroid adhesion protein CD239/Lu/BCAM for its known role in abnormal RBC adhesion in SCA,^{14,29,30} in particular to laminin,³¹ an important structural component of the splenic extracellular matrix. In addition, Lu/BCAM has an early increased expression on RBCs of infants with SCA, compared with age-matched controls.¹³ RBC adhesion to immobilized laminin was higher than control RBCs (data not shown) with a significant increase at 12, 18, and 24 months ($n = 15$; Figure 2A,C). This increase was associated with increased Lu/BCAM expression per cell with age (Figure 2D). To test whether the increase in RBC adhesion was secondary to the activation of Lu/BCAM, we determined the phosphorylation level of Lu/BCAM in the same blood samples at the 4 different time points. Lu phosphorylation began

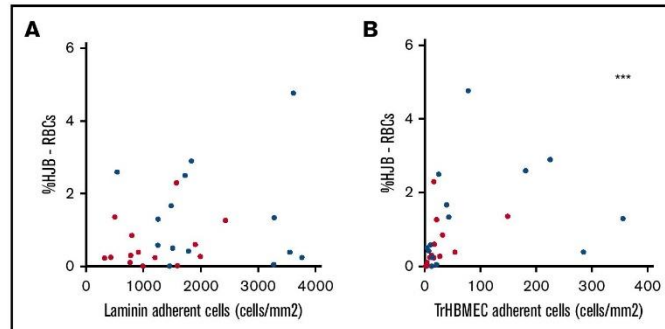
as early as 3 to 6 months of age, in accordance with the high adhesion levels observed at this stage. Lu phosphorylation ratio did not differ significantly between 3 to 6 and 24 months of age, indicating that both phospho-Lu and total Lu/BCAM were increasing at the same rate within this time frame (supplemental Figure 3).

There was no correlation between the number of adherent RBCs on laminin and splenic function measured by %HJB-RBCs ($P = .39$; Figure 3A). Conversely, a positive correlation was found between the number of adherent cells on TrHBMECs and the %HJB-RBCs (Spearman correlation $R^2 = 0.42$; $P < .0001$; Figure 3B) suggesting a role of adhesion, beyond Lu-BCAM, in the occurrence of decline of splenic function.

Incidence, determinants, and consequence of ASS

As previously reported,¹⁶ during the study period, 8 (17%) infants experienced at least 1 episode of ASS, at a median age of 13.4 months (8.0-15.9), an incidence rate within the

Figure 3. RBC adhesion and HJB-RBCs in children with SCA. Spearman correlation between the amount of adherent RBCs/mm² on laminin (A) and TrHBMEC and %HJB-RBCs (B). At 3 to 6 (red dots) and 18 months (blue dots). n = 28; R² = 0.43; ***P < .001.



expected range.^{32,33} Thirty-five infants remained asymptomatic during the follow-up period, and 14 experienced other SCD-related complications.

Analysis of routine laboratory parameters and more specific SCA-related biomarkers measured at enrollment showed that the level of HbF was the only factor that was prognostic of ASS.¹⁶ When the analysis was extended to %ISCs, the %HJB-RBCs and Lu/BCAM expression levels (in 7 and 22 patients of the ASS and asymptomatic groups, respectively, for whom samples were available) did not reveal an additional significant prognostic value of these markers.

Moving on to comparing %HJB-RBCs at enrollment in infants who later experienced ASS with those who remained asymptomatic showed no significant difference, demonstrating similar splenic function in both groups at 3 to 6 months of age and excluding intrinsic abnormalities of the spleen filtration function in the ASS group at this stage (Figure 4A). Likewise, no significant difference was noted between Lu/BCAM expression and Lu/BCAM-mediated adhesion levels in the 2 groups. Conversely, patients from the ASS group had a significantly higher %ISCs at enrollment than did those from the asymptomatic group (median: 1.61% vs 0.54%; P = .0025;

Figure 4B), suggesting that high levels of ISC in the circulation may be a contributing factor to ASS.

At 18 months, there was no difference in ISC level, Lu/BCAM expression, and Lu/BCAM-mediated adhesion levels, in both groups (data not shown). Importantly, %HJB-RBCs was significantly higher in the ASS group at 18 months, as compared with the asymptomatic group (Figure 4A), indicating altered splenic function after the occurrence of ASS.

Discussion

SCA is known to result in splenic dysfunction, with the spleen being the first organ to be severely injured, causing substantial morbidity and mortality. However, in clinical practice, exploration of splenic function is limited by the lack of easy, high-throughput, noninvasive tools, so that little is known about the timing and extent of splenic injury in SCA. In addition, direct access to spleen histology is rare because autosplenectomy is the natural outcome in SCA, and surgical splenectomy is therefore infrequently necessary.

A previous study, relying on pitted cell counts, an indirect peripheral measure of vesicle-containing RBCs, showed that splenic function was lost within the first 5 years of life in 90% of children with SCA.³⁴ More recently, the BABYHUG study using liver/spleen ^{99m}Tc

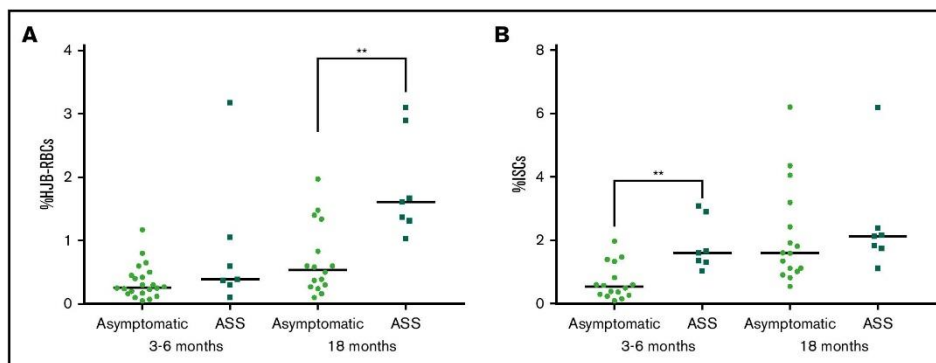


Figure 4. HJB-RBCs and ISCs in asymptomatic and ASS-affected infants. Comparison of %HJB-RBCs (A) and %ISCs (B) at 3 to 6 and 18 months in asymptomatic (n = 22) and ASS infants (n = 7, for whom samples were available for analysis). **P < .005, Wilcoxon test.

colloid scans showed that splenic function was impaired in 75% of the cases,³⁵ specifically in infants <12 months of age with SCA (n = 12, with the youngest aged 8 months). The present study went further by exploring longitudinally and specifically the filtration function of the spleen in a younger cohort. In fact, this splenic exploration could hardly be undertaken earlier (ie, before 6 months of age), given the time lapse between neonatal diagnosis and enrollment in the study, in addition to the difficulty in obtaining consent for an invasive spleen exploration in otherwise asymptomatic very young infants. Importantly, the longitudinal follow-up allowed insight into the dynamic dimension of splenic decline of function. Furthermore, splenic ^{99m}Tc heated RBC scintigraphy specifically explored the filtration function of the spleen (as opposed to ^{99m}Tc colloid spleen scanning that measures the phagocytic uptake by splenic macrophages), a relevant exploration given the major RBC deformability impairment occurring in SCA.

Our results show that at enrollment, 32% of patients had decreased filtration function evidenced by decreased splenic uptake. A previous study by Adekile et al,³⁶ based on a sequential use of colloid and heated RBC scintigraphy in a cohort of older patients (n = 17; mean age, 7 ± 3.5 years), suggested a temporal loss of splenic function, with an initial loss of the phagocytic function followed by the loss of the filtration function. If this temporal sequence is true, our results suggest that the onset of splenic phagocytic dysfunction may start earlier than 6 months and agree with the results from the baseline splenic exploration of the BABYHUG trial mentioned above. In addition to the known immaturity of splenic function in all infants below 2 years of age, which increases the risk of pneumococcal infection in this age group, our data support the early onset of an additional increased susceptibility to pneumococcal infections in infants with SCA and argues for very early penicillin prophylaxis therapy in infants with SCA.

The longitudinal follow-up further allowed insights into the natural history of splenic decline of function and its relationship with splenic volume. Almost half of patients (42%) showed a decrease in splenic function at 18 months—that is, within a year (increase in %HJB and decrease in splenic uptake). Furthermore, splenic volume measured by scintigraphy showed an increased volume in the majority of the children and, importantly, did not correlate with function, a finding not only illustrating functional asplenia,³⁷ but also demonstrating that splenic volume is not predictive of splenic function. Importantly, the very significant correlation between %HJB-RBCs and results of spleen scintigraphy demonstrates that the measurement of %HJB-RBCs by flow cytometry may allow accurate evaluation of the spleen's filtration function in future studies. In clinical practice, this measurement could help monitor spleen function and guide the appropriate timing of splenectomy in very young children with recurrent ASS, for instance, by demonstrating the absence of function and hence no additional infectious risk related to the surgical removal of the spleen. Beyond SCA, easily available measurement of HJB is a significant improvement, given the growing suspected role of the spleen in the occurrence of severe complications, such as autoimmune diseases, neoplasia, thromboembolic events, and pulmonary hypertension in other patients with hemolytic anemia and in healthy subjects.

We chose to focus on sickle RBC adhesion and deformability properties, as potential contributors to splenic injury, because determinants of splenic injury in SCD are not known and because

the splenic microcirculation specifically challenges these properties. Increased adhesion may play a role in splenic injury because the increased adhesive properties of sickle RBCs prolong transit time in the red pulp, favor HbS polymerization, and hence promote both sickling (and subsequent congestion) and increased cell–cell interaction (and subsequent phagocytosis) within the filtering beds. In this study, we confirmed the increase with time of the expression of Lu/BCAM on RBCs. We also showed that Lu/BCAM is activated. We further showed that this expression functionally translates into a significant increase in adhesion of RBCs on laminin-coated capillaries. Yet, no correlation (positive or negative) was observed between the percentage of adherent RBCs on laminin and the spleen function measured by %HJB-RBCs. This finding may pertain to the restricted interaction of Lu/BCAM with laminin 521, which may not be the major type of laminin present in the extracellular matrix of the spleen. Conversely, when adhesion assays were performed on TrHBMECs, we not only observed a significant increase in the number of adherent RBCs with age, we also observed a significant correlation with the %HJB-RBCs, implying a relation between splenic function and RBC adhesion. The activation of TrHBMECs leads to the expression of ICAM-1 and VCAM-1, which mediates cell adhesion,²³ and previous studies have indeed shown the presence of VCAM-1 in the red pulp of the spleen.^{38,39} Further immunohistological studies are needed to explore VCAM-1-mediated endothelial–sickle RBC adhesion within the human spleen.

In SCA, repeated HbS polymerization results in circulating ISCs. They have a short life span, correlate with hemolysis *in vivo*, and contribute to the pathophysiology of vaso-occlusion.¹⁸ We recently showed that ISCs are poorly deformable and prone to blocking capillaries *in vitro*.²⁰ We therefore chose to explore the role of ISCs in splenic function because we hypothesized that ISCs get trapped in the filtering beds of the red pulp, notably at the interendothelial slit barrier, because of their lack of deformability. In the present study, ISCs were indeed present in the circulation at a very young age and increased significantly with time, similar to %HJB-RBCs. Furthermore, the %ISCs correlated with splenic uptake, indicating that impaired deformability negatively affects splenic filtration.

Because ASS is the most life-threatening splenic complication in infants with SCA and is probably the extreme acute expression of spleen dysfunction, we specifically analyzed infants who experienced ASS and compared them to a selected subgroup of the cohort that remained asymptomatic throughout the follow-up. ASS caused further splenic dysfunction, as illustrated by the increase of %HJB-RBCs in those who experienced ASS, an unsurprising finding, yet one that is so far undemonstrated. Regarding determinants of ASS, while keeping in mind the small number of events, we found no correlation between increased RBC adhesion properties and the occurrence of this event. Conversely, the %ISCs was significantly elevated at 3 to 6 months of age in infants who later experienced ASS, a finding suggesting that ISCs, and hence decreased deformability, may be an important contributor to ASS. Trapping of ISCs may cause a decreased outflow, favoring further sickling and ultimately, ASS. Further studies on larger samples are necessary to confirm these findings.

In conclusion, our study demonstrated that flow cytometry analysis of %HJB-RBCs alone may accurately reflect spleen filtration function in very young children with SCA. Using the analysis, together with spleen scintigraphy, we showed that splenic loss of function is present very early in life (at 3 to 6 months of age) in SCA-affected infants,

declines further, and is unrelated to splenic volume. Hyposplenism results from both increased RBC adhesive properties and, critically, loss of deformability. ISCs are additionally a potential contributor to ASS, which in turn results in further loss of spleen function.

Acknowledgments

The authors thank Geneviève Milon, Peter David, Pierre Buffet, Gil Tchernia, Jacques Elion, and Naria Mohandas for intellectual contribution to the study; Thierry Peyrard, Dominique Gien, Eliane Vera, and Sirandou Tounkara at the Centre National de Référence pour les Groupes Sanguins for the management of blood samples; Frédérique Archambault for input into the design of the study and the acquisition and analysis of the spleen scintigraphy; Julien Picot and Catia Pereira for flow cytometry analyses; and Jean-Philippe Semblat for assistance.

This work was supported by the Projet Hospitalier de Recherche Clinique (Ministry of Health, Projet Hospitalier de Recherche Clinique 2008 AOM08171), INSERM, the Institut National de la Transfusion Sanguine, and the Laboratory of Excellence GR-Ex (grant ANR-11-LABX-0051). GR-Ex is funded by the program "Investissements d'avenir" of the French National Research Agency (grant ANR-11-IDEX-0005-02). S.E.H. was funded by the Ministère de l'Enseignement Supérieur et de la Recherche (Ecole Doctorale BioSPC) and received financial support from Club du Globule Rouge et du Fer and Société Française d'Hématologie.

Authorship

Contribution: S.E.H. conducted the experiments, acquired and analyzed the data, and wrote and edited the manuscript; S.C., M.M., C.L., and M.D. conducted the experiments and acquired the data; N.B. and C.E. performed the statistical analysis on the spleen scintigraphic data; M.d.M., C.A., C.G., B.P., M.H.O., and V.B. enrolled and were in charge of the patients; F.M. performed the spleen scintigraphy acquisition and analysis; C.L.V.K. and Y.C.A. edited the manuscript; W.E.N. contributed significantly to the design of the study, analyzed the data, and wrote and edited the manuscript; and V.B. designed and was responsible for the study, conducted the experiments, acquired and analyzed the data, and wrote and edited the manuscript.

Conflict-of-interest disclosure: The authors declare no competing financial interests.

ORCID profiles: M.M., 0000-0002-4094-022X; M.D., 0000-0002-6804-1621; M.d.M., 0000-0002-6318-0227; C.G., 0000-0001-5945-0469; C.L.V.K., 0000-0002-3251-1310; W.E.N., 0000-0001-8184-427X; V.B., 0000-0002-4984-754X.

Correspondence: Valentine Brousse, Service de Pédiatrie et Maladies Infectieuses, Hôpital Universitaire Necker-Enfants Malades, 149 rue de Sévres, 75015 Paris, France; e-mail: valentine.brousse@gmail.com.

References

1. Airede AL. Acute splenic sequestration in a five-week-old infant with sickle cell disease [letter]. *J Pediatr*. 1992;120(1):160.
2. Walterspiel JN, Rutledge JC, Bartlett BL. Fatal acute splenic sequestration at 4 months of age. *Pediatrics*. 1984;73(4):507-508.
3. Nickel RS, Seashore E, Lane PA, et al. Improved splenic function after hematopoietic stem cell transplant for sickle cell disease. *Pediatr Blood Cancer*. 2016;63(5):908-913.
4. Claster S, Vichinsky E. First report of reversal of organ dysfunction in sickle cell anemia by the use of hydroxyurea: splenic regeneration. *Blood*. 1996; 88(6):1951-1953.
5. Campbell PJ, Olatunji PO, Ryan KE, Davies SC. Splenic regrowth in sickle cell anaemia following hypertransfusion. *Br J Haematol*. 1997;96(1):77-79.
6. Brousse V, Buffet P, Rees D. The spleen and sickle cell disease: the sick(led) spleen. *Br J Haematol*. 2014;166(2):165-176.
7. Tubman VN, Makani J. Turf wars: exploring splenomegaly in sickle cell disease in malaria-endemic regions. *Br J Haematol*. 2017;177(6):938-946.
8. Gaston MH, Verter JI, Woods G, et al. Prophylaxis with oral penicillin in children with sickle cell anemia. A randomized trial. *N Engl J Med*. 1986;314(25): 1593-1599.
9. Mebius RE, Kraal G. Structure and function of the spleen. *Nat Rev Immunol*. 2005;5(8):606-616.
10. Buffet PA, Milon G, Brousse V, et al. Ex vivo perfusion of human spleens maintains clearing and processing functions. *Blood*. 2006;107(9):3745-3752.
11. Safeukui I, Correias JM, Brousse V, et al. Retention of Plasmodium falciparum ring-infected erythrocytes in the slow, open microcirculation of the human spleen. *Blood*. 2008;112(6):2520-2528.
12. Groom AC, Schmidt EE, MacDonald IC. Microcirculatory pathways and blood flow in spleen: new insights from washout kinetics, corrosion casts, and quantitative intravital videomicroscopy. *Scanning Microsc*. 1991;5(1):159-173, NaN-174.
13. Brousse V, Colin Y, Pereira C, et al. Erythroid adhesion molecules in sickle cell anaemia infants: Insights into early pathophysiology. *EBioMedicine*. 2014; 2(2):154-157.
14. El Nemer W, Gane P, Colin Y, et al. The Lutheran blood group glycoproteins, the erythroid receptors for laminin, are adhesion molecules. *J Biol Chem*. 1998;273(27):16686-16693.
15. Steiniger BS. Human spleen microanatomy: why mice do not suffice. *Immunology*. 2015;145(3):334-346.
16. Brousse V, El Hoss S, Bouazza N, et al. Prognostic factors of disease severity in infants with sickle cell anemia: A comprehensive longitudinal cohort study. *Am J Hematol*. 2018;93(11):1411-1419.
17. El Hoss S, Dussiot M, Renaud O, Brousse V, El Nemer W. A novel non-invasive method to measure splenic filtration function in humans. *Haematologica*. 2018;103(10):e436-e439.
18. Goodman SR. The irreversibly sickled cell: a perspective. *Cell Mol Biol*. 2004;50(1):53-58.

19. van Beers EJ, Samsel L, Mendelsohn L, et al. Imaging flow cytometry for automated detection of hypoxia-induced erythrocyte shape change in sickle cell disease. *Am J Hematol.* 2014;89(6):598-603.
20. Lizarralde Iragorri MA, El Hoss S, Brousse V, et al. A microfluidic approach to study the effect of mechanical stress on erythrocytes in sickle cell disease. *Lab Chip.* 2018;18(19):2975-2984.
21. Chaar V, Laurance S, Lapoumeroulie C, et al. Hydroxycarbamide decreases sickle reticulocyte adhesion to resting endothelium by inhibiting endothelial lutheran/basal cell adhesion molecule (Lu/BCAM) through phosphodiesterase 4A activation. *J Biol Chem.* 2014;289(16):11512-11521.
22. De Grandis M, Cambot M, Wautier MP, et al. JAK2V617F activates Lu/BCAM-mediated red cell adhesion in polycythemia vera through an EpoR-independent Rap1/Akt pathway. *Blood.* 2013;121(4):658-665.
23. Schweitzer KM, Vicart P, Delouis C, et al. Characterization of a newly established human bone marrow endothelial cell line: distinct adhesive properties for hematopoietic progenitors compared with human umbilical vein endothelial cells. *Lab Invest.* 1997;76(1):25-36.
24. Owunwanne A, Halkar R, Al-Rasheed A, Abubacker KC, Abdel-Dayem H. Radionuclide imaging of the spleen with heat denatured technetium-99m RBC when the splenic reticuloendothelial system seems impaired. *J Nucl Med.* 1988;29(3):320-323.
25. Adekile AD, Tuli M, Haider MZ, Al-Zaabi K, Mohammadi S, Owunwanne A. Influence of alpha-thalassemia trait on spleen function in sickle cell anemia patients with high HbF. *Am J Hematol.* 1996;53(1):1-5.
26. Klausner MA, Hirsch LJ, Leblond PF, Chamberlain JK, Klempner MR, Segel GB. Contrasting splenic mechanisms in the blood clearance of red blood cells and colloidal particles. *Blood.* 1975;46(6):965-976.
27. Nemati M, Hajalioghli P, Jahed S, Behzadmehr R, Rafeey M, Fouladi DF. Normal values of spleen length and volume: An ultrasonographic study in children. *Ultrasound Med Biol.* 2016;42(8):1771-1778.
28. Liu SC, Derick LH, Palek J. Dependence of the permanent deformation of red blood cell membranes on spectrin dimer-tetramer equilibrium: implication for permanent membrane deformation of irreversibly sickled cells. *Blood.* 1993;81(2):522-528.
29. Bartolucci P, Chaar V, Picot J, et al. Decreased sickle red blood cell adhesion to laminin by hydroxyurea is associated with inhibition of Lu/BCAM protein phosphorylation. *Blood.* 2010;116(12):2152-2159.
30. Udani M, Zen Q, Cottman M, et al. Basal cell adhesion molecule/lutheran protein. The receptor critical for sickle cell adhesion to laminin. *J Clin Invest.* 1998;101(11):2550-2558.
31. El Nemer W, Colin Y, Bauvy C, et al. Isoforms of the Lutheran/basal cell adhesion molecule glycoprotein are differentially delivered in polarized epithelial cells. Mapping of the basolateral sorting signal to a cytoplasmic di-leucine motif. *J Biol Chem.* 1999;274(45):31903-31908.
32. Emond AM, Collis R, Darvill D, Higgs DR, Maude GH, Serjeant GR. Acute splenic sequestration in homozygous sickle cell disease: natural history and management. *J Pediatr.* 1985;107(2):201-206.
33. Brousse V, Elie C, Benkerrou M, et al. Acute splenic sequestration crisis in sickle cell disease: cohort study of 190 paediatric patients. *Br J Haematol.* 2012;156(5):643-648.
34. Brown AK, Sleeper LA, Miller ST, Pegelow CH, Gill FM, Waclawiw MA; Cooperative Study of Sickle Cell Disease. Reference values and hematologic changes from birth to 5 years in patients with sickle cell disease. *Arch Pediatr Adolesc Med.* 1994;148(8):796-804.
35. Rogers ZR, Wang WC, Luo Z, et al; BABY HUG. Biomarkers of splenic function in infants with sickle cell anemia: baseline data from the BABY HUG Trial. *Blood.* 2011;117(9):2614-2617.
36. Adekile AD, Owunwanne A, Al-Za'abi K, Haider MZ, Tuli M, Al-Mohannadi S. Temporal sequence of splenic dysfunction in sickle cell disease. *Am J Hematol.* 2002;69(1):23-27.
37. Pearson HA, Spencer RP, Cornelius EA. Functional asplenia in sickle-cell anemia. *N Engl J Med.* 1969;281(17):923-926.
38. Dutta P, Hoyer FF, Grigoryeva LS, et al. Macrophages retain hematopoietic stem cells in the spleen via VCAM-1. *J Exp Med.* 2015;212(4):497-512.
39. Tada T, Inoue N, Widadayati DT, Fukuta K. Role of MAdCAM-1 and its ligand on the homing of transplanted hematopoietic cells in irradiated mice. *Exp Anim.* 2008;57(4):347-356.

Review

REVIEW



Considering the spleen in sickle cell disease

Sara El Hoss^{a,b,c} and Valentine Brousse^{a,b,c,d}

^aUniversité de Paris, Biologie Intégrée du Globule Rouge, UMR_S1134, BIGR, INSERM, F-75015, Paris, France; ^bInstitut National de la Transfusion Sanguine, Paris, France; ^cLaboratoire d'Excellence GR-Ex, Paris, France; ^dService de Pédiatrie Générale et Maladies Infectieuses, Hôpital Necker-Enfants Malades, Centre de Référence de la Drépanocytose, AP-HP, Paris, France

ABSTRACT

Introduction: In human physiology, the spleen is generally neglected, and its role is considered anecdotal. In sickle cell disease, splenic dysfunction is the main cause of life-threatening complications, particularly in early childhood with the risk of pneumococcal overwhelming sepsis and acute splenic sequestration crisis, notably. During the course of the disease, the spleen functionally declines and anatomically disappears, albeit with great individual variability depending on modulating genetic and environmental factors.

Areas covered: The present review aims to provide an overview of spleen structure and function in order to highlight its role in sickling disorders. The clinical features of spleen damage in sickle cell disease, as well as complications and short- and long-term consequences, are reviewed, along with the main therapeutic options.

Expert opinion: Management of acute splenic sequestration recurrence and timing of splenectomy in children with sickling disorders are two main areas in which clinical studies are needed.

ARTICLE HISTORY

Received 17 February 2019
Accepted 31 May 2019

KEYWORDS

Spleen; sickle cell disease; children; infectious risk; acute splenic sequestration

1. Introduction

The spleen has been a neglected organ up to date because it is not a vital organ in general and because its function is generally lost early in the course of sickle cell disease (SCD) in particular. It is, however, a unique and complex organ which, unlike other peripheral lymphoid organs, acts directly on the bloodstream. Its main functions are to filter the blood, particularly red blood cells (RBCs), and contribute to immune defense notably against blood-borne infections. In SCD, a single mutation in the β -globin gene results in the production of an abnormal hemoglobin (HbS) which, in homozygous patients, leads to subsequent RBC sickling: following the physiological release of oxygen, the deoxy-Hb S that is formed tends to form polymeric fibers that disrupt the architecture and flexibility of RBCs. In order to filter the blood, the spleen specifically challenges RBCs on their deformability and adhesion properties, the very properties that are impaired in patients with SCD. Early in the course of the disease therefore, the spleen is the site of a major interaction. This is particularly valid for the severe genotypes of sickling disorders, i.e. homozygous SS also referred to as sickle cell anemia (SCA) and S- β^0 thalassemia genotypes. Ultimately, repeated damage to the spleen can lead to its destruction. This review will first provide an updated description of the human spleen's structure and functions and will then focus on clinical manifestations and consequences of spleen damage in SCD, particularly in SCA.

2. Overview of the structure and function of the human spleen

The spleen is a combination of two main compartments, the red pulp and the white pulp, interconnected by the perifollicular zone that lies in between. These highly organized micro-anatomical structures serve the spleen's two main functions that are blood filtration and immune defense.

2.1. The red pulp

The red pulp represents the largest compartment of the spleen in humans (75%) and is mainly responsible for its filtering function. It is constituted of vascular structures, in particular specialized type of microvessels called venous sinuses, in addition to classical capillaries, within a meshwork of cords.

The filtration in the red pulp is allowed by a unique micro-circulation, which is termed open because when the arterial blood cells arrive into the cords of the red pulp, they exit their vascular endothelial-lined bed, thereafter flowing freely [1,2]. Due to a high hematocrit (approximately 60%), blood cells not only percolate freely but also slowly, favoring a close and prolonged cell-cell contact (Figure 1). During these interactions, RBCs that are coated with antibodies or senescent or abnormally structured are cleared by the macrophages of the red pulp, thus giving the red pulp its erythrophagocytic characteristic [3]. The collecting splenic sinuses, which will ultimately drain into portal veins, form a permeable vascular network with functional openings between the lining

Article highlights

- The spleen serves as a major filter for blood cells and blood-borne pathogens as it is the only immune lymphoid organ which acts directly on the bloodstream.
- Impaired properties of sickle red cells lead to splenic damage early in the course of the disease.
- Spleen damage results in early loss of function in children with sickle cell disease and subsequent life-long increased risk to encapsulated bacteria.
- Spleen-related complications are responsible for significant mortality and morbidity in children with sickle cell disease.
- Acute splenic sequestration of red blood cells is a life-threatening complication in early infancy.

endothelial cells. These possibly dynamic slits, which are very narrow (1–3 μm wide), allow the passage of RBCs back to the venous circulation if they are deformable enough to squeeze through [4]. During this vital checkpoint, an additional clearing process called pitting allows the removal of unwanted material within the RBCs (nuclear remnants or parasites for instance), while allowing the RBC to traverse [5,6]. RBCs that are not deformable enough may be retained upstream of the sinus wall. Consequently, if this checkpoint is altered, the removal of abnormal RBCs, for example, RBCs containing inclusion bodies, fails to happen and these are detected in the circulation. In splenectomized individuals or patients with a dysfunctional spleen like SCD patients, RBCs containing intracellular DNA remnants, i.e. Howell-Jolly Bodies (HJB), are found in the peripheral blood [7].

The cords are made of specialized fibroblasts and numerous macrophages lying upon a tridimensional network of reticular fibers, collagen type IV, and laminin composing the extracellular matrix (Figure 2) [8].

Macrophages in the red pulp play a specific role in recycling iron after the process of erythrophagocytosis [9]. They have unique characteristics when compared to monocytes or monocyte-derived macrophages by expressing differently FC γ receptors for instance and may, therefore, be a highly specialized self-renewing population established before birth [10,11].

2.2. The white pulp

The white pulp of the human spleen consists of B lymphocytes found in the follicles and T lymphocytes mainly organized in sheaths surrounding arteries. B follicles are composed of a germinal center (GC) surrounded by a mantle zone. The GC consists of mainly B-cells and of T-cells in the periphery, very much like a lymph node structure [8]. This compartment of the spleen is responsible for the recirculation and clearing of lymphocytes, and importantly, initiating an immune response for blood-borne antigens. In particular, the follicular B-cells initiate a T-cell dependent immune response, while IgM memory B-cells lining the mantle zone in the spleen initiate a T-cell independent response, critical for the phagocytosis of encapsulated bacteria, notably *Streptococcus pneumoniae*, *Neisseria meningitidis*, and *Haemophilus influenza* [12,13]. Splenic dysfunction, therefore, leads to an increased susceptibility to encapsulated bacterial infections, notably pneumococcal infection. Indeed, T-independent clearance of polysaccharidic germs requires both an intact splenic filtration and an efficient opsonization by IgM antibodies.

2.3. The perifollicular zone

The perifollicular zone connects the white pulp and the red pulp. It is a zone of intense circulation and termination of many arterioles that open up in this area. Whether there exists within this zone an additional closed microcirculatory pathway that would allow pathogen or cellular escape from the filtering beds is still matter of debate [2]. Unlike rodents, there is no perifollicular vascular structure like a marginal sinus [8]. In this zone of high cellular trafficking, specialized fibroblasts and macrophages provide a first line of cell sorting and allow selective circulation: the lymphocytes circulate towards the white pulp whereas the red cells will be directed towards the red pulp. Macrophages of the perifollicular zone have a specific phenotype with the expression for instance of sialoadhesins (CD169). Importantly, this zone is absent at birth in humans and becomes organized around 2 years of life, which

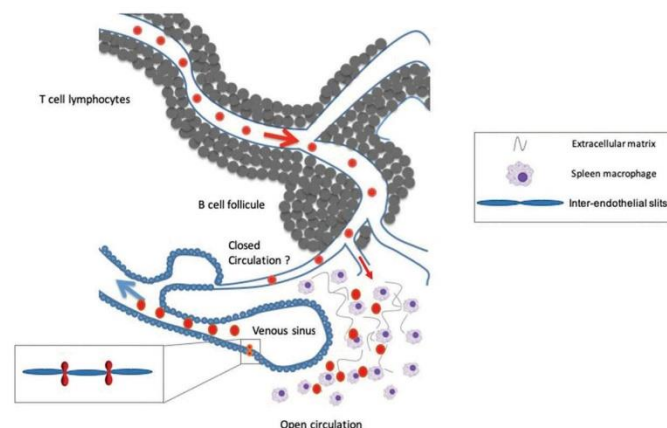


Figure 1. Schematic diagram of the microcirculation in the human spleen showing the close cellular interaction in the filtering beds of the red pulp and the inter-endothelial slits that red blood cells need to squeeze through in order to join the venous circulation.

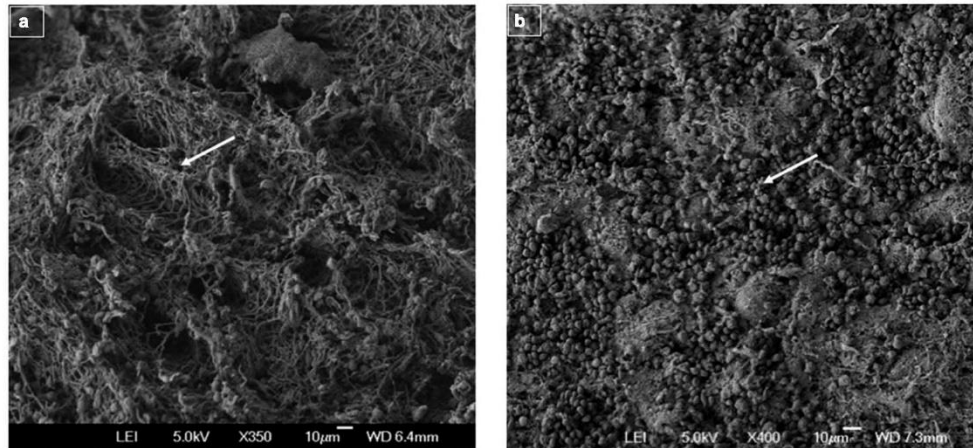


Figure 2. A. Scanning electron microscopy micrograph of a spleen sample from a 5-year-old boy with sickle cell anemia showing the tridimensional reticular matrix of the red pulp (arrow). Bar = 10µm. B. Scanning electron microscopy micrograph of a spleen sample from a healthy adult showing red blood cells present in the filtering beds of the red pulp (arrow). Bar = 10µm. (Courtesy of Pr. PA Buffet).

explains the susceptibility to pneumococci in all very young children, let alone SCD [14].

3. Pitfalls in measuring spleen function

Assessment of spleen function has remained challenging up to date due to a relative lack of non-invasive, accurate and readily available tools to measure its specific filtering or immune function.

Liver-spleen scintigraphic scanning has been and is possibly still the gold standard for assessing splenic function. This technique provides a qualitative and/or semi-quantitative measurement of splenic function by evaluating the splenic uptake of either heat-denatured RBCs or nano-colloids, labeled with technetium-99m [15]. While nanocolloids challenge the phagocytic ability of splenic macrophages, the heat-denatured RBCs challenge the mechanical filtration ability of the spleen [16]. Even though these techniques have proven reliable, they are time-consuming, invasive, and not readily available.

Counting of HJB-containing RBCs in circulation using May-Grunwald Giemsa staining on blood smears is one of the classical methods used to diagnose splenic dysfunction in clinical practice. This method is user-dependent and does not give exact percentages of HJB-containing RBCs because of the small number of counted cells (100–200 RBCs). Another similar commonly used method is to count ‘pitted’ RBCs by interference contrast microscopy [17].

A flow cytometry-based method using propidium iodide (PI) was developed to count HJB-containing RBCs [18], a technique that requires cell fixation, RNA digestion steps, and sample shipment to the laboratory. Recently, we developed a new widely available flow cytometry-based method to measure HJB-containing RBCs [19]. This method was first set up using imaging flow cytometry technology to specifically quantify HJB-containing RBCs. Using mathematical modeling, three different equations to deduce the percentage of HJB-containing RBCs from the percentage of Hoechst positive

events were thereafter proposed. This method reduces both the time needed for the analysis, the error due to RNA-related false-positive events and should be easily available in diverse settings. In clinical practice, this functional measurement can be used to monitor longitudinally splenic function, except in malaria-endemic countries, because the parasite would result in additional Hoechst staining.

Measuring spleen-related immune function is possible and relies on the peripheral blood analysis of splenic-specific lymphocyte subsets, for instance IgM memory B cells as a proportion of B cells. However, such analysis is time-consuming, expensive, and its clinical utility questionable as no discriminating threshold was associated with high sensitivity and specificity in a study that compared splenectomized patients with normal controls [20].

4. The spleen in sickle cell disease

4.1. Early and progressive loss of splenic function: a feature of SCD

In sickling disorders, the spleen is an organ of early and major interaction. In SCA in particular, depending on the technique used, splenic loss of function is evidenced very early in infants. Abnormally high pitted red cell counts were found in 23% of 130 homozygous infants at age 12 months, in 42% at age 24 months, and in 52% at age 36 months in a Jamaican cohort [21]. Using a combination of HJB counts (quantified by flow cytometry), pitted cells and (99m) Tc sulfur-colloid liver-spleen scan in 193 infants 8 to 18 months of age, a more recent study demonstrated that loss of splenic function began before 12 months of age in 86% of infants [22]. While this loss of function is a common feature in SCA, the age at which irreversible loss of the organ (autosplenectomy) occurs is variable, and reversal of splenic function with therapy has been described (see also section 8). Without intervention, autosplenectomy as evidenced by

ultrasound scanning was found in 35.7% of a cohort of 112 patients age 0 to 21 with SCD but in only 5% of children less than 5 years [23].

Less attention has been paid to other sickling genotypes (SC, S β + thalassemia for instance) and very few studies have in fact explored spleen function. In 201 subjects aged 6 months to 90 years with hemoglobin SC, a significantly increased count of pitted cells was found with age. Interestingly, however, none of the 59 subjects less than 4 years of age had abnormally high pitted cells, while the counts rose in 19 of 86 subjects (22%) 4 to 12 years of age, and 25 of 56 subjects (45%) greater than 12 years of age. Spleen loss of function occurs, therefore, later in life, and to a lesser extent than in patients with SCA [24].

4.2. Insights from histological studies

Seminal histological studies have allowed insight into spleen pathological changes as early as 1935 [25]. These studies, principally based on necropsies in patients with SCA, described the 'progressive changes from congestive enlargement to fibrotic atrophy'. These changes resulted from the 'pooling and intense packing of the red pulp by circulating RBCs' [26].

In more severe cases or after a longer duration of the disease, fibrosis and specific splenic lesions such as subcapsular infarcts and sclero-siderotic nodules called Gamna-Gandy bodies are observed [27]. These pioneering studies, however, did not allow refined correlations between clinical course and pathological findings. More recent studies have supported further understanding, although they are based on an inevitable selection bias, since splenic specimens are derived from individuals with SCD who undergo surgical removal for spleen-

related complications (mainly splenomegaly, recurrent acute splenic sequestration or hypersplenism). A study analyzing the nature and role of Gamna-Gandy bodies (that are not pathognomonic of SCD and may also be extra splenic) demonstrated its crystal nature composed of calcium and iron, and showed that their number correlated with age in children with SCA [28]. More recently, a comparative study of spleens from SCD patients ($n = 7$, mean age 6.4 ± 1.7 years) with control spleens ($n = 10$, mean age 9.6 ± 3.4 years) and spleens from patients with hereditary spherocytosis (HS) ($n = 32$, mean age 8.7 ± 1.2) showed that SCD spleens displayed marked alterations of both the white and red pulp [29]. In particular, immuno-histological staining showed that in SCD, there was a significantly lower sinus density, increased microvessel density and higher prevalence of fibrosis and Gamna-Gandy bodies compared to HS or control spleens. The authors concluded that these specific changes seen in SCD suggested damage secondary to chronic vascular occlusion, RBC hemolysis and heme release with subsequent red pulp fibrosis and proliferation of non-specialized microvessels.

4.3. Pathophysiology of SCD splenic damage

In patients with SCD, complications derive from both hemolysis and the entrapment of blood cells in small capillary networks causing vaso-occlusion and subsequent downstream ischemic damage. In the spleen, however, the precise mechanism whereby damage occurs is not completely understood: in the splenic red pulp, RBCs are not contained in capillaries so that classical vaso occlusion does not occur. The red pulp is instead congested by RBCs, implying an active flow rather than an upstream blockade (Figure 3). The term vaso occlusion is therefore inappropriate when considering splenic damage.

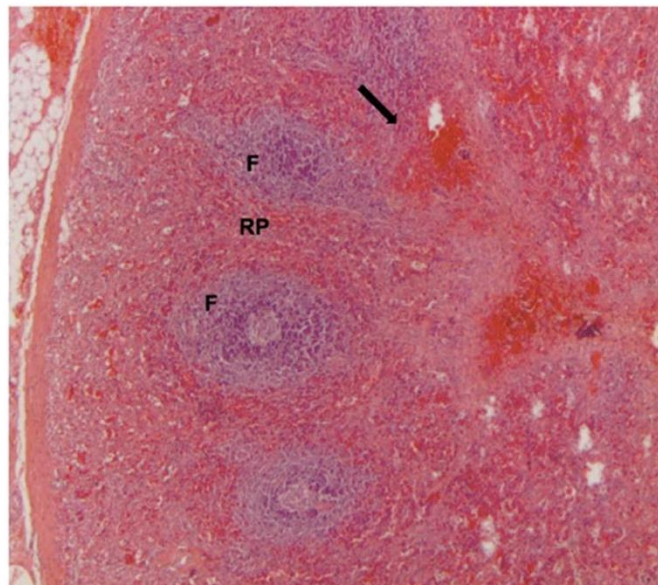


Figure 3. Hematin eosin saffron-stained spleen sample following splenectomy for recurrent acute splenic sequestration in a 5-year-old girl with sickle cell anemia, showing intense red blood cell congestion or hemorrhage (black arrow). RP: Red pulp. F: Follicle. Original magnification $\times 100$.

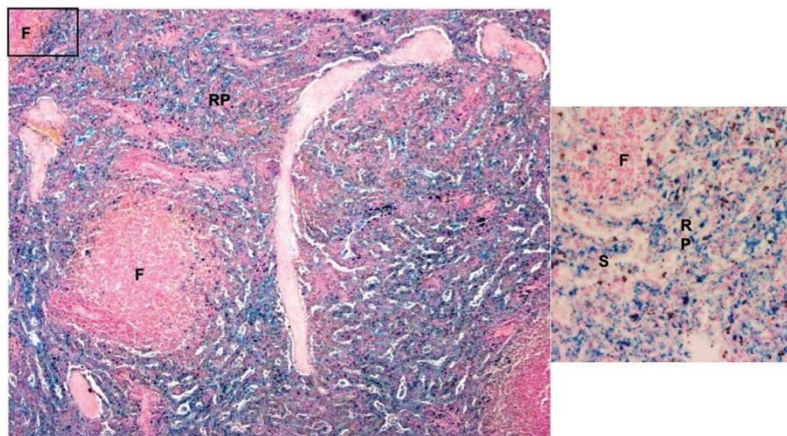


Figure 4. Perls' staining of a spleen sample following splenectomy in a 4-year-old boy with sickle cell anemia, showing intense iron deposition (in blue) along and around the venous sinuses of the red pulp. RP: Red pulp. F: Follicle. S: Sinus. Original magnification x200. Insert: same sample. Original magnification x 400.

Congestion is most probably caused by sickle RBCs main characteristics, i.e. markedly reduced deformability and increased adhesion properties, favored by the splenic environment: slow transit time, high hematocrit, high concentration of specialized clearing macrophages. It is possible that an additional systemic signal (infectious for instance) may trigger further congestion. Consequences include hemorrhage followed by inflammation and fibrosis. Hypothetically hemodynamic diversion of RBCs towards other circulatory pathways shunting blood away from the filtration beds may occur. In addition, repeated acute or chronic hemolysis may result in low-grade iron deposit, inflammation, and fibrosis (Figure 4). Up to date, however, there is no clear sequence of events or repeated pattern that may unequivocally explain the natural history of splenic pathological changes.

5. Consequences of splenic loss of function in SCD

5.1. Increased susceptibility to encapsulated bacteria

Functional or anatomical asplenia is a common feature in sickling disorders although its onset may vary across genotypes and environments. Loss of spleen function results in an increased infectious susceptibility to encapsulated bacteria, first of all *Streptococcus pneumoniae* [13]. As mentioned above, the risk of pneumococcal infection is high in all infants below 2 years of age due to the immaturity of the perifollicular zone of the spleen harboring specialized IgM memory B lymphocytes. Splenic damage in infants with SCA further increases the risk of pneumococcal infection by impairing innate mechanisms that allow defense against encapsulated bacteria, the red pulp efficient phagocytosis by specialized macrophages favored by the T independent immune response by IgM memory B lymphocytes. In high-income settings, the increased risk of invasive pneumococcal infection is well tackled by early diagnosis, penicillin prophylaxis, pneumococcal immunization, and aggressive antibiotic treatment, so that infection-related mortality in childhood has drastically

decreased [30,31]. Daily penicillin prophylaxis has indeed proven very effective in infants with SCA, although the age at which the treatment may be safely discontinued is still under debate. Similarly, pneumococcal immunization by 13 valent-conjugated vaccines followed at 2 years of age by 23 valent polysaccharidic vaccines is strongly recommended and has proven great efficacy in reducing pneumococcal-related morbidity and mortality [32]. By contrast, in sub-Saharan Africa, where over 300,000 babies with sickling disorders are born annually [33], more than half of them will die by age 5 [34] with infection and malaria being presumably the major contributors [35]. In particular, the specific susceptibility of children with SCA to *Streptococcus pneumoniae* and *Haemophilus influenzae B* was elegantly demonstrated in this setting [36], as well as its related mortality with a quarter of these children admitted with bacteremia dying in hospital, a rate further underestimated since only a minority of patients actually present to hospital in their final illness.

5.2. Additional consequences of splenic loss of function

In SCD, splenic loss of function is the natural fate. In addition, there is extreme variability not only in spleen function but in disease severity altogether. There is therefore much difficulty in assessing long-term consequences of asplenia in this population, beyond the well-documented infectious risk. Case-control studies to compare outcomes in patients with SCD according to their splenic functional status would be complex to implement. While ASS has not been demonstrated so far to be prognostic of disease severity, it is however expected that patients with early splenic damage may also be the most severe patients [37,38]. In addition, splenic loss presumably shifts intra tissular hemolysis towards vascular hemolysis with more early systemic damage. In other hemoglobinopathies or RBC membrane disorders, the deleterious consequences of asplenia following splenectomy have emerged in the last years [39]. Furthermore, in healthy subjects, recent large epidemiological studies have demonstrated the increased long-

term risk of cancer and thromboembolism after splenectomy [40]. Altogether, this data underscores the emerging role of the spleen in maintaining blood and immune homeostasis.

6. Clinical manifestations of splenic dysfunction

While splenic loss of function, a clinical feature of SCD, is in the majority of cases clinically silent, acute or chronic splenic complications may also occur: acute splenic sequestration (ASS), splenomegaly, and hypersplenism. These occur with a variable incidence, depending on age, genotype, and various protective biological and genetic factors.

6.1. Acute splenic sequestration

Acute splenic sequestration (ASS) results from a massive trapping of RBCs in the spleen. It is defined by the sudden enlargement of the spleen with an acute drop of Hb level $>2\text{g/dL}$. The classic clinical signs are splenomegaly, abdominal pain and tenderness, pallor, and irritability or pain. While there is a wide spectrum of severity, urgent treatment based on top-up transfusion or red blood cell exchange is mandatory as transfusion delay can lead to hypovolemic shock and death from acute anemia. Of note, transfusion usually leads to a decrease in the size of the spleen while the hematocrit rises above post-transfusional target as a result of blood unpooling. ASS occurs in approximately 7% to 30% of infants with SCA [41–43]. Predictive factors are unknown, although high fetal hemoglobin (HbF) is a strong protective factor [44].

ASS is one of the earliest life-threatening complications seen in patients with SCD. Such a complication has been reported in a 5-week old and 4-month old [45,46]. The median age range for this complication is between 6 months and 5 years, with a median age of 1.4 years in a French cohort study [43]. Over two-thirds of infants (67%) experience more than one ASS episode, with a higher risk, when ASS occurs before the age of 2. Precipitating factors are largely unknown although an infectious triggering event is often associated. Studies have reported an association between the occurrence of a parvovirus B19 infection and ASS and highlighted the need to monitor patients with an active parvovirus B19 infection for ASS episodes [47]. More recently in a longitudinal cohort of 57 SCA infants enrolled at 6 months, eight (17%) suffered from at least one ASS episode at a median age of 13.4 months, five of the patients experienced a reoccurrence during the study period [44].

Despite the expected decline in spleen function with time, ASS, which presumably requires an active spleen to occur, has also been described in older patients, both in SCA and SC disease, with a higher risk of a fatal outcome given the difficulty of recognition in adult patients [48].

ASS was considered as the second cause of death after infections in the first decade of life, but ASS-related mortality has decreased in the last years in areas where neonatal screening is available and parental awareness allows prompt medical assistance in case of ASS [42,47,49]. Nonetheless, more educational campaigns directed toward SCD patients' families are required in low-income countries to decrease ASS-related mortality rate [50].

6.2. Splenomegaly

Splenomegaly is presumably the result of moderate trapping of rigid RBCs and translates into a limited enlargement of the spleen with no or very mild hematological consequences. Its prevalence is variable depending on genetic and environmental determinants. In a Jamaican setting, splenomegaly reached its highest incidence in the first year of life in patients with SCA, followed by a progressive decrease. More recently, in the US, spleen volume assessed by ultrasonography in a large cohort of infants aged 7.5–18 months showed a mean volume significantly greater than normal age-matched controls [51,52].

SC disease is characterized by a high prevalence of splenomegaly. Splenomegaly by palpation or imaging has been reported in up to 50–60% of adult patients with Hb SC disease and 34% of children at a mean age of $10. \pm 4.6$ years [53,54].

Genetic modifiers of disease severity such as co-inheritance of alpha thalassemia [55] or beta-globin haplotypes associated with high fetal hemoglobin (HbF) levels prolong spleen function and hence in certain cases splenomegaly to adulthood [56,57].

In malaria endemic settings, splenomegaly has a higher and a prolonged incidence in patients with SCD [58,59]. This finding has been partly attributed to malaria exposure, with an association between splenomegaly and anti-malarial IgG titers [60]. Historically, splenomegaly was in fact used as a marker of malaria prevalence, but scarce data are available in patients with SCD. Pathological studies of spleens from children with SCD living in malaria-endemic countries would greatly contribute to understand the mechanisms underlying splenomegaly in those settings [61].

Conflicting results of spleen size and function have been published. Increased pitted cells and HbJ-containing RBCs together with decreased scintigraphic uptake have been reported in SCD patients suffering from an enlarged spleen, a finding that gave rise to the concept of functional asplenia, i.e., a palpable spleen with decreased function [62]. However, other studies show a significant inverted relationship between pitted RBC count and spleen size [60]. It is now considered that there is no relationship between spleen size and function so that splenomegaly can result in either a normal or a decreased function [52].

6.3. Hypersplenism

Hypersplenism is the consequence of chronic blood sequestration in the spleen with subsequent cytopenia. It occurs when the spleen is chronically enlarged and probably partly fibrotic, preventing it from shrinking back to a normal size, notably after transfusion. Hypersplenism has overlapping features with ASS or splenomegaly so that the diagnosis may sometimes be difficult and consequently the exact prevalence ill-defined. Like splenomegaly, hypersplenism has a higher frequency in patients with high HbF levels and co-inheritance of alpha thalassemia. One consequence of hypersplenism in children is its impact on growth due to the metabolic cost of severe anemia and increased erythropoiesis to compensate [63].

6.4. Other clinical findings

Splenic imaging by CT scanning, ultrasound or MRI in patients with SCD may be normal or evidence multiple abnormalities ranging from mild heterogeneity to a fibrotic calcified splenic remnant. Infarcts are seen as peripheral wedge-shaped defects with decreased signal intensities on both T1 and T2-weighted images with no enhancement following IV contrast administration [64]. ASS may appear on CT scans as multiple peripheral non-enhancing low-density areas or large diffuse areas of low density in the majority of the splenic tissue [65]. Hypoechoic rounded intrasplenic masses of preserved functioning splenic tissue may be found within echogenic spleen on ultrasound and should not be mistaken for splenic abscess. Such 'sterile abscesses' were first described in patients with sickle trait and correspond to infarction and colliquation secondary to intrasplenic RBC sickling, even in sickle cell carriers [64].

7. Management of splenic complications

7.1. General management

7.1.1. ASS

The treatment of ASS is both corrective and prophylactic. Urgent transfusion is vital to correct hypovolemia and anemia. Regarding prophylactic measures, there are no evidence-based guidelines for the management after the first episode of ASS [66]. Depending on the severity of the episode, the family's access to medical facilities and the age of the child, a watchful attitude may be advocated after first ASS. In all other situations, a transfusion program is usually initiated [67]. No particular target of HbS is defined as transfusion does not prevent a recurrence. However, transfusion may alleviate the severity in case of recurrence by increasing the Hb level. In all cases, parents are taught to palpate the spleen and require assistance in case of sudden and/or massive splenomegaly and/or any sign of acute anemia. Pneumococcal immunization is continued as in all other children with SCD, as well as antibiotic prophylaxis. Splenectomy is generally advocated in children older than 3 years, following the first severe episode or recurrence, although this age limit has never been appropriately explored. In exceptional cases of massive ASS, life-saving urgent splenectomy can be performed [68].

7.1.2. Splenomegaly and hypersplenism

Generally, moderate splenomegaly does not require specific management, as it will disappear spontaneously. Conversely, hypersplenism generally prompts splenectomy. While no specific evidence-based management guideline is currently available in SCD regarding hypersplenism, but it is a general recommendation to surgically remove the spleen in order to correct cytopenia, improve growth, decrease discomfort and reduce the risk of traumatic injury [63].

7.2. Splenectomy in SCD

Splenectomy is rarely necessary for patients with SCD given the natural loss of the organ without medical

intervention. However, in cases of ASS (first severe episode or recurrence) or hypersplenism, total laparoscopic splenectomy is performed (see also previous section 7.1 General Management) [69]. The main questions pertaining to splenectomy in children with SCD are the timing of the procedure according to age and to what extent the surgical removal of the spleen further alters the residual immune functions and consequently increases the infectious risk. In a study that compared outcomes following splenectomy in 130 homozygous children with a control group matched for age and sex, the authors demonstrated no greater mortality nor bacteremic episodes in the splenectomized group [70]. Splenectomy had been performed in 46 children with recurrent ASS and 84 with hypersplenism at a median age of 2.3 and 5.9 years, respectively, with a follow-up of 5 years. While age is a central parameter as pneumococcal risk is highest in children below 2 years of age, there is, in fact, no available data to address this question and propose 'a safe age for splenectomy'. No large study has monitored markers of spleen function longitudinally with HJB or pitted cells, in particular before and after splenectomy. Indications and procedures regarding splenectomy, therefore, vary across settings. Altogether, indications for splenectomy are mostly based on local guidelines and a case by case benefit/risk ratio, particularly in children with recurrent ASS episodes.

8. Reversal of splenic loss of function in SCD

Reversal of splenic loss of function in patients with SCD has been reported following transfusion by the early pioneers of spleen exploration and thereafter following hematopoietic stem cell transplantation (HSCT) or hydroxyurea therapy [71–73].

Recently a study carried on 90 SCA patients investigated splenic function prior to and two years following HSCT. Using liver-spleen scintigraphy splenic function was improved with splenic uptake demonstrated in 14/38 (37%) pre-HSCT versus 34/38 (89%) post-HSCT [74]. HSCT at a young age may, therefore, preserve the function at a time when spleen damage is still reversible.

Hydroxyurea also called hydroxycarbamide (HC), one of the two FDA approved treatment for SCA, among its multiple effects, increases HbF levels that interrupts HbS polymerization and hence decreases RBC sickling. Various studies in the literature have evaluated the effect of HC on spleen function in SCD patients. While the Baby Hug trial that compared HC to placebo in very young children failed to demonstrate the efficacy of HC in preserving splenic function after 2 years of treatment, a more recent study in a group of 40 patients (mean age of 9.1 years) showed that after 3 years of HC treatment, 33% of patients had preservation or restitution of splenic filtration function evaluated by liver/spleen scan [75].

Altogether, it is highly probable that maintenance of splenic function or restoration of function may occur when SCD modifying therapy is given early in the course of splenic damage before irreversible fibrosis has occurred.

42. Powell RW, Levine GL, Yang YM, et al. Acute splenic sequestration crisis in sickle cell disease: early detection and treatment. *J Pediatr Surg*. 1992;27:215–218, discussion 218–9
43. Brousse V, Elie C, Benkerrou M, et al. Acute splenic sequestration crisis in sickle cell disease: cohort study of 190 paediatric patients. *Br J Haematol*. 2012;156:643–648.
44. Brousse V, El Hoss S, Bouazza N, et al. Prognostic factors of disease severity in infants with sickle cell anemia: A comprehensive longitudinal cohort study. *Am J Hematol*. 2018;93:1411–1419.
45. Airede AI. Acute splenic sequestration in a five-week-old infant with sickle cell disease. *J Pediatr*. 1992;120:160.
46. Walterspiel JN, Rutledge JC, Bartlett BL. Fatal acute splenic sequestration at 4 months of age. *Pediatrics*. 1984;73:507–508.
47. Emond AM, Collis R, Darvill D, et al. Acute splenic sequestration in homozygous sickle cell disease: natural history and management. *J Pediatr*. 1985;107:201–206.
48. Naymagon L, Pendurti G, Billett HH. Acute splenic sequestration crisis in adult sickle cell disease: a report of 16 cases. *Hemoglobin*. 2015;39:375–379.
49. Telfer P, Coen P, Chakravorty S, et al. Clinical outcomes in children with sickle cell disease living in England: a neonatal cohort in East London. *Haematologica*. 2007;92:905–912.
50. Khoriaty E, Halaby R, Berro M, et al. Incidence of sickle cell disease and other hemoglobin variants in 10,095 Lebanese neonates. *PLoS ONE*. 2014;9:e105109.
51. Rogers DW, Vaidya S, Serjeant GR. Early splenomegaly in homozygous sickle-cell disease: an indicator of susceptibility to infection. *Lancet*. 1978;2:963–965.
52. McCarville MB, Luo Z, Huang X, et al. Abdominal ultrasound with scintigraphic and clinical correlates in infants with sickle cell anemia: baseline data from the BABY HUG trial. *AJR Am J Roentgenol*. 2011;196:1399–1404.
53. Ballas SK, Lewis CN, Noone AM, et al. Clinical, hematological, and biochemical features of Hb SC disease. *Am J Hematol*. 1982;13:37–51.
54. Zimmerman SA, Ware RE. Palpable splenomegaly in children with haemoglobin SC disease: haematological and clinical manifestations. *Clin Lab Haematol*. 2000;22:145–150.
55. Embury SH, Clark MR, Monroy G, et al. Concurrent sickle cell anemia and alpha-thalassemia. Effect on pathological properties of sickle erythrocytes. *J Clin Invest*. 1984;73:116–123.
56. Chopra R, Al-Mulhim AR, Al-Baharani AT. Fibrocongestive splenomegaly in sickle cell disease: a distinct clinicopathological entity in the Eastern province of Saudi Arabia. *Am J Hematol*. 2005;79:180–186.
57. Alsultan A, Alabdulaali MK, Griffin PJ, et al. Sickle cell disease in Saudi Arabia: the phenotype in adults with the Arab-Indian haplotype is not benign. *Br J Haematol*. 2014;164:597–604.
58. Tubman VN, Makani J. Turf wars: exploring splenomegaly in sickle cell disease in malaria-endemic regions. *Br J Haematol*. 2017;177:938–946.
- **A recent review exploring splenomegaly in sickle cell disease in sub Saharan Africa**
59. Sadarangani M, Makani J, Komba AN, et al. An observational study of children with sickle cell disease in Kilifi, Kenya. *Br J Haematol*. 2009;146:675–682.
60. Adekile AD, McKie KM, Adeodu OO, et al. Spleen in sickle cell anemia: comparative studies of Nigerian and U.S. patients. *Am J Hematol*. 1993;42:316–321.
61. Edington GM. Pathology of malaria in West Africa. *Br Med J*. 1967;1:715–718.
62. Pearson HA, Spencer RP, Cornelius EA. Functional asplenia in sickle-cell anemia. *N Engl J Med*. 1969;281:923–926.
63. Singhal A, Thomas P, Kearney T, et al. Acceleration in linear growth after splenectomy for hypersplenism in homozygous sickle cell disease. *Arch Dis Child*. 1995;72:227–229.
64. Luzzatto L. Sterile 'Abscess' of the spleen and the sickle cell trait. *Mediterr J Hematol Infect Dis* [Internet]. 2018. Available from: <https://www.ncbi.nlm.nih.gov/pmc/articles/PMC5760069/>
65. Sheth S, Ruzal-Shapiro C, Piomelli S, et al. CT imaging of splenic sequestration in sickle cell disease. *Pediatr Radiol*. 2000;30:830–833.
66. Owusu-Ofori S, Remington T. Splenectomy versus conservative management for acute sequestration crises in people with sickle cell disease. *Cochrane Database Syst Rev*. 2017;11:CD003425.
67. Brousse V, Buffet P, Rees D. The spleen and sickle cell disease: the sick(led) spleen. *Br J Haematol*. 2014;166:165–176.
68. Al-Salem AH. Massive splenic infarction in children with sickle cell anemia and the role of splenectomy. *Pediatr Surg Int*. 2013;29:281–285.
69. Al-Salem AH, Qaisaruddin S, Nasserullah Z, et al. Splenectomy and acute splenic sequestration crises in sickle cell disease. *Pediatr Surg Int*. 1996;11:26–28.
70. Wright JG, Hambleton IR, Thomas PW, et al. Postsplenectomy course in homozygous sickle cell disease. *J Pediatr*. 1999;134:304–309.
71. Pearson HA, Cornelius EA, Schwartz AD, et al. Transfusion-reversible functional asplenia in young children with sickle-cell anemia. *N Engl J Med*. 1970;283:334–337.
72. Ferster A, Bujan W, Corazza F, et al. Bone marrow transplantation corrects the splenic reticuloendothelial dysfunction in sickle cell anemia. *Blood*. 1993;81:1102–1105.
73. Hankins JS, Helton KJ, McCarville MB, et al. Preservation of spleen and brain function in children with sickle cell anemia treated with hydroxyurea. *Pediatr Blood Cancer*. 2008;50:293–297.
74. Nickel RS, Seashore E, Lane PA, et al. Improved splenic function after hematopoietic stem cell transplant for sickle cell disease. *Pediatr Blood Cancer*. 2016;63:908–913.
75. Nottage KA, Ware RE, Winter B, et al. Predictors of splenic function preservation in children with sickle cell anemia treated with hydroxyurea. *Eur J Haematol*. 2014;93:377–383.
76. Tadayon S, Dunkel J, Takeda A, et al. Clever-1 contributes to lymphocyte entry into the spleen via the red pulp. *Sci Immunol*. 2019;(4).
77. Buffet PA, Safeukui I, Deplaine G, et al. The pathogenesis of *Plasmodium falciparum* malaria in humans: insights from splenic physiology. *Blood*. 2011;117:381–392.
78. Safeukui I, Buffet PA, Deplaine G, et al. Quantitative assessment of sensing and sequestration of spherocytic erythrocytes by the human spleen. *Blood*. 2012;120:424–430.